SANDIA NATIONAL LABORATORIES
WASTE ISOLATION PILOT PLANT

ANALYSIS PACKAGE FOR PARAMETER SAMPLING IN THE 2019 COMPLIANCE RECERTIFICATION APPLICATION PERFORMANCE ASSESSMENT (CRA-2019 PA)

REVISION 0

	Print	Signature	Date
Author:	Todd R. Zeitler	[signature]	6/10/2019
Technical Reviewer:	Sarah Brunell	Sarah Brunell	6/10/2019
QA Reviewer:	Shelly Nielsen	Shelly R. Nielsen	6-10-19
Management Reviewer:	Chris Camphouse	[signature]	6-10-19

ERMS #571367
JUNE 2019
WIPP:4.2.1:PA:QA-L:571155

This page intentionally left blank.

TABLE OF CONTENTS

LIST OF TABLES

LIST OF FIGURES

Executive Summary

The Land Withdrawal Act requires that the U.S. Department of Energy (DOE) apply for recertification of the Waste Isolation Pilot Plant (WIPP) every five years following the initial 1999 waste shipment. The 2019 Compliance Recertification Application (CRA-2019) is the fourth WIPP recertification application submitted for approval by the U.S. Environmental Protection Agency. A performance assessment (PA) has been executed by Sandia National Laboratories in support of the DOE submittal of the CRA-2019. Results found in the CRA-2019 PA are compared to those obtained in the 2014 Compliance Recertification Application (CRA-2014) in order to assess repository performance in terms of the current regulatory baseline. This package documents the parameter sampling component of the CRA-2019 PA. Changes incorporated into the CRA-2019 PA include repository planned changes, parameter updates, and refinements to PA implementation. Changes included in the CRA-2019 PA that potentially affect parameter sampling results as compared to the CRA-2014 PA are:

- Refinement of the gas generation process model to include brine radiolysis.
- An update to the probability that a drilling intrusion into a repository excavated region will intersect the Castile brine reservoir modeled in BRAGFLO.
- Refinement to the corrosion rates of steel under humid and inundated conditions.
- Refinement to the effective shear strength of WIPP waste.
- Refinement to colloid enhancement parameters associated with actinide mobilization.
- Refinement to the hydromagnesite to magnesite conversion rate.
- Updates to radionuclide solubilities and their associated uncertainty.
- Hardware and computational code updates.

LHS was used to generate 100 vectors of sampled parameter values for each of three replicates for the CRA19 analysis of the CRA-2019 PA. A unique random number seed was assigned to each of the three replicates. These seed values were identical to those used in the CRA14 analysis. Sixty-four parameters were sampled for the CRA19 analysis, including two new parameters (also, one parameter from the CRA14 analysis was not sampled). Updated distributions were sampled for six additional parameters. All 300 sets of sampled parameters were written to the WIPP PA Results Database (PA_Results) for use by other WIPP PA codes.

The resulting sampled data had the expected correlation structure and the values fell within the expected ranges. The distributions of sampled values matched the expected cumulative distribution functions (CDFs).

This page intentionally left blank.

1.0 INTRODUCTION

The Waste Isolation Pilot Plant (WIPP), located in southeastern New Mexico, has been developed by the U.S. Department of Energy (DOE) for the geologic (deep underground) disposal of transuranic (TRU) waste. Containment of TRU waste at the WIPP is regulated by the U.S. Environmental Protection Agency (EPA) according to the regulations set forth in Title 40 of the Code of Federal Regulations (CFR), Part 191. The DOE demonstrates compliance with the containment requirements according to the Certification Criteria in Title 40 CFR Part 194 by means of performance assessment (PA) calculations performed by Sandia National Laboratories (SNL). WIPP PA calculations estimate the probability and consequence of potential radionuclide releases from the repository to the accessible environment for a regulatory period of 10,000 years after facility closure. The models used in PA are maintained and updated with new information as part of an ongoing process. Improved information regarding important WIPP features, events, and processes typically results in refinements and modifications to PA models and the parameters used in them. Planned changes to the repository and/or the components therein also result in updates to WIPP PA models. WIPP PA models are used to support the repository recertification process that occurs at five-year intervals following the receipt of the first waste shipment at the site in 1999.

PA calculations were included in the 1996 Compliance Certification Application (CCA) (U.S. DOE 1996), and in a subsequent Performance Assessment Verification Test (PAVT) (MacKinnon and Freeze 1997a, 1997b and 1997c). Based in part on the CCA and PAVT PA calculations, the EPA certified that the WIPP met the regulatory containment criteria. The facility was approved for disposal of transuranic waste in May 1998 (U.S. EPA 1998). PA calculations were an integral part of the 2004 Compliance Recertification Application (CRA-2004) (U.S. DOE 2004). During their review of the CRA-2004, the EPA requested an additional PA calculation, referred to as the CRA-2004 Performance Assessment Baseline Calculation (PABC) (Leigh et al. 2005), be conducted with modified assumptions and parameter values (Cotsworth 2005). Following review of the CRA-2004 and the CRA-2004 PABC, the EPA recertified the WIPP in March 2006 (U.S. EPA 2006).

PA calculations were completed for the second WIPP recertification and documented in the 2009 Compliance Recertification Application (CRA-2009). The CRA-2009 PA resulted from continued review of the CRA-2004 PABC, including a number of technical changes and corrections, as well as updates to parameters and improvements to the PA computer codes (Clayton et al. 2008). To incorporate additional information which was received after the CRA-2009 PA was completed, but before the submittal of the CRA-2009, the EPA requested an additional PA calculation, referred to as the 2009 Compliance Recertification Application Performance Assessment Baseline Calculation (PABC-2009) (Clayton et al. 2010), be undertaken which included updated information (Cotsworth 2009). Following the completion and submission of the PABC-2009, the WIPP was recertified in 2010 (U.S. EPA 2010).

PA calculations were completed for the third WIPP recertification and documented in the 2014 Compliance Recertification Application (CRA-2014). Following the completion and submission of the CRA-2014, the WIPP was recertified in 2017 (U.S. EPA 2017a).

The Land Withdrawal Act (U.S. Congress 1992) requires that the DOE apply for WIPP recertification every five years following the initial 1999 waste shipment. The 2019 Compliance Recertification Application (CRA-2019) is the fourth WIPP recertification application submitted by the DOE for EPA approval. The PA executed by SNL in support of the CRA-2019 is detailed in AP-181 (Zeitler 2019a). The CRA-2019 PA includes a repository planned changes, parameter updates, and refinements to PA implementation. Results found in the CRA-2019 PA are compared to those obtained in the CRA-2014 in order to assess repository performance in terms of the current regulatory baseline. This analysis package documents the parameter sampling component of the CRA-2019 PA analysis.

1.1 Changes Since the CRA-2014

Several changes are incorporated in the CRA-2019 PA relative to the CRA-2014 that potentially impact parameter sampling results. The changes are:

- Refinement of the gas generation process model to include brine radiolysis.
- An update to the probability that a drilling intrusion into a repository excavated region will intersect the Castile brine reservoir modeled in BRAGFLO.
- Refinement to the corrosion rates of steel under humid and inundated conditions.
- Refinement to the effective shear strength of WIPP waste.
- Refinement to colloid enhancement parameters associated with actinide mobilization.
- Refinement to the hydromagnesite to magnesite conversion rate.
- Updates to radionuclide solubilities and their associated uncertainty.
- Hardware and computational code updates.

Changes listed above are discussed in more detail in the sections that follow.

1.1.1 Parameterization of Brine Radiolysis (GLOBAL:GDEPFAC)

The CRA-2019 PA calculations include radiolytic gas generation as a refinement to the gas generation process model implemented in BRAGFLO calculations (Zeitler 2019a). Radiolytic gas generation was screened out of PA calculations for the CRA-2014 PA, but for the CRA-2019 PA, radiolytic gas generation due to brine is included (radiolyis of cellulosics, plastics, and rubbers is still screened out) (Day 2019). As part of the implementation for the CRA-2019 PA, a new parameter, GLOBAL:GDEPFAC, has been defined to represent the energy deposition probability for wetted solid radionuclides and a uniform distribution over the range [0, 0.5] (unitless) has been assigned.

1.1.2 Update to Brine Intrusion Probability (GLOBAL:PBRINE)

The CRA-2019 PA calculations include an update to the parameter distribution assigned to the GLOBAL:PBRINE parameter, which represents the probability that a drilling intrusion into a repository excavated region will intersect the Castile brine reservoir modeled in BRAGFLO

(Zeitler 2019a). It is used by the CCDFGF code. The normal distribution used in CRA-2014 PA calculations has been replaced by a cumulative distribution derived by the EPA. The cumulative distribution for the GLOBAL:PBRINE parameter has a range of [0.04, 0.57] (unitless), is described in detail in U.S. EPA (2017b), and is summarized in Zeitler (2019b).

1.1.3 Refinement to Steel Corrosion Rates (STEEL:HUMCORR and STEEL:CORRMCO2)

The CRA-2019 PA calculations include refinements to the parameters for the rates of steel corrosion under humid (STEEL:HUMCORR) and inundated (STEEL:CORRMCO2) conditions (Zeitler 2019a). Both parameters are used by the BRAGFLO code. The constant value of zero used in the CRA-2014 PA for the STEEL:HUMCORR parameter has been replaced by a cumulative distribution with a range of [0, 1.03E-15] m/s and is described in detail in Zeitler (2018a). The Student distribution in the the CRA-2014 PA for the STEEL:CORRMCO2 parameter has been replaced by a cumulative distribution with a range of [0, 7.92E-14] m/s and is described in detail in Zeitler (2018b).

1.1.4 Refinement to Waste Shear Strength (BOREHOLE:TAUFAIL)

The CRA-2019 PA calculations include an update to the parameter distribution assigned to the BOREHOLE:TAUFAIL parameter, which represents effective shear strength of WIPP waste (Zeitler 2019a). It is used by the CUTTINGS_S code. The lower end of the uniform distribution used in CRA-2014 PA calculations has been revised following a request by the EPA. The uniform distribution for the BOREHOLE:TAUFAIL parameter has a range of [1.6, 77.0] (Pa), is described in detail in U.S. EPA (2017c), and is summarized in Zeitler (2019b).

1.1.5 Refinement to Humic Colloid Proportionality Constant (+III, Castile Brine) (PHUMOX3:PHUMCIM)

The CRA-2019 PA calculations include an update to the PHUMOX3:PHUMCIM parameter, which is the proportionality constant for humic colloids of oxidation state +III in Castile brine (Zeitler 2019a, Mariner 2019). The cumulative distribution used in CRA-2014 PA calculations has been replaced by a constant value. In CRA-2014 PA calculations, it was used by the PANEL code; for CRA-2019 PA calculations, it is used by the PANEL code as well as the BRAGFLO code due to its role in radiolytic gas generation. Because the PHUMOX3:PHUMCIM parameter is now represented by a constant value, it was not sampled for the CRA-2019 PA and thus will not be discussed further in this document.

1.1.6 Refinement to Hydromagnesite Conversion Rate (WAS_AREA:HYMAGCON)

The CRA-2019 PA calculations include a refinement to the parameter distribution assigned to the WAS_AREA:HYMAGCON parameter, which represents the rate of conversion of hydromagnesite to magnesite (Zeitler 2019a). It is used by the BRAGFLO code. The uniform distribution used in CRA-2014 PA calculations has been replaced by a uniform distribution derived by the EPA. The uniform distribution for the WAS_AREA:HYMAGCON parameter has a range of [0, 3.4E-10] (mol kg^{-1} sec^{-1}), is described in detail in U.S. EPA (2017d), and is summarized in Zeitler (2019b).

1.1.7 Updates to Actinide Solubility Uncertainty Multipliers (SOLMOD3:SOLVAR and SOLMOD4:SOLVAR)

The CRA-2019 PA calculations include updates to the parameter distributions assigned to the actinide uncertainty multiplier parameters for +III (SOLMOD3:SOLVAR) and +IV (SOLMOD4:SOLVAR) actinides (Zeitler 2019a, Domski 2019a). In CRA-2014 PA calculations, these two parameters were used by the PANEL code; for CRA-2019 PA calculations, they are used by the PANEL code as well as the BRAGFLO code due to their role in radiolytic gas generation. The cumulative distributions for these parameters used in CRA-2014 PA calculations have been replaced by cumulative distributions derived by Domski (2019a). The cumulative distribution for the SOLMOD3:SOLVAR parameter has a range of [-1.14251, 2.97147] (unitless) and the cumulative distribution for the SOLMOD4:SOLVAR parameter has a range of [-2.0098, 1.4266] (unitless).

1.1.8 LHS Code Updates

Calculations for the CRA-2014 PA were performed on the WIPP PA Alpha Cluster (Long 2013). WIPP PA codes were later migrated to the WIPP PA Solaris Cluster (Kirchner 2012, Kirchner et al. 2014, Kirchner et al. 2015). The migration process consisted of recompilation, retesting, and requalification of codes. Additional code changes have been made since the migration to the Solaris system, as described below.

1.1.8.1 PRELHS Code

The PRELHS code v2.40 was used in CRA-2014 PA calculations and code v2.41 was a product of the migration to the Solaris system. Code v2.42 was created to include new command line arguments that aide in informal (not production) runs of the code (WIPP PA 2015a). Code v2.43 was created to correct an error in retrieving non-zero analysis revisions (WIPP PA 2015b). Finally, code v2.44 was created as a recompilation with new compile options that support running the code on all Solaris cluster nodes (WIPP PA 2016a). For the CRA-2019 PA, PRELHS code v.2.44 was used.

1.1.8.2 LHS Code

In the case of the LHS code, the migration process also included incorporation of functionality from the LHS_EDIT code. For the CRA-2014 PA, the LHS_EDIT utility code v1.0 was used to post-process LHS files created by LHS code v2.42 to impose conditional relationships between pairs of variables for the case where: 1) one variable was restricted to having values less than or equal to the other "controlling" variable; and 2) the restricted, or conditioned, variable has a uniform distribution. Additionally, the port of the LHS code to the Solaris system included a modification of the code to have some of the output data exported directly to database tables for easier access by analysts (Kirchner 2014).

The LHS code v2.43 was a product of the migration to the Solaris system. The LHS code v2.44 was created later to link to an updated database object library (DB_LIB) and to correct an error in writing very small numbers (≤ E-100) to the results database. For the CRA-2019 PA, LHS code v.2.44 was used, which now includes the functionality of the LHS_EDIT code and thus the LHS_EDIT code is no longer needed.

1.1.8.3 POSTLHS Code

The POSTLHS code is not a necessary part of the parameter sampling process, because the LHS code does the sampling and populates the WIPP PA Parameter Database (ParamDB). However, given its relationship to the LHS code (i.e., that it queries the database for sampled parameter values) and its use in the workflow of various other codes, changes to the POSTLHS code are described here. The POSTLHS code v4.07A was used in CRA-2014 PA calculations and code v4.08 was a product of the migration to the Solaris system. Code v4.09 was created later to link to an updated database object library (DB_LIB) (WIPP PA 2015c). Code v4.10 was created to allow termination of the program with an error message when attempting to retrieve an analysis with no records in the requested database (WIPP PA 2015d). Finally, code v4.11 was created as a recompilation with new compile options that support running the code on all Solaris cluster nodes (WIPP PA 2016b). For the CRA-2019 PA, POSTLHS code v.4.11 was used.

This page intentionally left blank.

2.0 CONCEPTUAL APPROACH FOR THE CRA-2019 PA

No changes have been made to the conceptualization of parameter sampling since the CRA-2014 PA. Under the standard approach, a determination is first made as to which parameters are epistemically uncertain and parameter distributions are defined for those parameters and entered into the WIPP PA Parameter Database (ParamDB) (Kim and Feng 2019). Uncertain parameters are sampled from these defined distributions using a Latin Hypercube sampling design. Care is taken to ensure that distributions that have not changed since the CRA-2014 PA are sampled identically as was done for CRA-2014 PA calculations. Three sets ("replicates") of 100 samples each are assembled for use in PA calculations performed by various PA codes. The LHS code is used to perform the sampling and populate database tables from which sampled values may be accessed.

This page intentionally left blank.

3.0 PARAMETER SAMPLING METHODOLOGY

The LHS code is used to sample the distributions of parameters having epistemic uncertainty using a Latin Hypercube sampling design (WIPP PA 2005). Epistemic uncertainty represents lack of knowledge about parameters that are considered constants and hence represents a distribution of confidence rather than of variability. Sampled parameters are written to the WIPP PA Results Database (PA_Results) for use by other WIPP PA codes.

However, the LHS code is also used to sample variables that represent model uncertainty rather than parameter uncertainty. In two cases (SOLMOD3:SOLVAR and SOLMOD4:SOLVAR), LHS samples distributions that represent prediction error due to imperfectly known thermodynamic data (logarithm of observed/predicted) in the aqueous speciation code EQ3/6 v.8a as the uncertainty on solubility projections (Domski 2019b). These two parameters are sampled to account for uncertainty in the solubility of the +III and +IV actinides. The S_MB139:RELPMOD parameter is used to select one of two relative permeability models for use in anhydrite. The WAS_AREA:PROBDEG parameter is the probability of biodegradation of plastics and rubber and takes on only one of two values, either 1 for microbial degradation of cellulose only or 2 for microbial degradation of cellulose, plastic and rubber.

The PRELHS code is run prior to the LHS code and is used to obtain from the WIPP Parameter Database (ParamDB) the data describing the distributions and to create an input file for the LHS code based on that data. PRELHS Version 2.44 was used in CRA-2019 PA calculations. A user-created input file for PRELHS specifies which parameters are to be sampled using their "material" and "property" identifiers. PRELHS performs limited error checking on the data extracted from the database.

The LHS code can reorder sampled data to induce or restrict correlations among the parameters based on specified correlation relationships. The LHS code generates a correlation matrix that can be used to help identify correlations among sampled parameters. Additionally, other conditional relationships may be user-specified. These conditional relationships restrict the value for one parameter to be less than or equal to the sampled value of another parameter. For CRA-2014 calculations, this conditional relationship was enforced using the utility LHS_EDIT v1.0 to modify the output file generated by LHS—for CRA-2019 calculations, this capability is available via the LHS code itself, so a separate LHS_EDIT code is not necessary and no longer used (Section 1.1.8.2).

This report documents the use of PRELHS Version 2.44 and LHS Version 2.44 to provide three sets of sampled data for use in the CRA-2019 PA (Zeitler 2019a). These three sets represent three replicates of one hundred samples for each of 75 variables. Sixty-four of these variables are associated with model parameters (Table 1). However, there are also 11 "placeholder" variables sampled. These placeholders are included to enable users to add additional parameters and run LHS while preserving the ability to regenerate the values previously sampled for the model parameters. The ability to regenerate values previously sampled (e.g., for the CRA-2014 PA calculations) is also ensured by maintaining identical values of random seeds in the PRELHS input files. This approach enables comparison of CRA-2019 and CRA-2014 PA results on a vector-by-vector basis.

3.1 Parameters Sampled for the CRA-2019 PA

The 64 parameters listed in Table 1 are sampled for the CRA-2019 PA. In CRA-2014 PA calculations, 63 parameters were sampled; the parameters GLOBAL:GDEPFAC and STEEL:HUMCORR are new to LHS sampling for the CRA-2019 PA and the PHUMOX3:PHUMCIM parameter, which was sampled for the CRA-2014 PA, is not sampled.

Table 1 – Parameters Sampled by LHS for the CRA-2019 PA

Parameter	Description
AM+3:MKD_AM	Americium III, matrix partition coefficient for americium
BH_SAND:PRMX_LOG	Borehole filled with silty sand, log of intrinsic permeability, x-direction
BOREHOLE:DOMEGA	Borehole and fill, drill string angular velocity (0)
BOREHOLE:TAUFAIL	Borehole and fill, effective shear strength for erosion
CASTILER:COMP_RCK	Castile brine reservoir, bulk compressibility
CASTILER:PRESSURE	Castile brine reservoir, brine far-field pore pressure
CASTILER:PRMX_LOG	Castile brine reservoir, log of intrinsic permeability, x-direction
CONC_PLG:PRMX_LOG	Concrete plug, surface and rustler, log of intrinsic permeability, x-direction
CULEBRA:APOROS	Culebra member of the rustler formation, Culebra advective porosity
CULEBRA:DPOROS	Culebra member of the rustler formation, diffusive porosity for Culebra dolomite
CULEBRA:HMBLKLT	Culebra member of the rustler formation, Culebra half matrix-block length
CULEBRA:MINP_FAC	Culebra member of the rustler formation, mining transmissivity multiplier
DRZ_1:PRMX_LOG	Disturbed rock zone during the time period that begins with facility closure (0 years) and ends when DRZ healing is complete, log of intrinsic permeability, x-direction
DRZ_PCS:PRMX_LOG	DRZ directly above the panel closure system, log of intrinsic permeability, x-direction
GLOBAL:CLIMTIDX	Information that applies globally, climate index
GLOBAL:GDEPFAC	Information that applies globally, energy deposition probability for wetted solid radionuclides
GLOBAL:OXSTAT	Information that applies globally, index for the oxidation state

Parameter	Description
GLOBAL:PBRINE	Information that applies globally, prob. that drilling intrusion in excavated area encounteres pressurized brine
GLOBAL:TRANSIDX	Information that applies globally, index for selecting realizations of the transmissivity field
PCS_T1:PORE_DIS	Panel closure system for an initial time duration, Brooks-Corey pore distribution parameter
PCS_T1:POROSITY	Panel closure system for an initial time duration, effective porosity
PCS_T1:PRMX_LOG	Panel closure system for an initial time duration, log of intrinsic permeability, x-direction
PCS_T1:SAT_RBRN	Panel closure system for an initial time duration, residual brine saturation
PCS_T1:SAT_RGAS	Panel closure system for an initial time duration, residual gas saturation
PCS_T2:POR2PERM	Panel closure system for a secondary time duration, distribution used to calculate permeability from sampled porosity values
PCS_T2:POROSITY	Panel closure system for a secondary time duration, effective porosity
PCS_T3:POROSITY	Run-of-mine panel closure system, tertiary time period, effective porosity
PU+3:MKD_PU	Plutonium III, matrix partition coefficient for plutonium
PU+4:MKD_PU	Plutonium IV, matrix partition coefficient for plutonium
S_HALITE:COMP_RCK	Salado halite, intact, bulk compressibility
S_HALITE:POROSITY	Salado halite, intact, effective porosity
S_HALITE:PRESSURE	Salado halite, intact, brine far-field pore pressure
S_HALITE:PRMX_LOG	Salado halite, intact, log of intrinsic permeability, x-direction
S_MB139:PORE_DIS	Salado marker bed 139, intact and fractured, Brooks-Corey pore distribution parameter
S_MB139:PRMX_LOG	Salado marker bed 139, intact and fractured, log of intrinsic permeability, x-direction
S_MB139:RELP_MOD	Salado marker bed 139, intact and fractured, model number, relative permeability model
S_MB139:SAT_RBRN	Salado marker bed 139, intact and fractured, residual brine saturation

Parameter	Description
SHFTL_T1:PRMX_LOG	Lower portion of simplified shaft from 0 - 200 years, log of intrinsic permeability, x-direction
SHFTL_T2:PRMX_LOG	Lower portion of simplified shaft from 200 - 10,000 years, log of intrinsic permeability, x-direction
SHFTU:PRMX_LOG	Upper portion of simplified shaft, log of intrinsic permeability, x-direction
SHFTU:SAT_RBRN	Upper portion of simplified shaft, residual brine saturation
SHFTU:SAT_RGAS	Upper portion of simplified shaft, residual gas saturation
SOLMOD3:SOLVAR	Oxidation state III model, solubility multiplier
SOLMOD4:SOLVAR	Oxidation state IV model, solubility multiplier
SPALLMOD:PARTDIAM	Material developed for DRSPALL, particle diameter of disaggregated waste
SPALLMOD:REPIPERM	Material developed for DRSPALL, waste permeability to gas local to intrusion borehole
SPALLMOD:REPIPOR	Material developed for DRSPALL, waste porosity at time of drilling intrusion
SPALLMOD:TENSLSTR	Material developed for DRSPALL, tensile strength of waste
STEEL:CORRMCO2	Generic steel in waste, inundated corrosion rate for steel without CO2 present
STEEL:HUMCORR	Generic steel in waste, humid corrosion rate for steel
TH+4:MKD_TH	Thorium IV, matrix partition coefficient for thorium
U+4:MKD_U	Uranium IV, matrix partition coefficient for uranium
U+6:MKD_U	Uranium VI, matrix partition coefficient for uranium
WAS_AREA:BIOGENFC	Waste emplacement area and waste, probability of attaining sampled microbial-gas-generation rates
WAS_AREA:BRUCITEC	Waste emplacement area and waste, MgO inundated hydration rate in ERDA-6 brine
WAS_AREA:BRUCITEH	Waste emplacement area and waste, MgO humid hydration rate
WAS_AREA:BRUCITES	Waste emplacement area and waste, MgO inundated hydration rate in GWB brine
WAS_AREA:GRATMICH	Waste emplacement area and waste, humid biodegradation rate for cellulose

Parameter	Description
WAS_AREA:GRATMICI	Waste emplacement area and waste, inundated biodegradation rate for cellulose
WAS_AREA:HYMAGCON	Waste emplacement area and waste, rate of conversion of hydromagnesite to magnesite
WAS_AREA:PROBDEG	Waste emplacement area and waste, probability of plastics and rubber biodegradation in event of microbial gas generation
WAS_AREA:SAT_RBRN	Waste emplacement area and waste, residual brine saturation
WAS_AREA:SAT_RGAS	Waste emplacement area and waste, residual gas saturation
WAS_AREA:SAT_WICK	Waste emplacement area and waste, index for computing wicking

3.2 Correlation Matrix Assignments

As was done for the CRA-2014 PA, correlations between variables are assigned in two cases. First a correlation of -0.99 is assigned to the correlation between the S_HALITE:PRMX_LOG and S_HALITE:COMP_RCK parameters. Also, a correlation of -0.75 is assigned to the correlation between the CASTILER:PRMX_LOG and CASTILER:COMP_RCK parameters. Rank correlations are calculated for each possible pair of variables and are written to the WIPP PA Results Database (PA_Results); significant correlations are reported in Section 4.3.

3.3 Conditional Relationship Assignments

The LHS code is used to enforce a conditional relationship between three pairs of variables (the LHS_EDIT code used for CRA-2014 calculations is now incorporated into the LHS code—see Section 1.1.8.2). The relationships are WAS_AREA:GRATMICH ≤ WAS_AREA:GRATMICI (Clayton 2008, Nemer and Stein 2005) and PCS_T3: POROSITY ≤ PCS_T2: POROSITY ≤ PCS_T1:POROSITY (Camphouse 2013).

For each pair of variables, the sampled value of the "restricted" variable (i.e., the parameter to the left of the ≤ symbol) is rescaled to the new, conditioned value using the equation:

$$v_i' = \frac{v_i - U_{V,lower}}{U_{V,upper} - U_{V,lower}} \times \left(Min(x_i, U_{V,upper}) - U_{V,lower} \right) + U_{V,lower} \quad (1)$$

Where v'_i is the conditioned value of restricted parameter, v_i is the sampled value of the restricted variable, x_i is the sampled value of the "controlling" variable (i.e., the parameter to the right of the ≤ symbol), and $U_{V,lower}$ and $U_{V,upper}$ are the bounds of the distribution assigned to the restricted variable. This method preserves the probability associated with the value of the restricted variable.

The nature of these correlations is fundamentally different than that which LHS could induce between the variables. LHS achieves correlations between variables by reordering the sampled data whereas the conditional relationship changes the range of the restricted variable. If instead of limiting the value of the restricted variable, an equivalent correlation had been specified between the variables in the input file to LHS, then LHS would have generated values for the restricted variable that could have exceeded the corresponding value for the controlling variable.

3.3.1 MgO Hydration Rates

Humid MgO hydration rates are given by the WAS_AREA:BRUCITEH parameter. Inundated hydration rates are defined by the WAS_AREA:BRUCITEC and WAS_AREA:BRUCITES parameters (BRUCITEC when Castile brine is assumed and BRUCITES when Salado brine is assumed). For a given BRAGFLO or PANEL calculation, only one of the WAS_AREA:BRUCITEC and WAS_AREA:BRUCITES parameters are used. Support for the conditional relationship between the humid and inundated rates for biodegradation of cellulose (i.e., that the humid rate should not be expected to exceed the inundated rate or WAS_AREA:GRATMICH ≤ WAS_AREA:GRATMICI (Clayton 2008, Nemer and Stein 2005)) could potentially be extended to the humid and inundated rates for hydration of MgO (i.e., WAS_AREA:BRUCITEH ≤ WAS_AREA:BRUCITEC and WAS_AREA:BRUCITEH ≤ WAS_AREA:BRUCITES). Because there is no overlap between the BRUCITEH parameter distribution and either of the BRUCITEC or BRUCITES parameter distributions, there is zero probability that a BRUCITEH sampled value could exceed a sampled BRUCITEC or BRUCITES value (Table 2). Therefore, no conditional relationship is enforced between humid and inundated MgO hydration rates.

Table 2 – Comparison of MgO Hydration Rate Distributions

Material:Property	Normal Distribution Limits (mol kg^{-1} sec^{-1})	
	Min	Max
WAS_AREA:BRUCITEH	1.81E-8	2.19E-8
WAS_AREA:BRUCITEC	4.76E-8	5.64E-8
WAS_AREA:BRUCITES	4.27E-8	6.13E-8

3.3.2 Steel Corrosion Rates

Humid steel corrosion rates are given by the STEEL:HUMCORR parameter. Inundated steel corrosion rates are defined by the STEEL:CORRMCO2 parameter. Support for the conditional relationship between the humid and inundated rates for biodegradation of cellulose (i.e., that the humid rate should not be expected to exceed the inundated rate or WAS_AREA:GRATMICH ≤ WAS_AREA:GRATMICI (Clayton 2008, Nemer and Stein 2005)) could potentially be extended to the humid and inundated rates for corrosion of steel (i.e., STEEL:HUMCORR ≤ STEEL:CORRMCO2). However, the algorithm used to control conditional relationships in the LHS code (Equation 1) is only applicable to uniform distributions of the restricted value and the distribution defined for the STEEL:HUMCORR distribution is a cumulative distribution. Therefore, a conditional relationship between STEEL:HUMCORR and STEEL:CORRMCO2 was not enforced in CRA-2109 PA calculations.

However, there is only a small overlap in the defined distributions for the two rates and thus only a small probability of the humid rate exceeding the inundated rate (Figure 1). As a result, the humid steel corrosion exceeds the inundated rate in only one case out of the 300 sampled pairs (Replicate 3, Vector 42)—in that case, the humid rate is 4.51E-16 m/s and the inundated rate is 1.39E-16 m/s. Because a conditional relationship was not enforced, the humid rate of steel corrosion is higher than it would have been had a conditional relationship been enforced.

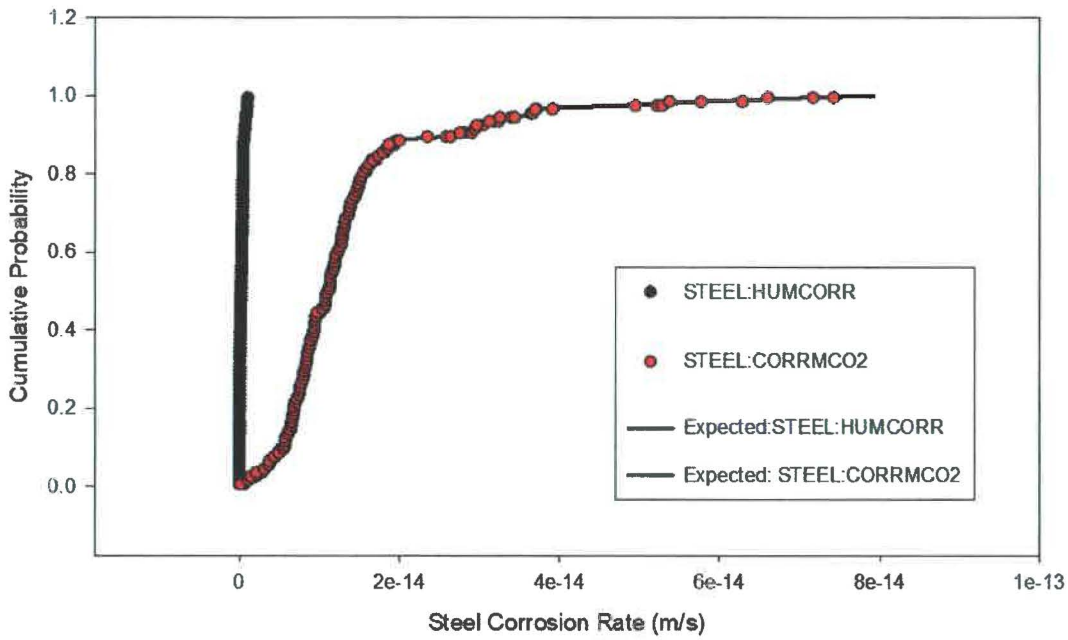

Figure 1 – Comparison of STEEL:HUMCORR and STEEL:CORRMCO2 Distributions for the CRA-2019 PA.

3.4 Student vs. Normal Distribution for MgO Hydration Rates

The parameters WAS_AREA:BRUCITEC, WAS_AREA:BRUCITEH and WAS_AREA:BRUCITES, which represent MgO hydration rates, were once treated as constants but were assigned distributions for the CRA14 analysis (Kirchner 2013). As described by Clayton (2013) and Kirchner (2013), the distribution of uncertainty on these parameters should be a Student-t distribution because the parameters represent the slopes of lines from linear regressions. However, at that time, the Student distribution of LHS could not be parameterized using a mean, standard error, and degrees of freedom and so a normal distribution was substituted.

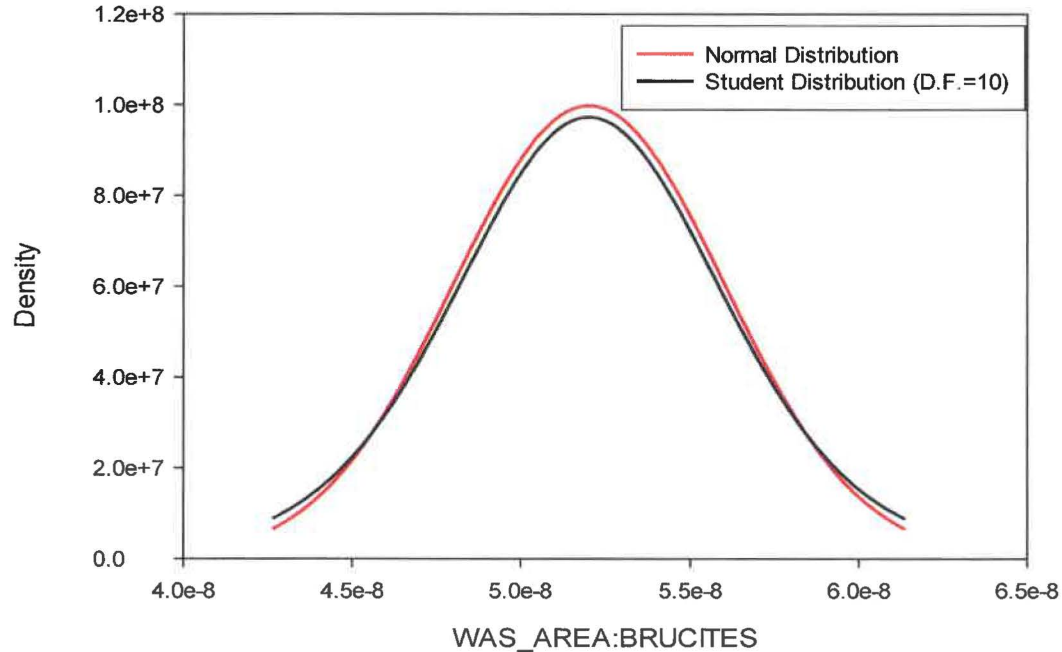

Figure 2 – Difference Between a Normal and Student-t Distribution (d.f. = 10; from Kirchner (2013)).

Figure 2 represents the WAS_AREA:BRUCITES distribution which, having the fewest degrees of freedom of the three parameters, shows the greatest difference between the Student and normal distributions. As shown in Figure 2 and stated by Kirchner (2013), the differences between the normal and Student distributions are inconsequential. Kirchner (2013) also noted that the LHS code would be modified to accommodate a Student distribution defined by a mean, standard error, and degrees of freedom. As part of the code migration to the Solaris system, the capability to handle such a Student distribution was added to PRELHS v2.41 and LHS v2.43. However, the MgO hydration rate parameters have not been redefined in the WIPP PA Parameter Database (ParamDB), so a normal distribution identical to the one used for the CRA14 analysis was used for the CRA19 analysis.

3.5 Run Control

A full description of the run control for the CRA19 analysis, including names and locations of input and output files, can be found in Long (2019). As outlined in AP-181 (Zeitler 2019a), in cases where comparisons are made to the CRA-2014 PA results, the CRA14 (Rev. 2) results from the Solaris migration integration tests are used (Kirchner et al. 2014, Kirchner et al. 2015)—for LHS sampled values, these CRA14 (Rev. 2) results are the same as the CRA14 (Rev. 0) values (Kirchner (2013) and Long (2013)).

3.5.1 PRELHS Input and Output Files

AP-181 specifies that three replicates be run for the CRA19 analysis. The input files for PRELHS for the CRA19 analysis are named lhs1_CRA19_r1_con.inp, lhs1_CRA19_r2_con.inp, and lhs1_CRA19_r3_con.inp, respectively for replicates 1 to 3. Except for the title, internal comments, and random seed value, these three files are identical. Different random seeds are assigned in each input file to cause LHS to generate three unique sets of values. The random seeds used were identical to those used in the CRA-2014 PA, as specified in AP-181. This sampling design facilitates the comparison of results from one analysis to the next by ensuring that identically numbered vectors have, to the greatest extent possible, the same collection of parameter values.

The output "transfer" files for the CRA19 analysis are named lhs1_CRA19_r1_con.trn, lhs1_CRA19_r2_con.trn, and lhs1_CRA19_r3_con.trn, respectively for replicates 1 to 3. The three transfer files are identical except for titles and the random seed values. All input and output files were inspected to verify that the data used to construct the distributions were properly extracted from the WIPP PA Parameter Database (ParamDB).

3.5.2 LHS Output Files

The transfer files created by running the PRELHS code were used as inputs to the LHS calculations. The output files for LHS for the CRA19 analysis are named lhs2_CRA19_r1_con.trn. The sampled values written to the WIPP PA Results Database (PA_Results) by the LHS code were examined for errors. The ranges of the sampled variables were compared to the range specified as input for the distribution (Table 5, Appendix A). No values were found to exceed the specified ranges of the distributions although in a few cases, as was discussed in Kirchner (2013), the range of sampled values was found to cover less than 90% of the specified range (e.g. 77.4 % of the range was covered by the samples for the S_MB139:PRMX_LOG parameter in replicate 3 (Figure 179)). These low coverage cases are in part due to the shape of the distribution; the tails of CDF curves from nonuniform distributions may be nearly horizontal, such that the width of 1 % and 99 % quantiles sampled by LHS are relatively wide. The width of the quantiles (each covering 1 % of the probability) is set by the number of LHS samples in the replicate (100).

This page intentionally left blank.

4.0 RESULTS

Results of parameter sampling are presented in this section for all 64 uncertain parameters. Two parameters are new to LHS sampling analysis for the CRA-2019 PA: GLOBAL:GDEPFAC and STEEL:HUMCORR. Additionally, six other parameters have updated distributions since the CRA-2014 PA: GLOBAL:PBRINE, STEEL:CORRMCO2, BOREHOLE:TAUFAIL, WAS_AREA:HYMAGCON, SOLMOD3:SOLVAR, and SOLMOD4:SOLVAR.

4.1 Parameters New to Parameter Sampling for the CRA-2019 PA

There are two parameters sampled as part of the CRA19 analysis that were not sampled as part of the CRA14 analysis, the GLOBAL:GDEPFAC and STEEL:HUMCORR parameters. Their input distributions and sampled values are discussed below.

4.1.1 GLOBAL:GDEPFAC

The GLOBAL:GDEPFAC parameter is new to WIPP PA and is used in the calculation of radiolytic gas generation from brine in BRAGFLO calculations. For the CRA-2019 PA, it has been assigned a uniform distribution from 0 to 0.5 (unitless). Comparison of all sampled values against the expected distribution is shown in Figure 3. Comparisons on a replicate basis are shown in Figure 32, Figure 96, and Figure 160.

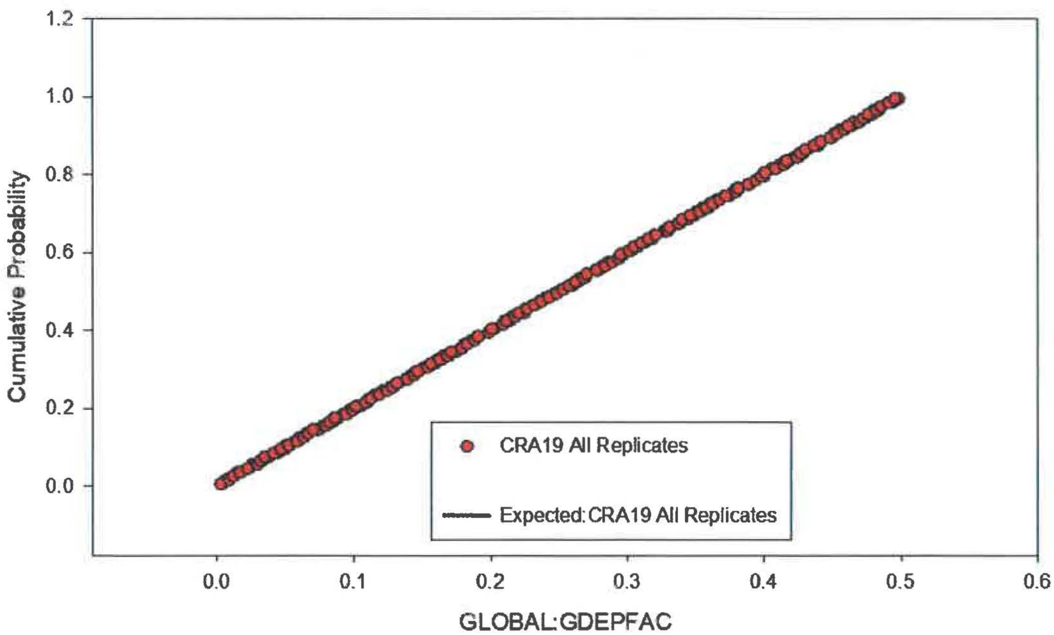

Figure 3 – Observed and Expected CDFs for GLOBAL:GDEPFAC (Uniform Distribution), All Replicates

4.1.2 STEEL:HUMCORR

A constant value of zero for the STEEL:HUMCORR parameter has previously been used in the calculation of gas generation due to steel corrosion in BRAGFLO calculations. For the CRA-2019 PA, it has been assigned a cumulative distribution with range from 0 to 1.03E-15 m/s. Comparison of all sampled values against the expected distribution is shown in Figure 4. Comparisons on a replicate basis are shown in Figure 66, Figure 130, and Figure 194.

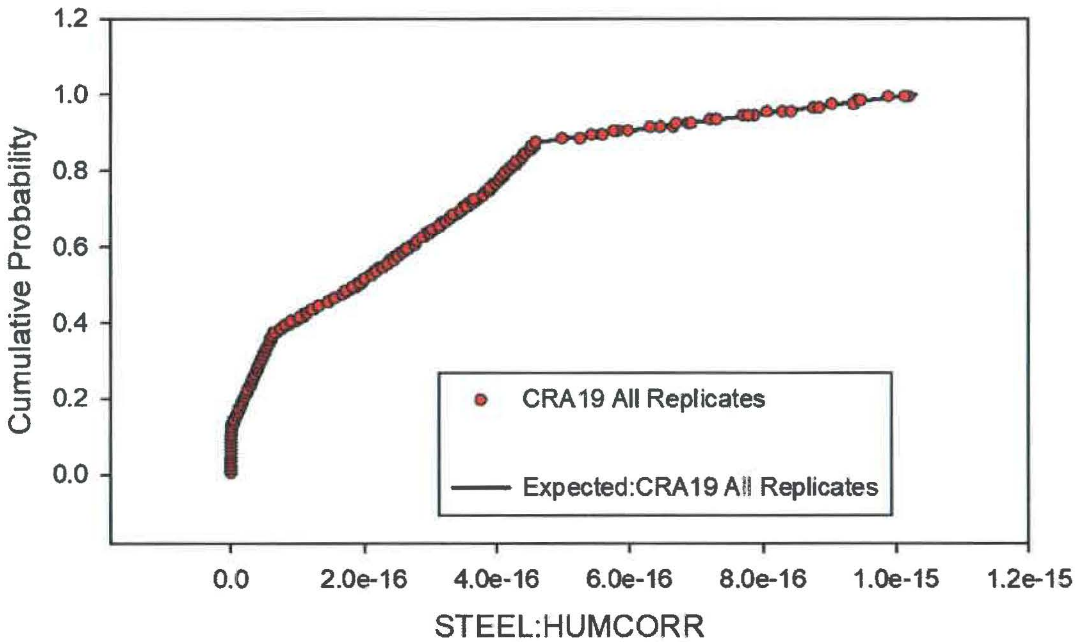

Figure 4 – Observed and Expected CDFs for STEEL:HUMCORR (Cumulative Distribution), All Replicates

4.2 Parameters With Updated Distributions Since the CRA-2014 PA

Parameter distributions for six parameters have changed since the CRA-2014 PA (additionally, the parameter distribution for the PHUMOX3:PHUMCIM parameter has been replaced by a constant value for BRAGFLO and PANEL calculations). Parameter distributions from the CRA19 analysis are compared with those from the CRA14 analysis for the six parameters below. Sampled parameter values for all parameters are tabulated in Kim and Feng (2019).

4.2.1 GLOBAL:PBRINE

The distribution for the GLOBAL:PBRINE parameter has been changed for CRA-2019 PA calculations (Section 1.1.2). Comparison of all sampled values for the CRA19 analyis against the expected distribution is shown in Figure 5, along with the same comparison for the CRA-2014 PA.

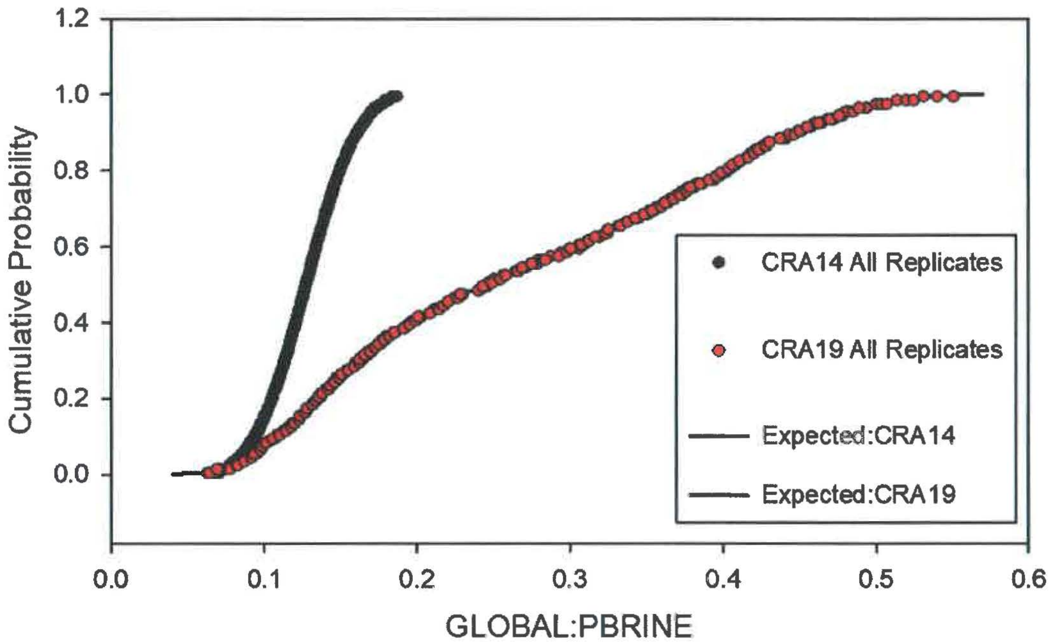

Figure 5 – Observed and Expected CDFs for GLOBAL:PBRINE, All Replicates for CRA14 and CRA19 Analyses

4.2.2 STEEL:CORRMCO2

The distribution for the STEEL:CORRMCO2 parameter has been changed for CRA-2019 PA calculations (Section 1.1.3). Comparison of all sampled values for the CRA19 analsyis against the expected distribution is shown in Figure 6, along with the same comparison for the CRA14 analysis.

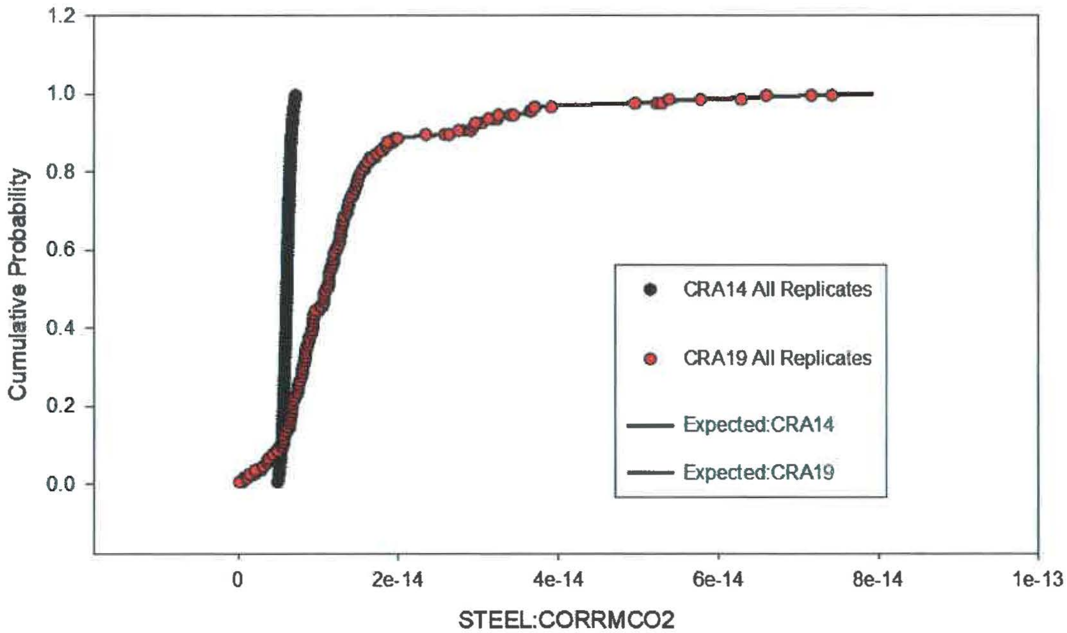

Figure 6 – Observed and Expected CDFs for STEEL:CORRMCO2, All Replicates for CRA14 and CRA19 Analyses

4.2.3 BOREHOLE:TAUFAIL

The distribution for the BOREHOLE:TAUFAIL parameter has been changed for CRA-2019 PA calculations (Section 1.1.4). Comparison of all sampled values for the CRA19 analysis against the expected distribution is shown in Figure 7, along with the same comparison for the CRA14 analysis. The differences between sampled values for the CRA14 and CRA19 analyses are small and not easily discernable from the figure.

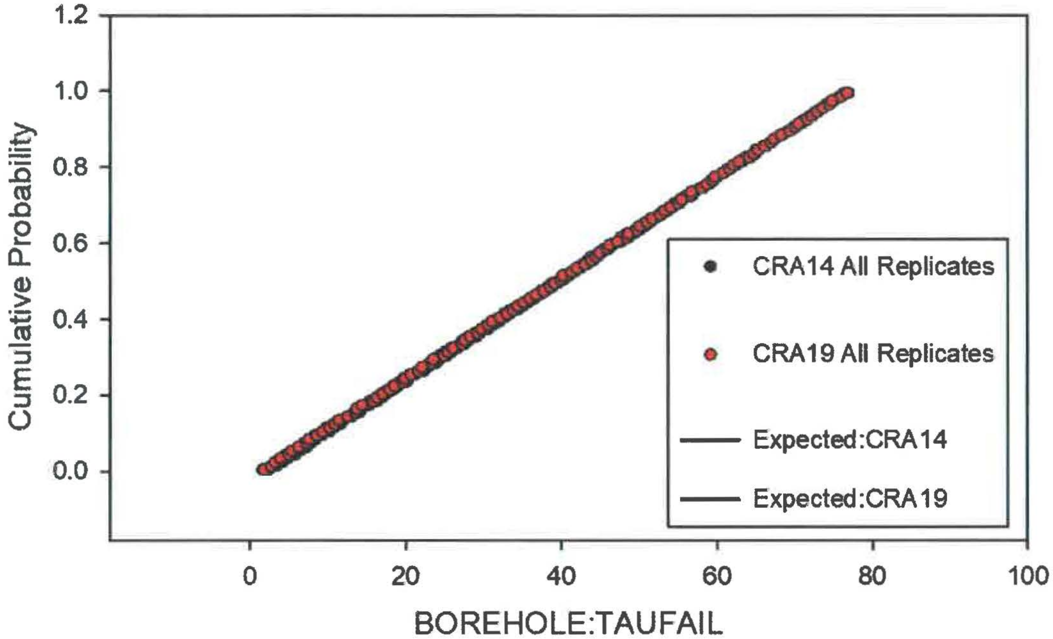

Figure 7 – Observed and Expected CDFs for BOREHOLE:TAUFAIL, All Replicates for CRA14 and CRA19 Analyses

4.2.4 WAS_AREA:HYMAGCON

The distribution for the WAS_AREA:HYMAGCON parameter has been changed for CRA-2019 PA calculations (Section 1.1.6). Comparison of all sampled values for the CRA19 analysis against the expected distribution is shown in Figure 8, along with the same comparison for the CRA14 analysis.

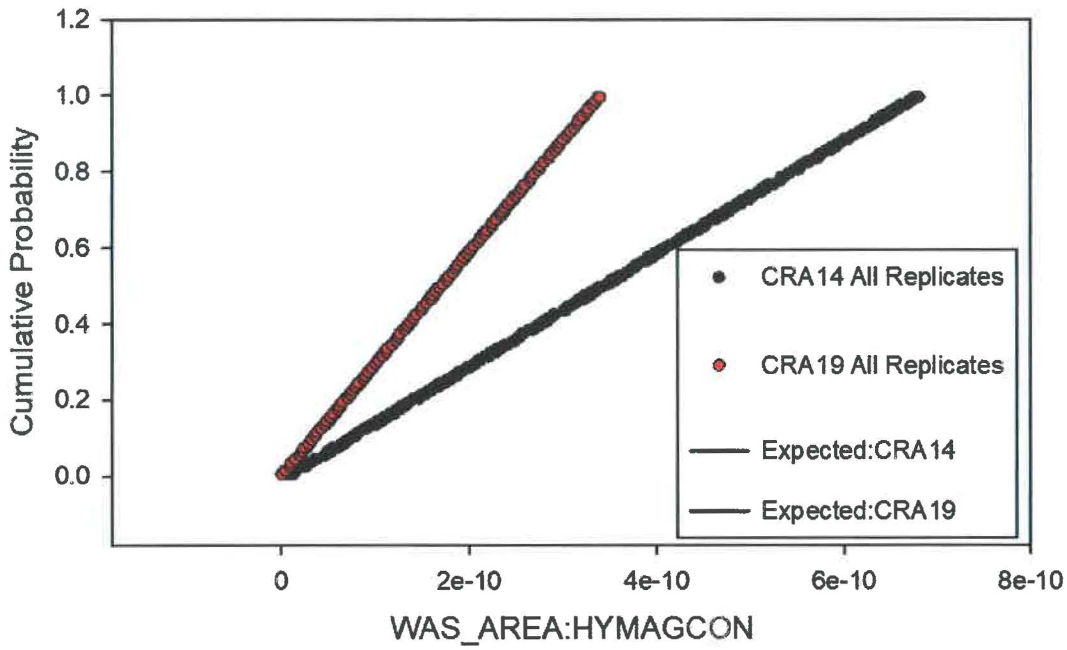

Figure 8 – Observed and Expected CDFs for WAS_AREA:HYMAGCON, All Replicates for CRA14 and CRA19 Analyses

4.2.5 SOLMOD3:SOLVAR

The distribution for the SOLMOD3:SOLVAR parameter has been changed for CRA-2019 PA calculations (Section 1.1.7). Comparison of all sampled values for the CRA19 analysis against the expected distribution is shown in Figure 9, along with the same comparison for the CRA-2014 PA.

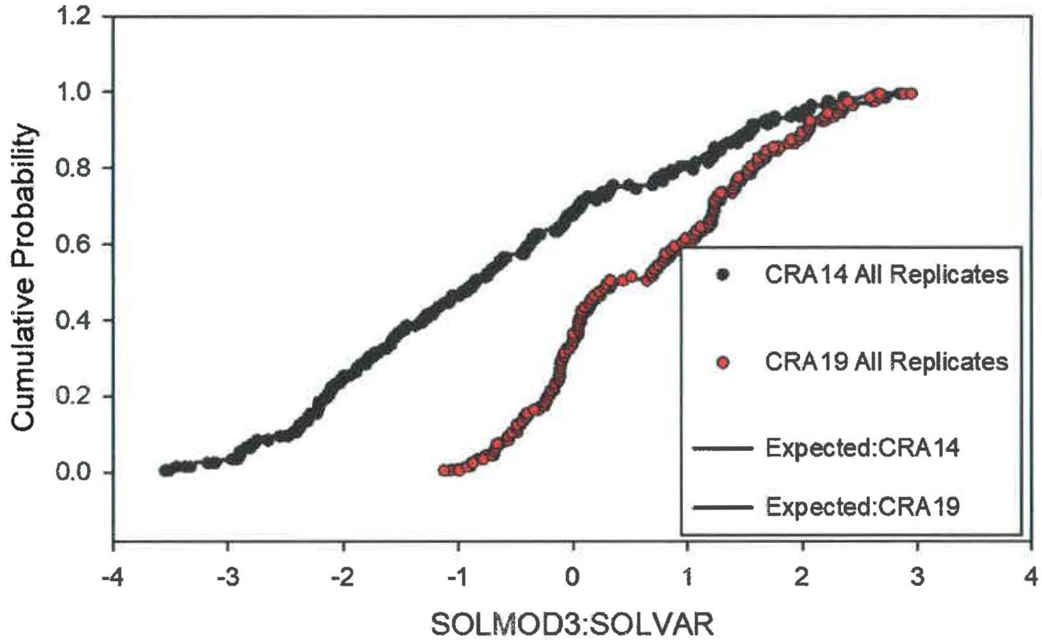

Figure 9 – Observed and Expected CDFs for SOLMOD3:SOLVAR, All Replicates for CRA14 and CRA19 Analyses

4.2.6 SOLMOD4:SOLVAR

The distribution for the SOLMOD4:SOLVAR parameter has been changed for CRA-2019 PA calculations (Section 1.1.7). Comparison of all sampled values for the CRA19 analyis against the expected distribution is shown in Figure 10, along with the same comparison for the CRA-2014 PA.

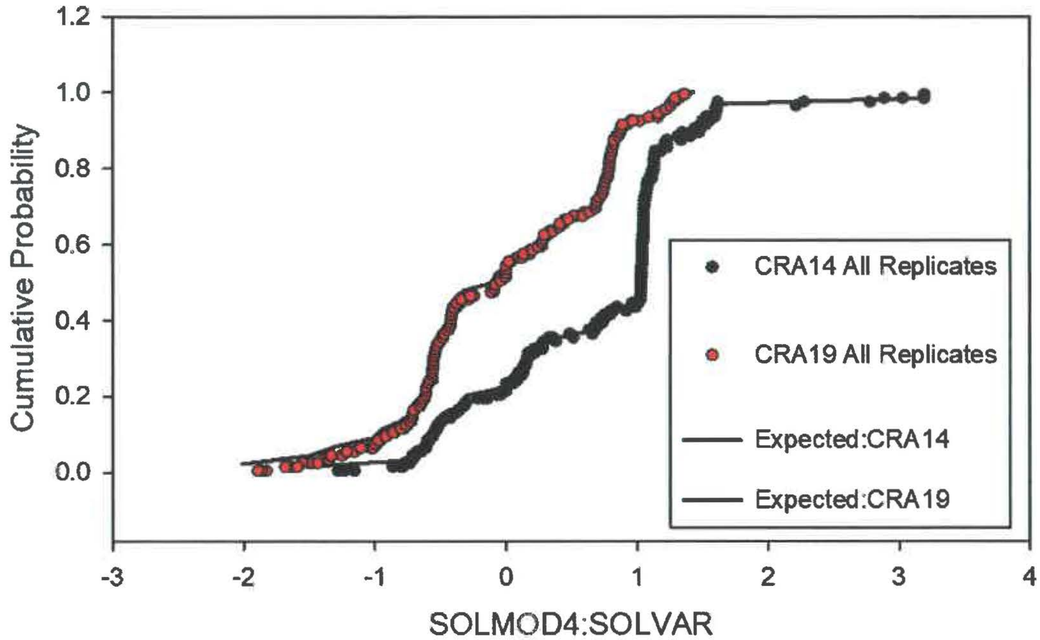

Figure 10 – Observed and Expected CDFs for SOLMOD4:SOLVAR, All Replicates for CRA14 and CRA19 Analyses

4.3 Calculated Correlations Between Variables

Rank correlations between pairs of sampled variables (i.e., the strength of a linear association between the sampled values) are written directly to the WIPP PA Results Database (PA_Results) and are also found in the LHS output file (e.g., lhs2_CRA19_r1_con.trn) and the correlations output file (e.g., lhs2_CRA19_r1_con.trn_CORR) for each replicate. The rank correlations in the WIPP PA Results Database (PA_Results) were examined and those that exceeded specified test statistics are noted in Table 3.[1]

The rankings of sampled data for those variables for which a correlation relationship was assigned showed correlations that were close to those specified. Positive, significant correlations were also observed between the WAS_AREA:GRATMICH and WAS_AREA:GRATMICI parameters in all replicates, which is a result of the assigned conditional relationship (Section 3.3). No significant (at the $\alpha = 0.01$ significance level; α is the probability of a Type I error, or the probability of rejecting a null hypothesis when it is in fact true) spurious correlations were observed among the uncorrelated variables, although in replicate 2 the correlation between the ranks of the variables CASTILER:PRESSURE and WAS_AREA:PROBDEG was -0.234 which is significant at the $\alpha = 0.05$ level. However, the WAS_AREA:PROBDEG parameter is a

[1] A test statistic of 0.195 was used to determine the $\alpha = 0.05$ level of significance and a test statistic of 0.254 was used for the $\alpha = 0.01$ level of significance. These are the same values used by Kirchner (2013) and are appropriate for a sample size of 100.

discrete user-specified distribution (delta distribution) having only 2 possible values (Figure 77). This restriction limits the ability of LHS to rearrange the sampled values to enforce a correlation near zero. In addition, the significance test on the correlation coefficient is questionable in any case because the data fails to even come close to meeting the assumptions of normality of the data (Kirchner 2013).

To evaluate the frequency with which high correlation coefficients would be expected in such variables, a test was conducted by Kirchner (2009), the results of which continue to be valid as no new correlations have been specified for the CRA-2019 PA. In the test, 1000 LHS samples were generated and the correlation coefficients were tabulated. For this test, all correlations were specified to be zero. Out of the 1000 samples, "significant" correlations were generated in 502 cases at the $\alpha = 0.05$ level and 2 cases at the $\alpha = 0.01$ level. All of these correlations involved either the WAS_AREA:PROBDEG or S_MB139:RELP_MOD parameters, both of which have discrete distributions having only two possible values. These results suggest that the number of values exceeding the standard test statistics for correlation coefficients may be relatively high when LHS samples discrete distributions having few possible values.

Table 3 – Significant Correlations Between Parameters

Rep	Parameters in Comparison (Mat:Prop)		Exp. Corr.	Obs. Corr.	Signif[a]
1	S_HALITE:COMP_RCK	S_HALITE:PRMX_LOG	-0.99	-0.9869	**
	WAS_AREA:GRATMICH	WAS_AREA:GRATMICI	0.00	0.7347	**[b]
	CASTILER:COMP_RCK	CASTILER:PRMX_LOG	-0.75	-0.7281	**
2	S_HALITE:COMP_RCK	S_HALITE:PRMX_LOG	-0.99	-0.9907	**
	CASTILER:COMP_RCK	CASTILER:PRMX_LOG	-0.75	-0.7242	**
	WAS_AREA:GRATMICH	WAS_AREA:GRATMICI	0.00	0.6920	**[b]
	CASTILER:PRESSURE	WAS_AREA:PROBDEG	0.00	-0.2340	*[c]
3	S_HALITE:COMP_RCK	S_HALITE:PRMX_LOG	-0.99	-0.9834	**
	WAS_AREA:GRATMICH	WAS_AREA:GRATMICI	0.00	0.7604	**[b]
	CASTILER:COMP_RCK	CASTILER:PRMX_LOG	-0.75	-0.7252	**
	PCS_T3:POROSITY	PCS_T2:POROSITY	0.00	0.2711	**[b]

[a]Significance level (see text): * = Significant at $p<0.05$, ** = Significant at $p<0.01$

[b]No correlation specified, but conditional relationship assigned (Section 3.3)

[c]This correlation is spurious.

4.4 Parameters With Conditional Relationships

As was done for the CRA-2014 PA, conditional relationships were imposed for three variables in the CRA-2019 PA. The CDFs for the original sampled values and the conditioned values are shown in Figure 11, Figure 13, and Figure 15 of Section 4.4 for the WAS_AREA:GRATMICH, PCS_T2:POROSITY, and PCS_T3:POROSITY parameters, respectively. The correlations between variables involved in conditional relationships are shown in Table 4.

Table 4 – Correlations Between Parameters With Conditional Relationships

Rep	Parameters in Comparison (Mat:Prop)		Observed Correlation
1	WAS_AREA:GRATMICH	WAS_AREA:GRATMICI	0.7347
	PCS_T2:POROSITY	PCS_T1:POROSITY	-0.0506
	PCS_T3:POROSITY	PCS_T2:POROSITY	0.1227
2	WAS_AREA:GRATMICH	WAS_AREA:GRATMICI	0.6920
	PCS_T2:POROSITY	PCS_T1:POROSITY	-0.0161
	PCS_T3:POROSITY	PCS_T2:POROSITY	0.1833
3	WAS_AREA:GRATMICH	WAS_AREA:GRATMICI	0.7604
	PCS_T2:POROSITY	PCS_T1:POROSITY	-0.0143
	PCS_T3:POROSITY	PCS_T2:POROSITY	0.2711

4.4.1 WAS_AREA:GRATMICH

As was done for the CRA-2014 PA, the conditional relationship WAS_AREA:GRATMICH ≤ WAS_AREA:GRATMICI has been imposed for the CRA-2019 PA, which ensures that the humid rate of cellulose degradation does not exceed the inundated rate by adjusting the sampled value of WAS_AREA:GRATMICH, if necessary. The values used in the CRA19 analysis are input into the WIPP PA Results Database (PA_Results), while values sampled prior to conditioning are only available in the LHS output debug file (lhs2_CRA19_r1_con.dbg for Replicate 1). A comparison of the values for WAS_AREA:GRATMICH prior to conditioning with those used in the CRA19 analysis for all replicates is shown in Figure 11. All values are identical to those for the CRA-2014 PA. The correlation between the two variables as a result of the applied conditional relationship is shown in Figure 12. Relatively strong correlations of 0.73, 0.69, and 0.76 were calculated for replicates 1, 2, and 3.

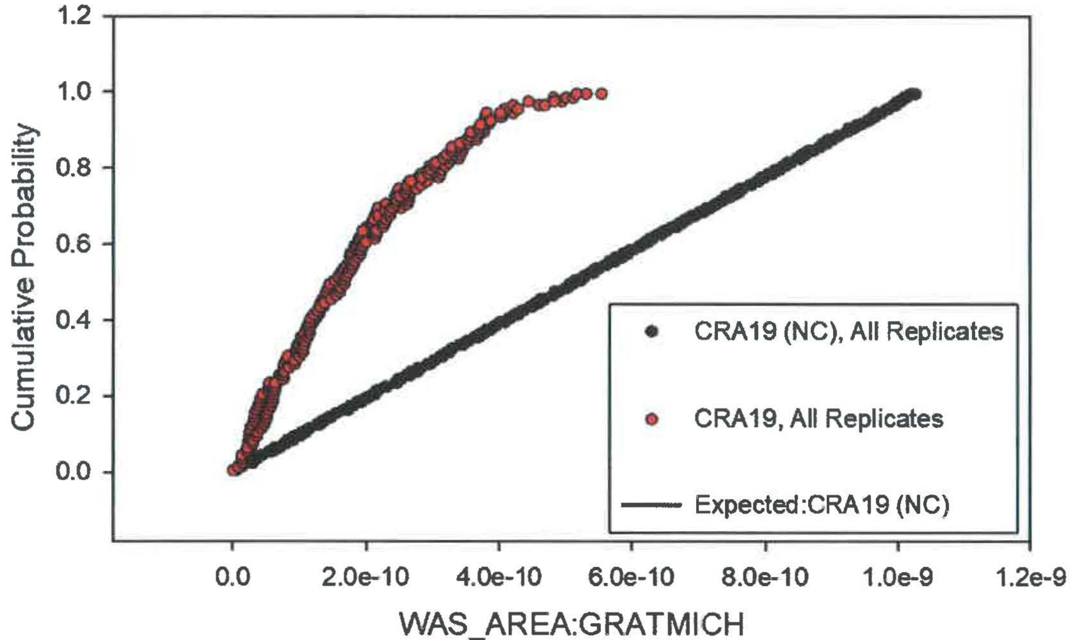

Figure 11 – Observed and Expected CDFs for WAS_AREA:GRATMICH Including Data Prior to Conditioning (NC)

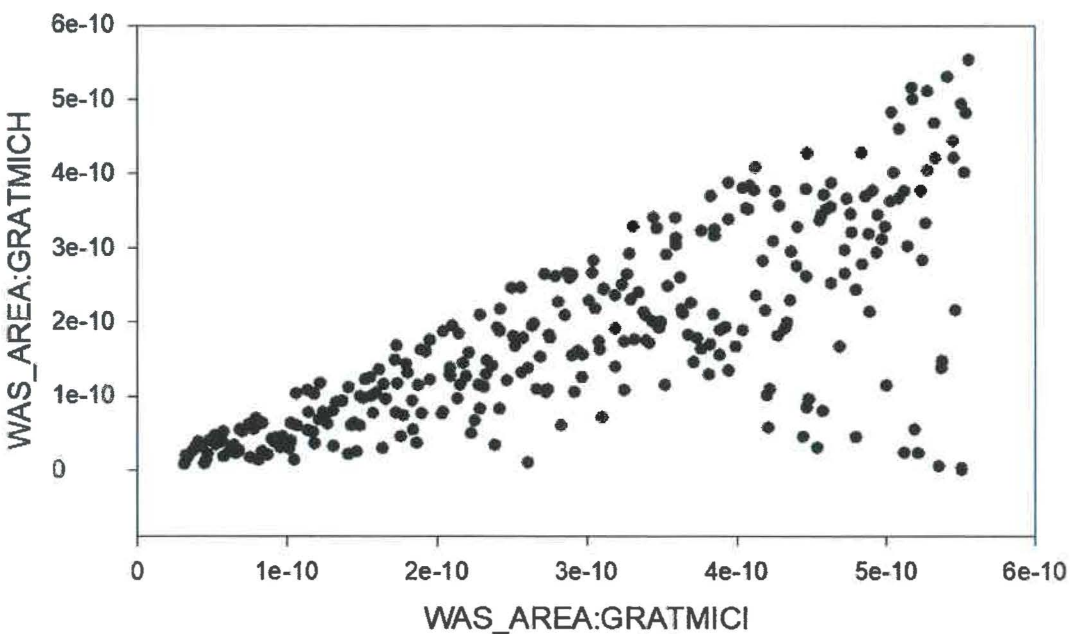

Figure 12 – Correlation Between WAS_AREA:GRATMICI and WAS_AREA:GRATMICH, All Replicates

4.4.2 PCS_T2:POROSITY

As was done for the CRA-2014 PA, the conditional relationship PCS_T2:POROSITY ≤ PCS_T1:POROSITY has been imposed for the CRA-2019 PA, which ensures that the panel closure porosity decreases with time by adjusting the sampled value of PCS_T2:POROSITY, if necessary. The values used in the CRA19 analysis are input into the WIPP PA Results Database (PA_Results), while values sampled prior to conditioning are only available in the LHS output debug file (lhs2_CRA19_r1_con.dbg for Replicate 1). A comparison of the values for PCS_T2:POROSITY prior to conditioning with those used in the CRA19 analysis for all replicates is shown in Figure 13. In only a few cases was the conditional relationship applied; therefore, the differences between values prior to and subsequent to conditioning are relatively rare and not easily discernable from the figure. All values are identical to those for the CRA-2014 PA. The correlation between the two variables as a result of the applied conditional relationship is shown in Figure 12. Relatively weak correlations of -0.05, -0.02, and -0.01 were calculated for replicates 1, 2, and 3.

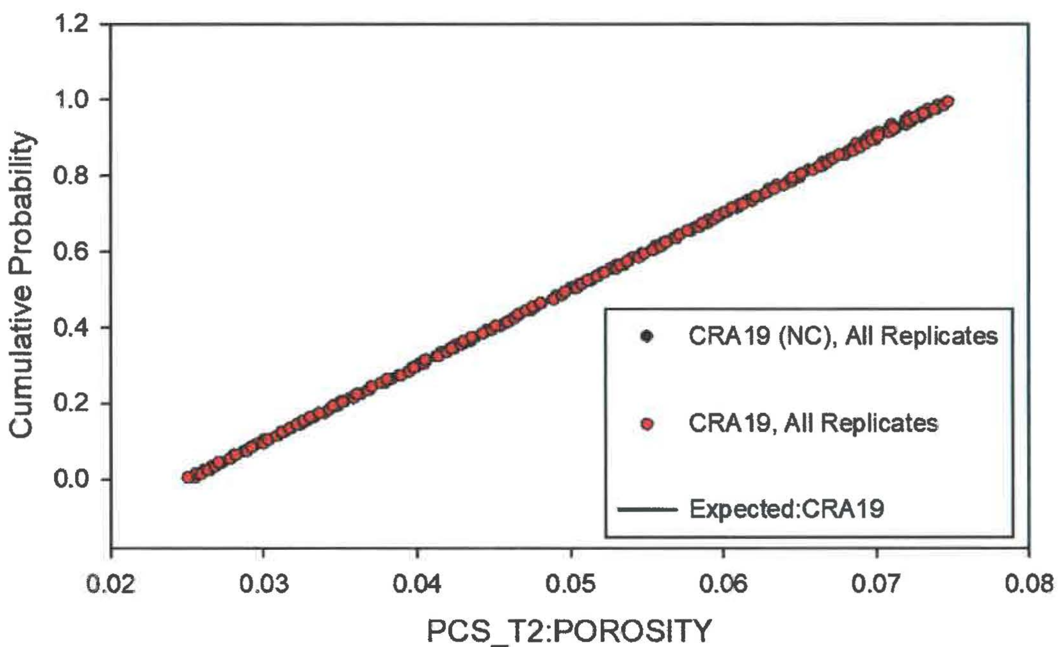

Figure 13 – Observed and Expected CDFs for PCS_T2:POROSITY Including Data Prior to Conditioning (NC)

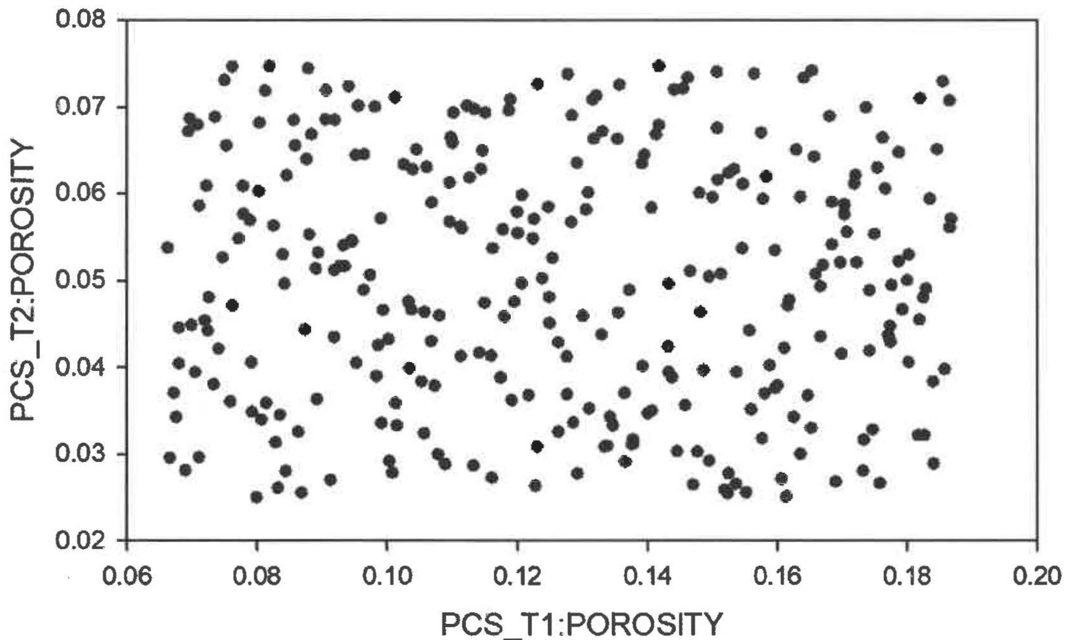

Figure 14 – Correlation Between PCS_T1:POROSITY and PCS_T2:POROSITY, All Replicates

4.4.3 PCS_T3:POROSITY

As was done for the CRA-2014 PA, the conditional relationship PCS_T3:POROSITY ≤ PCS_T2:POROSITY has been imposed for the CRA-2019 PA, which ensures that the panel closure porosity decreases with time by adjusting the sampled value of PCS_T3:POROSITY, if necessary. The values used in the CRA19 analysis are input into the WIPP PA Results Database (PA_Results), while values sampled prior to conditioning are only available in the LHS output debug file (lhs2_CRA19_r1_con.dbg for Replicate 1). A comparison of the values for PCS_T3:POROSITY prior to conditioning with those used in the CRA19 analysis for all replicates is shown in Figure 15. All values are identical to those for the CRA-2014 PA. The correlation between the two variables as a result of the applied conditional relationship is shown in Figure 12. Relatively weak correlations of 0.12, 0.18, and 0.27 were calculated for replicates 1, 2, and 3.

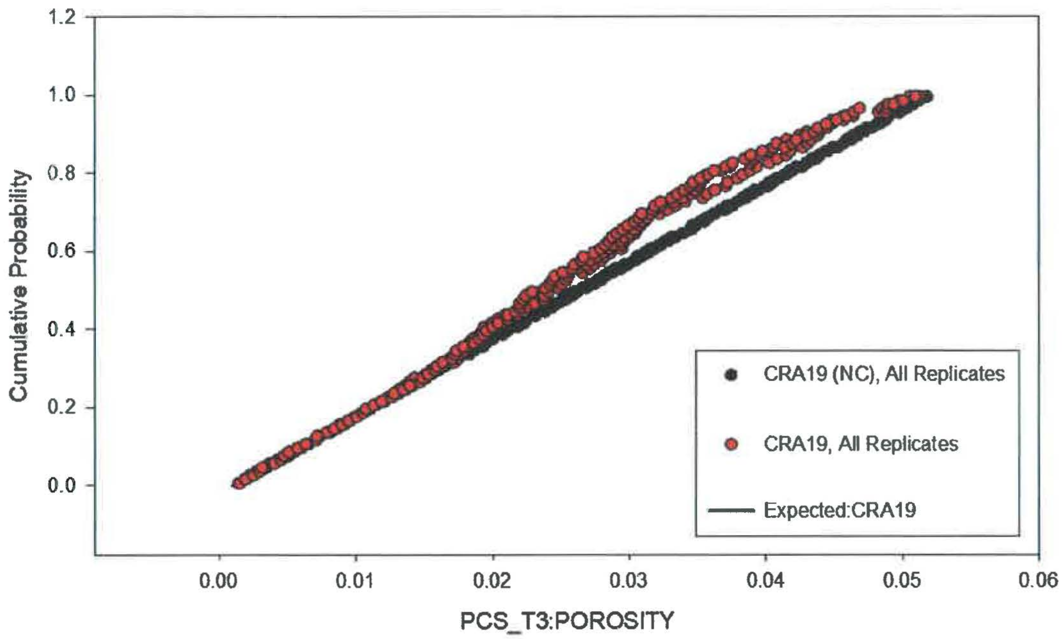

Figure 15 – Observed and Expected CDFs for PCS_T3:POROSITY Including Data Prior to Conditioning (NC)

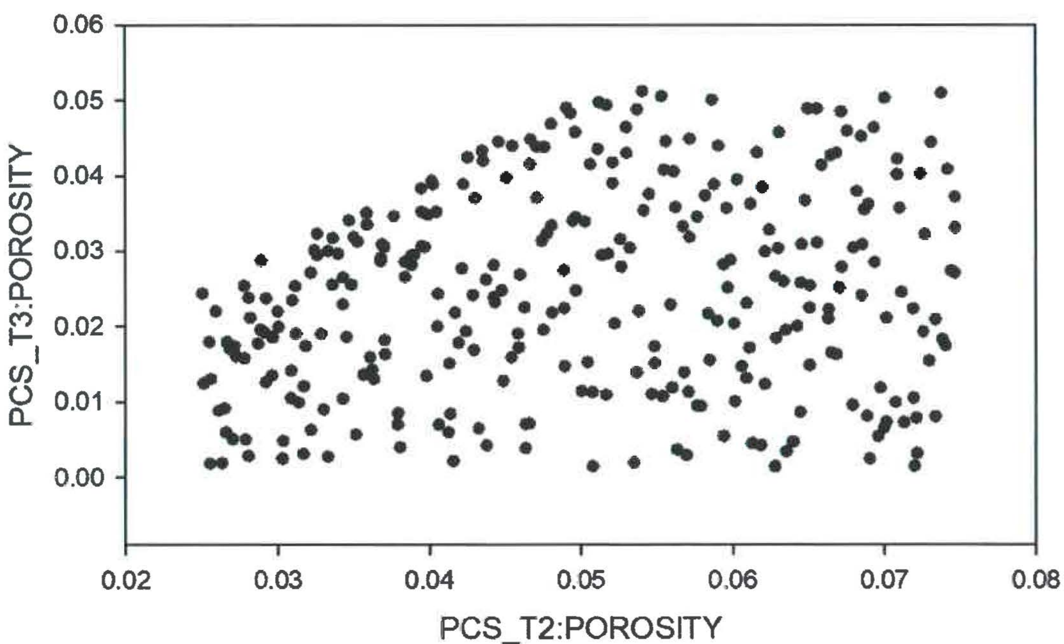

Figure 16 – Correlation Between PCS_T2:POROSITY and PCS_T3:POROSITY, All Replicates

4.5 Sampled CDF Comparisons to Input Distributions

In this section, sampled distributions are compared to the expected distributions. Cumulative distribution functions (CDFs) for the sampled data were constructed by ordering the data from smallest to largest value and assigning the probability *i*/100-0.005 to the *i*th ordered value (i.e. the midpoint of the interval containing the value based on order statistics). With the exception of the variables modified based on assigned conditional relationships (Section 4.4), the differences between the CDFs of the sampled values and the CDFs of the expected distributions are due to the differences between the estimated probability assigned to the values and the true probability associated with the data.

Comparisons between the sampled parameters and input distributions ("expected distributions") for all 64 sampled parameters are found in the CDFs plotted from Figure 17 through Figure 208. Figure 17 through Figure 80 show comparisons for Replicate 1, Figure 81 through Figure 144 show comparisons for Replicate 2, and Figure 145 through Figure 208 show comparisons for Replicate 3. Sampled parameter values for all parameters are tabulated in Kim and Feng (2019).

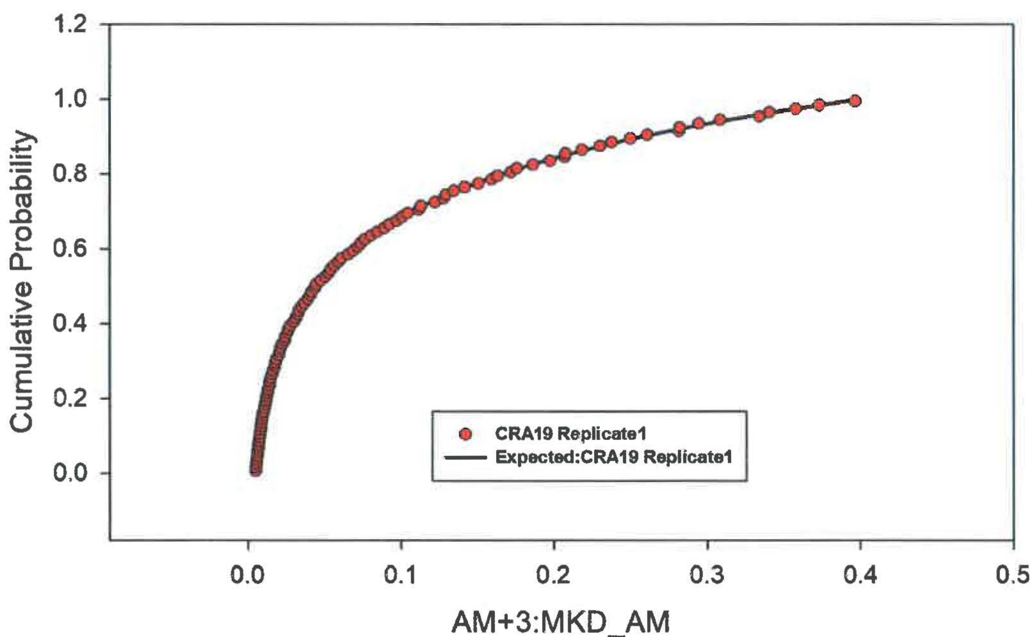

Figure 17 – Observed and Expected CDFs for AM+3:MKD_AM (Loguniform Distribution) Replicate 1.

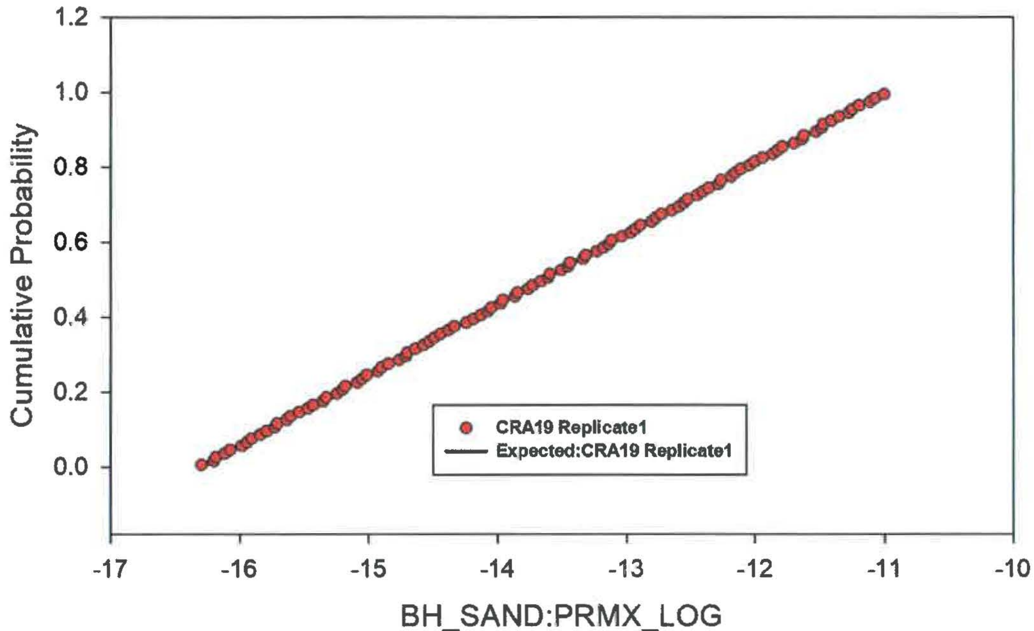

Figure 18 – Observed and Expected CDFs for BH_SAND:PRMX_LOG (Uniform Distribution) Replicate 1.

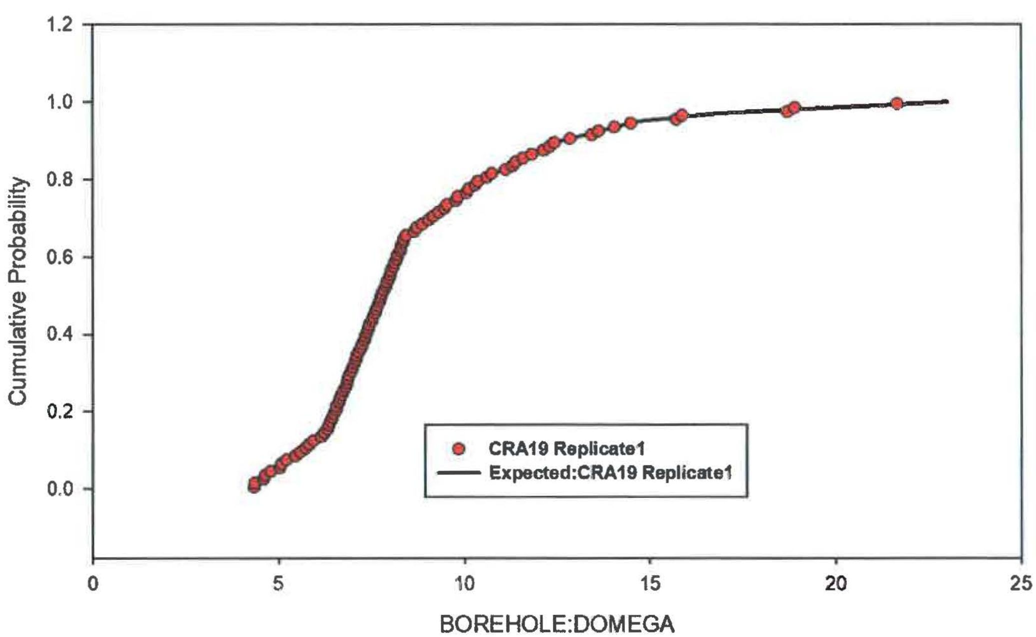

Figure 19 – Observed and Expected CDFs for BOREHOLE:DOMEGA (Cumulative Distribution) Replicate 1.

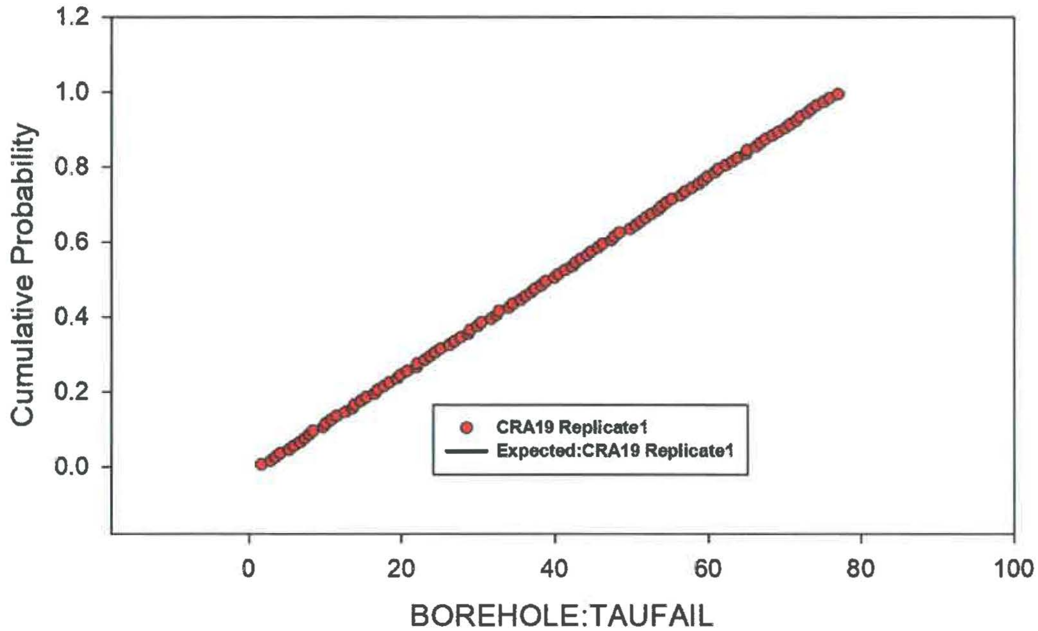

Figure 20 – Observed and Expected CDFs for BOREHOLE:TAUFAIL (Uniform Distribution) Replicate 1.

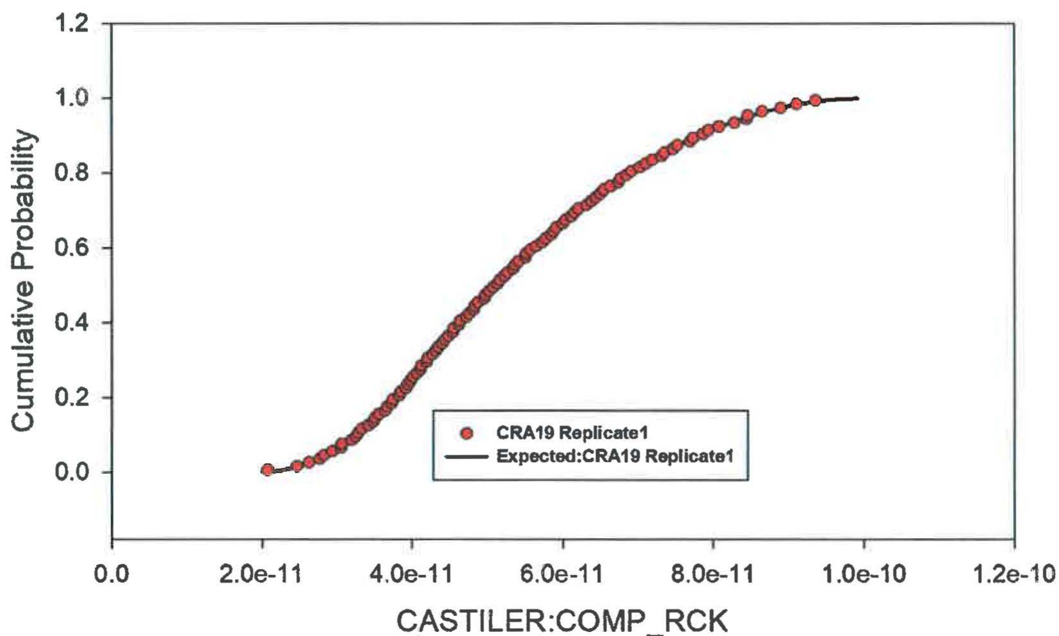

Figure 21 – Observed and Expected CDFs for CASTILER:COMP_RCK (Triangular Distribution) Replicate 1.

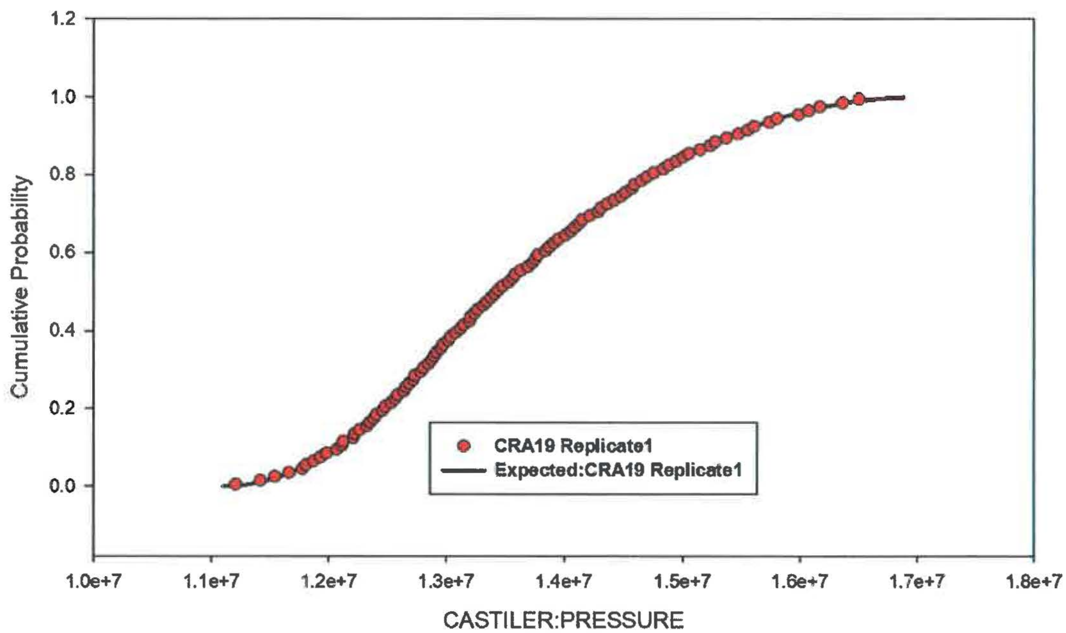

Figure 22 – Observed and Expected CDFs for CASTILER:PRESSURE (Triangular Distribution) Replicate 1.

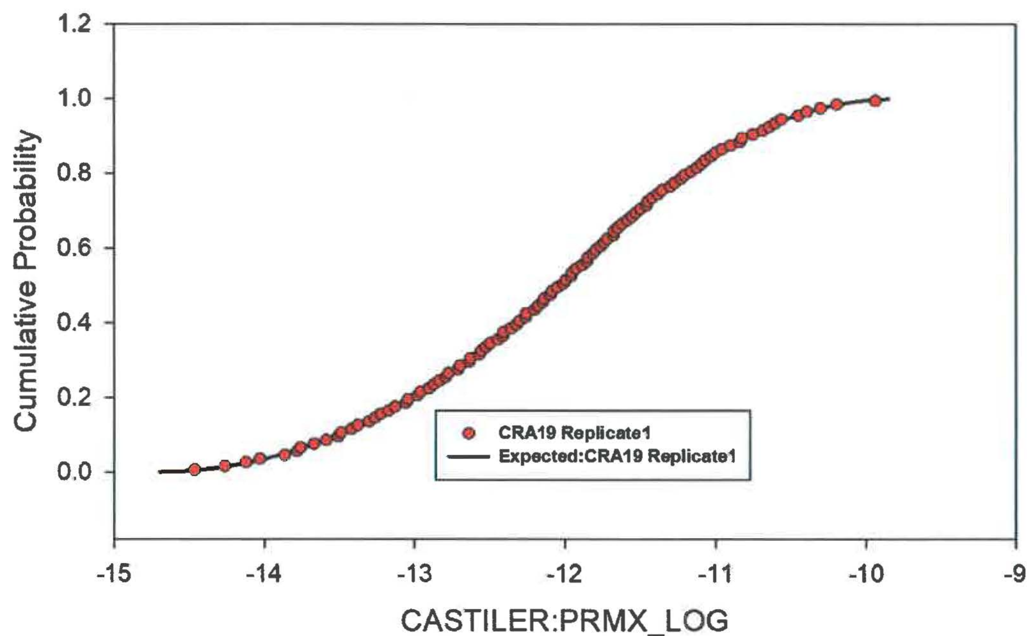

Figure 23 – Observed and Expected CDFs for CASTILER:PRMX_LOG (Triangular Distribution) Replicate 1.

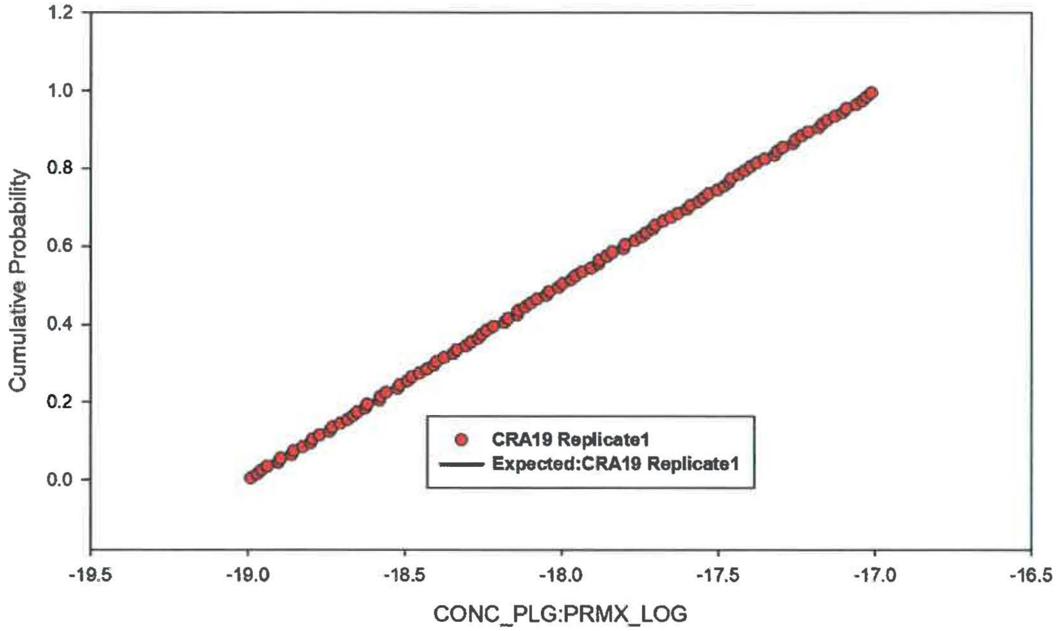

Figure 24 – Observed and Expected CDFs for CONC_PLG:PRMX_LOG (Uniform Distribution) Replicate 1.

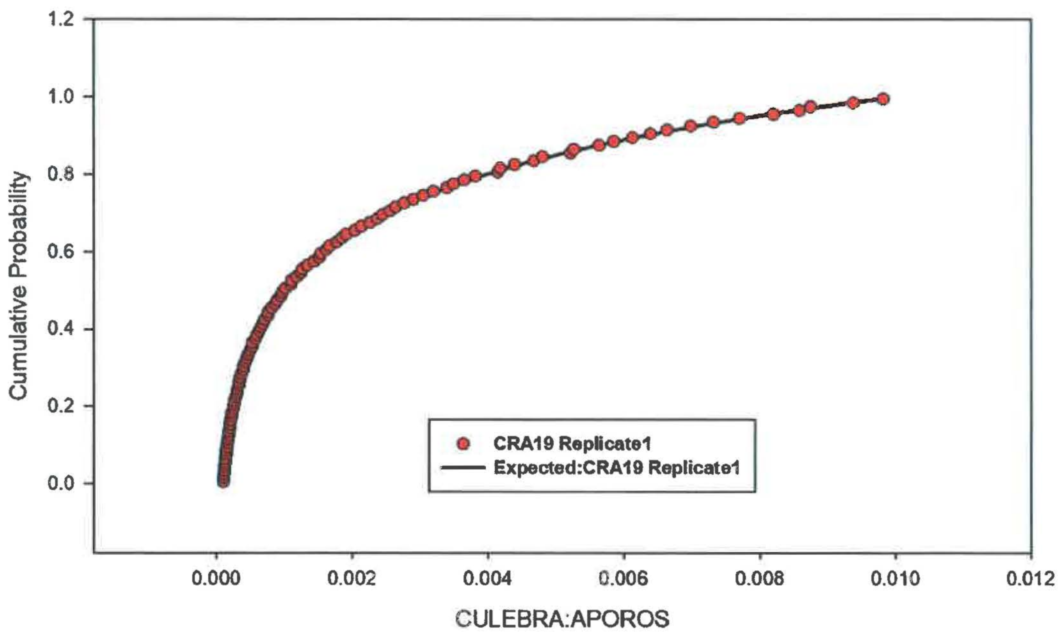

Figure 25 – Observed and Expected CDFs for CULEBRA:APOROS (Loguniform Distribution) Replicate 1.

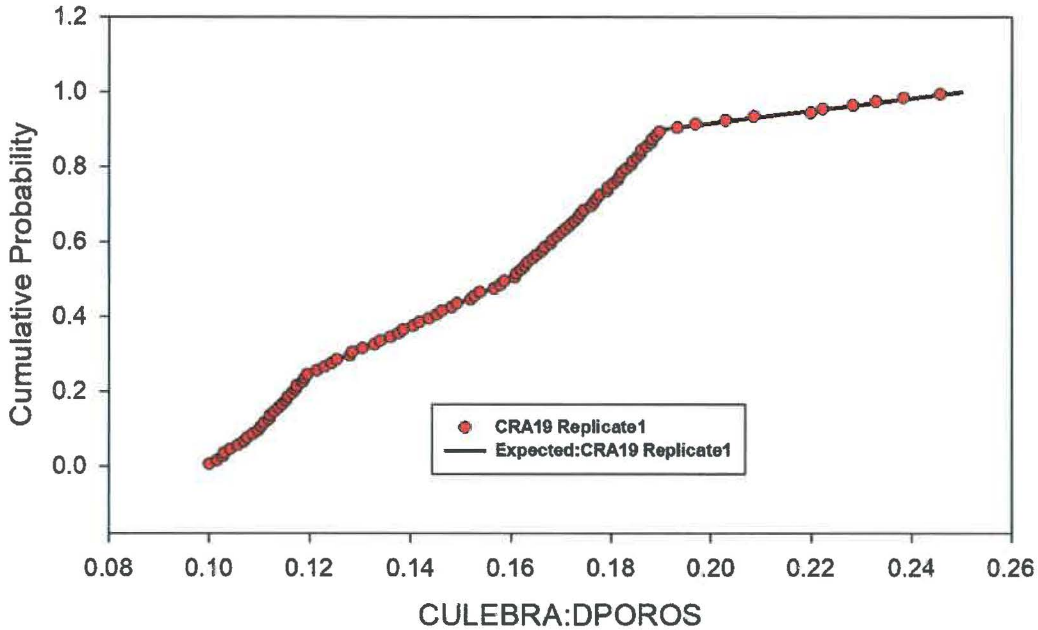

Figure 26 – Observed and Expected CDFs for CULEBRA:DPOROS (Cumulative Distribution) Replicate 1.

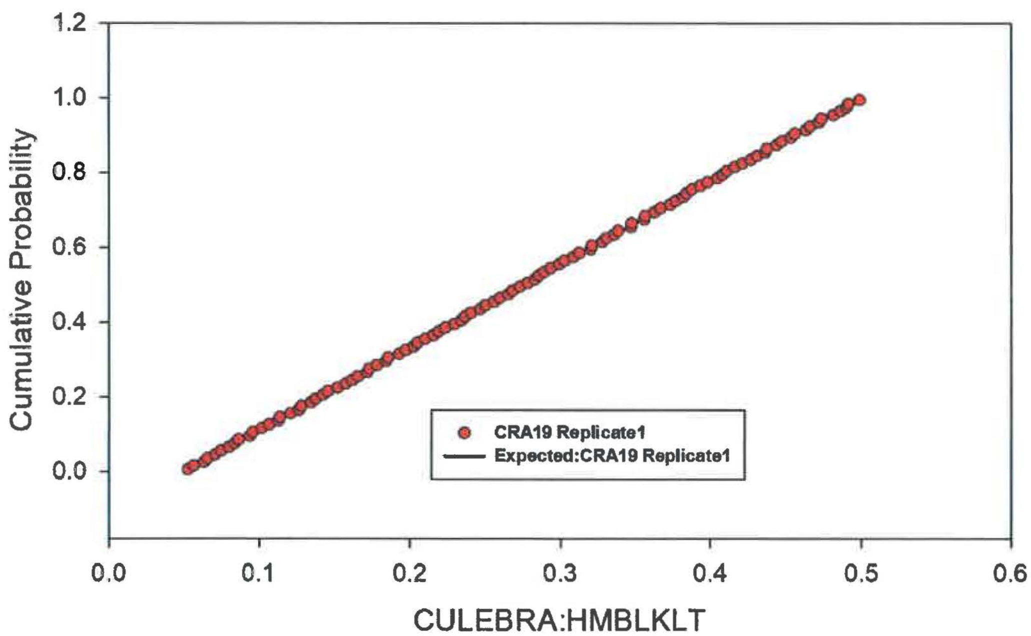

Figure 27 – Observed and Expected CDFs for CULEBRA:HMBLKLT (Uniform Distribution) Replicate 1.

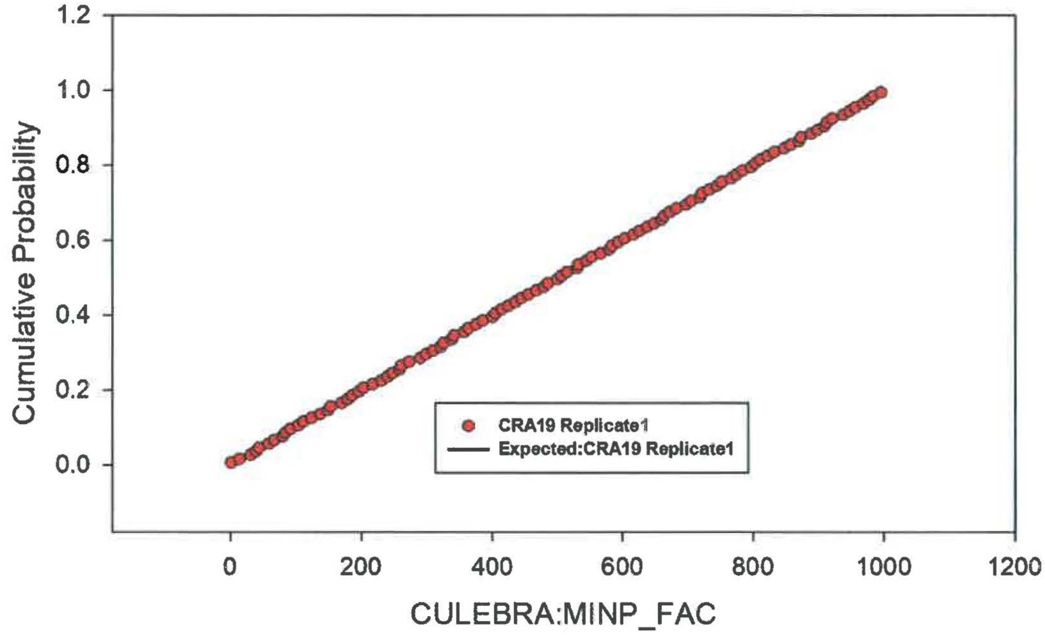

Figure 28 – Observed and Expected CDFs for CULEBRA:MINP_FAC (Uniform Distribution) Replicate 1.

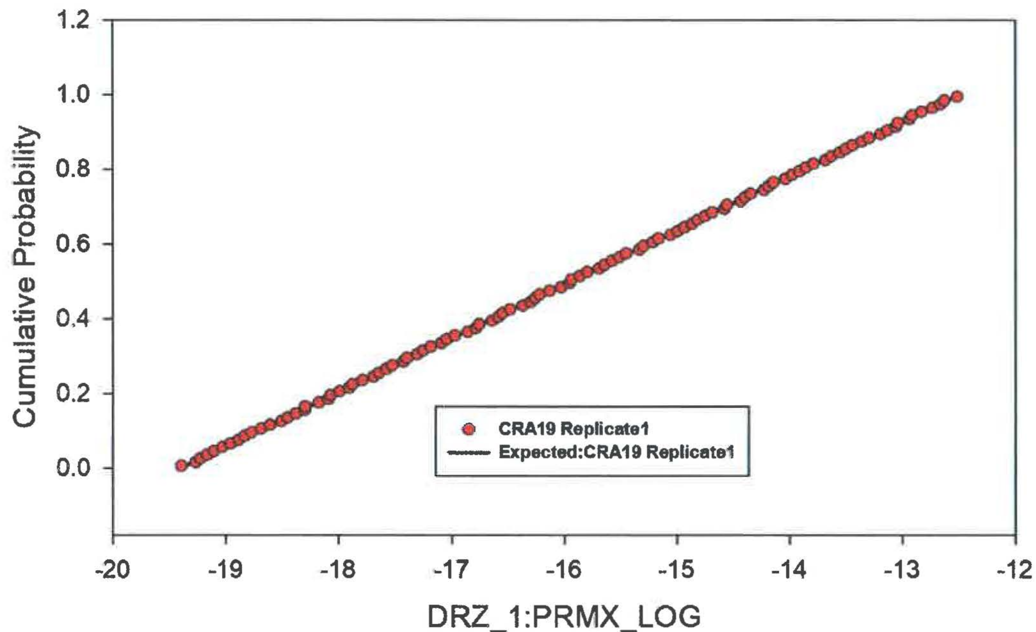

Figure 29 – Observed and Expected CDFs for DRZ_1:PRMX_LOG (Uniform Distribution) Replicate 1.

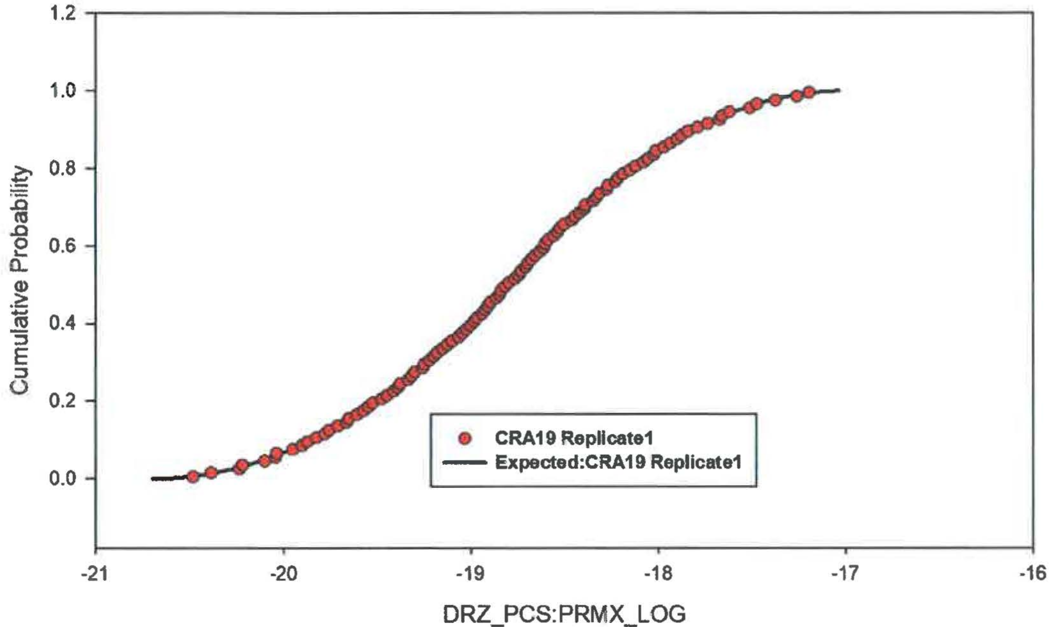

Figure 30 – Observed and Expected CDFs for DRZ_PCS:PRMX_LOG (Triangular Distribution) Replicate 1.

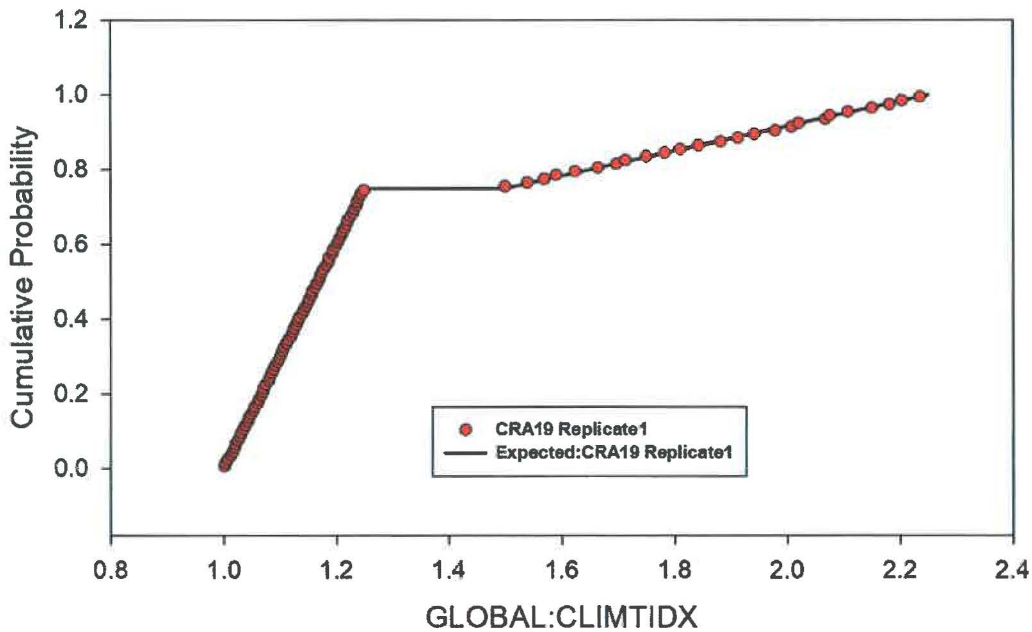

Figure 31 – Observed and Expected CDFs for GLOBAL:CLIMTIDX (Cumulative Distribution) Replicate 1.

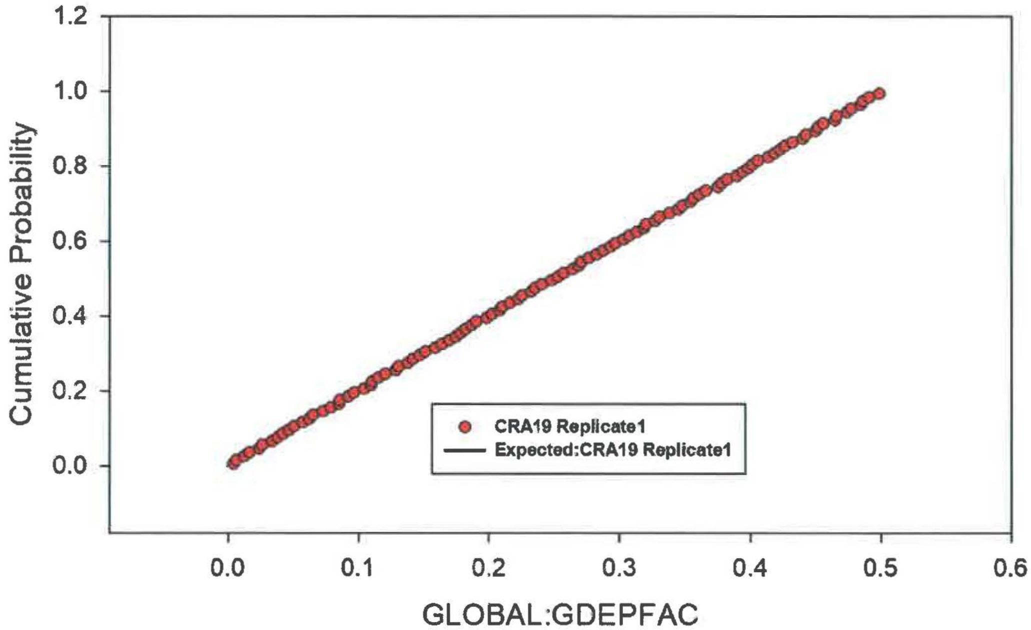

Figure 32 – Observed and Expected CDFs for GLOBAL:GDEPFAC (Uniform Distribution) Replicate 1.

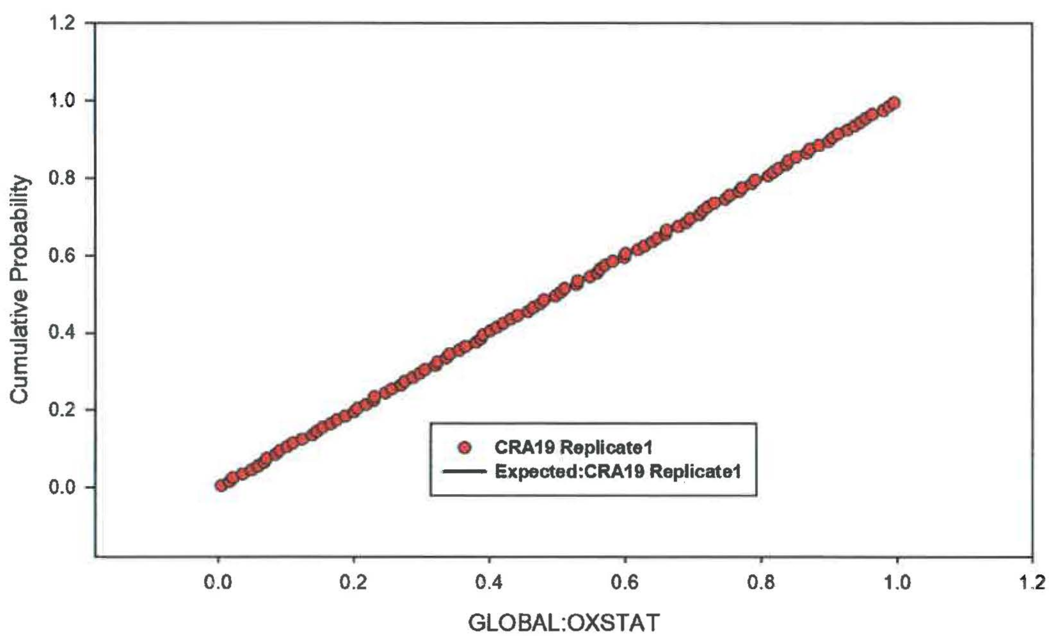

Figure 33 – Observed and Expected CDFs for GLOBAL:OXSTAT (Uniform Distribution) Replicate 1.

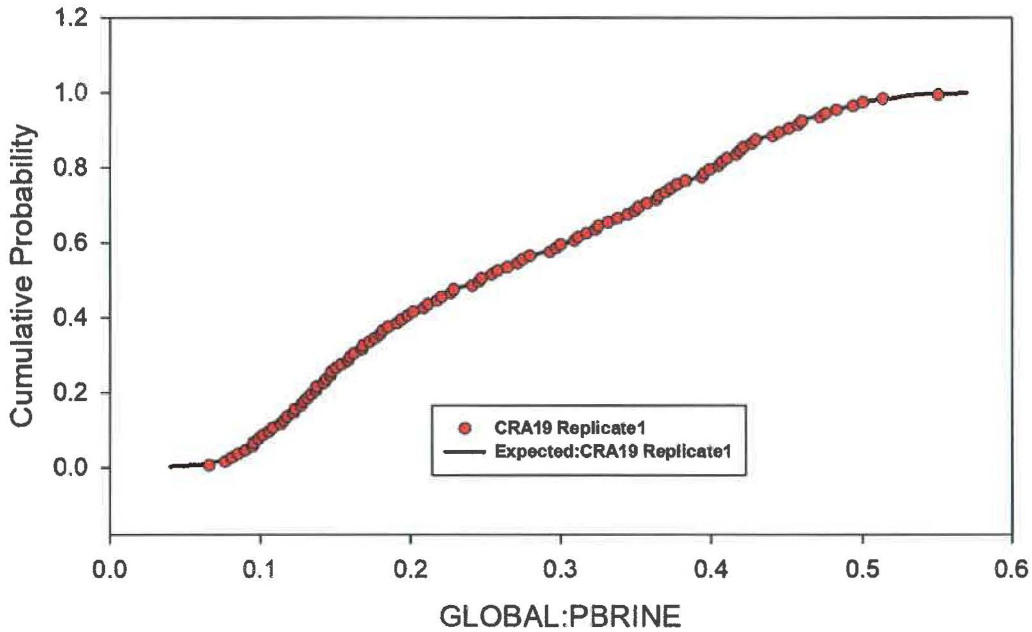

Figure 34 – Observed and Expected CDFs for GLOBAL:PBRINE (Cumulative Distribution) Replicate 1.

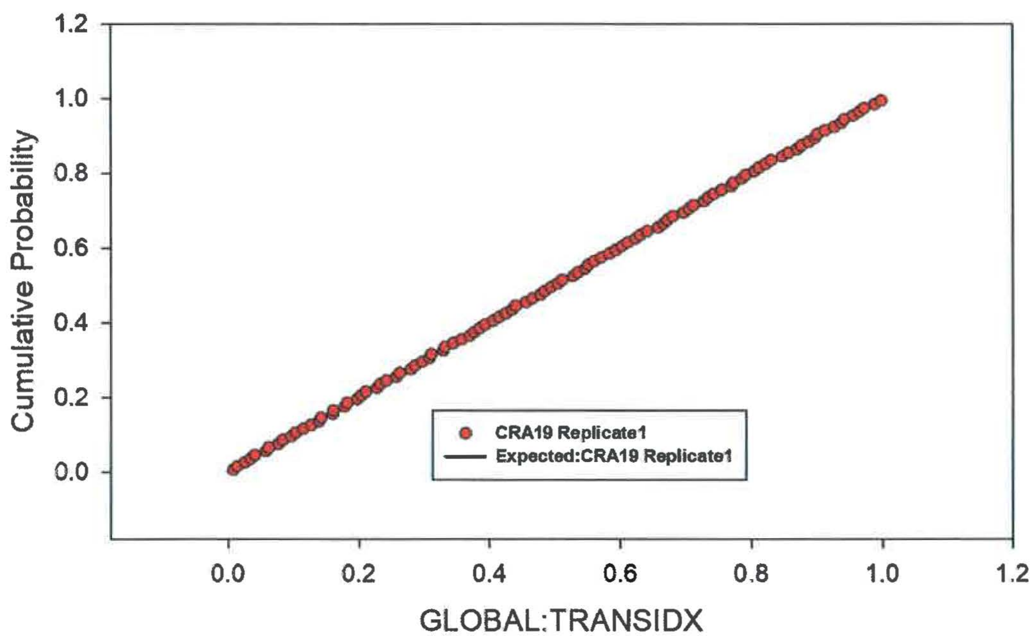

Figure 35 – Observed and Expected CDFs for GLOBAL:TRANSIDX (Uniform Distribution) Replicate 1.

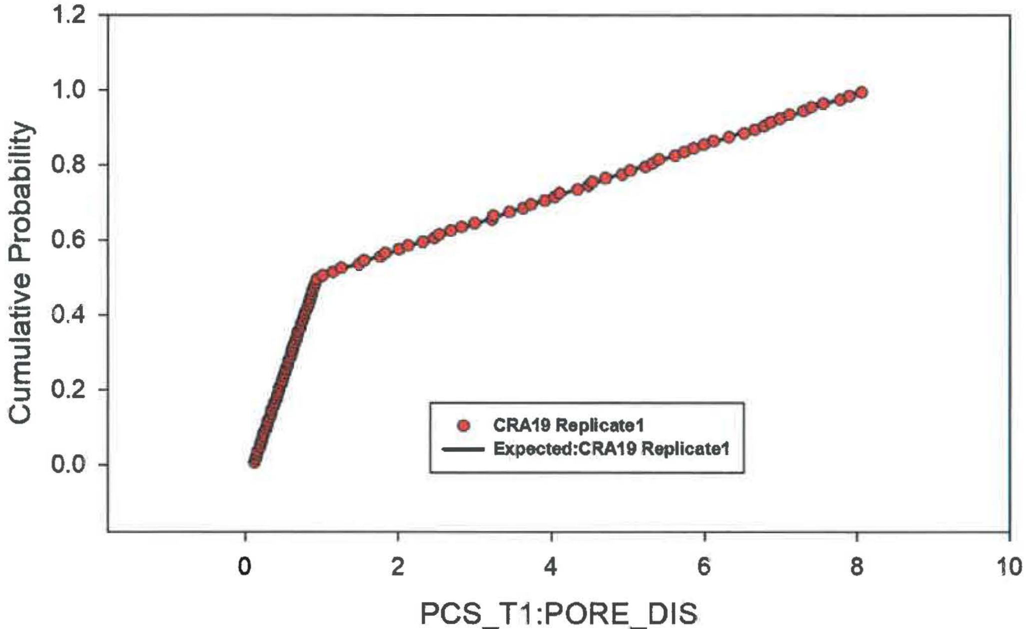

Figure 36 – Observed and Expected CDFs for PCS_T1:PORE_DIS (Cumulative Distribution) Replicate 1.

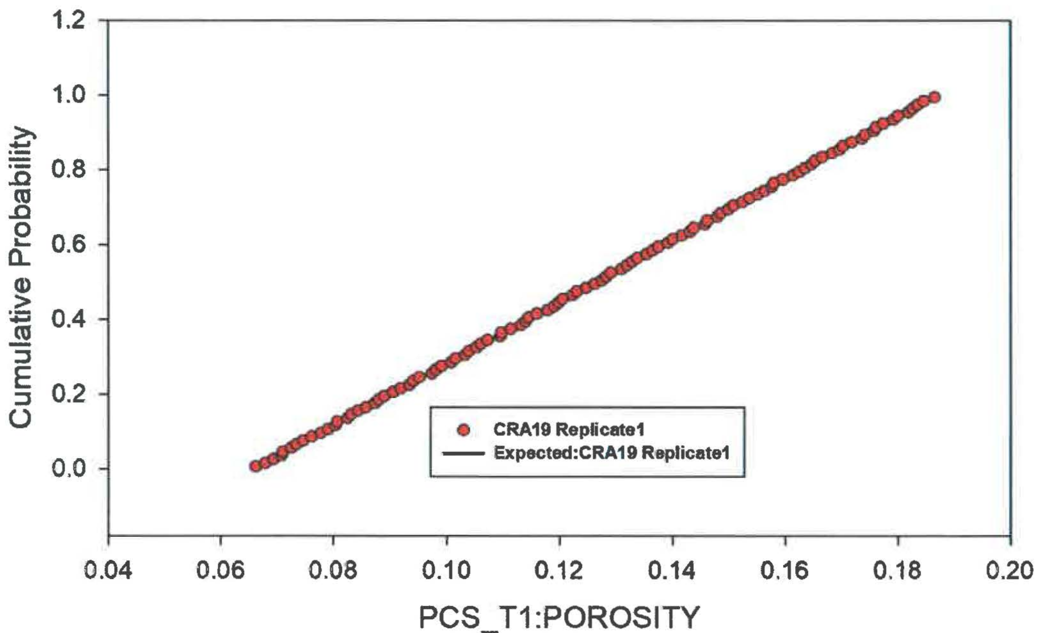

Figure 37 – Observed and Expected CDFs for PCS_T1:POROSITY (Uniform Distribution) Replicate 1.

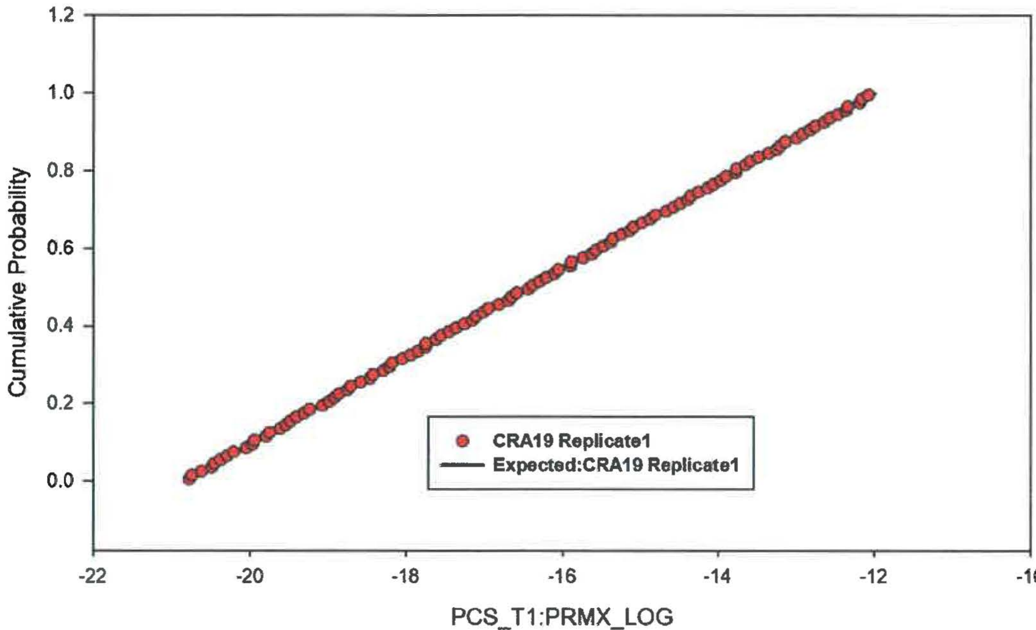

Figure 38 – Observed and Expected CDFs for PCS_T1:PRMX_LOG (Uniform Distribution) Replicate 1.

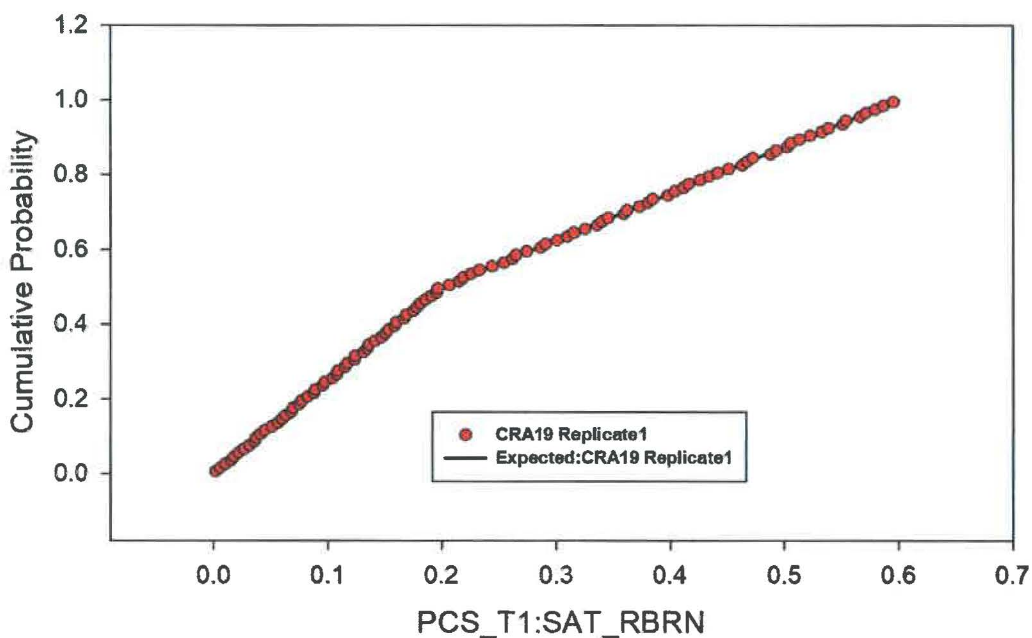

Figure 39 – Observed and Expected CDFs for PCS_T1:SAT_RBRN (Cumulative Distribution) Replicate 1.

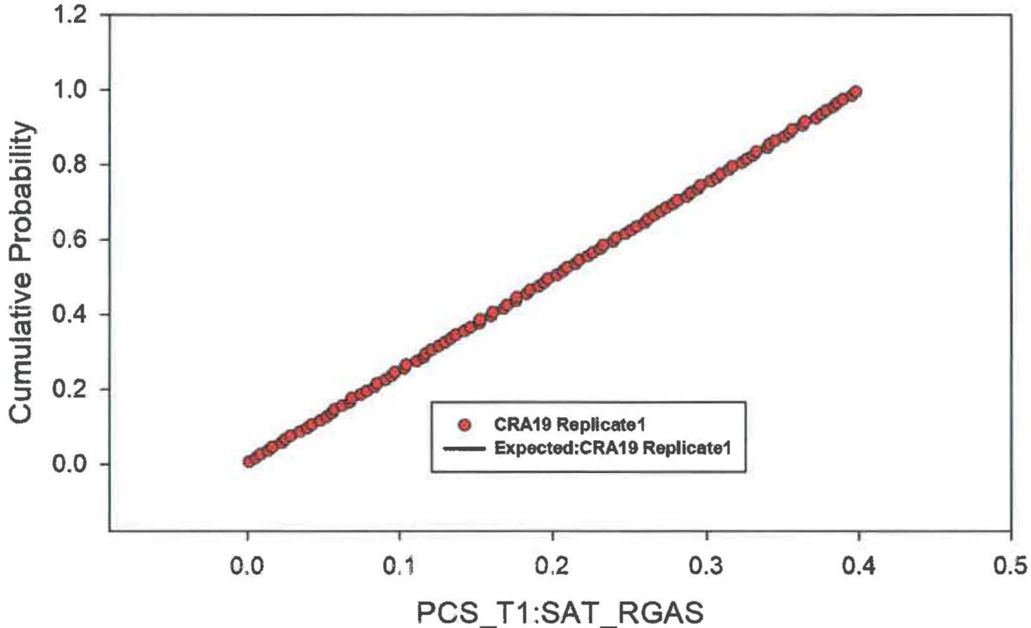

Figure 40 – Observed and Expected CDFs for PCS_T1:SAT_RGAS (Uniform Distribution) Replicate 1.

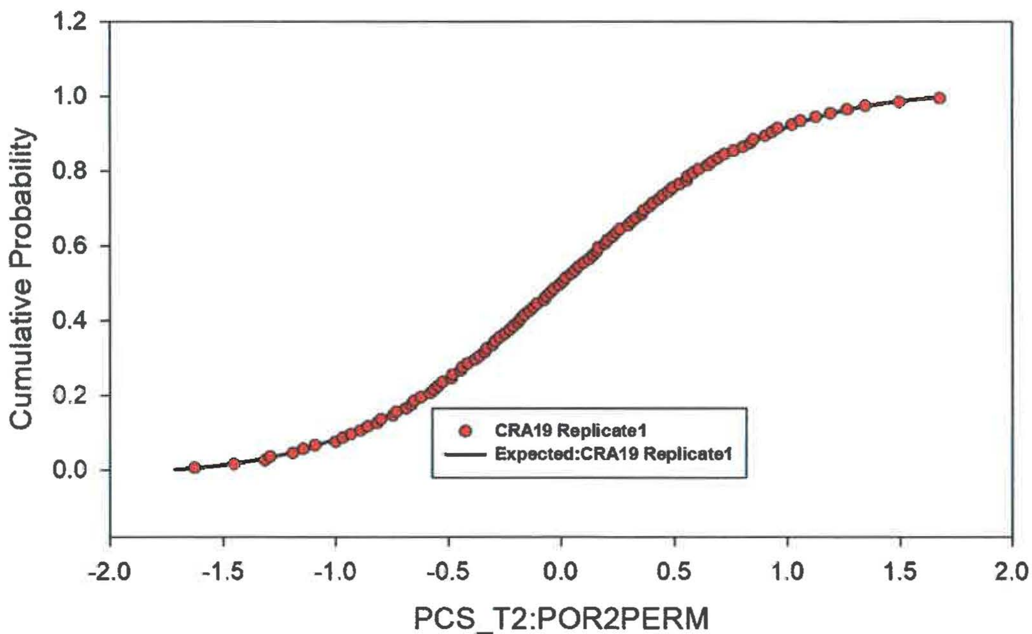

Figure 41 – Observed and Expected CDFs for PCS_T2:POR2PERM (Normal Distribution) Replicate 1.

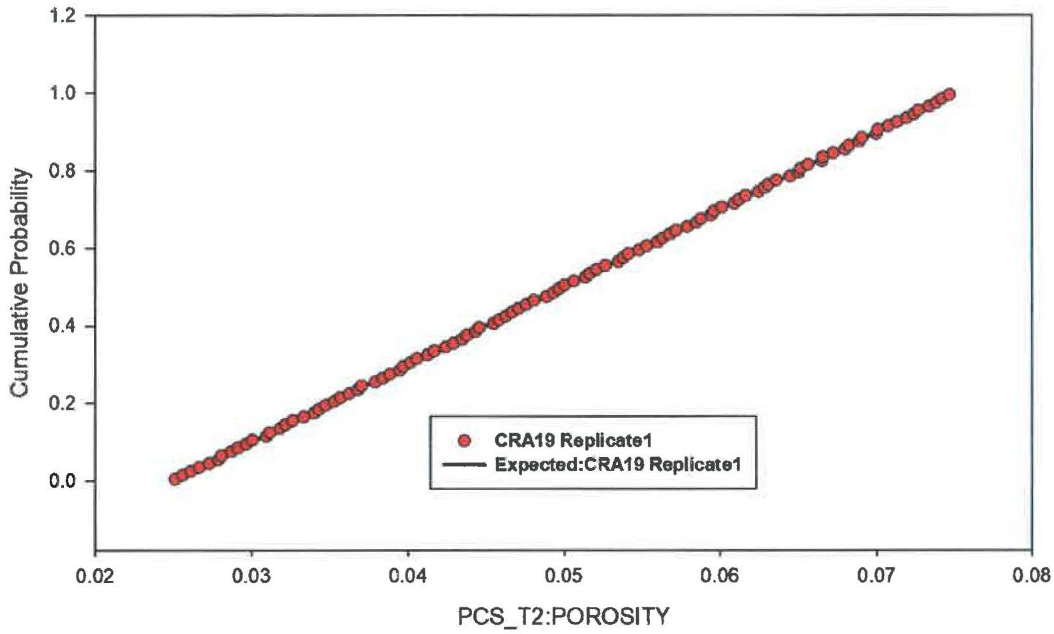

Figure 42 – Observed and Expected CDFs for PCS_T2:POROSITY (Uniform Distribution) Replicate 1.

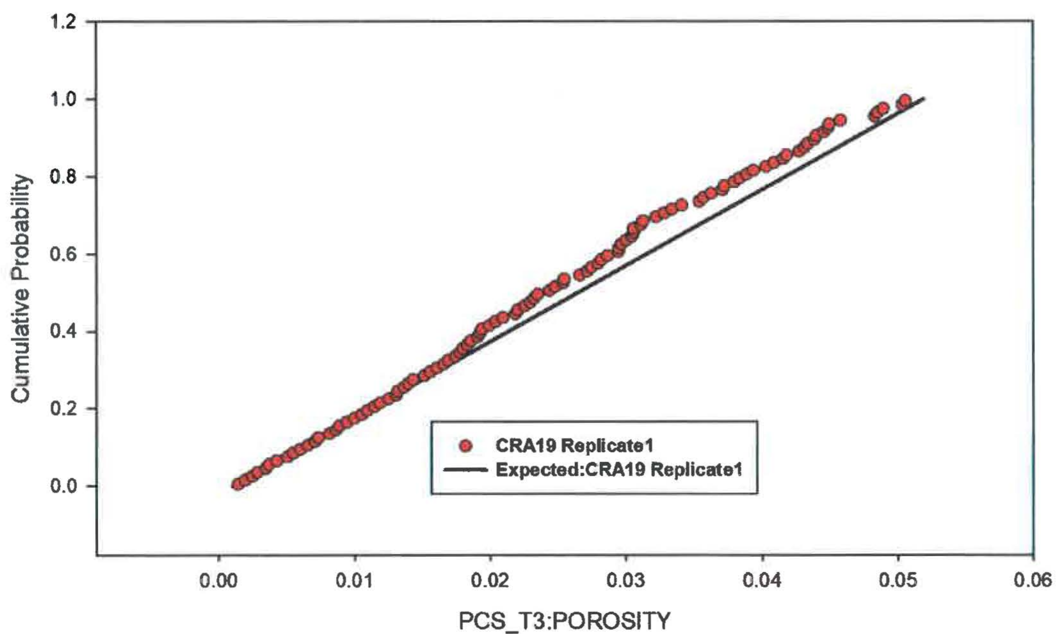

Figure 43 – Observed and Expected CDFs for PCS_T3:POROSITY (Uniform Distribution) Replicate 1.

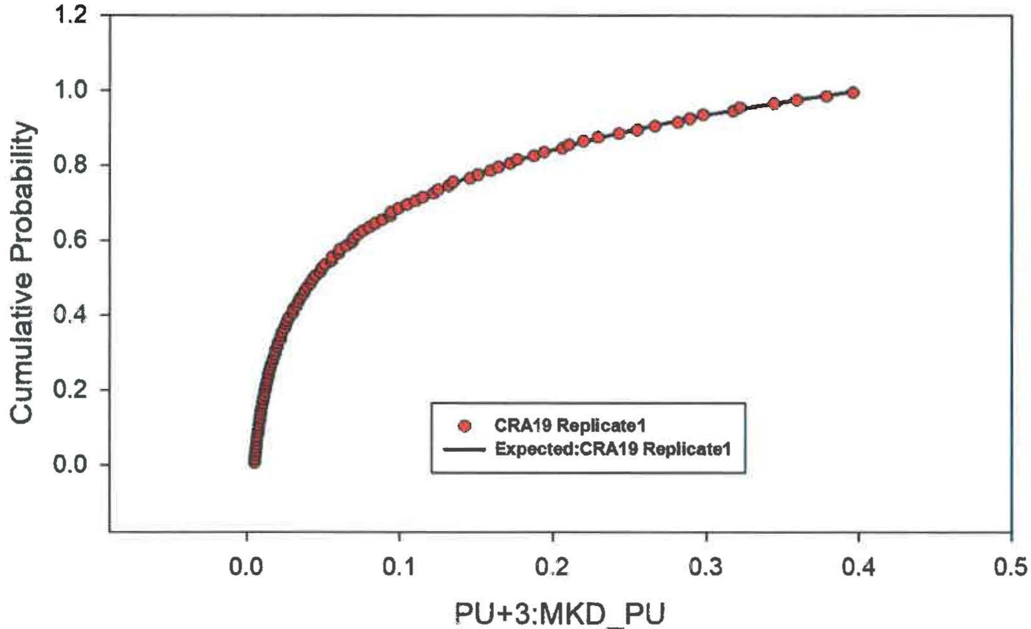

Figure 44 – Observed and Expected CDFs for PU+3:MKD_PU (Loguniform Distribution) Replicate 1.

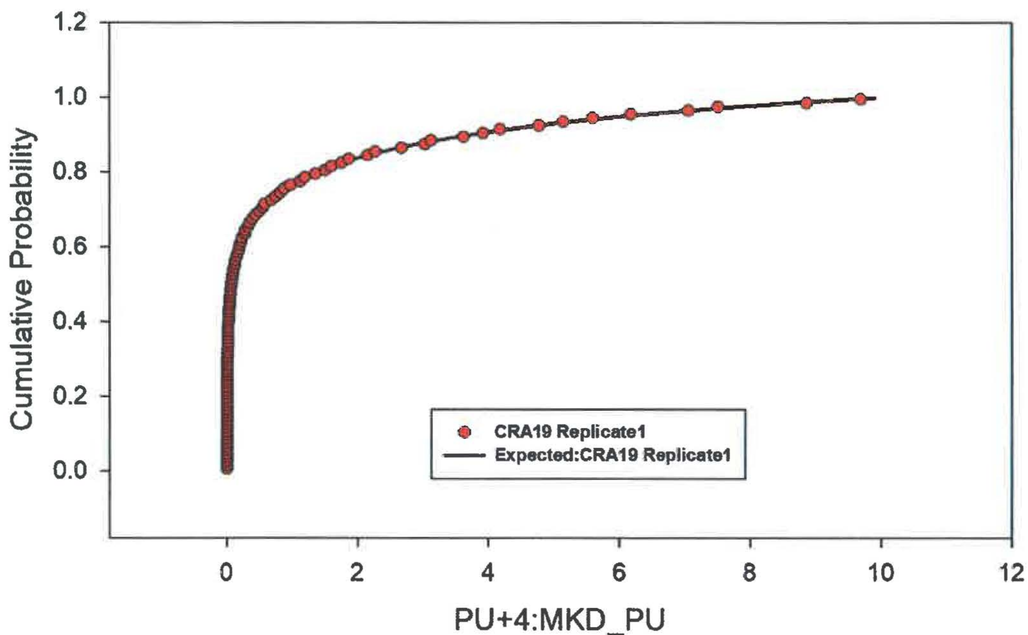

Figure 45 – Observed and Expected CDFs for PU+4:MKD_PU (Loguniform Distribution) Replicate 1.

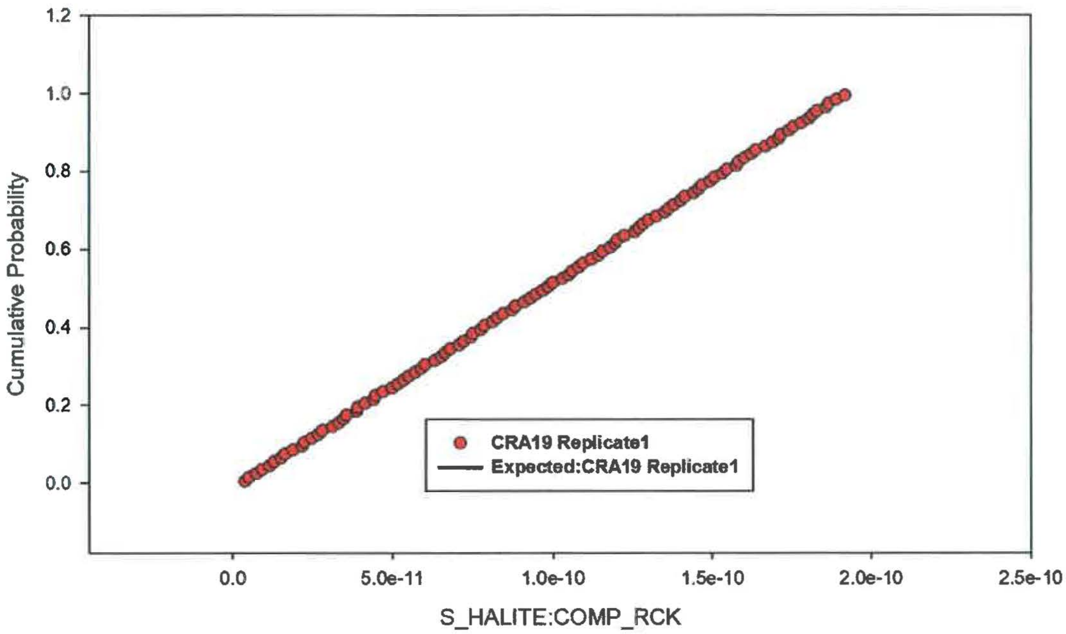

Figure 46 – Observed and Expected CDFs for S_HALITE:COMP_RCK (Uniform Distribution) Replicate 1.

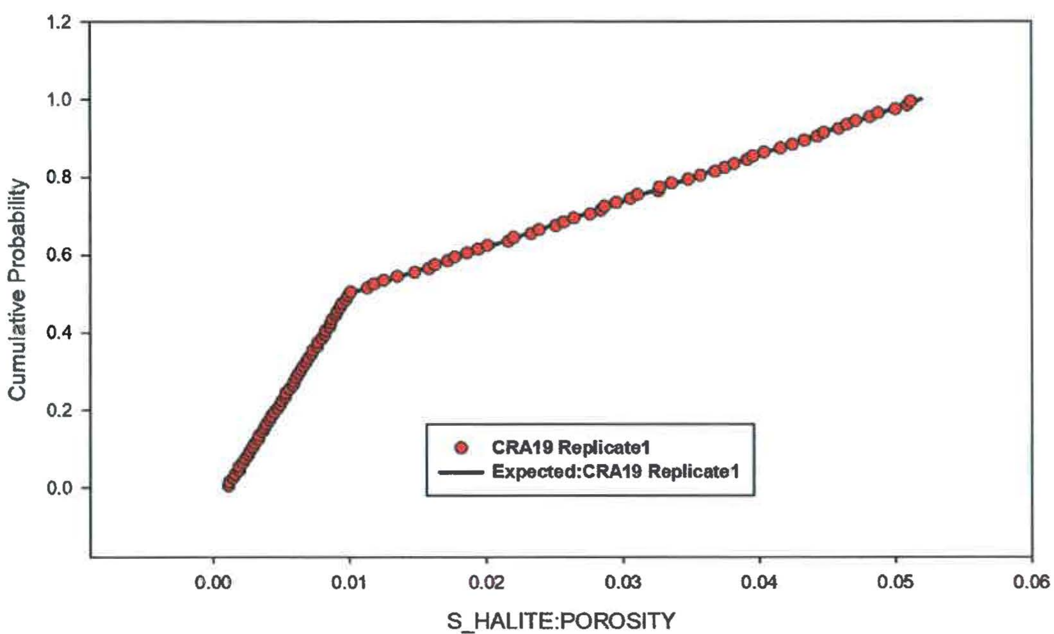

Figure 47 – Observed and Expected CDFs for S_HALITE:POROSITY (Cumulative Distribution) Replicate 1.

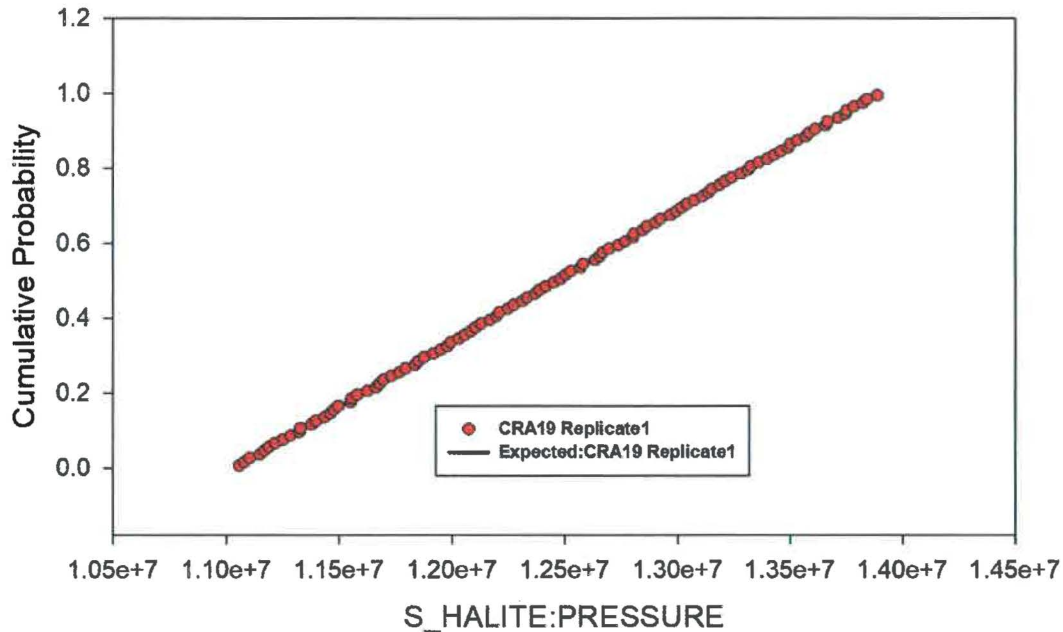

Figure 48 – Observed and Expected CDFs for S_HALITE:PRESSURE (Uniform Distribution) Replicate 1.

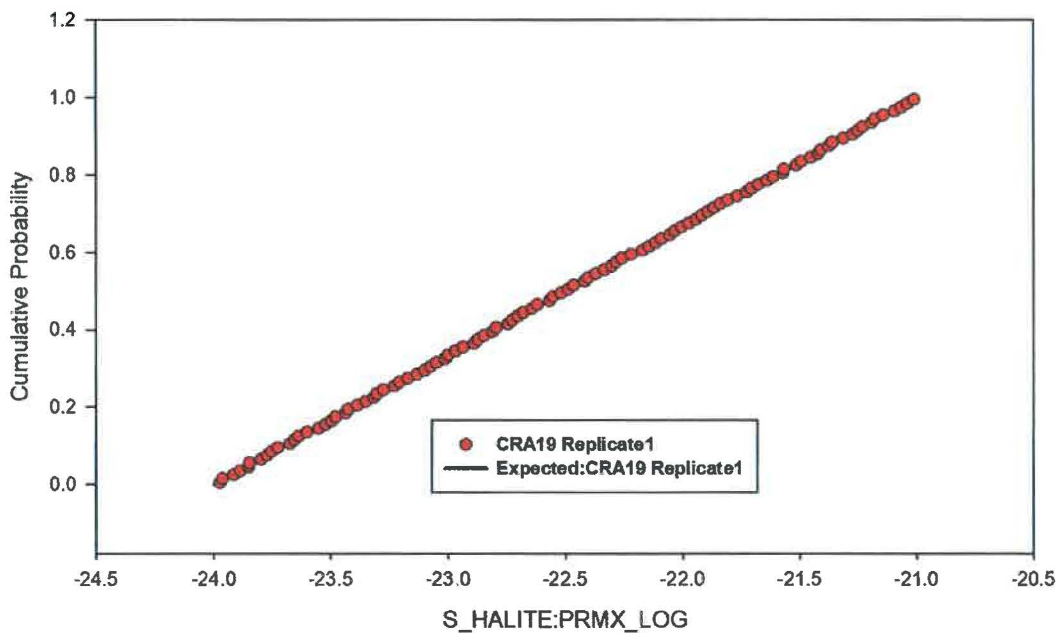

Figure 49 – Observed and Expected CDFs for S_HALITE:PRMX_LOG (Uniform Distribution) Replicate 1.

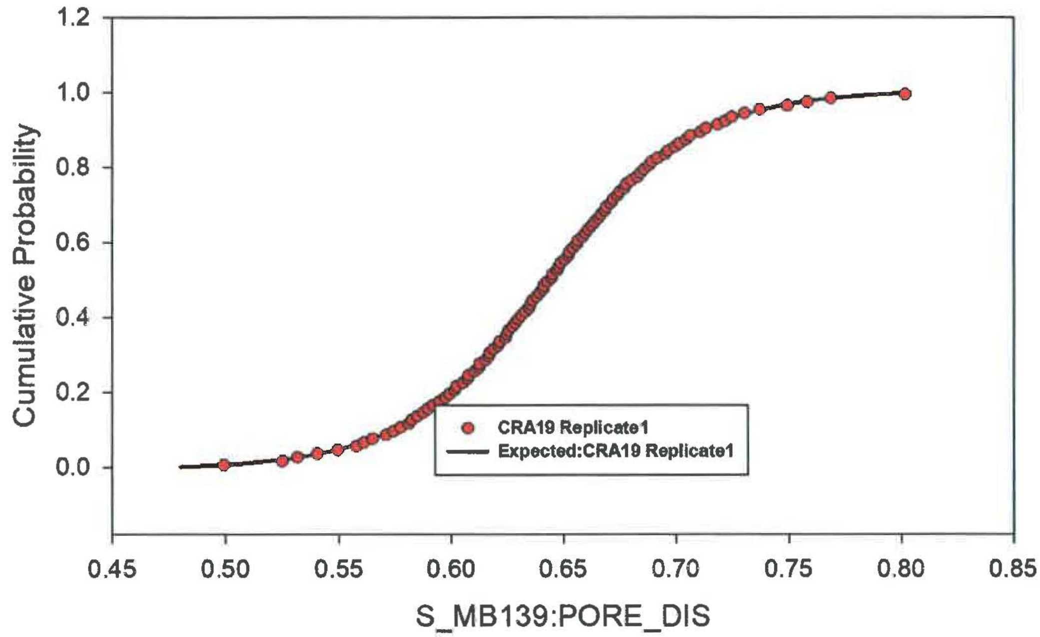

Figure 50 – Observed and Expected CDFs for S_MB139:PORE_DIS (Student Distribution) Replicate 1.

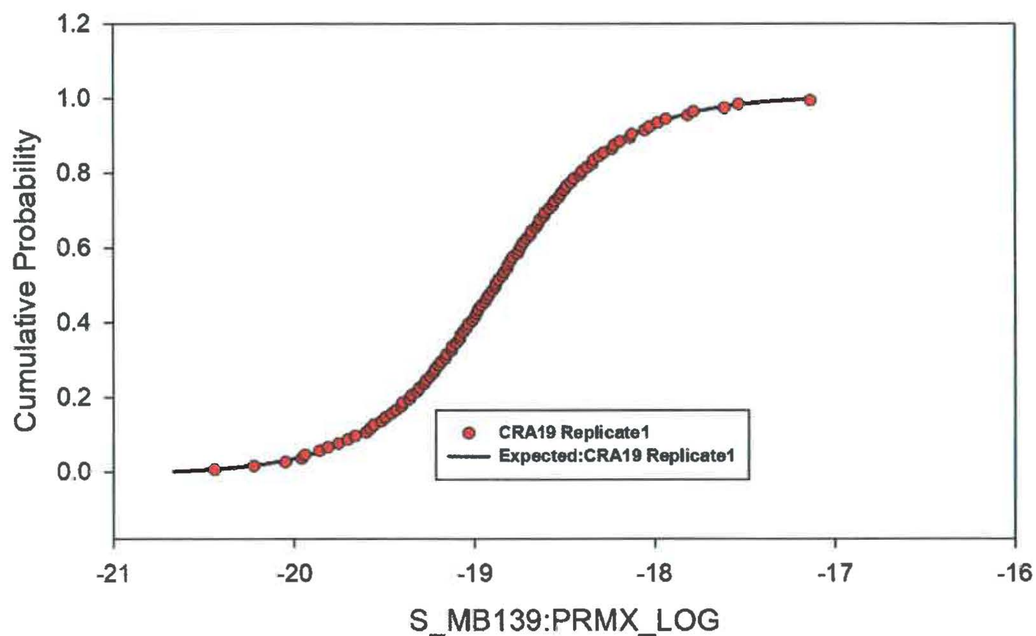

Figure 51 – Observed and Expected CDFs for S_MB139:PRMX_LOG (Student Distribution) Replicate 1.

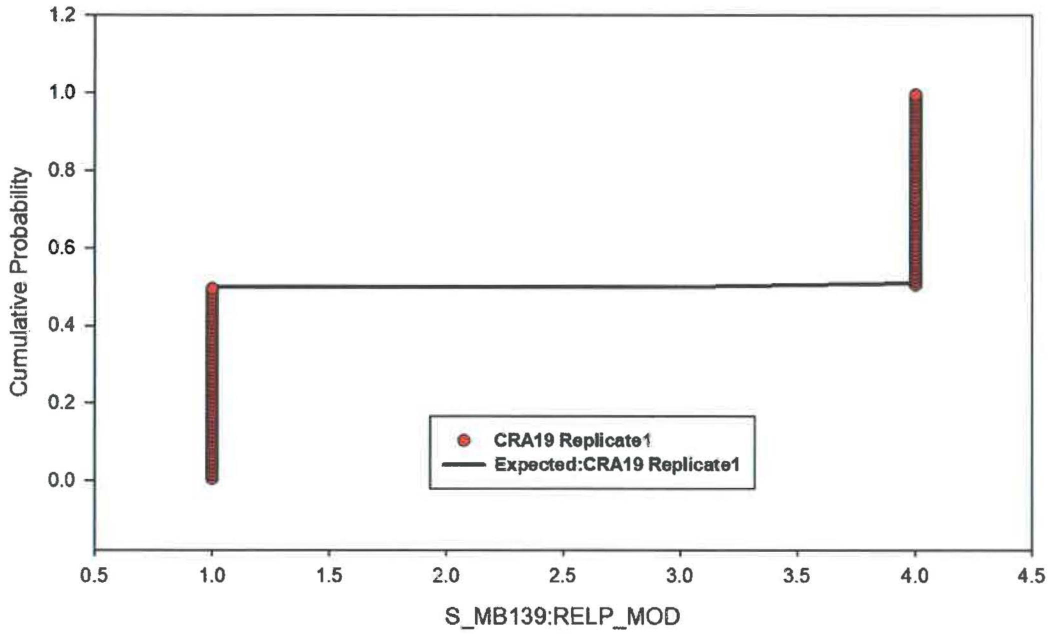

Figure 52 – Observed and Expected CDFs for S_MB139:RELP_MOD (Delta Distribution) Replicate 1.

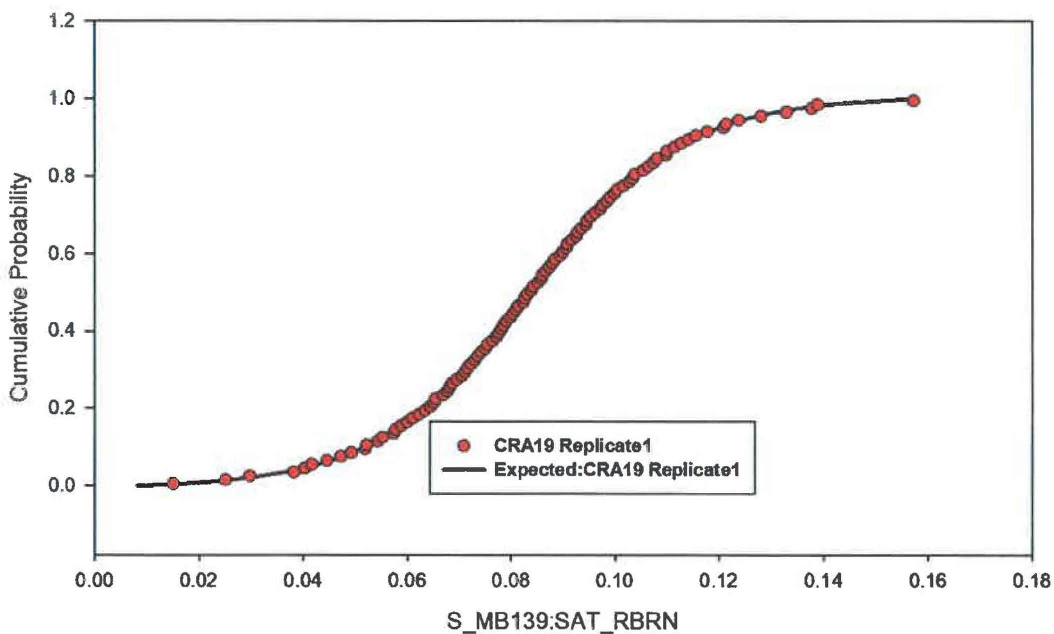

Figure 53 – Observed and Expected CDFs for S_MB139:SAT_RBRN (Student Distribution) Replicate 1.

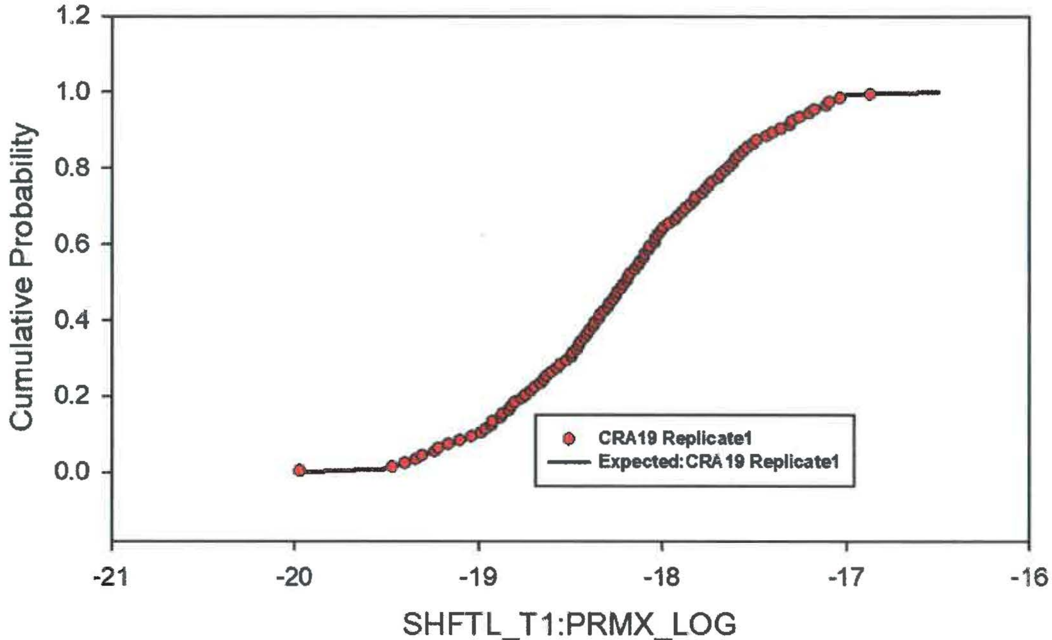

Figure 54 – Observed and Expected CDFs for SHFTL_T1:PRMX_LOG (Cumulative Distribution) Replicate 1.

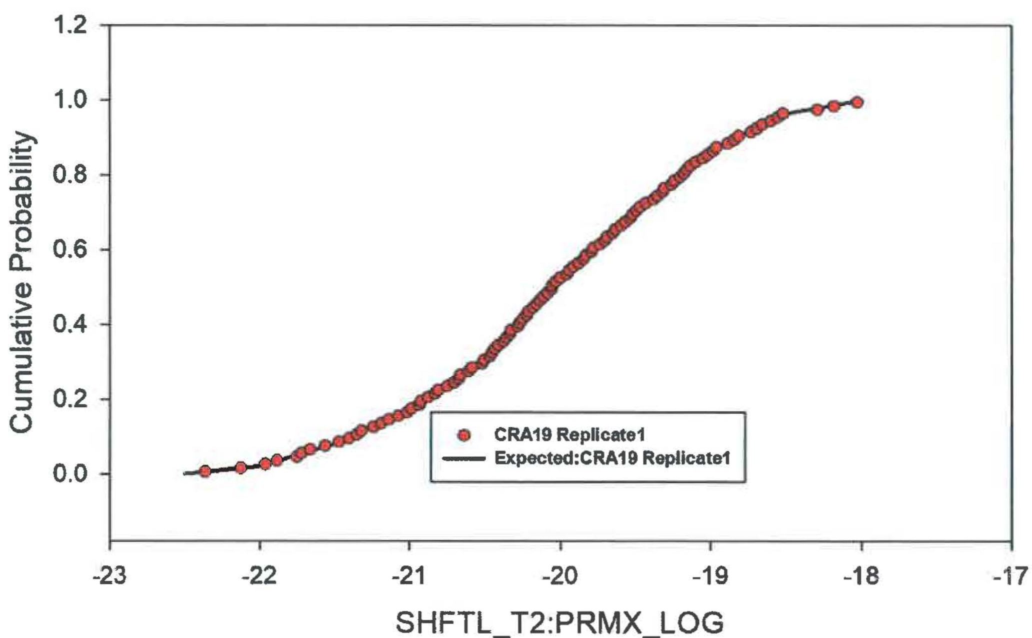

Figure 55 – Observed and Expected CDFs for SHFTL_T2:PRMX_LOG (Cumulative Distribution) Replicate 1.

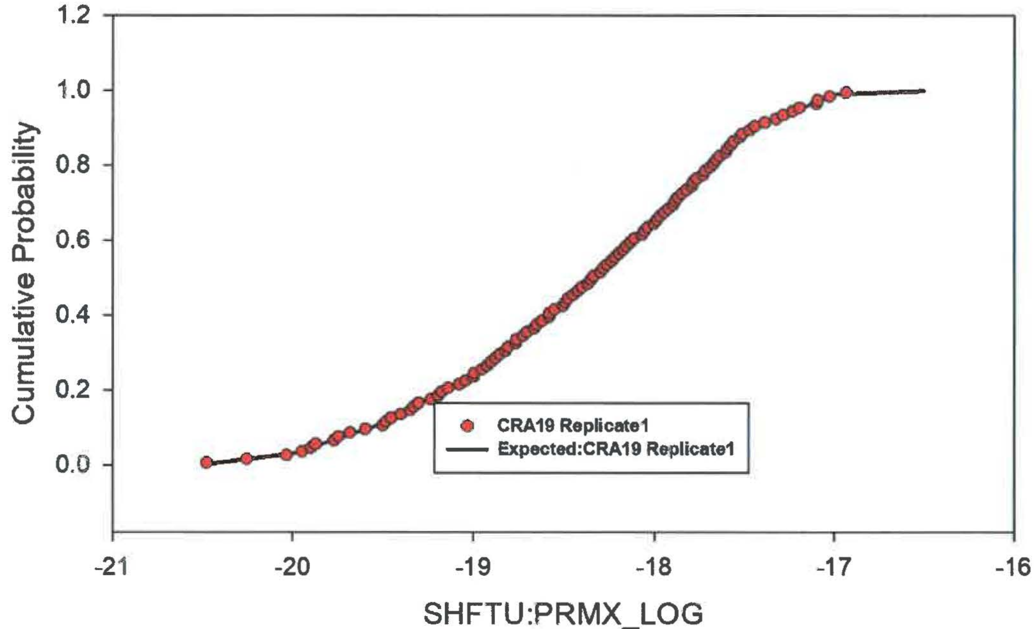

Figure 56 – Observed and Expected CDFs for SHFTU:PRMX_LOG (Cumulative Distribution) Replicate 1.

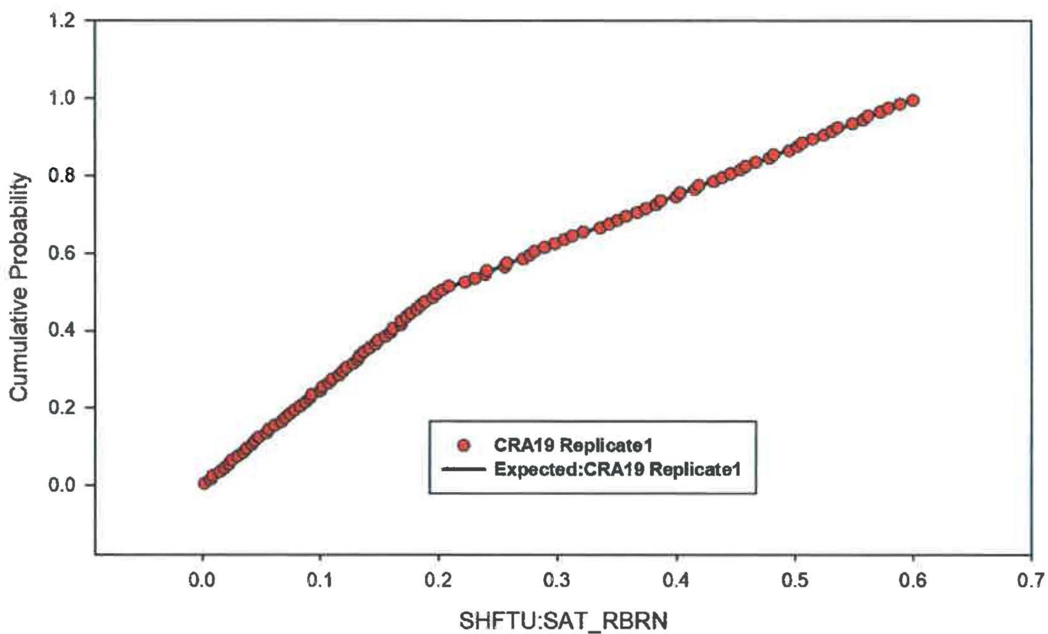

Figure 57 – Observed and Expected CDFs for SHFTU:SAT_RBRN (Cumulative Distribution) Replicate 1.

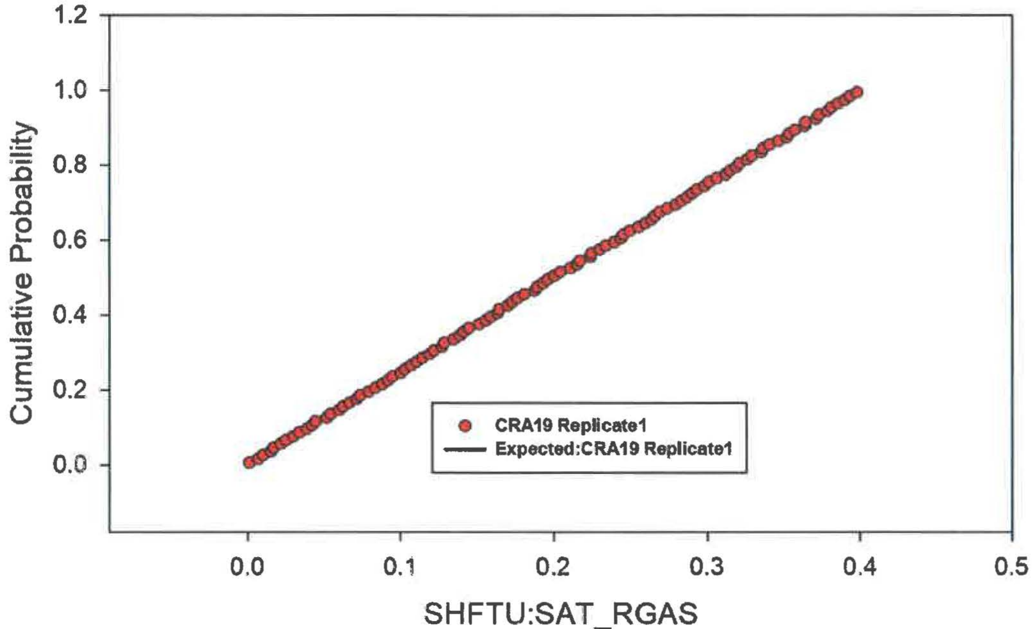

Figure 58 – Observed and Expected CDFs for SHFTU:SAT_RGAS (Uniform Distribution) Replicate 1.

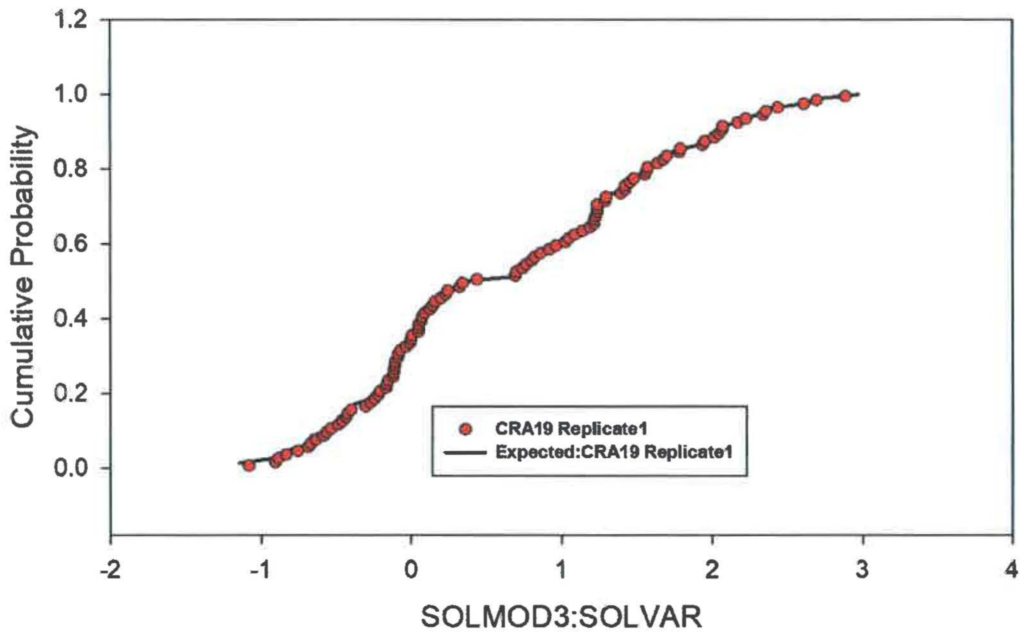

Figure 59 – Observed and Expected CDFs for SOLMOD3:SOLVAR (Cumulative Distribution) Replicate 1.

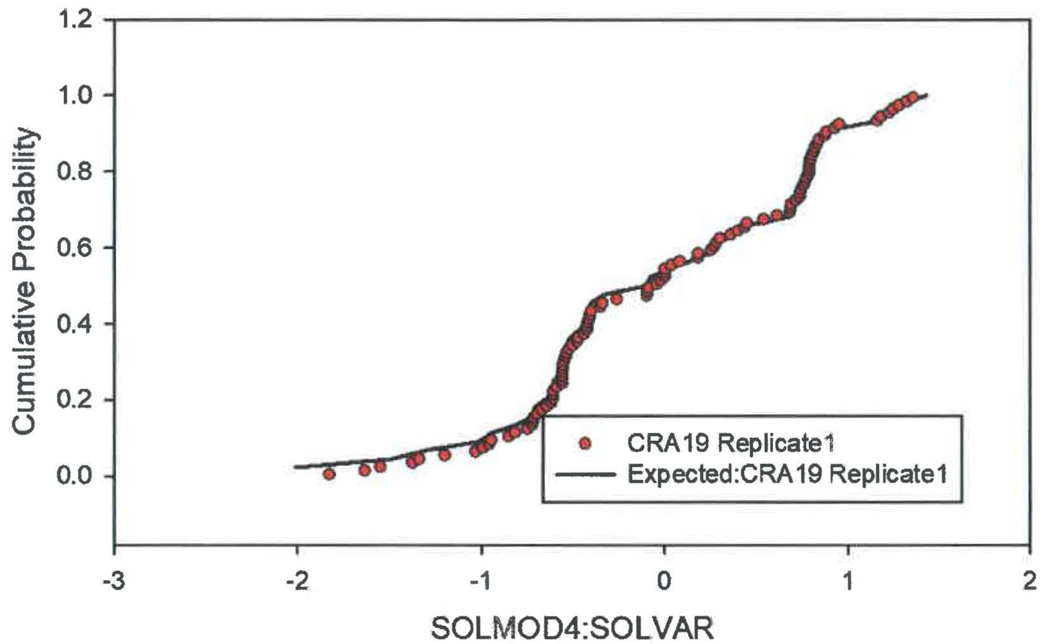

Figure 60 – Observed and Expected CDFs for SOLMOD4:SOLVAR (Cumulative Distribution) Replicate 1.

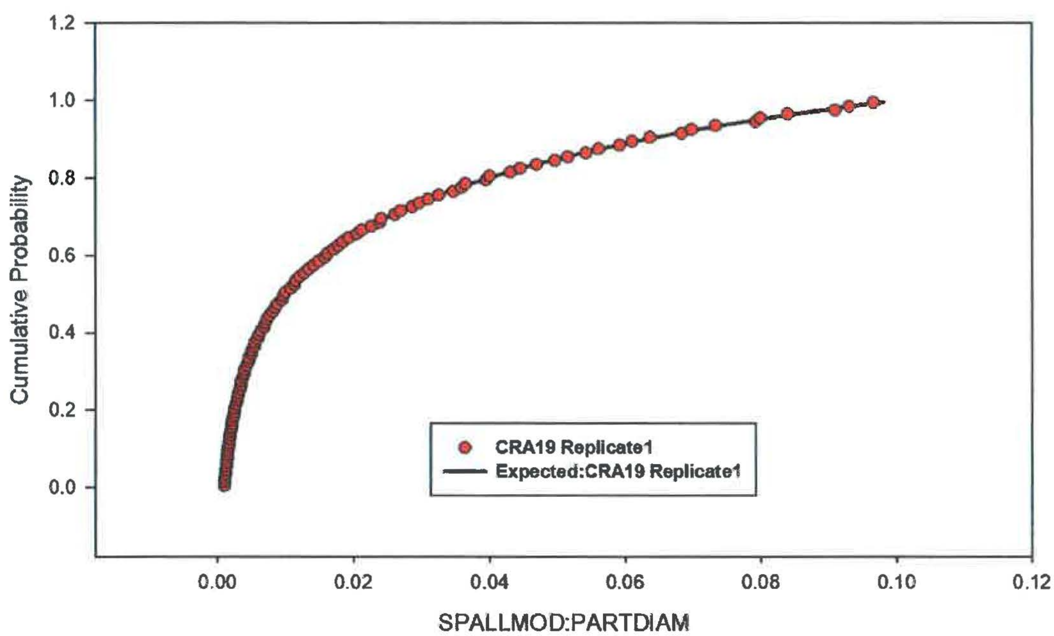

Figure 61 – Observed and Expected CDFs for SPALLMOD:PARTDIAM (Loguniform Distribution) Replicate 1.

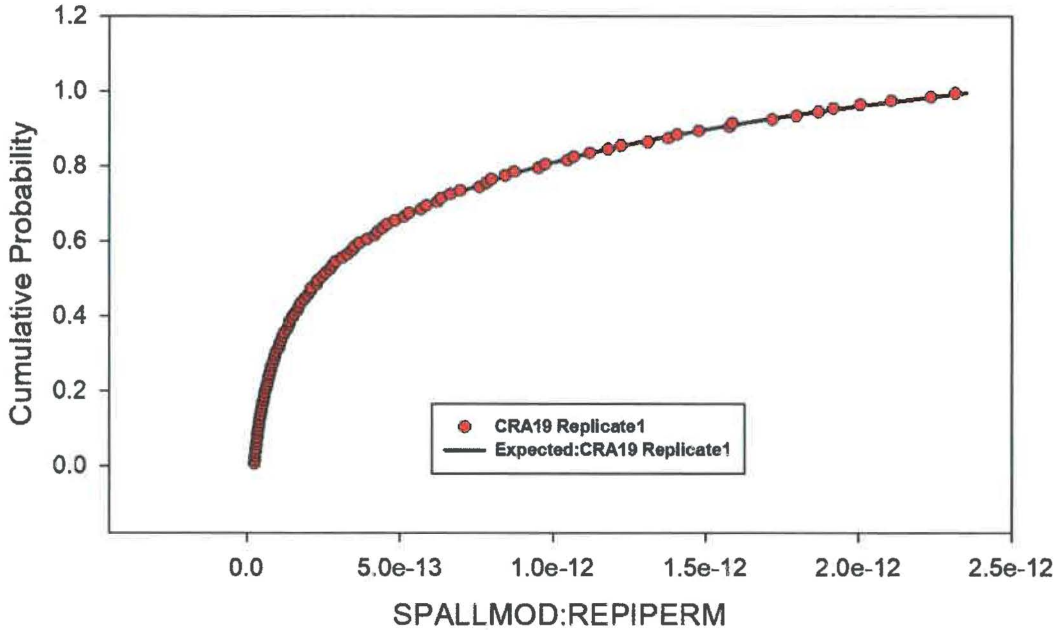

Figure 62 – Observed and Expected CDFs for SPALLMOD:REPIPERM (Loguniform Distribution) Replicate 1.

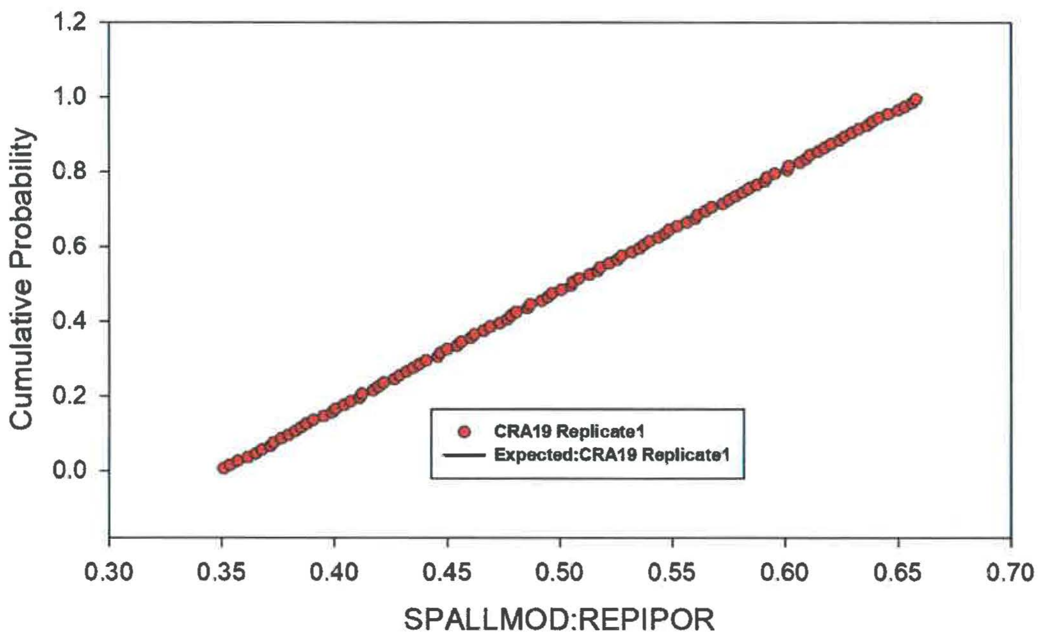

Figure 63 – Observed and Expected CDFs for SPALLMOD:REPIPOR (Uniform Distribution) Replicate 1.

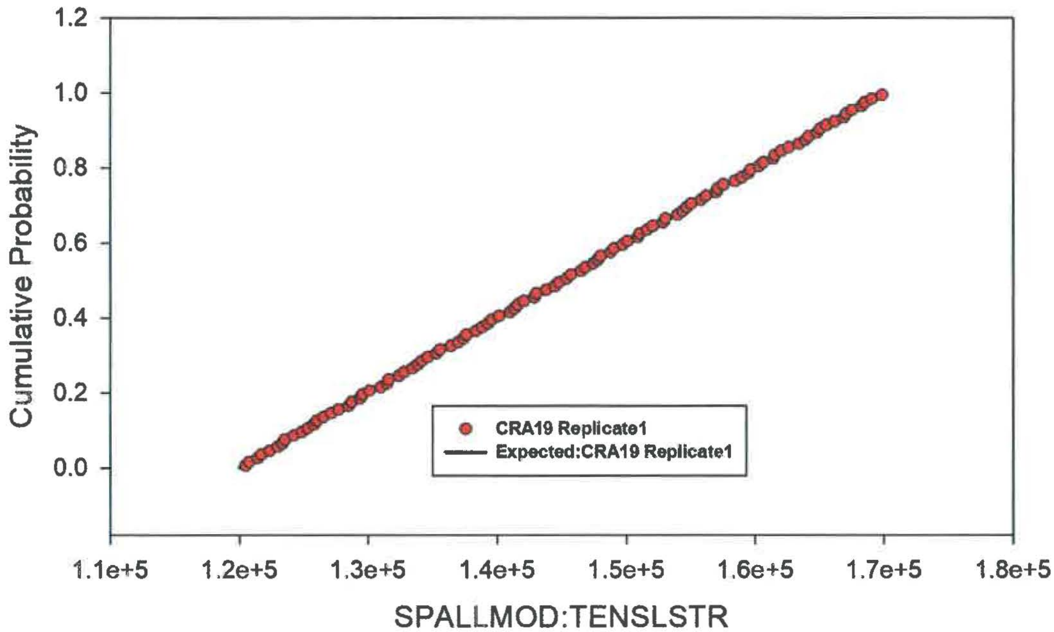

Figure 64 – Observed and Expected CDFs for SPALLMOD:TENSLSTR (Uniform Distribution) Replicate 1.

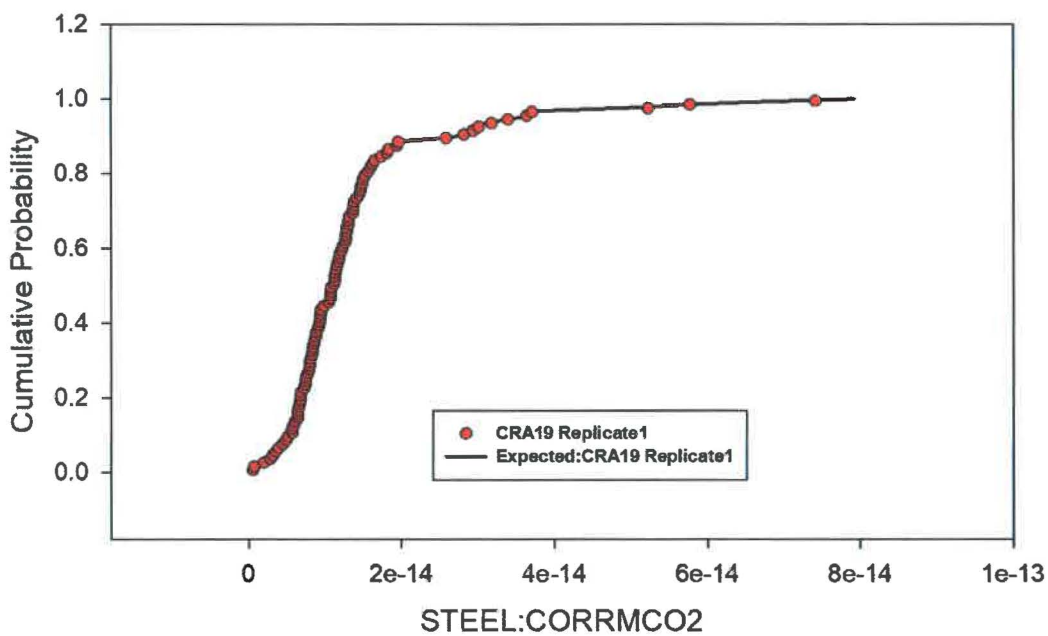

Figure 65 – Observed and Expected CDFs for STEEL:CORRMCO2 (Cumulative Distribution) Replicate 1.

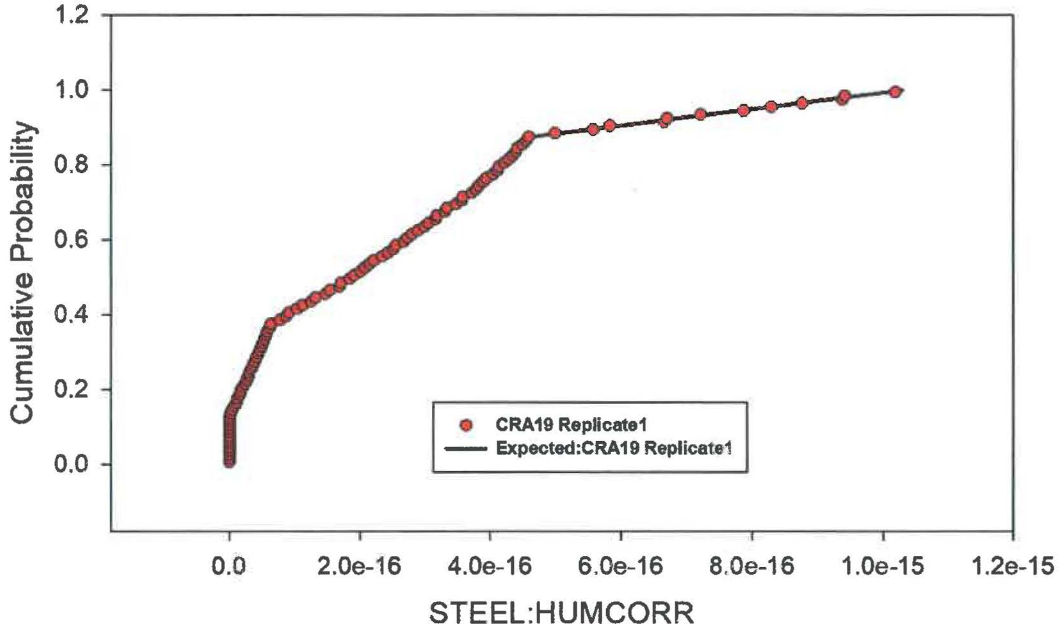

Figure 66 – Observed and Expected CDFs for STEEL:HUMCORR (Cumulative Distribution) Replicate 1.

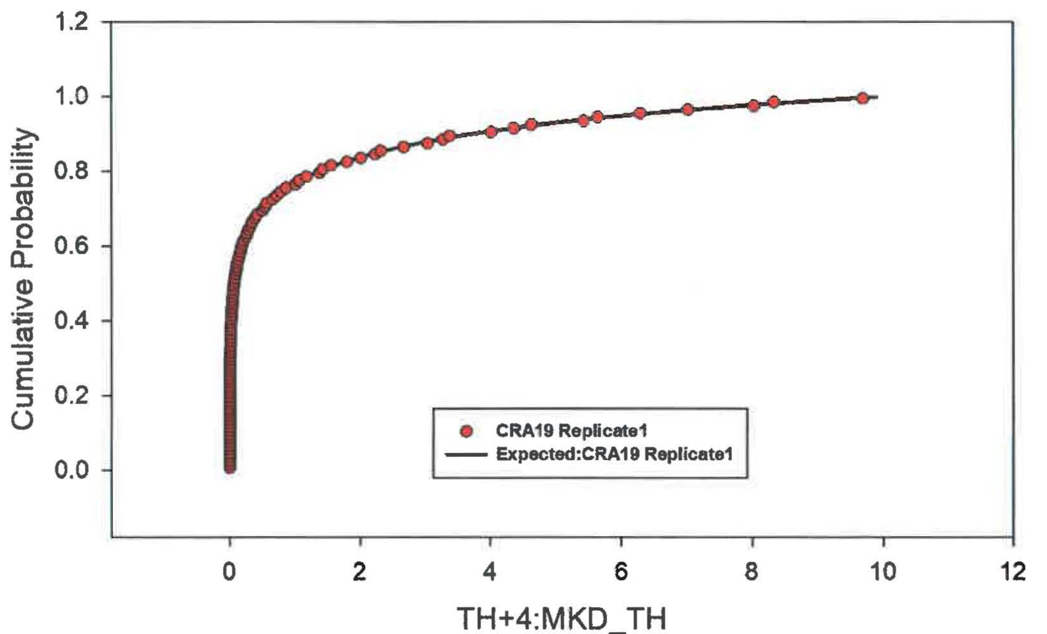

Figure 67 – Observed and Expected CDFs for TH+4:MKD_TH (Loguniform Distribution) Replicate 1.

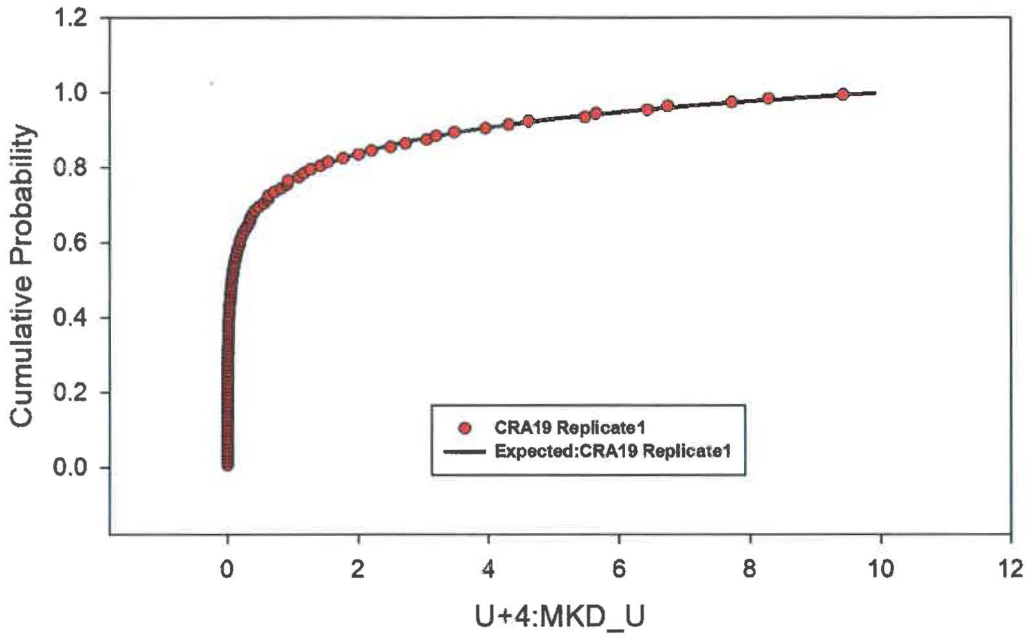

Figure 68 – Observed and Expected CDFs for U+4:MKD_U (Loguniform Distribution) Replicate 1.

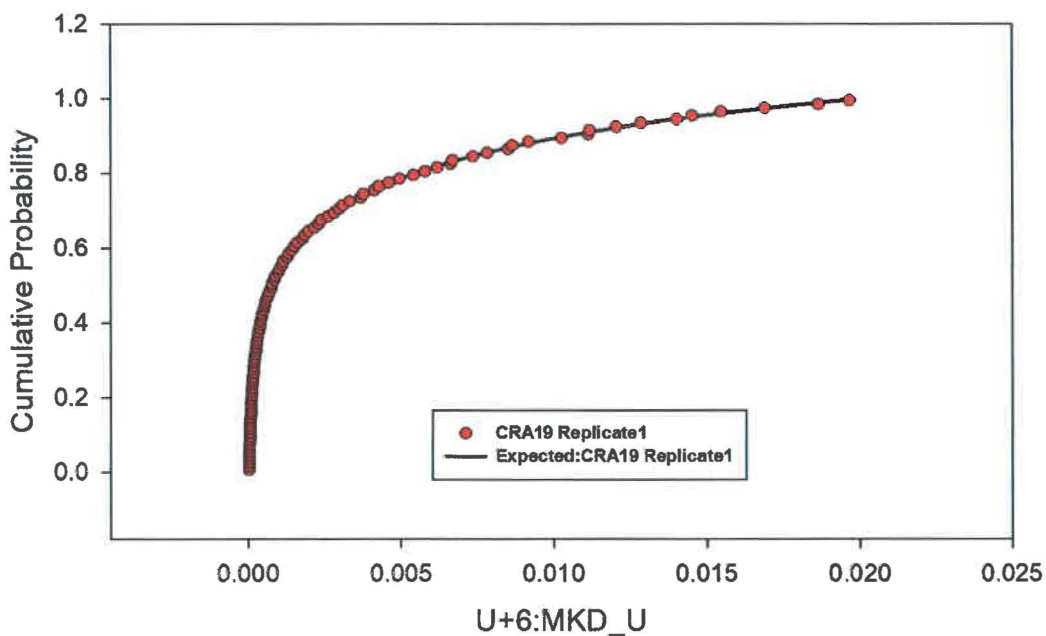

Figure 69 – Observed and Expected CDFs for U+6:MKD_U (Loguniform Distribution) Replicate 1.

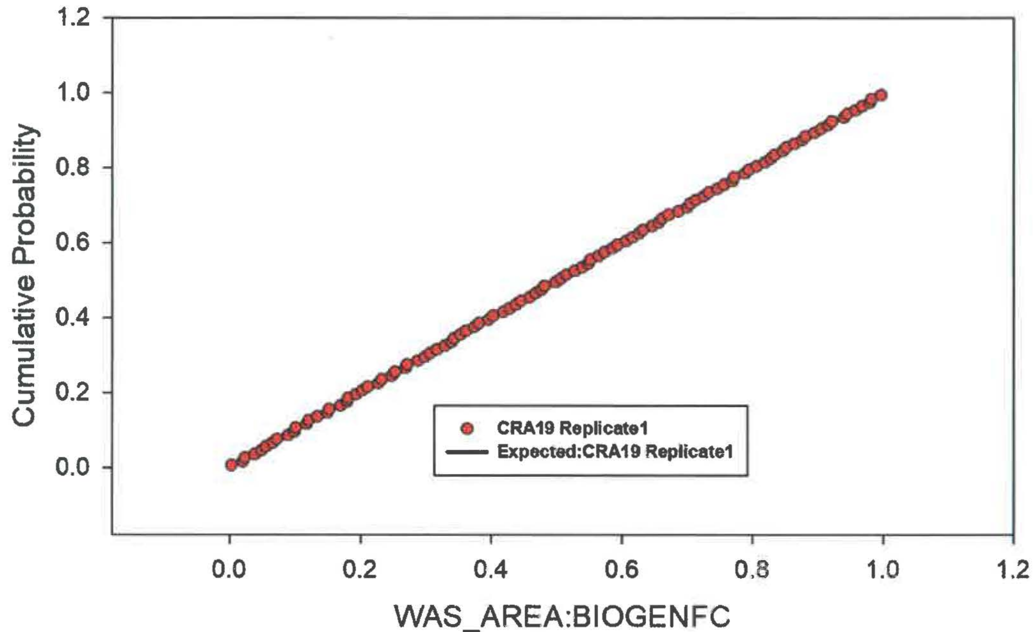

Figure 70 – Observed and Expected CDFs for WAS_AREA:BIOGENFC (Uniform Distribution) Replicate 1.

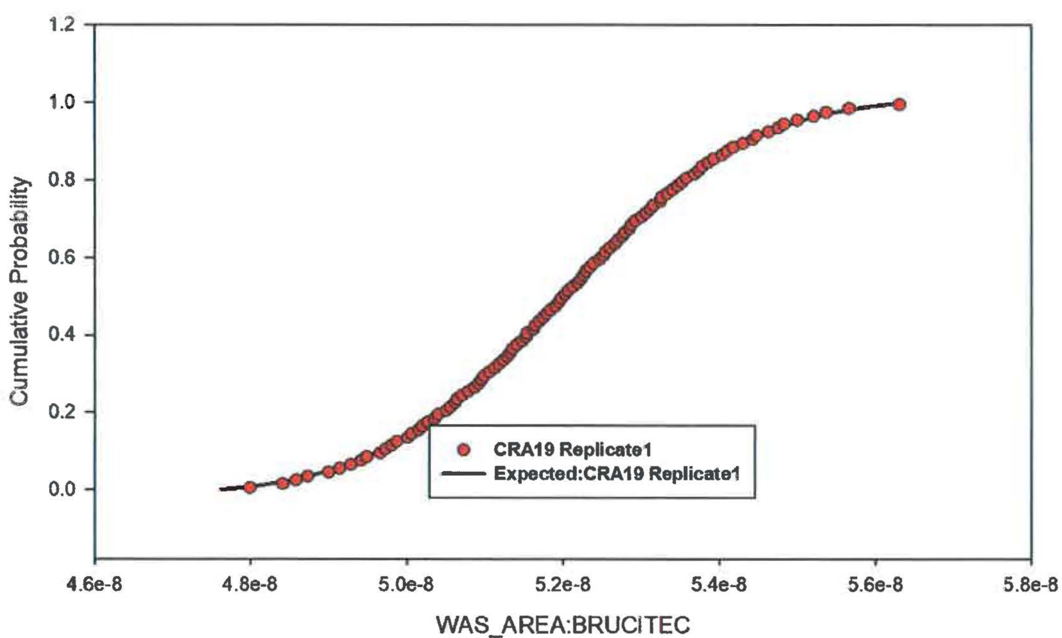

Figure 71 – Observed and Expected CDFs for WAS_AREA:BRUCITEC (Normal Distribution) Replicate 1.

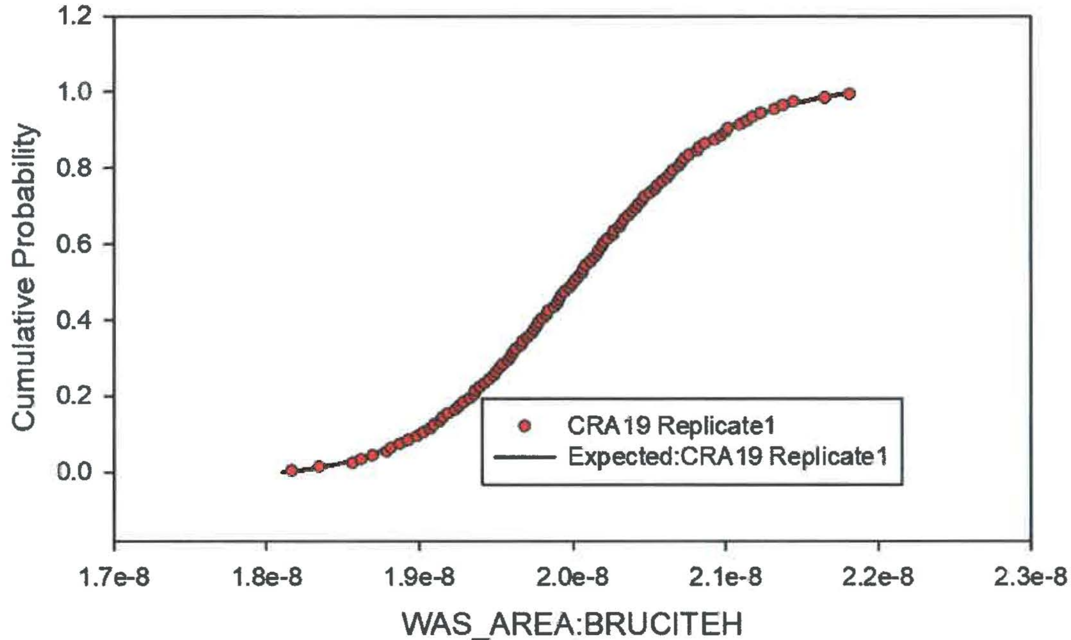

Figure 72 – Observed and Expected CDFs for WAS_AREA:BRUCITEH (Normal Distribution) Replicate 1.

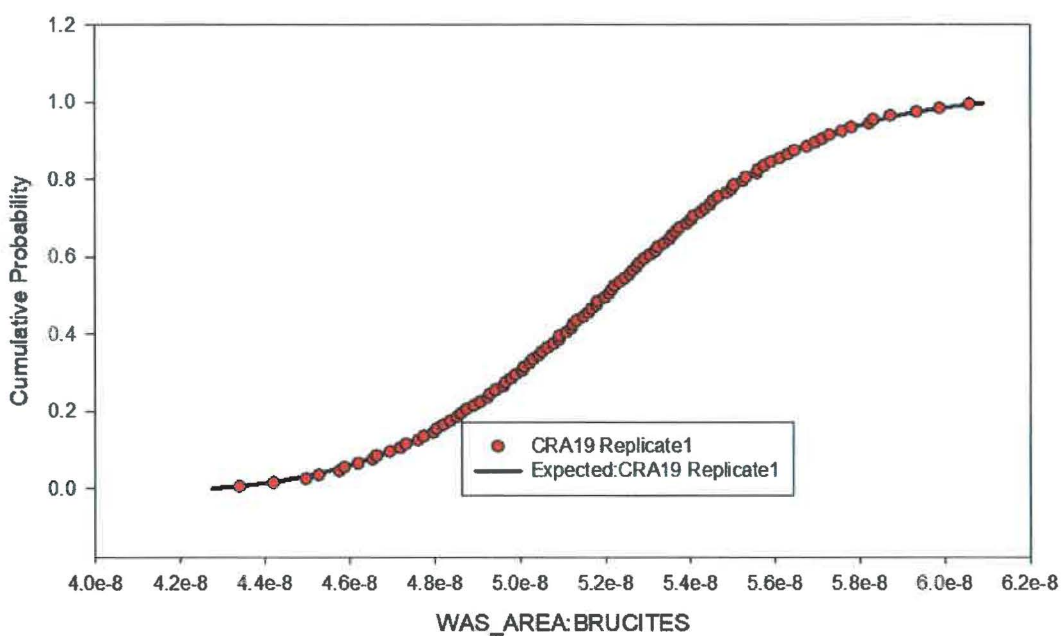

Figure 73 – Observed and Expected CDFs for WAS_AREA:BRUCITES (Normal Distribution) Replicate 1.

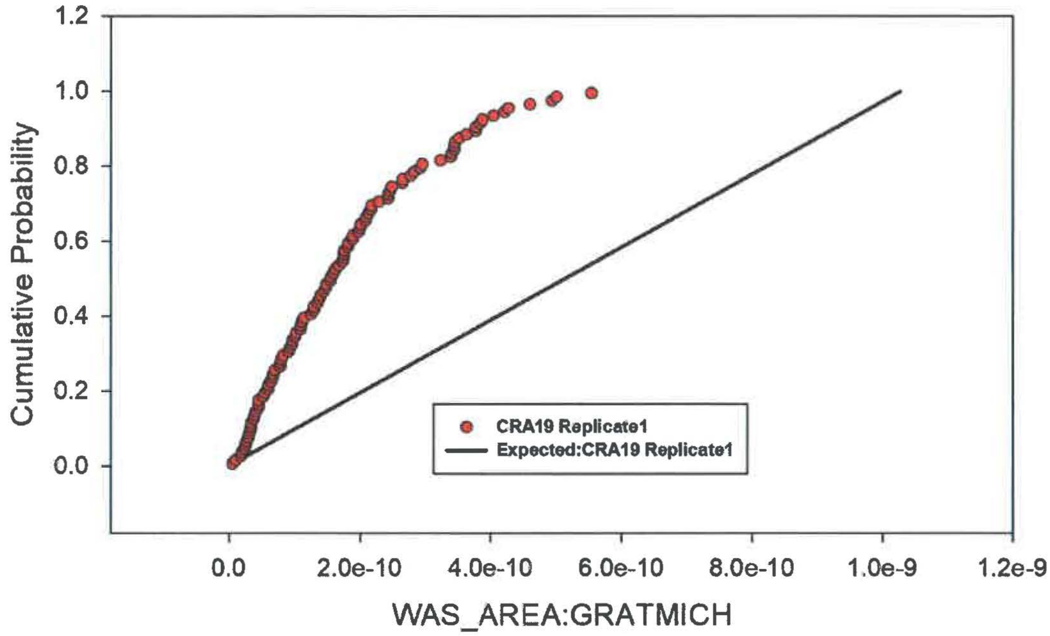

Figure 74 – Observed and Expected CDFs for WAS_AREA:GRATMICH (Uniform Distribution) Replicate 1.

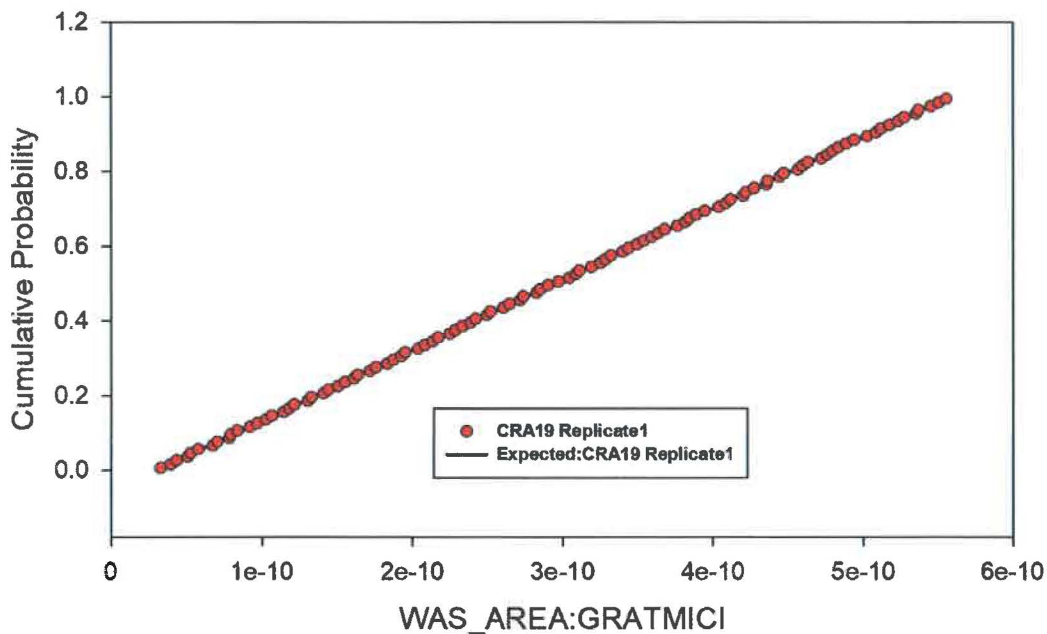

Figure 75 – Observed and Expected CDFs for WAS_AREA:GRATMICI (Uniform Distribution) Replicate 1.

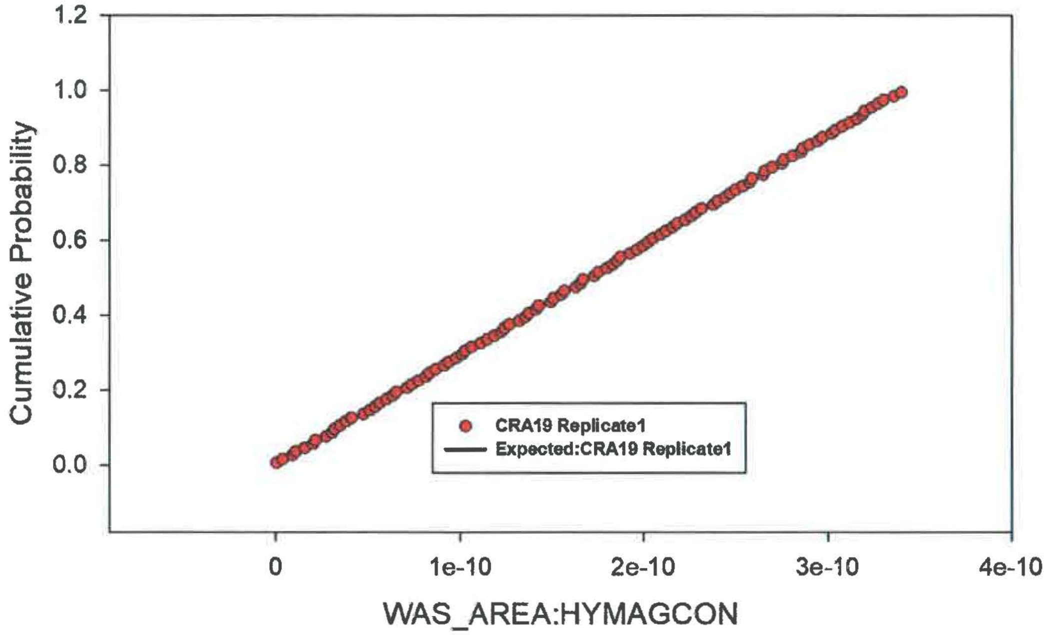

Figure 76 – Observed and Expected CDFs for WAS_AREA:HYMAGCON (Uniform Distribution) Replicate 1.

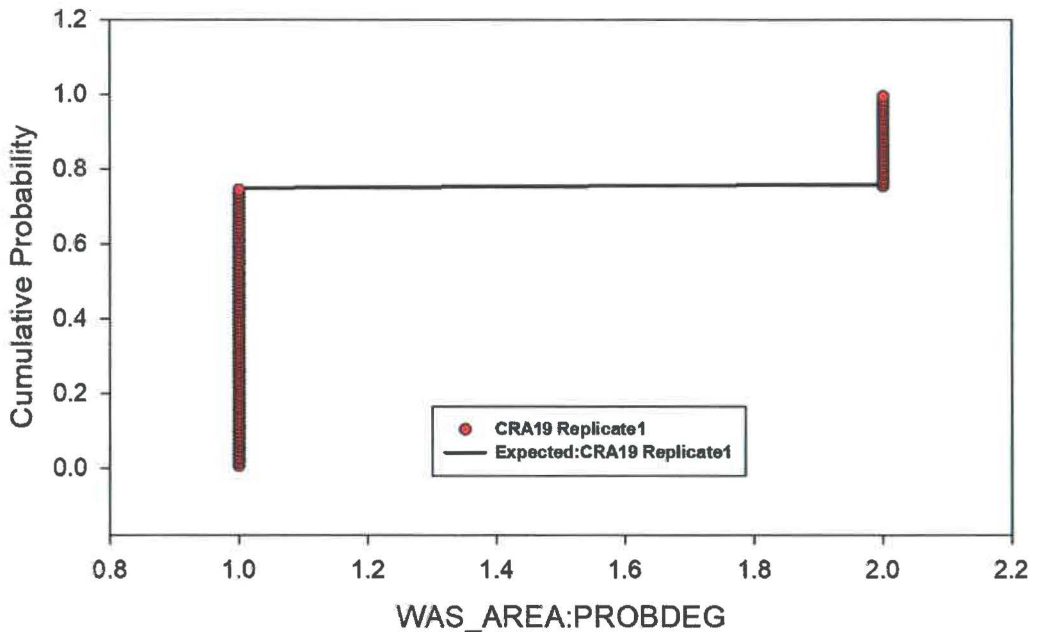

Figure 77 – Observed and Expected CDFs for WAS_AREA:PROBDEG (Delta Distribution) Replicate 1.

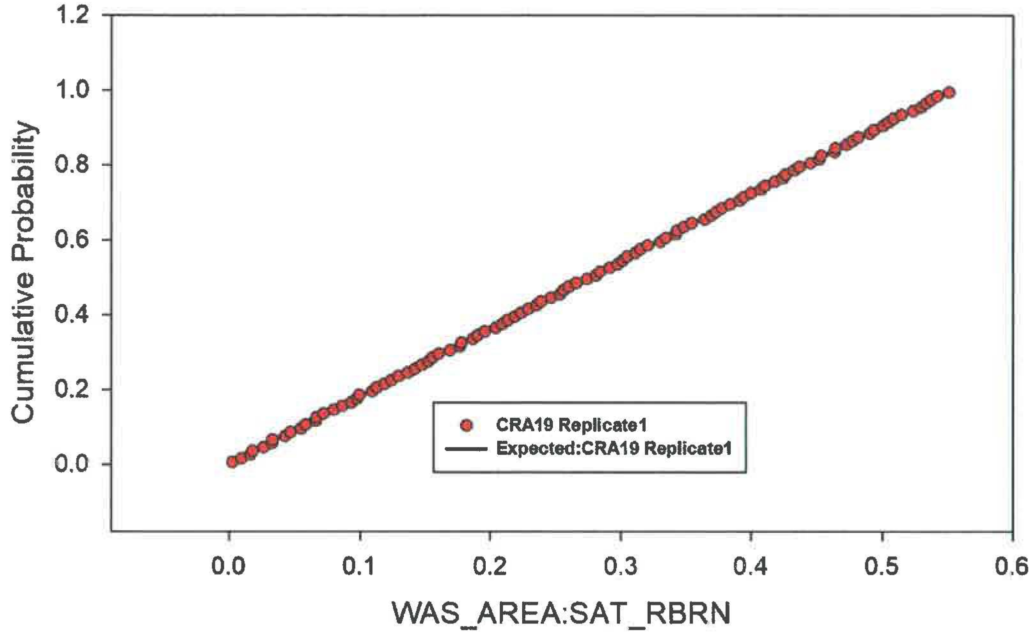

Figure 78 – Observed and Expected CDFs for WAS_AREA:SAT_RBRN (Uniform Distribution) Replicate 1.

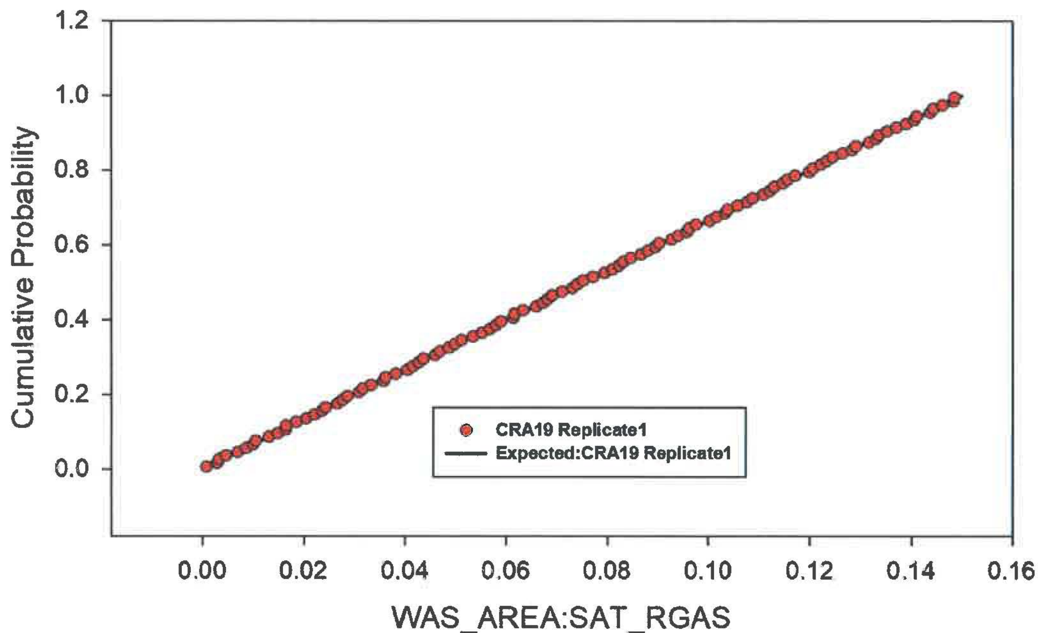

Figure 79 – Observed and Expected CDFs for WAS_AREA:SAT_RGAS (Uniform Distribution) Replicate 1.

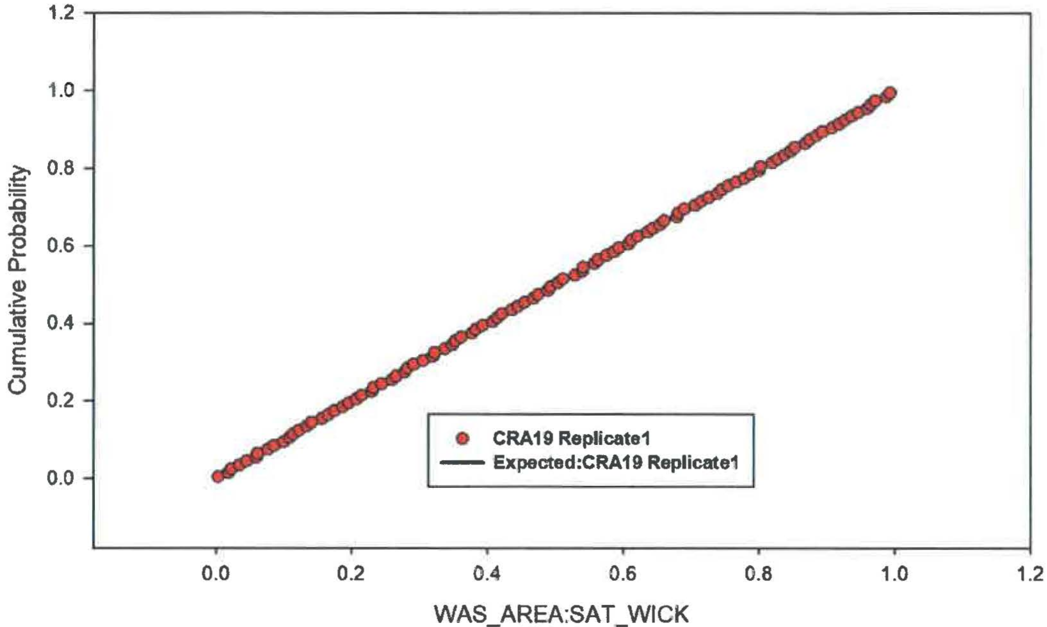

Figure 80 – Observed and Expected CDFs for WAS_AREA:SAT_WICK (Uniform Distribution) Replicate 1.

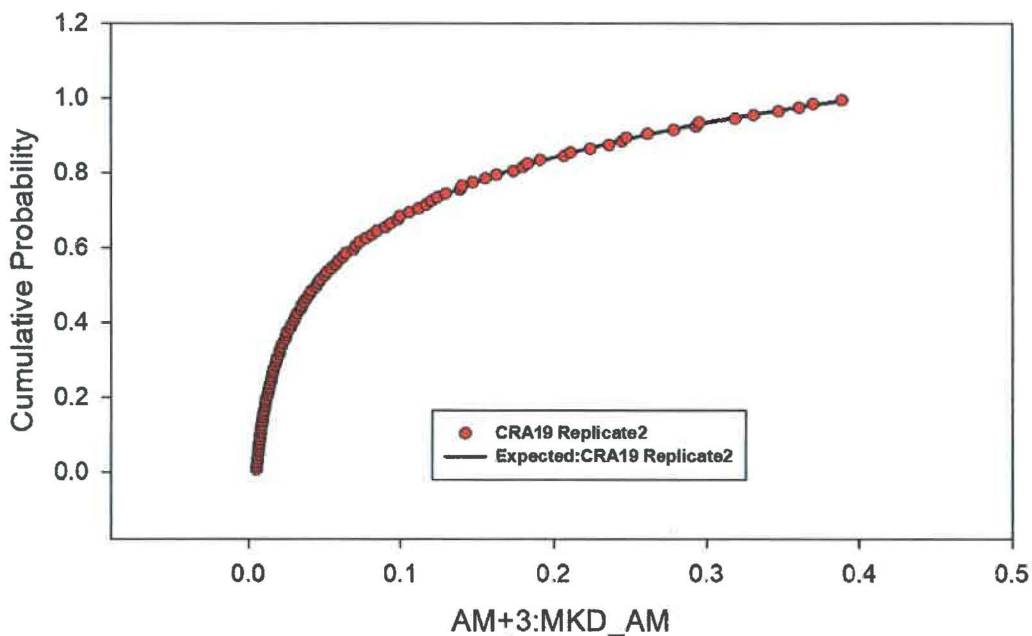

Figure 81 – Observed and Expected CDFs for AM+3:MKD_AM (Loguniform Distribution) Replicate 2.

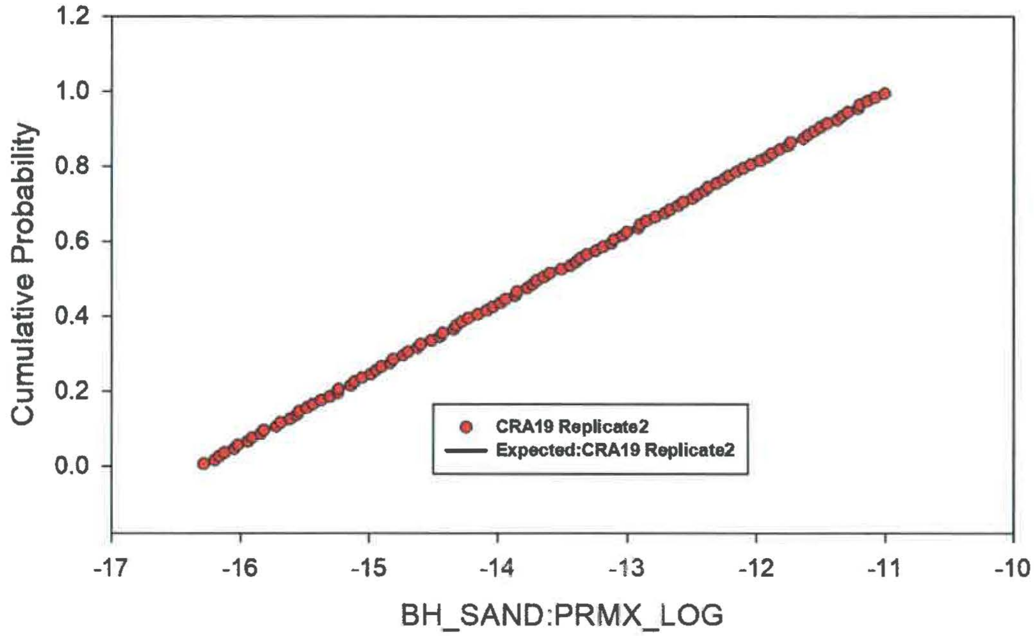

Figure 82 – Observed and Expected CDFs for BH_SAND:PRMX_LOG (Uniform Distribution) Replicate 2.

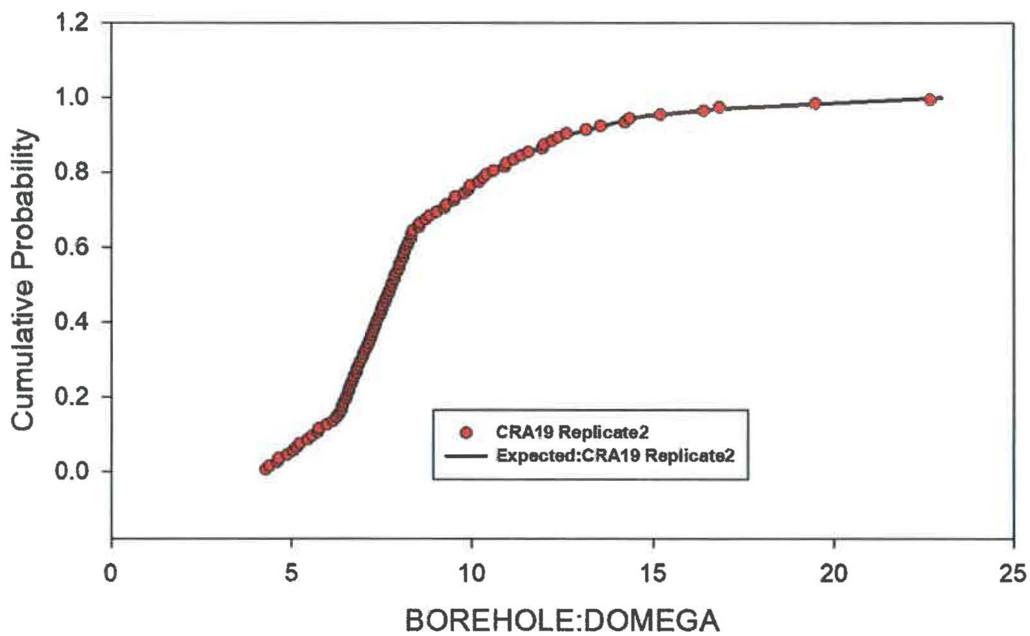

Figure 83 – Observed and Expected CDFs for BOREHOLE:DOMEGA (Cumulative Distribution) Replicate 2.

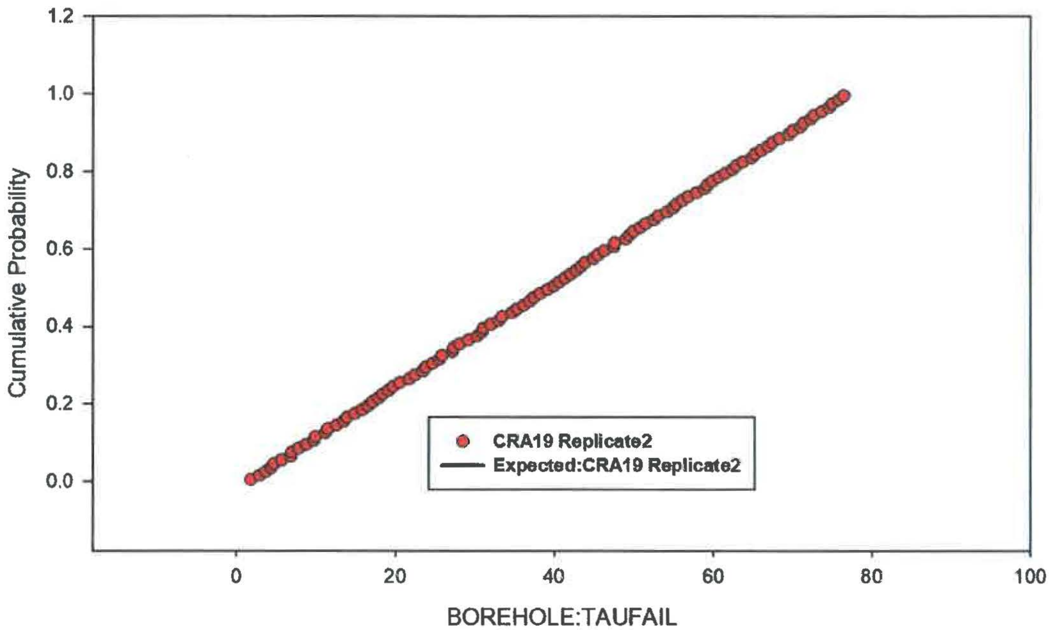

Figure 84 – Observed and Expected CDFs for BOREHOLE:TAUFAIL (Uniform Distribution) Replicate 2.

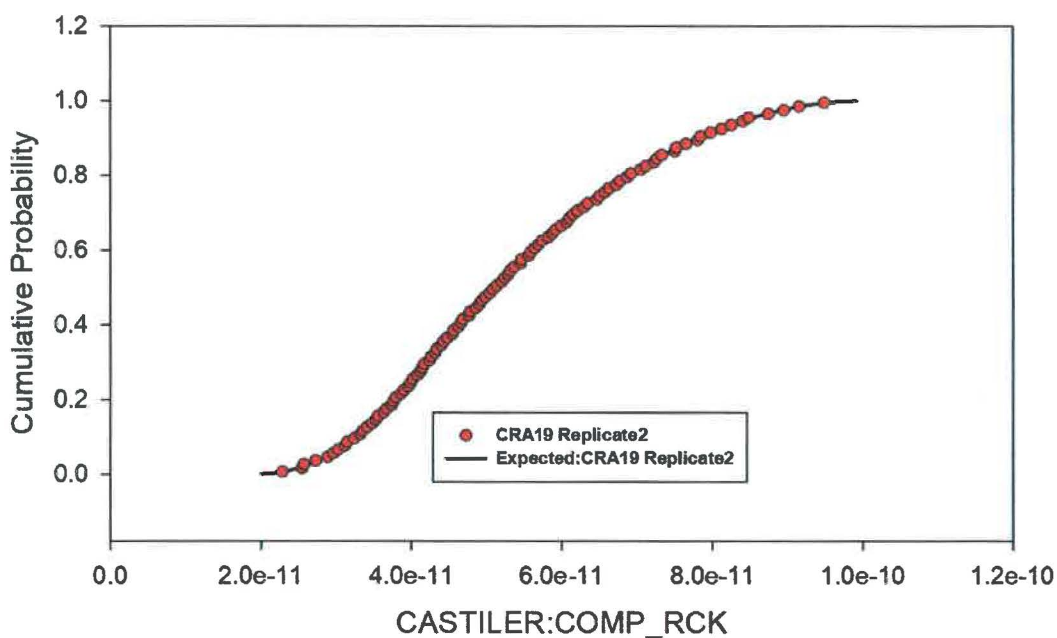

Figure 85 – Observed and Expected CDFs for CASTILER:COMP_RCK (Triangular Distribution) Replicate 2.

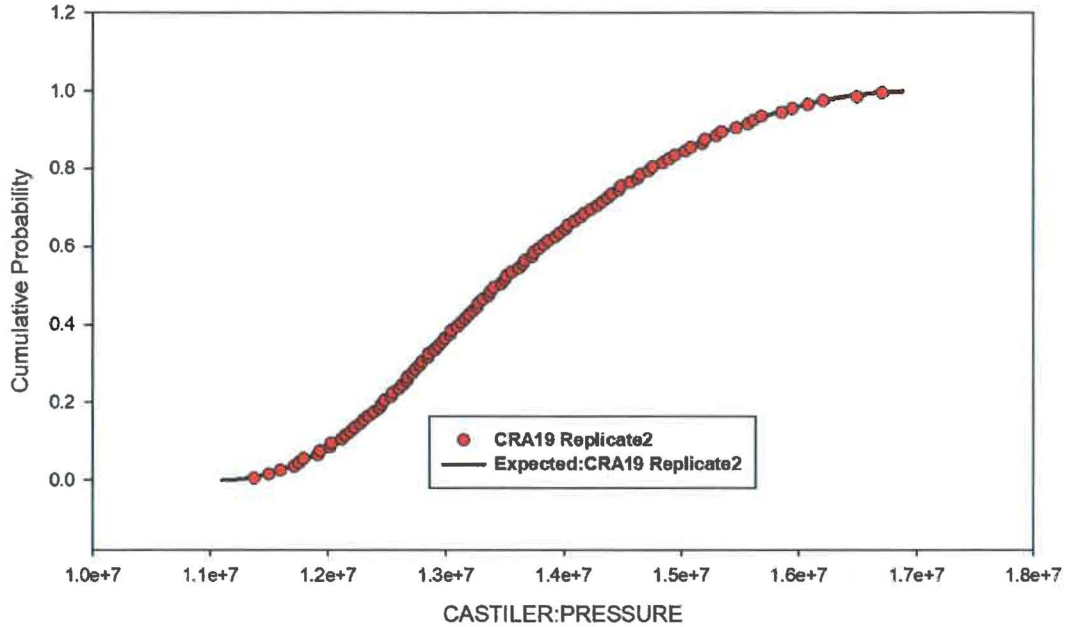

Figure 86 – Observed and Expected CDFs for CASTILER:PRESSURE (Triangular Distribution) Replicate 2.

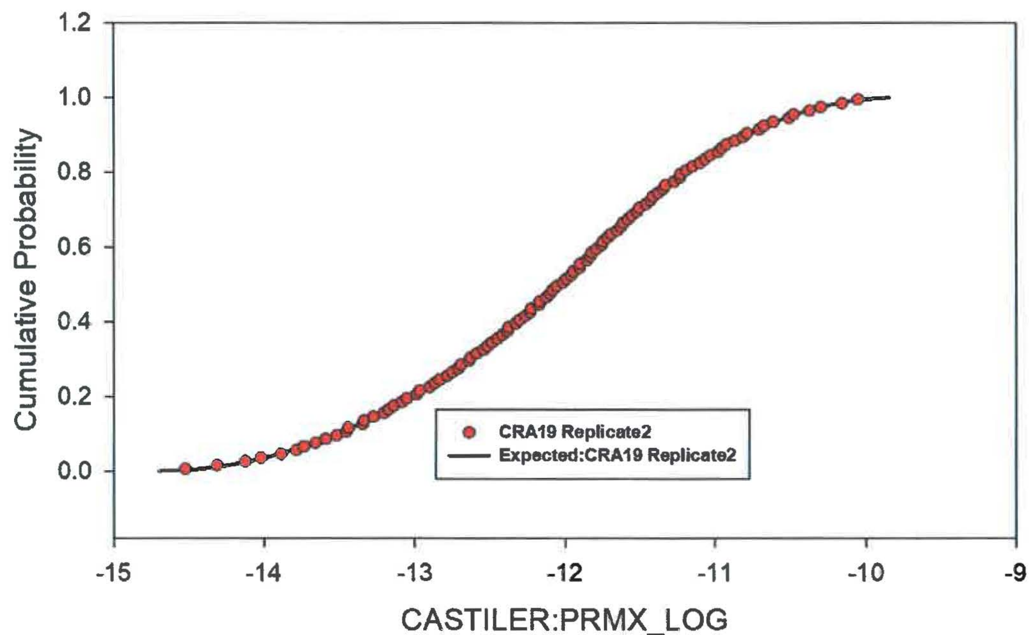

Figure 87 – Observed and Expected CDFs for CASTILER:PRMX_LOG (Triangular Distribution) Replicate 2.

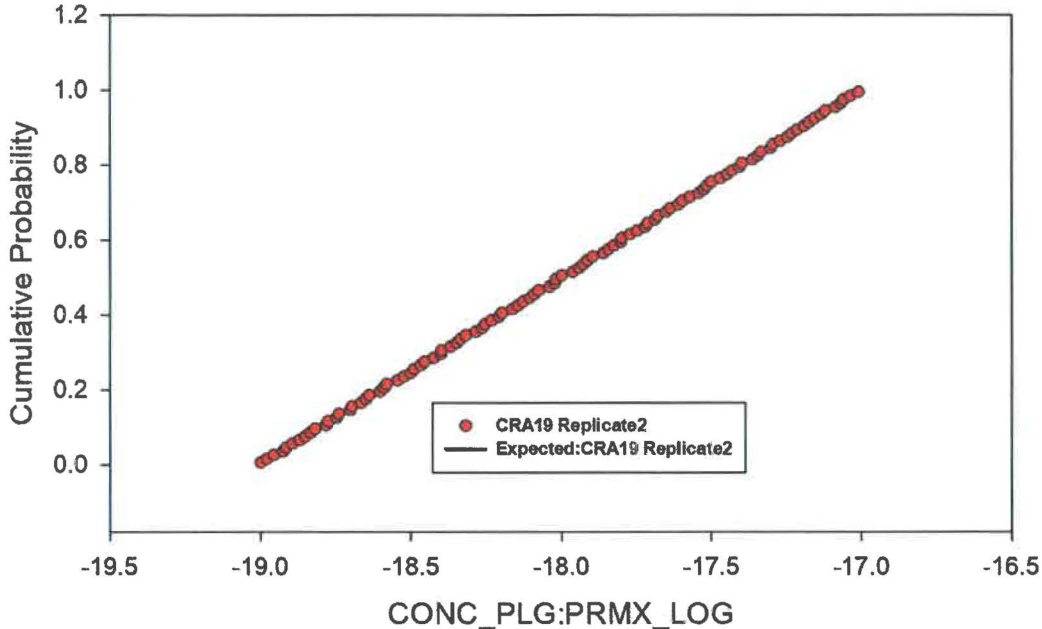

Figure 88 – Observed and Expected CDFs for CONC_PLG:PRMX_LOG (Uniform Distribution) Replicate 2.

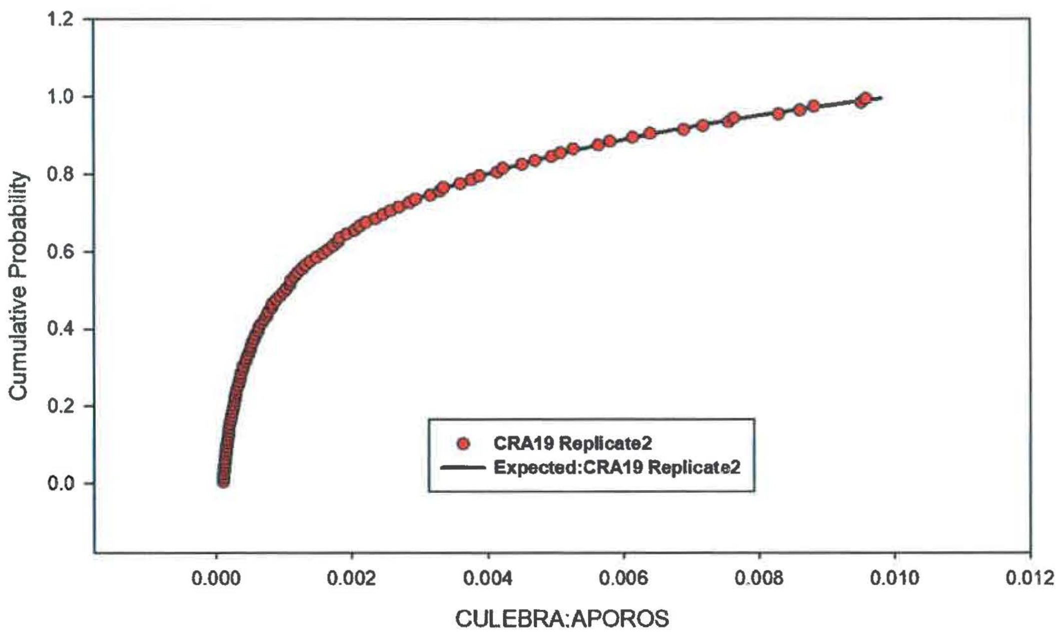

Figure 89 – Observed and Expected CDFs for CULEBRA:APOROS (Loguniform Distribution) Replicate 2.

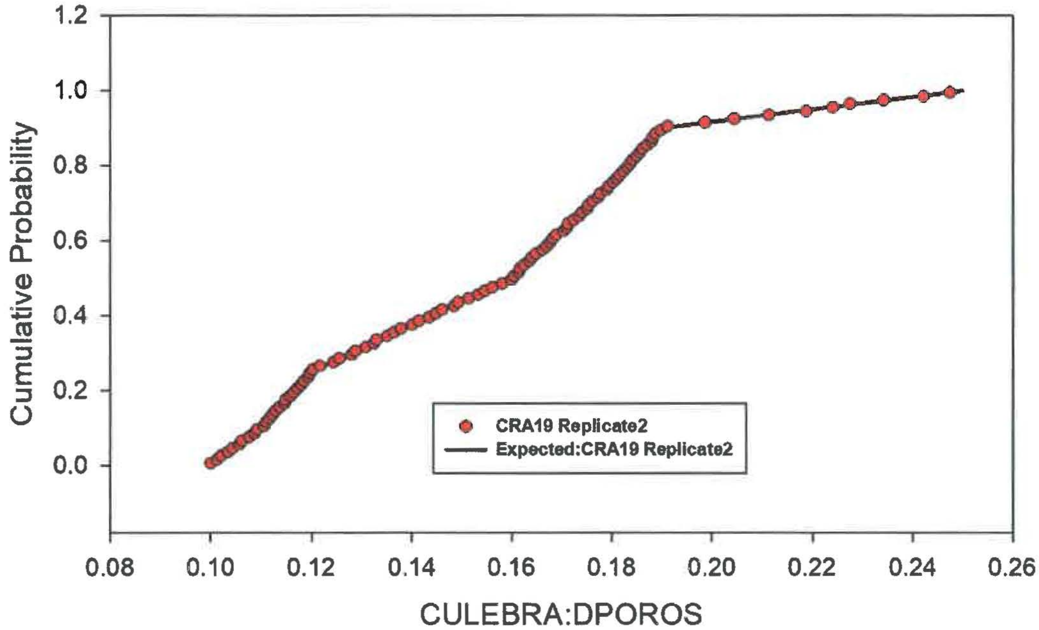

Figure 90 – Observed and Expected CDFs for CULEBRA:DPOROS (Cumulative Distribution) Replicate 2.

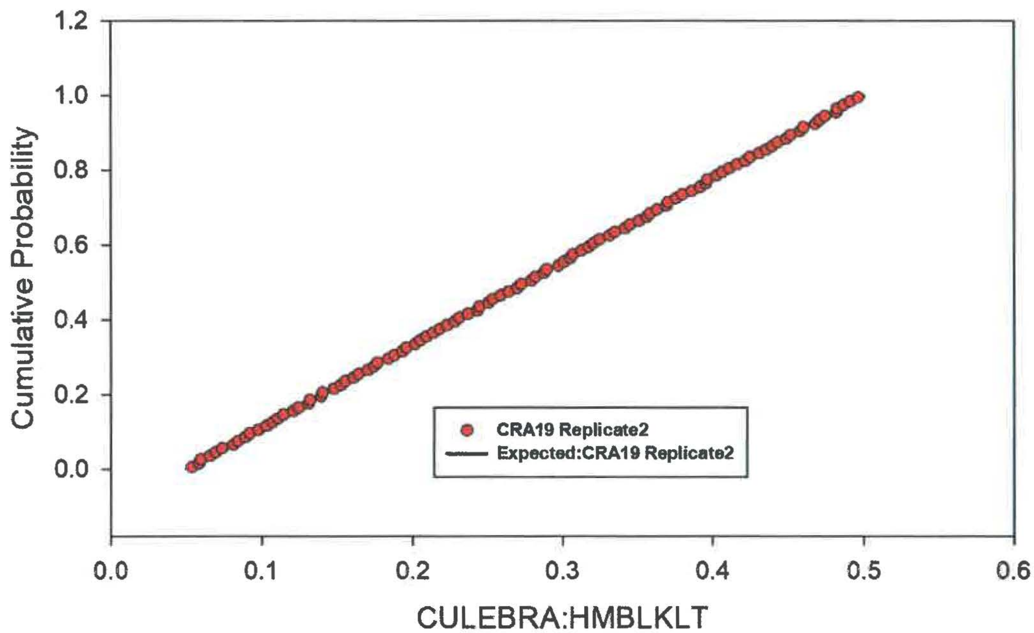

Figure 91 – Observed and Expected CDFs for CULEBRA:HMBLKLT (Uniform Distribution) Replicate 2.

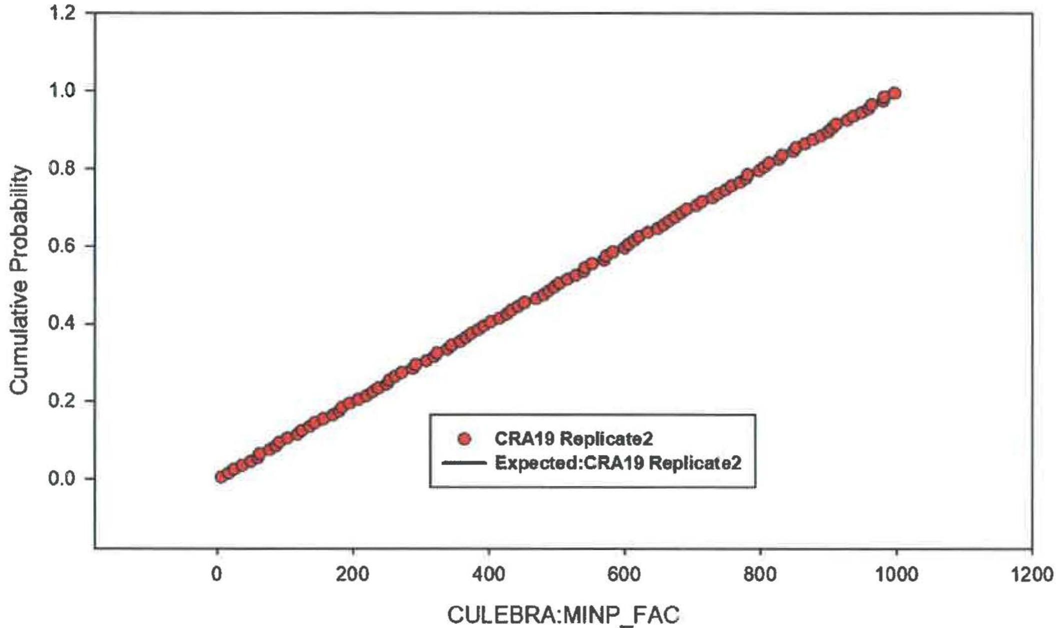

Figure 92 – Observed and Expected CDFs for CULEBRA:MINP_FAC (Uniform Distribution) Replicate 2.

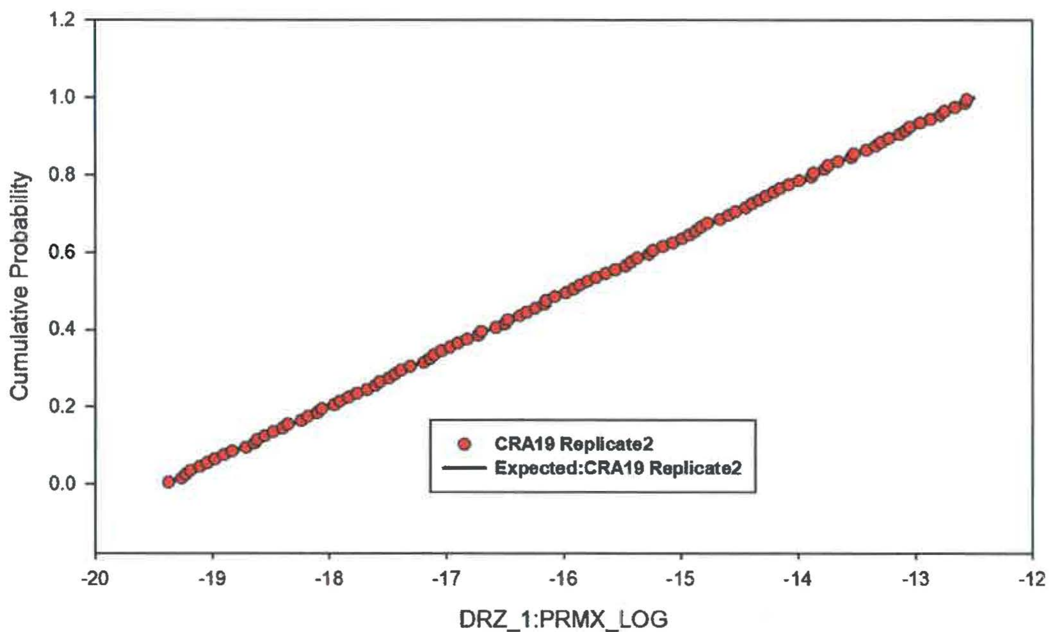

Figure 93 – Observed and Expected CDFs for DRZ_1:PRMX_LOG (Uniform Distribution) Replicate 2.

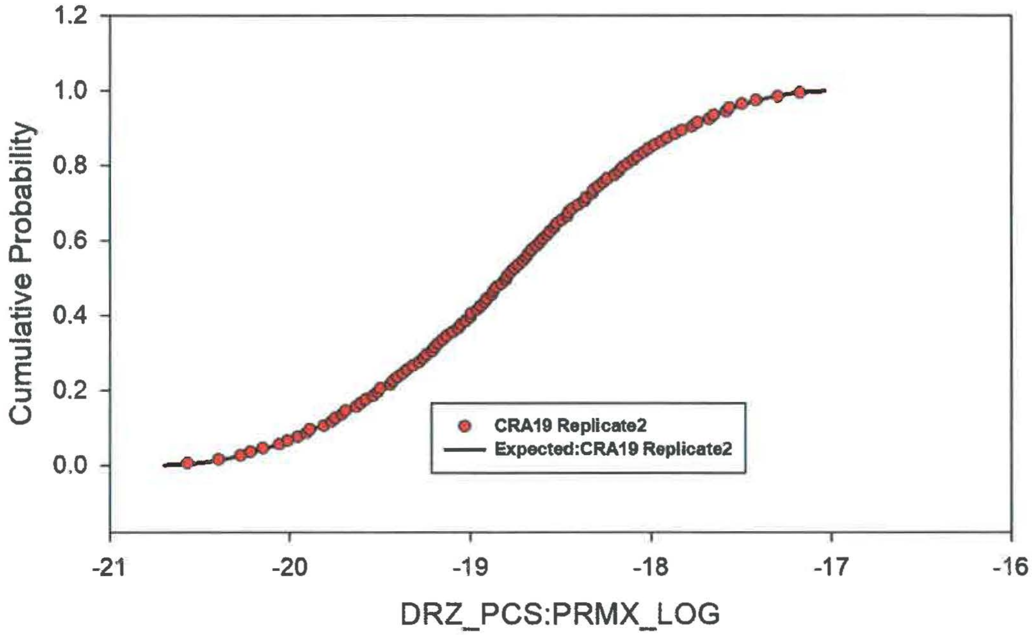

Figure 94 – Observed and Expected CDFs for DRZ_PCS:PRMX_LOG (Triangular Distribution) Replicate 2.

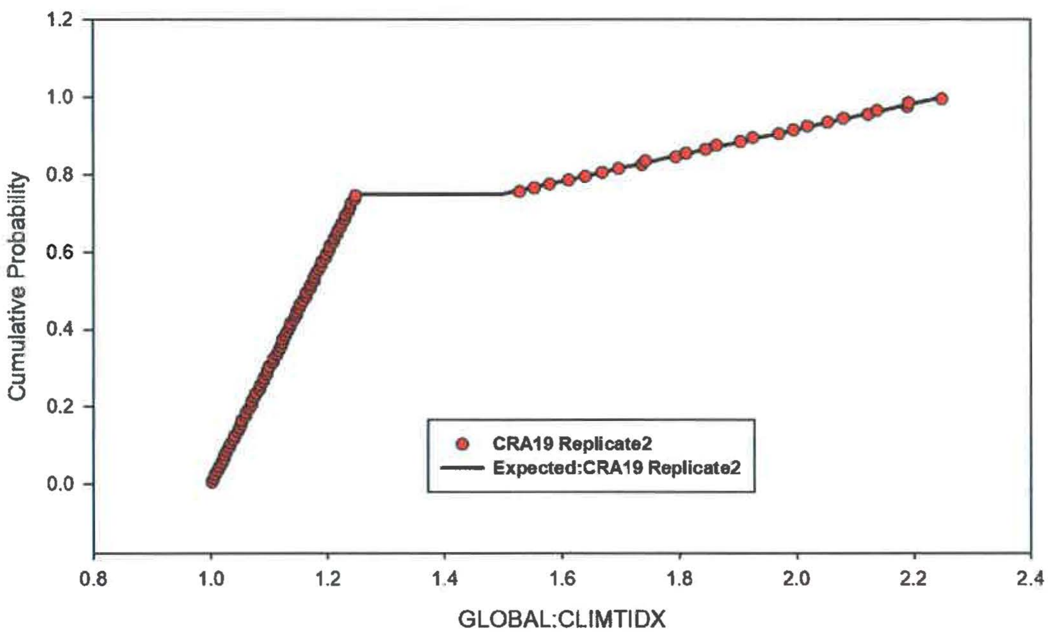

Figure 95 – Observed and Expected CDFs for GLOBAL:CLIMTIDX (Cumulative Distribution) Replicate 2.

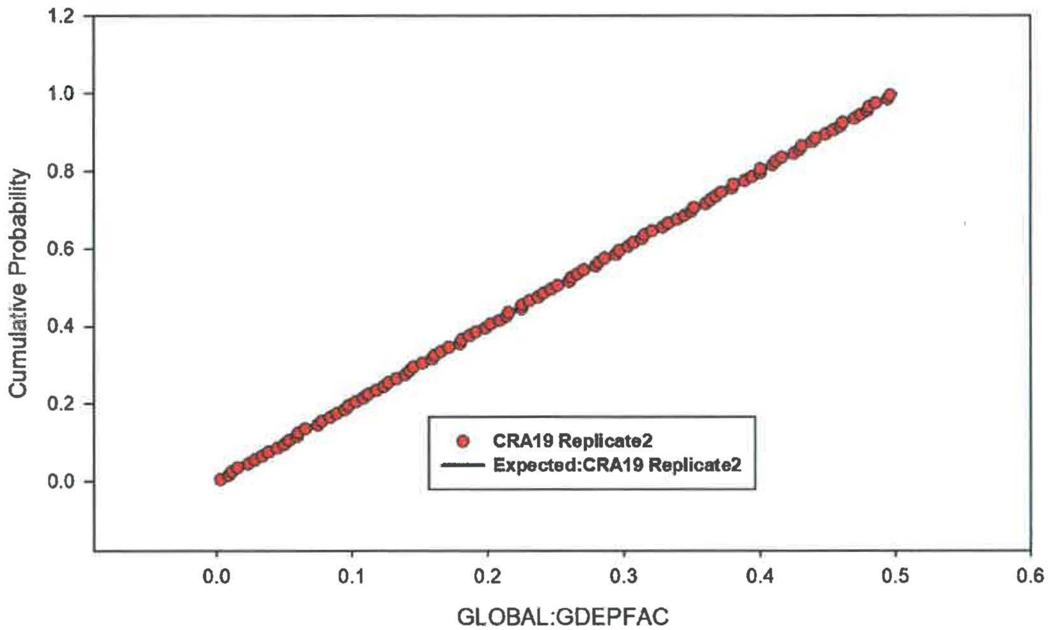

Figure 96 – Observed and Expected CDFs for GLOBAL:GDEPFAC (Uniform Distribution) Replicate 2.

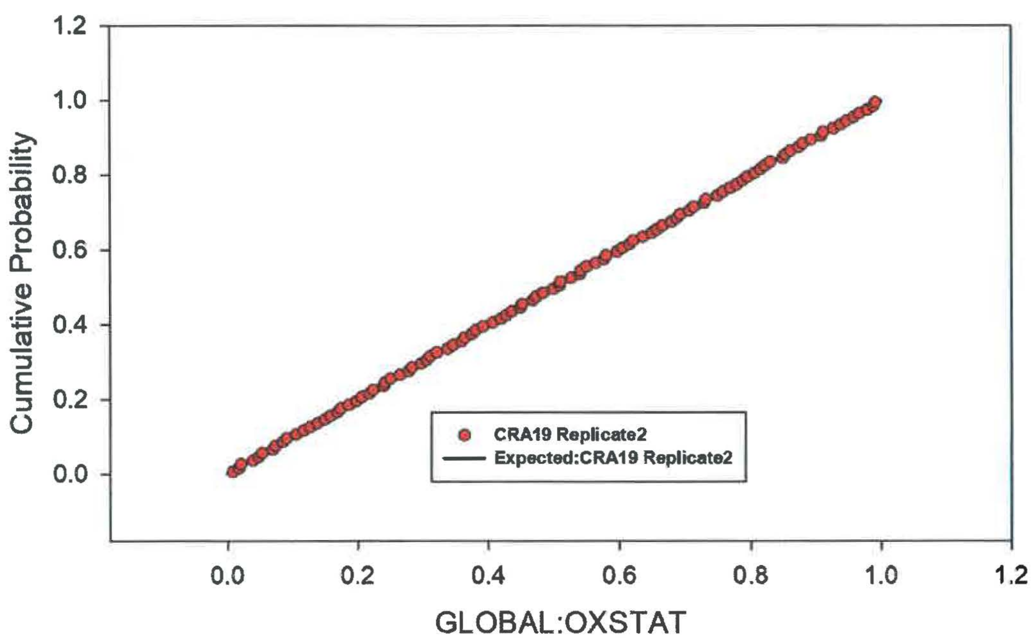

Figure 97 – Observed and Expected CDFs for GLOBAL:OXSTAT (Uniform Distribution) Replicate 2.

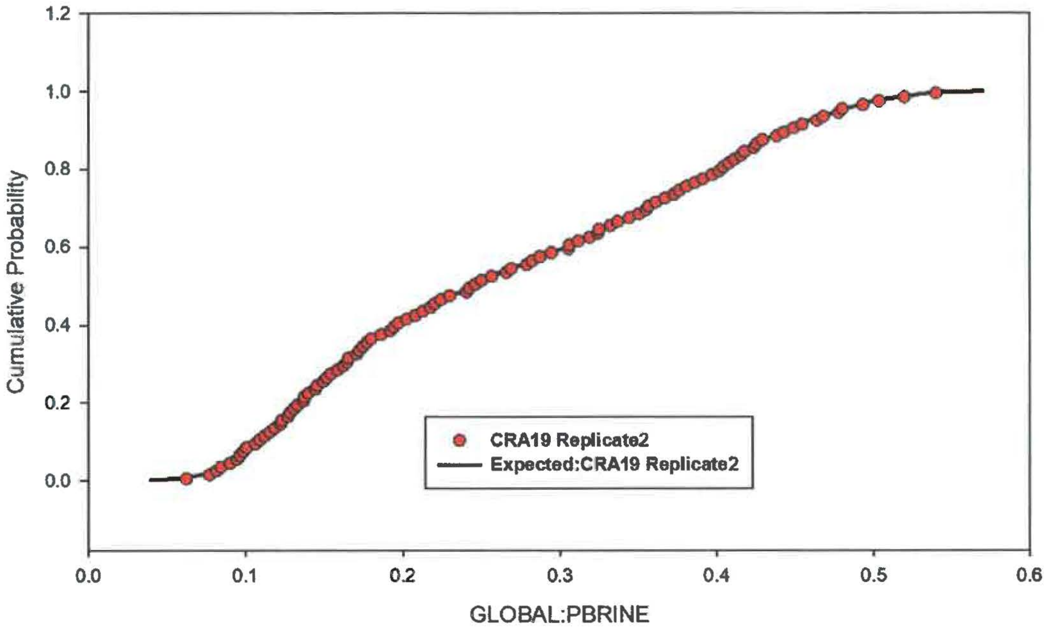

Figure 98 – Observed and Expected CDFs for GLOBAL:PBRINE (Cumulative Distribution) Replicate 2.

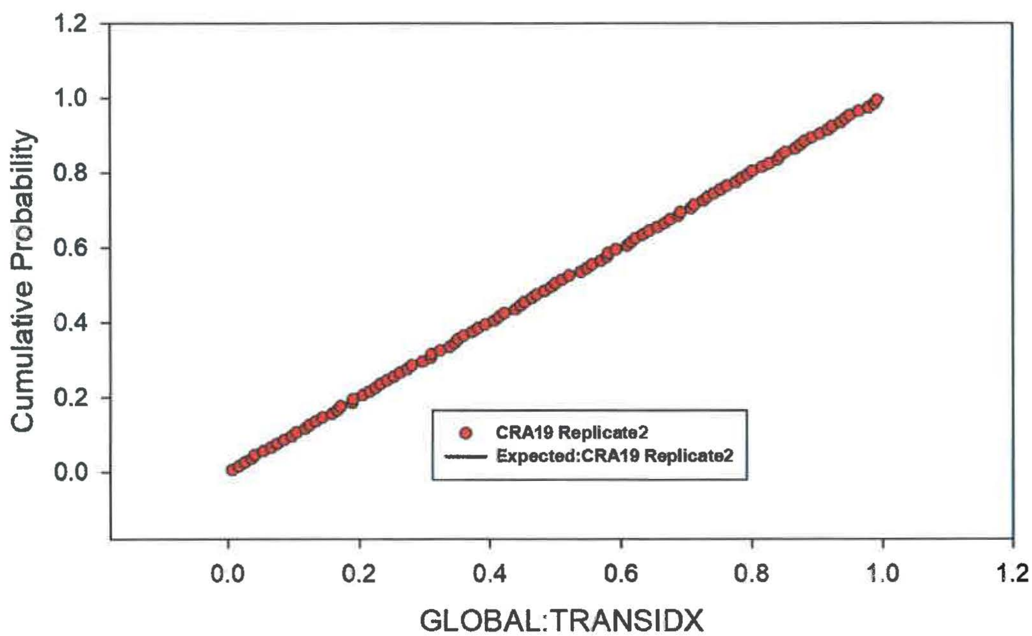

Figure 99 – Observed and Expected CDFs for GLOBAL:TRANSIDX (Uniform Distribution) Replicate 2.

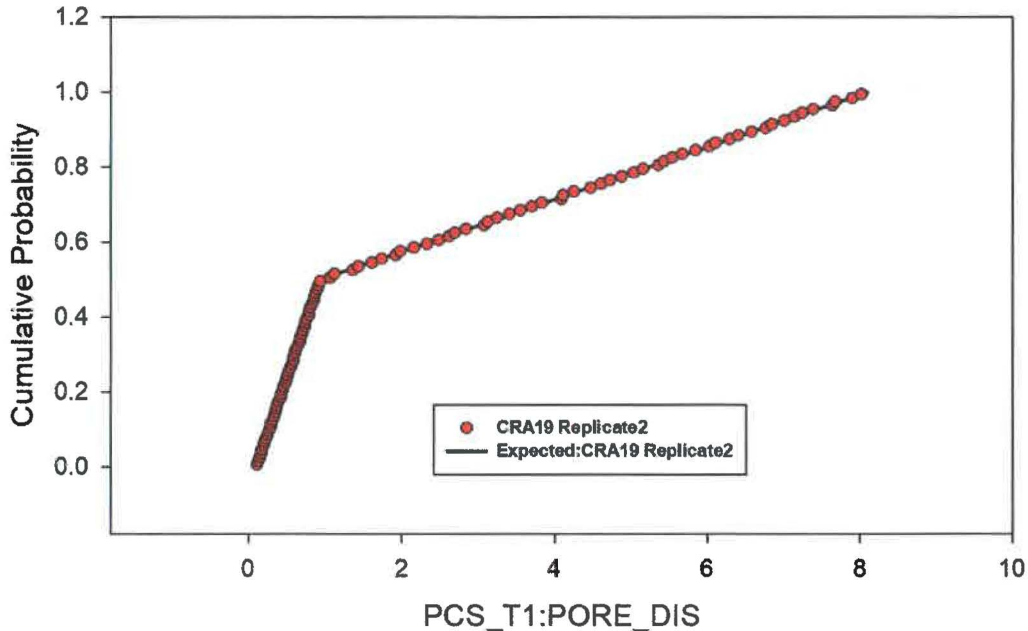

Figure 100 – Observed and Expected CDFs for PCS_T1:PORE_DIS (Cumulative Distribution) Replicate 2.

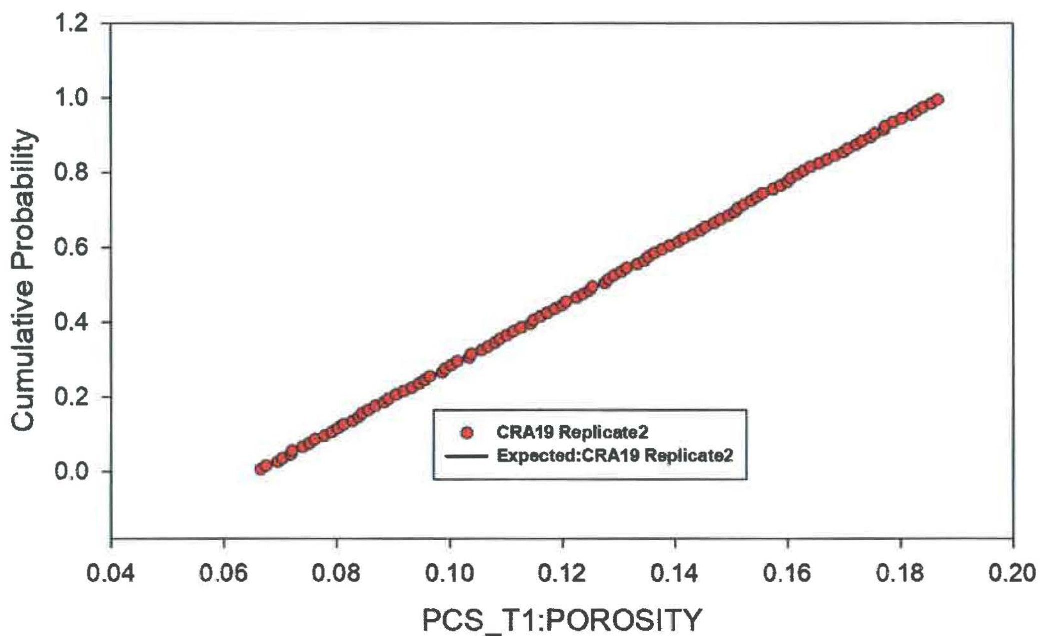

Figure 101 – Observed and Expected CDFs for PCS_T1:POROSITY (Uniform Distribution) Replicate 2.

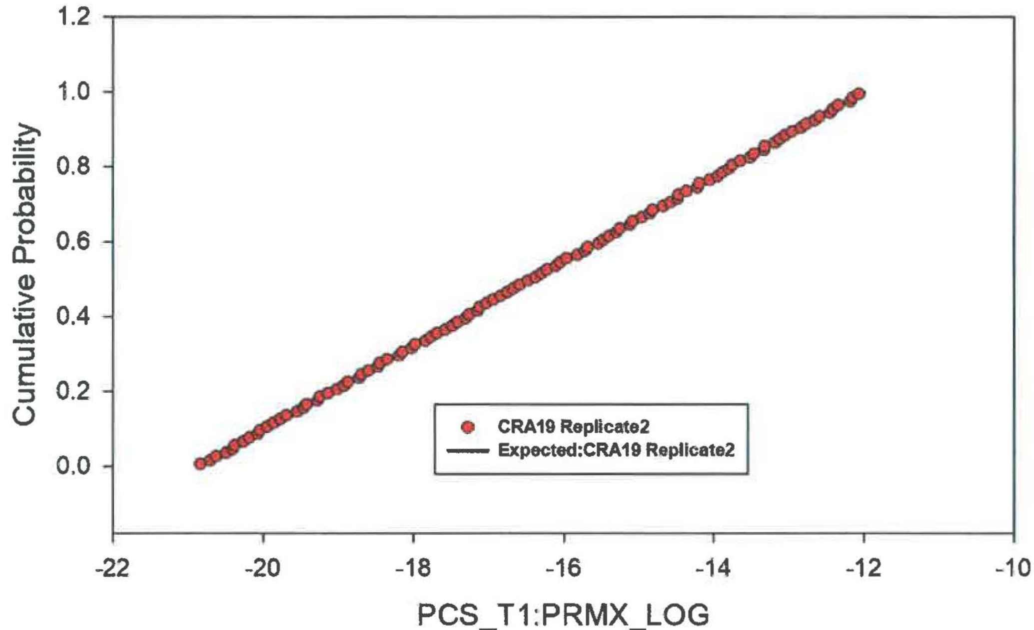

Figure 102 – Observed and Expected CDFs for PCS_T1:PRMX_LOG (Uniform Distribution) Replicate 2.

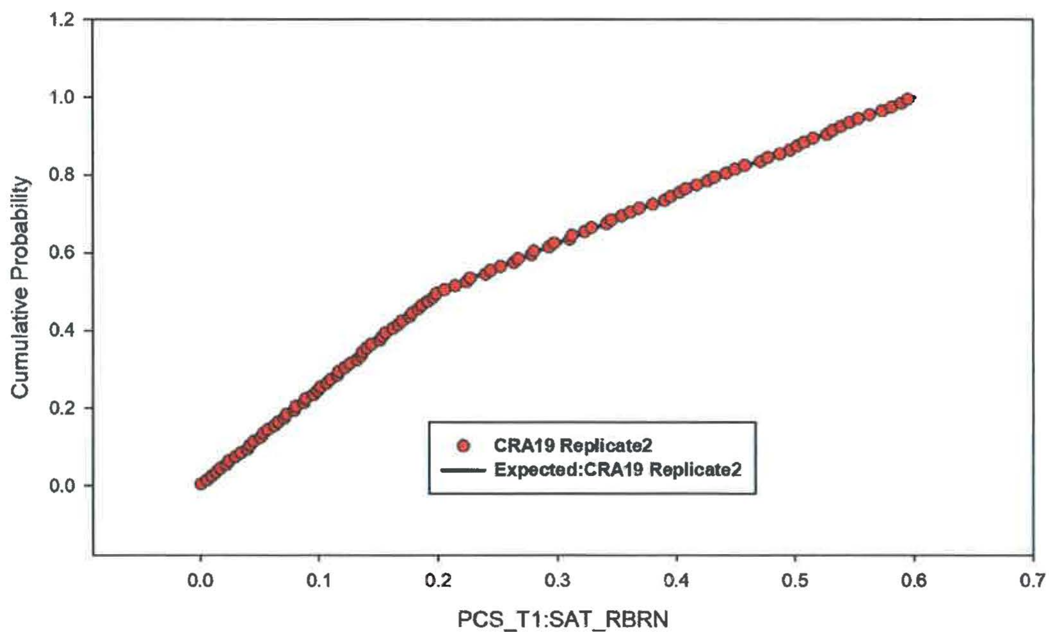

Figure 103 – Observed and Expected CDFs for PCS_T1:SAT_RBRN (Cumulative Distribution) Replicate 2.

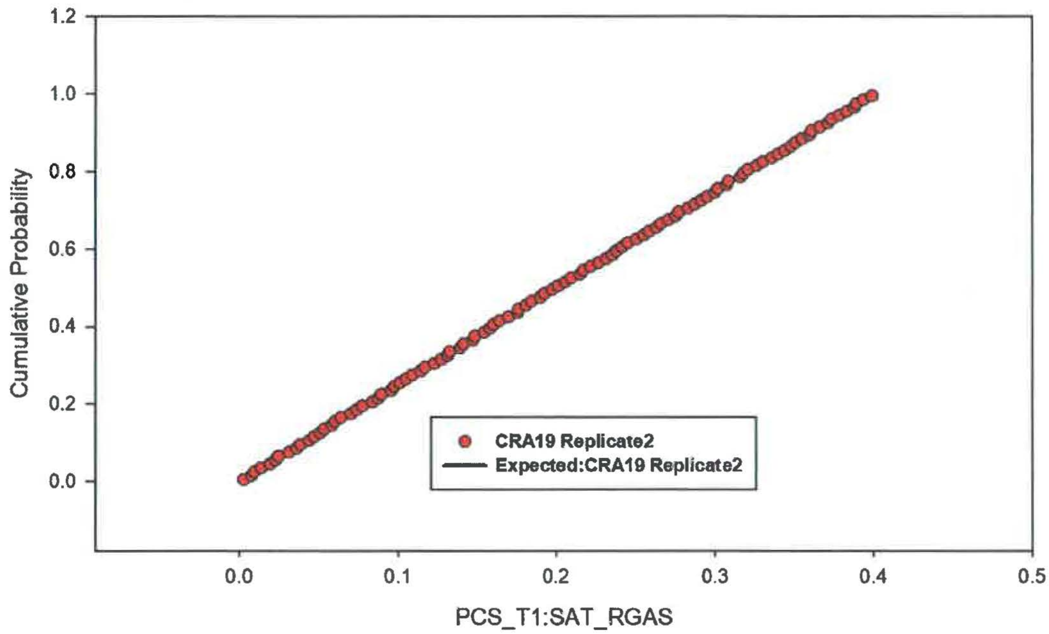

Figure 104 – Observed and Expected CDFs for PCS_T1:SAT_RGAS (Uniform Distribution) Replicate 2.

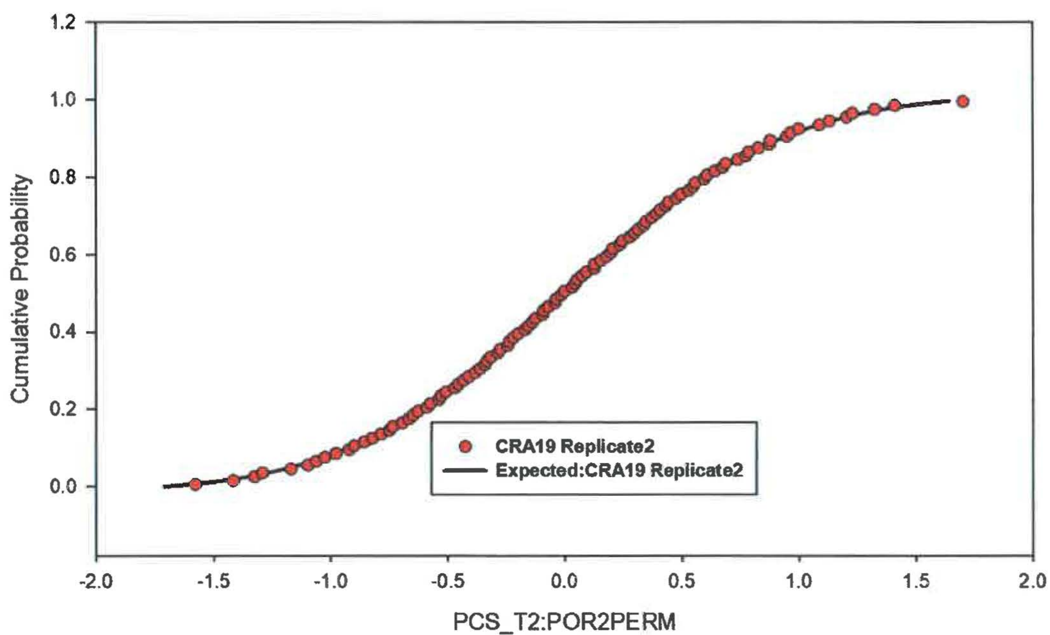

Figure 105 – Observed and Expected CDFs for PCS_T2:POR2PERM (Normal Distribution) Replicate 2.

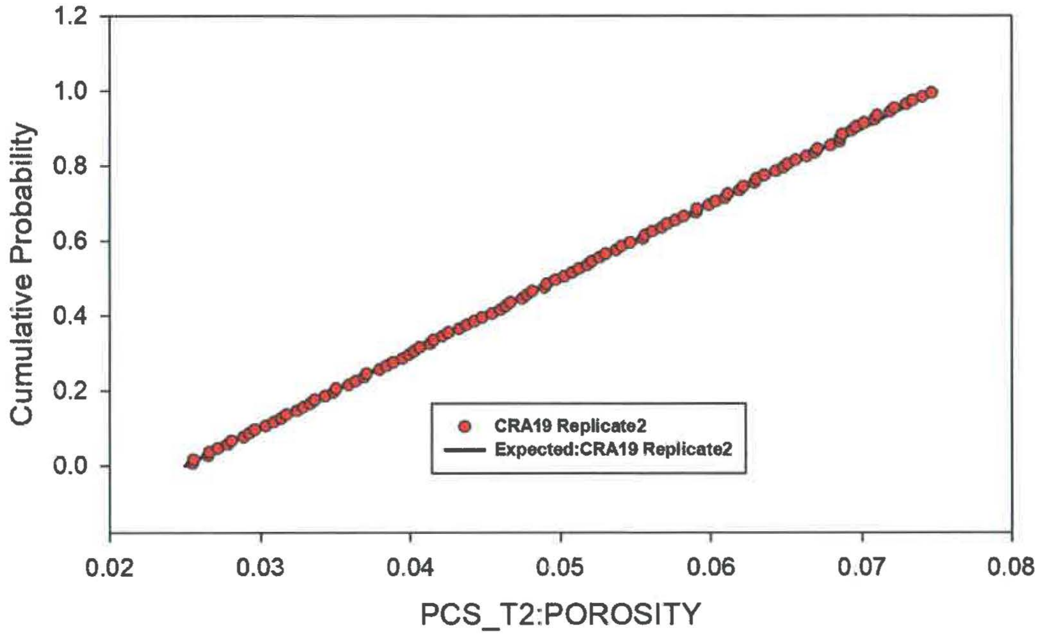

Figure 106 – Observed and Expected CDFs for PCS_T2:POROSITY (Uniform Distribution) Replicate 2.

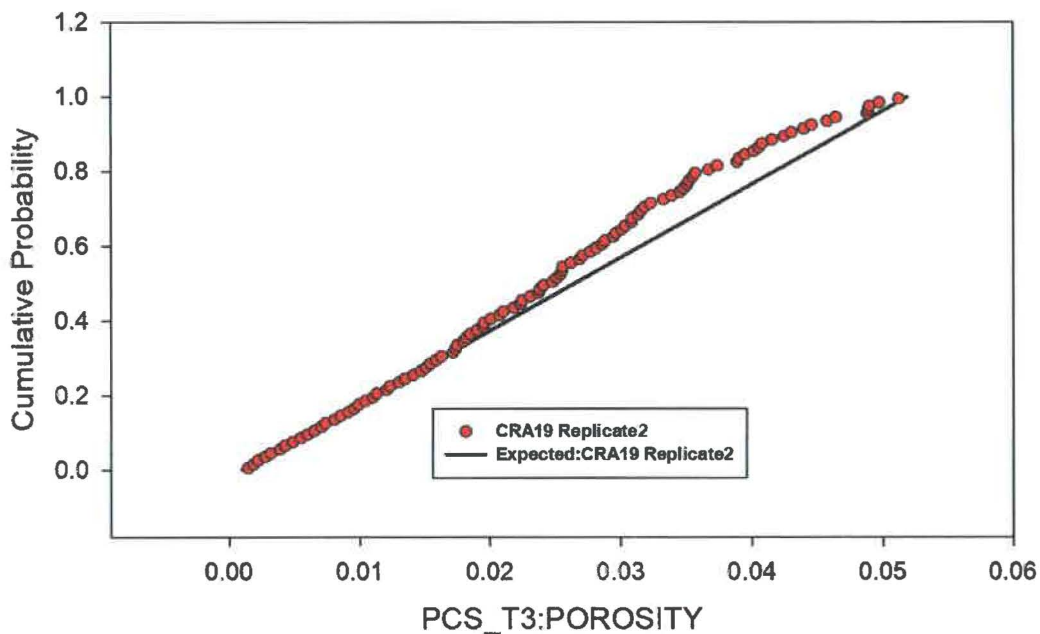

Figure 107 – Observed and Expected CDFs for PCS_T3:POROSITY (Uniform Distribution) Replicate 2.

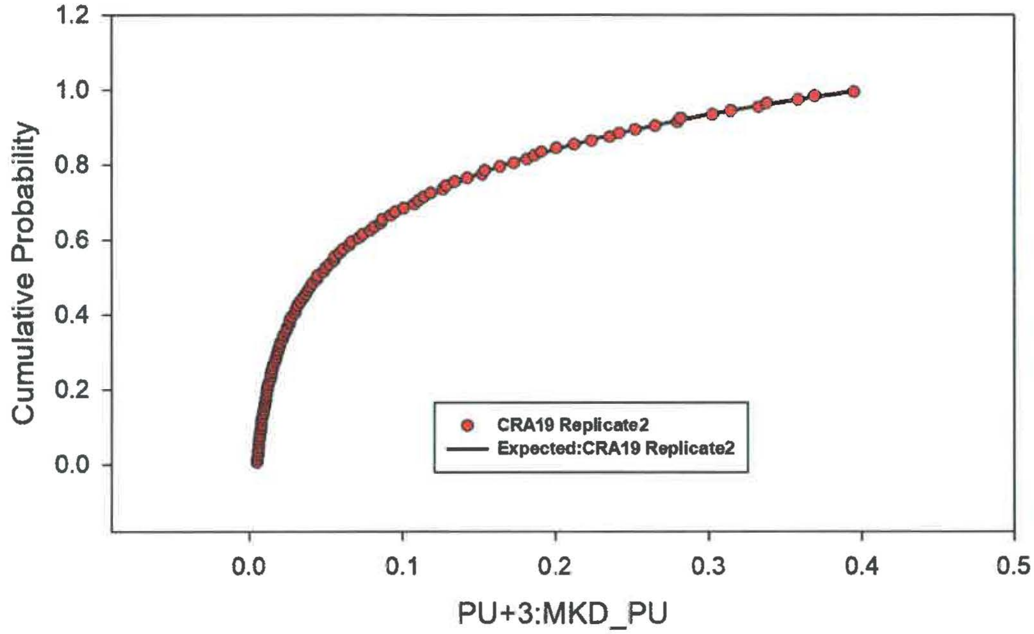

Figure 108 – Observed and Expected CDFs for PU+3:MKD_PU (Loguniform Distribution) Replicate 2.

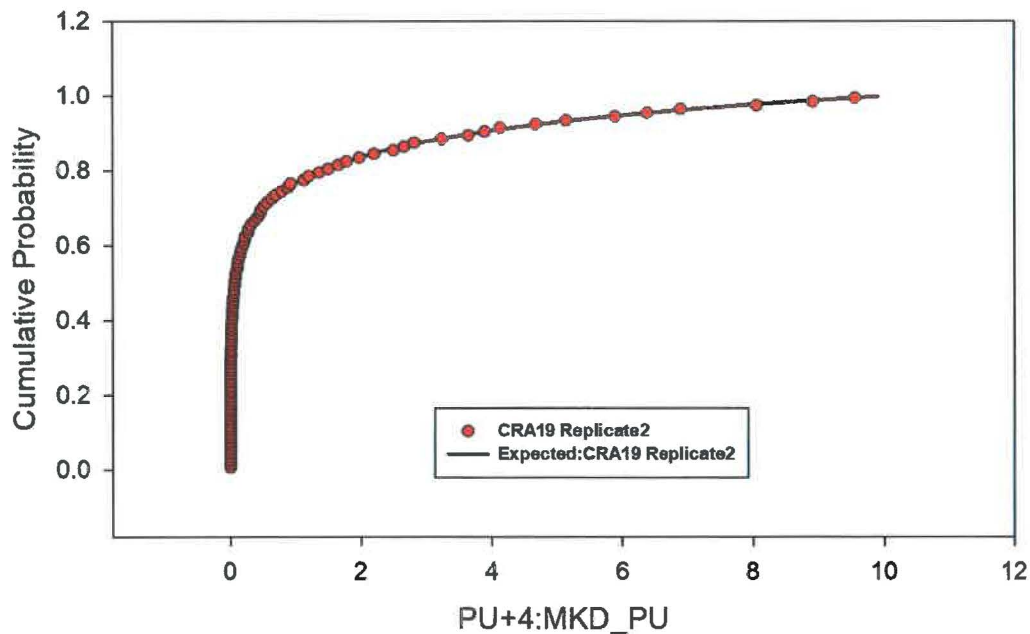

Figure 109 – Observed and Expected CDFs for PU+4:MKD_PU (Loguniform Distribution) Replicate 2.

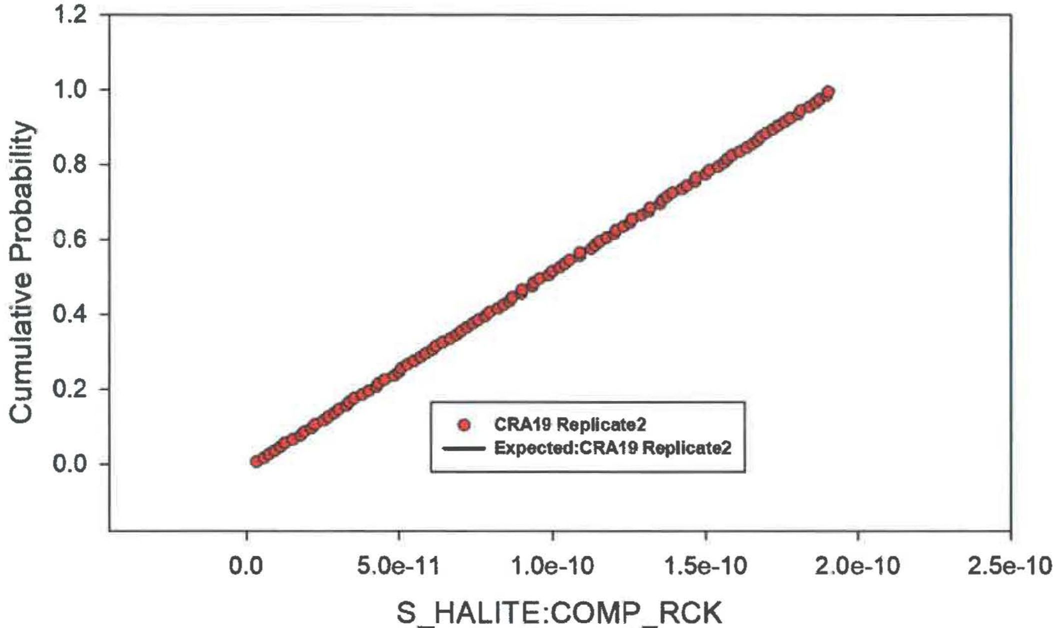

Figure 110 – Observed and Expected CDFs for S_HALITE:COMP_RCK (Uniform Distribution) Replicate 2.

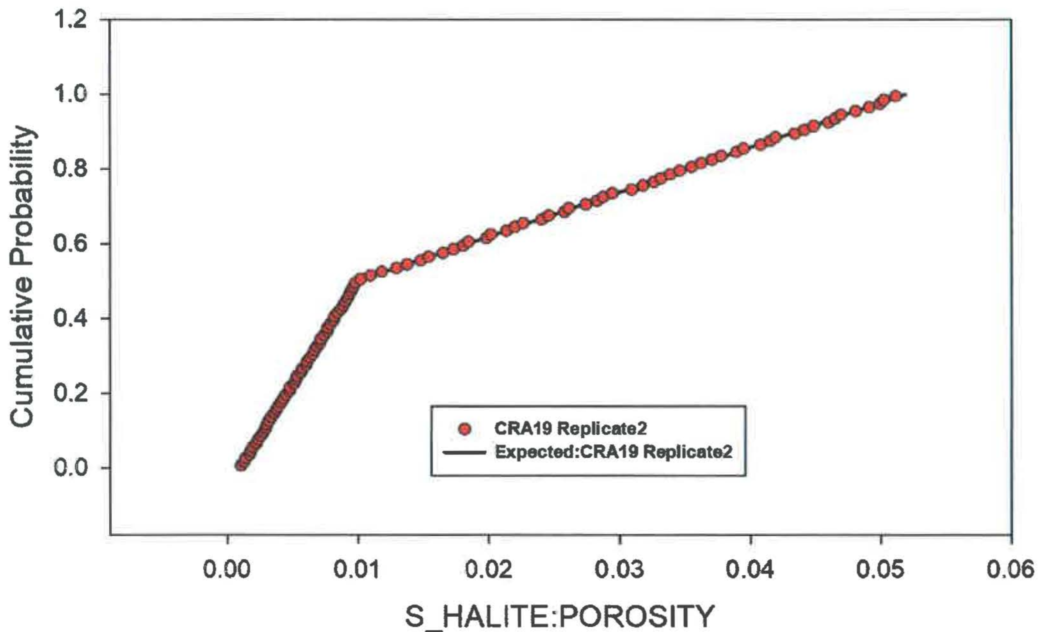

Figure 111 – Observed and Expected CDFs for S_HALITE:POROSITY (Cumulative Distribution) Replicate 2.

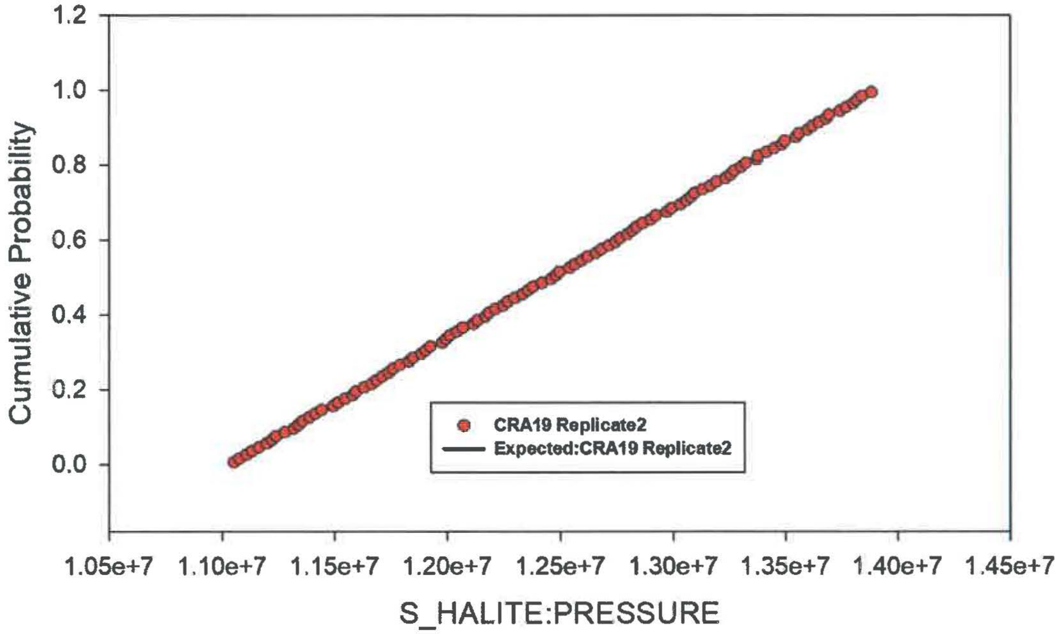

Figure 112 – Observed and Expected CDFs for S_HALITE:PRESSURE (Uniform Distribution) Replicate 2.

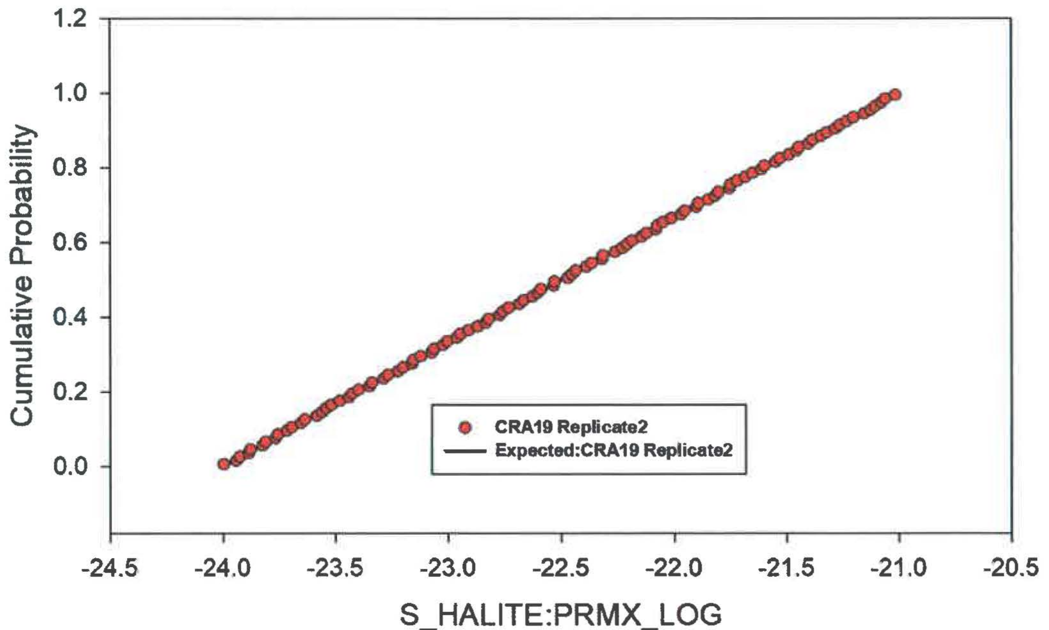

Figure 113 – Observed and Expected CDFs for S_HALITE:PRMX_LOG (Uniform Distribution) Replicate 2.

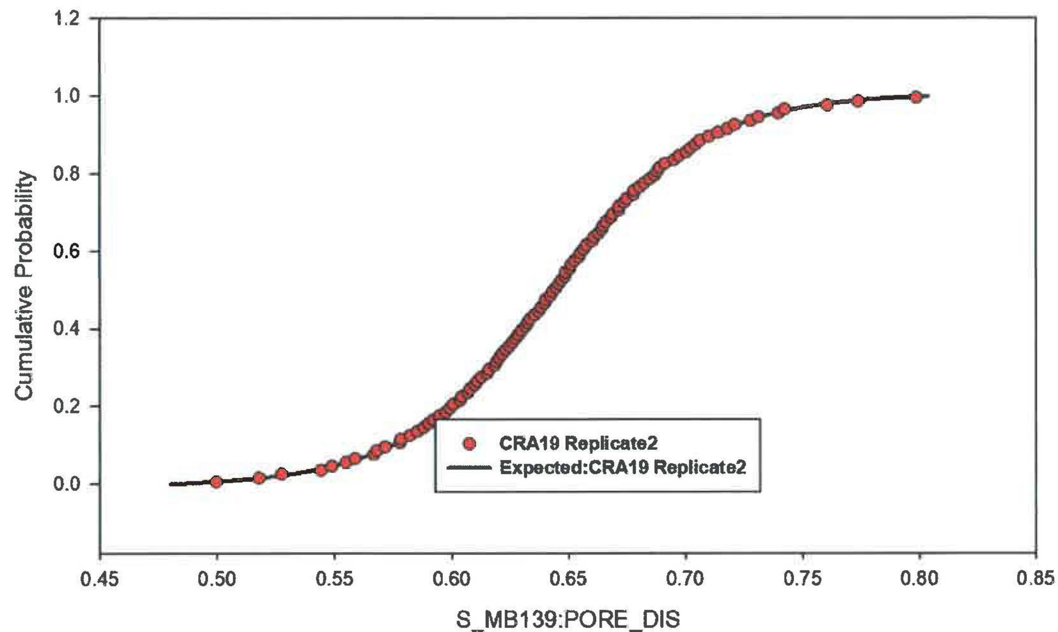

Figure 114 – Observed and Expected CDFs for S_MB139:PORE_DIS (Student Distribution) Replicate 2.

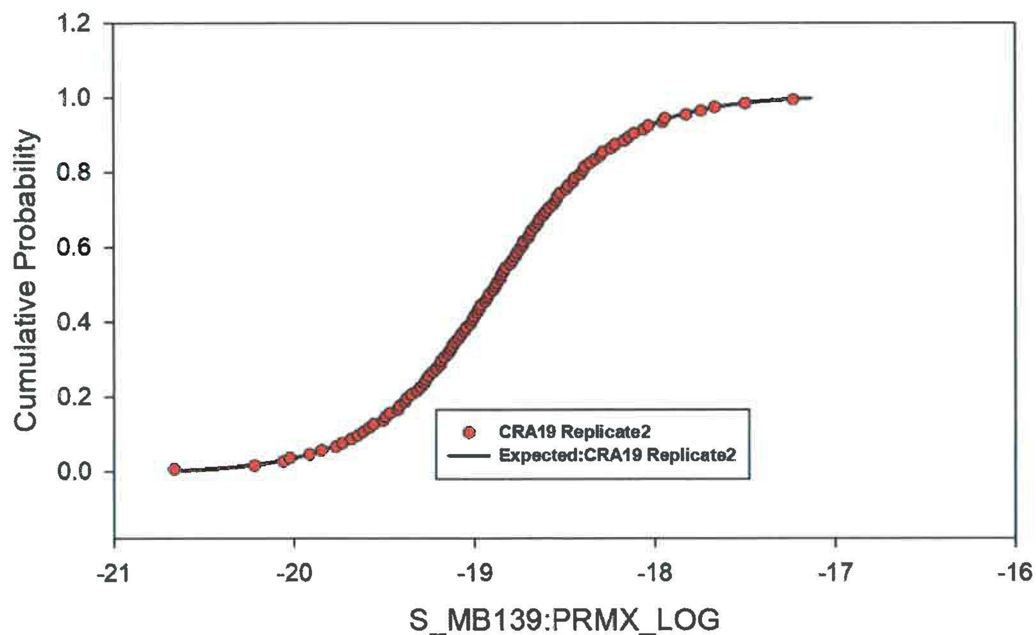

Figure 115 – Observed and Expected CDFs for S_MB139:PRMX_LOG (Student Distribution) Replicate 2.

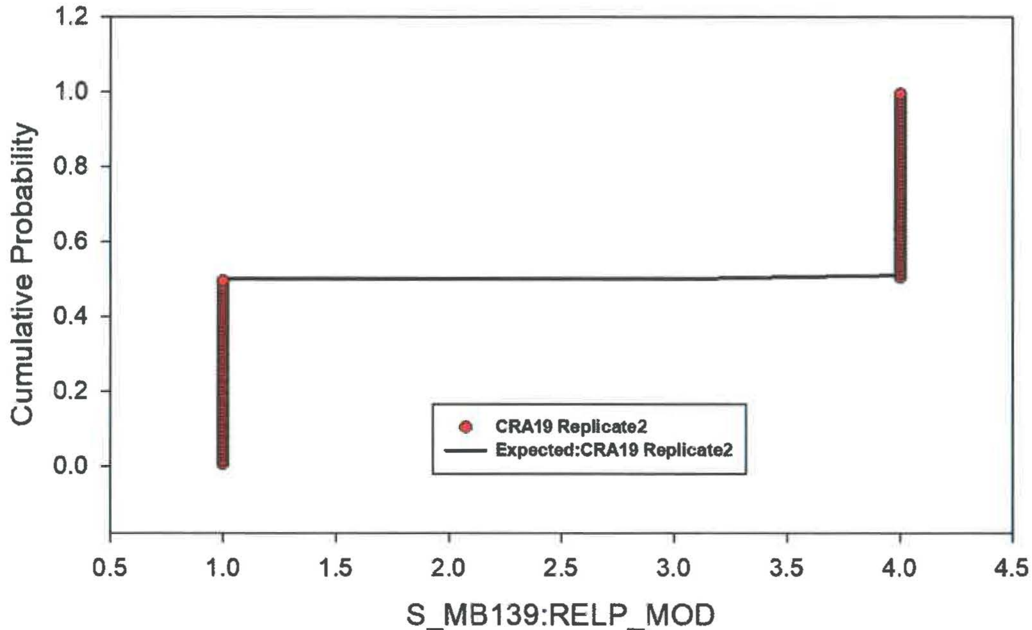

Figure 116 – Observed and Expected CDFs for S_MB139:RELP_MOD (Delta Distribution) Replicate 2.

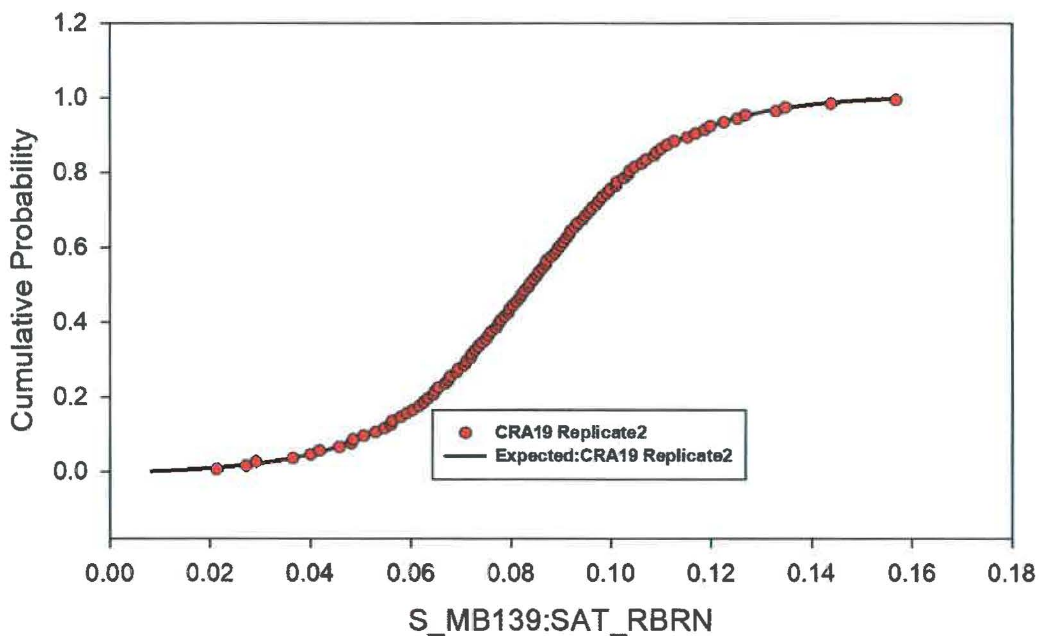

Figure 117 – Observed and Expected CDFs for S_MB139:SAT_RBRN (Student Distribution) Replicate 2.

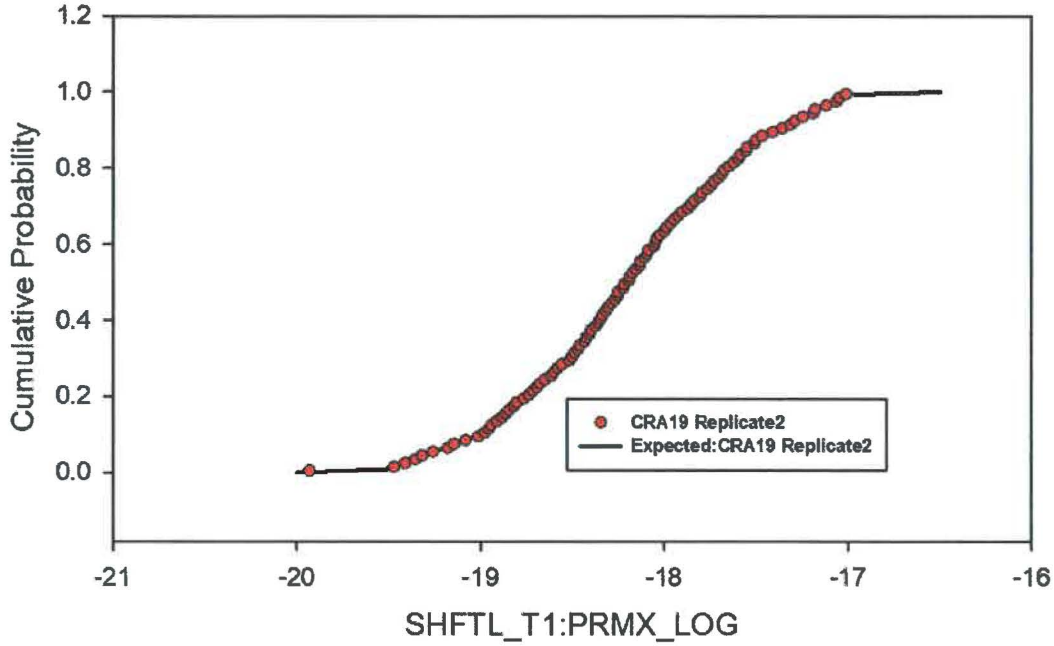

Figure 118 – Observed and Expected CDFs for SHFTL_T1:PRMX_LOG (Cumulative Distribution) Replicate 2.

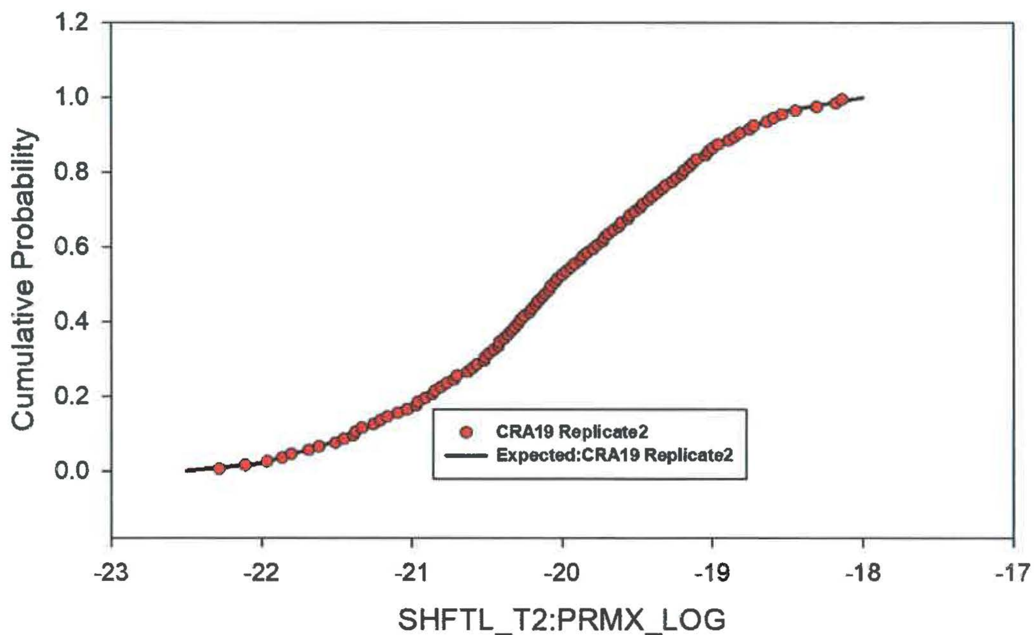

Figure 119 – Observed and Expected CDFs for SHFTL_T2:PRMX_LOG (Cumulative Distribution) Replicate 2.

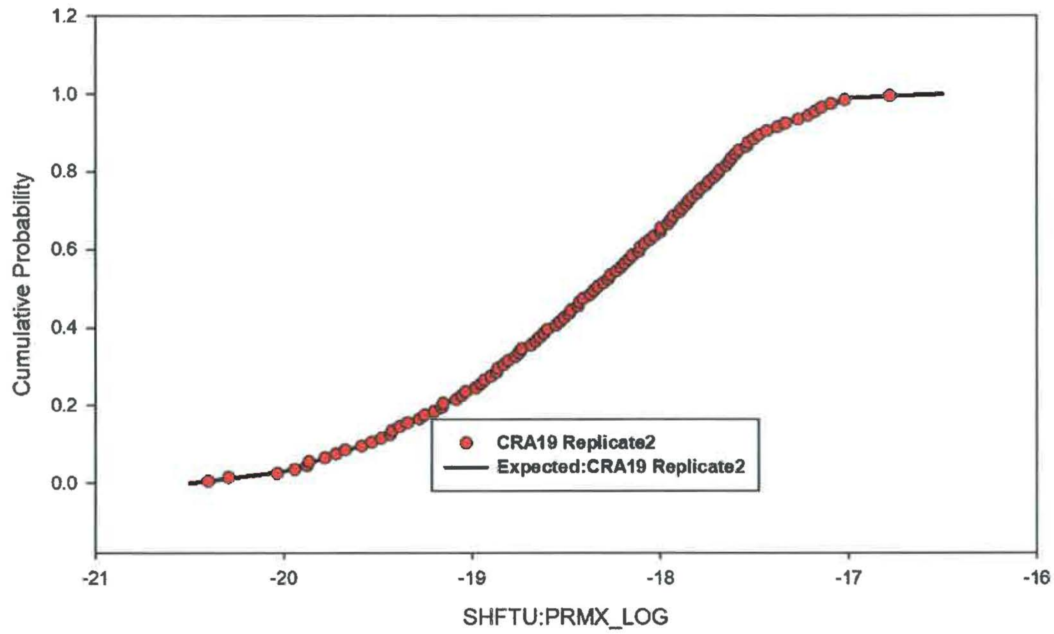

Figure 120 – Observed and Expected CDFs for SHFTU:PRMX_LOG (Cumulative Distribution) Replicate 2.

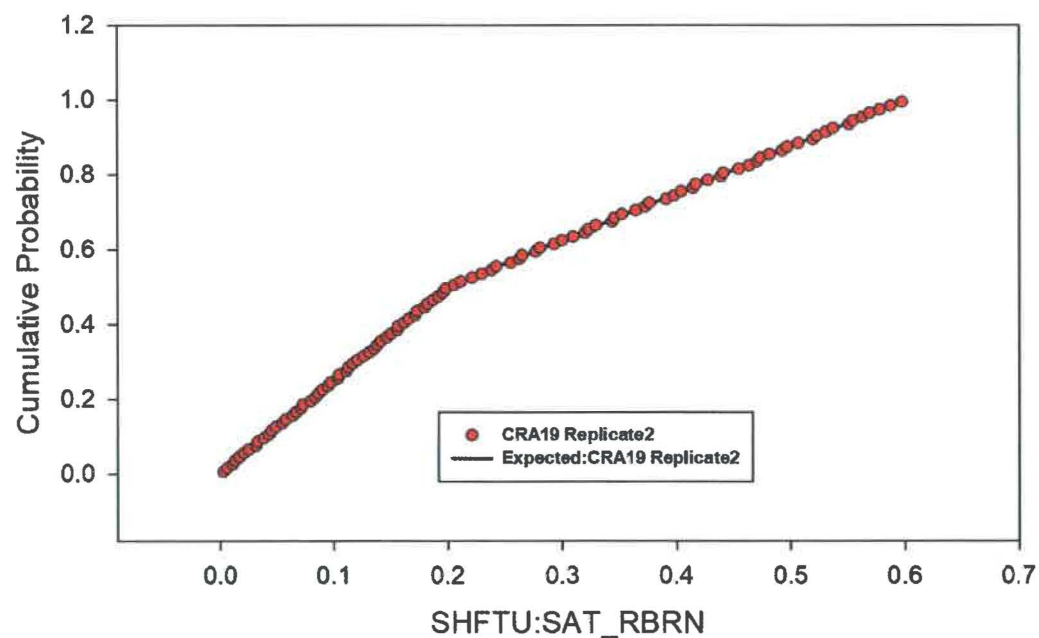

Figure 121 – Observed and Expected CDFs for SHFTU:SAT_RBRN (Cumulative Distribution) Replicate 2.

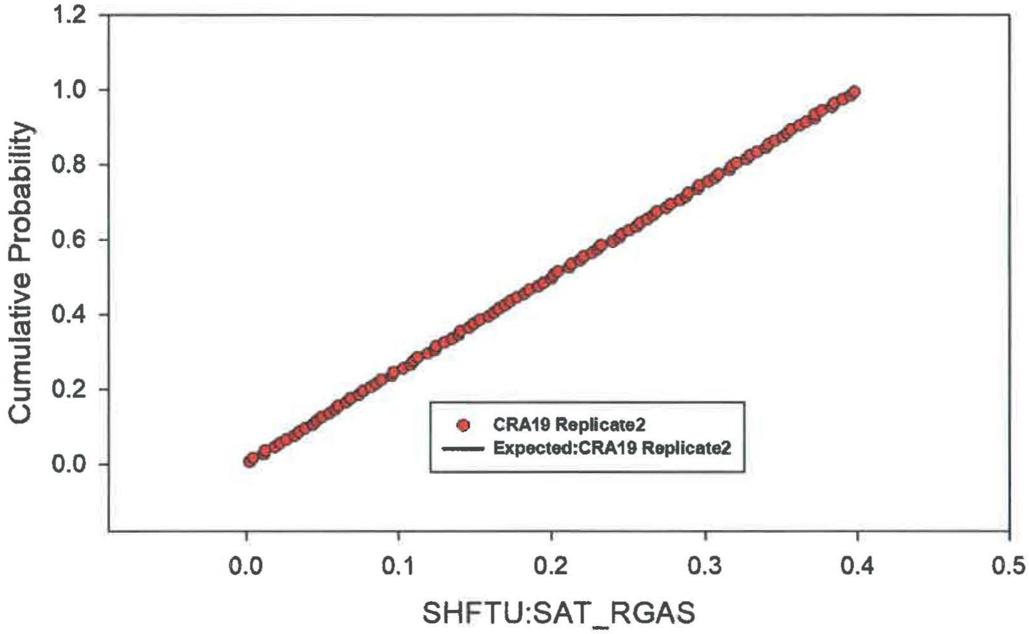

Figure 122 – Observed and Expected CDFs for SHFTU:SAT_RGAS (Uniform Distribution) Replicate 2.

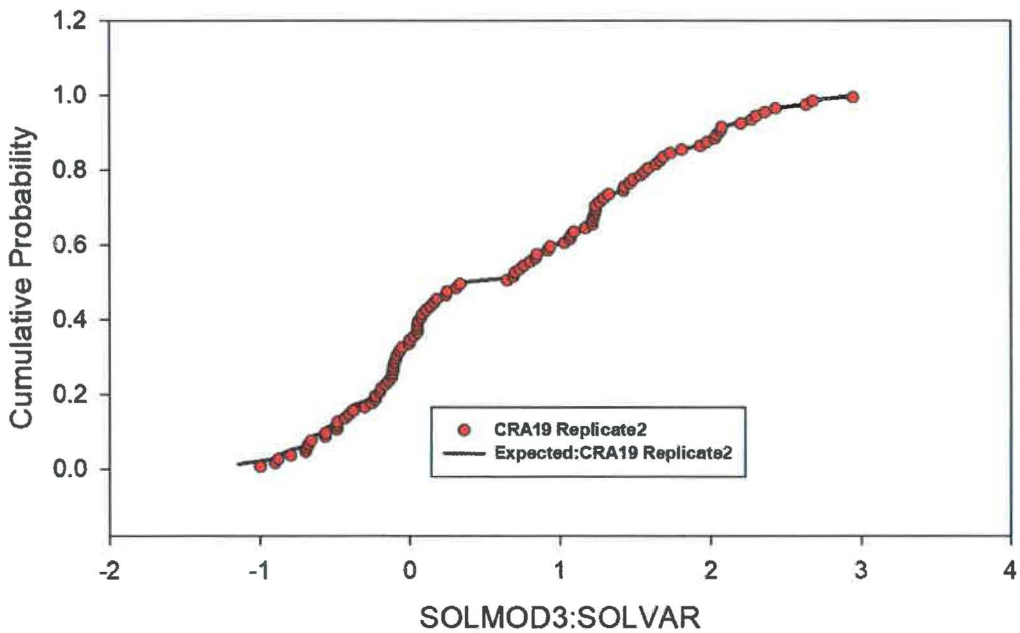

Figure 123 – Observed and Expected CDFs for SOLMOD3:SOLVAR (Cumulative Distribution) Replicate 2.

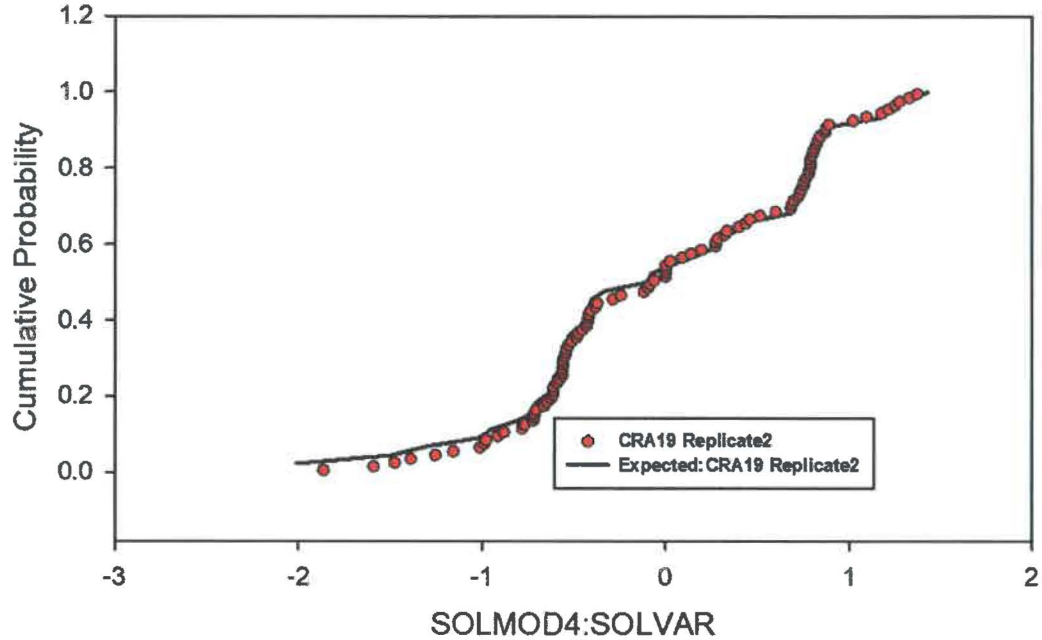

Figure 124 – Observed and Expected CDFs for SOLMOD4:SOLVAR (Cumulative Distribution) Replicate 2.

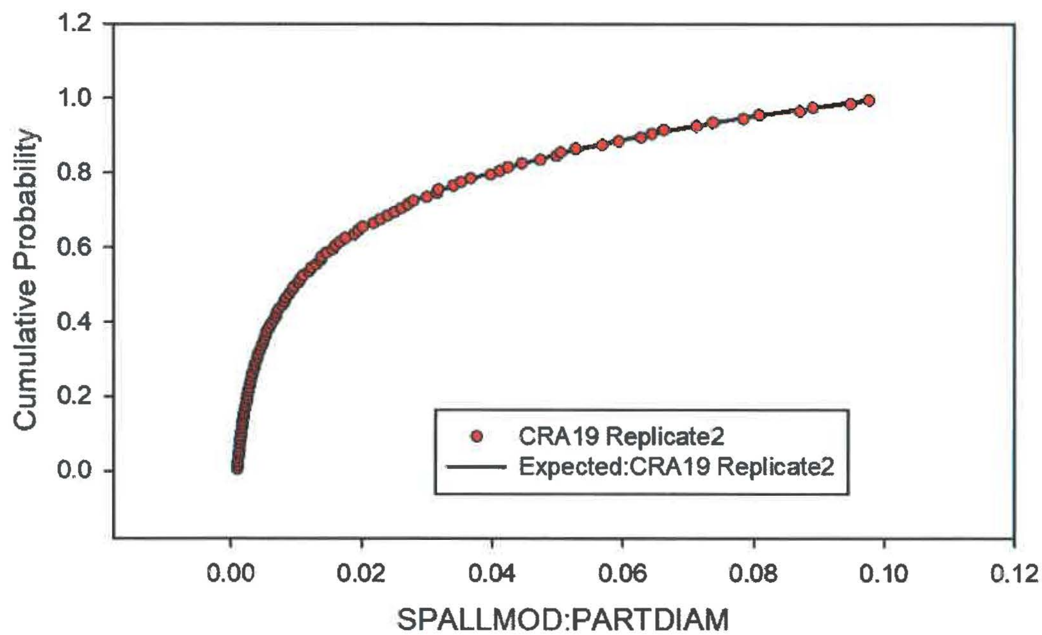

Figure 125 – Observed and Expected CDFs for SPALLMOD:PARTDIAM (Loguniform Distribution) Replicate 2.

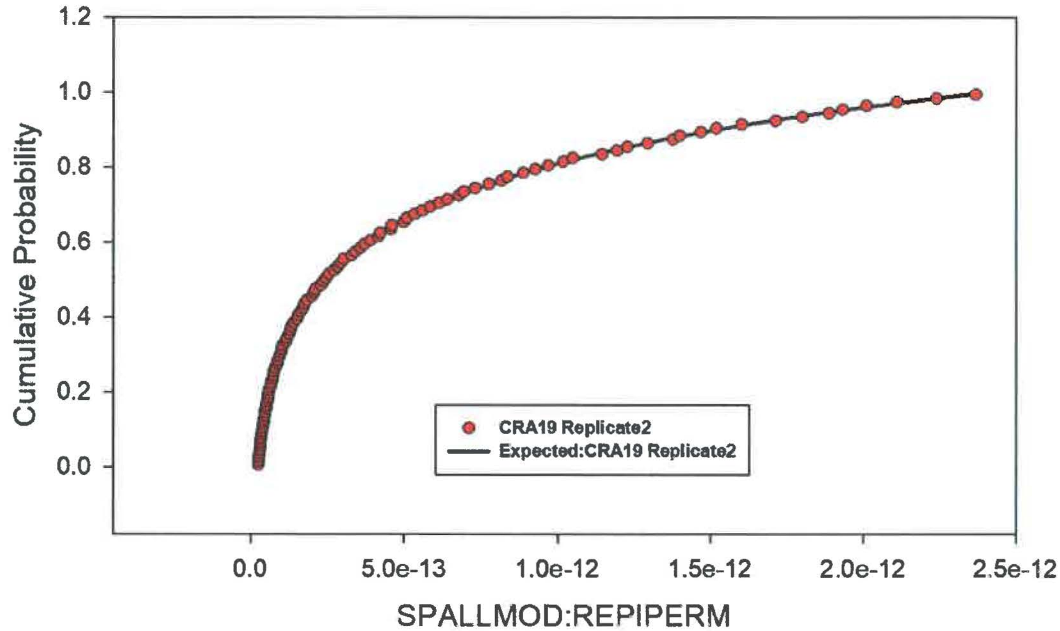

Figure 126 – Observed and Expected CDFs for SPALLMOD:REPIPERM (Loguniform Distribution) Replicate 2.

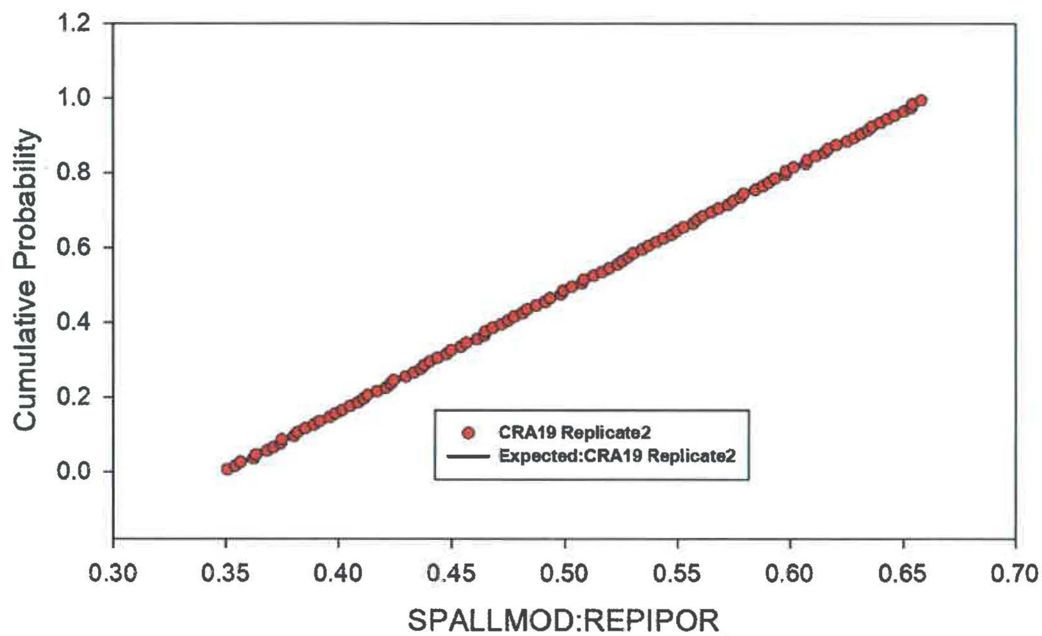

Figure 127 – Observed and Expected CDFs for SPALLMOD:REPIPOR (Uniform Distribution) Replicate 2.

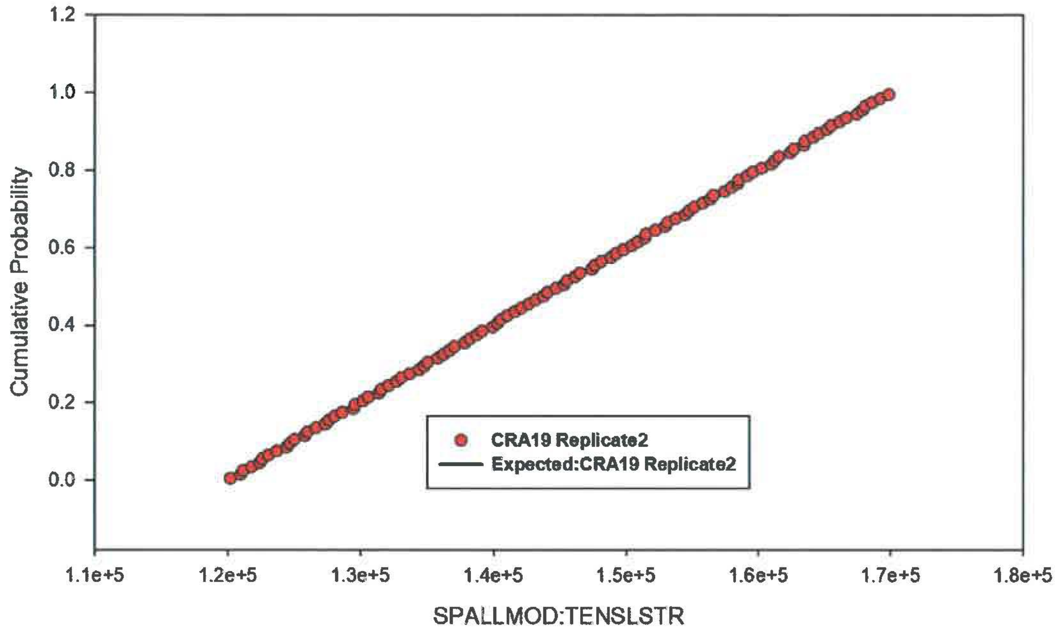

Figure 128 – Observed and Expected CDFs for SPALLMOD:TENSLSTR (Uniform Distribution) Replicate 2.

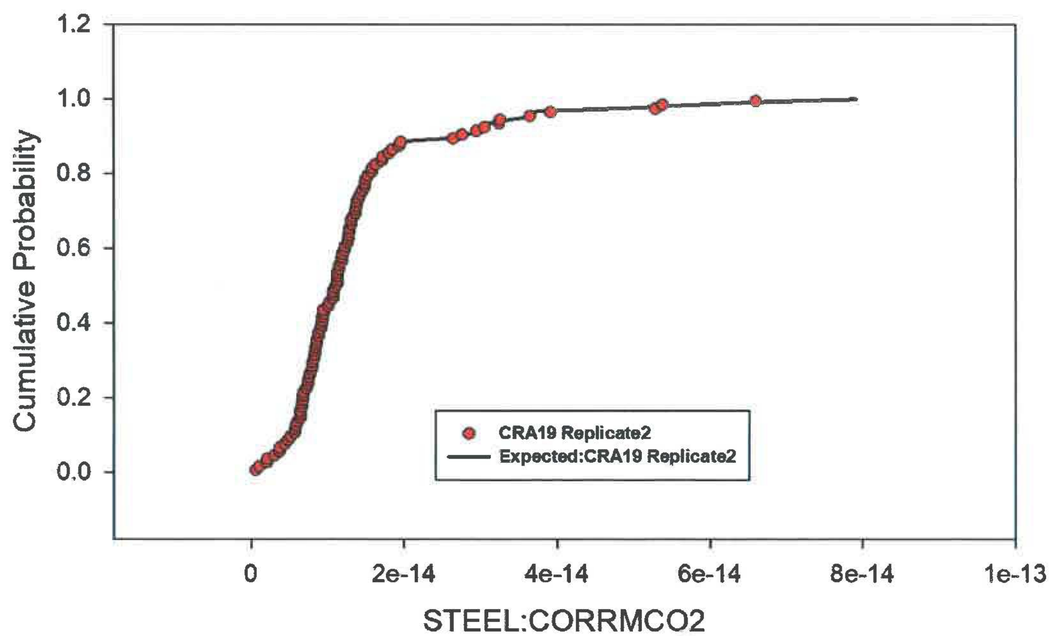

Figure 129 – Observed and Expected CDFs for STEEL:CORRMCO2 (Cumulative Distribution) Replicate 2.

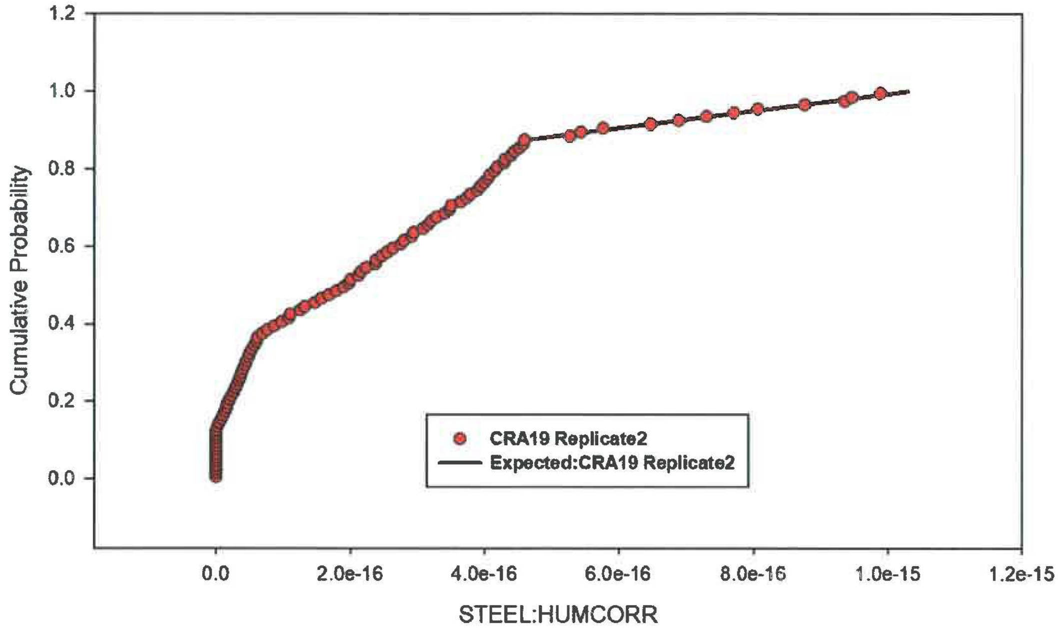

Figure 130 – Observed and Expected CDFs for STEEL:HUMCORR (Cumulative Distribution) Replicate 2.

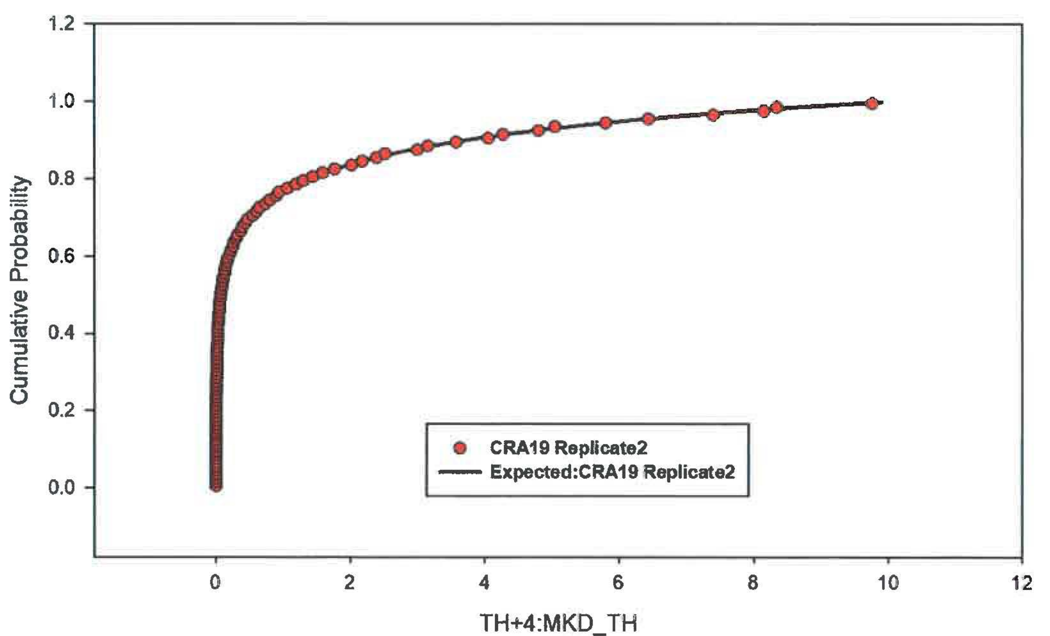

Figure 131 – Observed and Expected CDFs for TH+4:MKD_TH (Loguniform Distribution) Replicate 2.

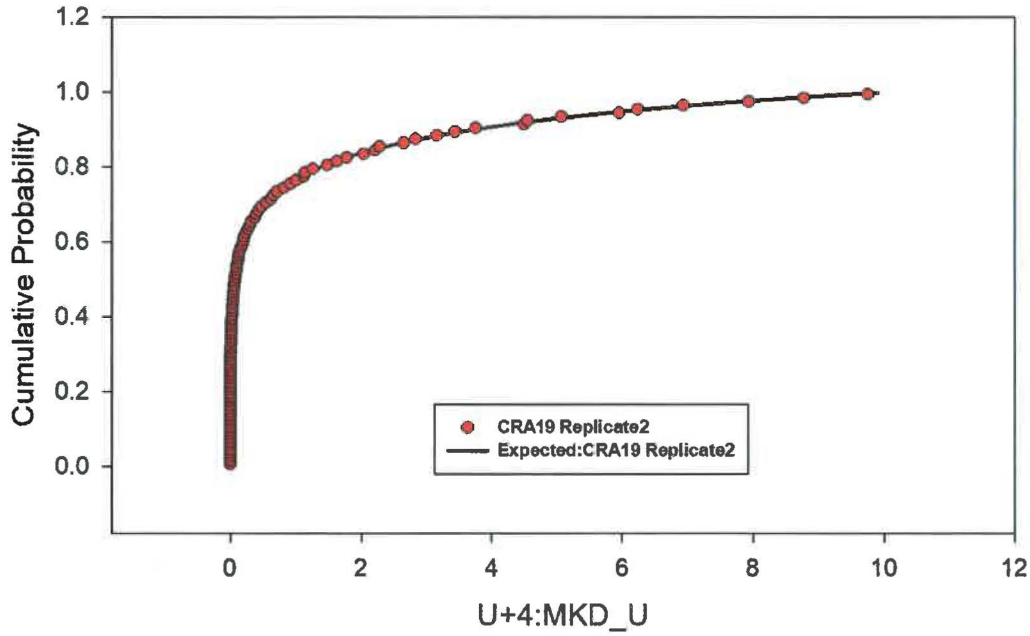

Figure 132 – Observed and Expected CDFs for U+4:MKD_U (Loguniform Distribution) Replicate 2.

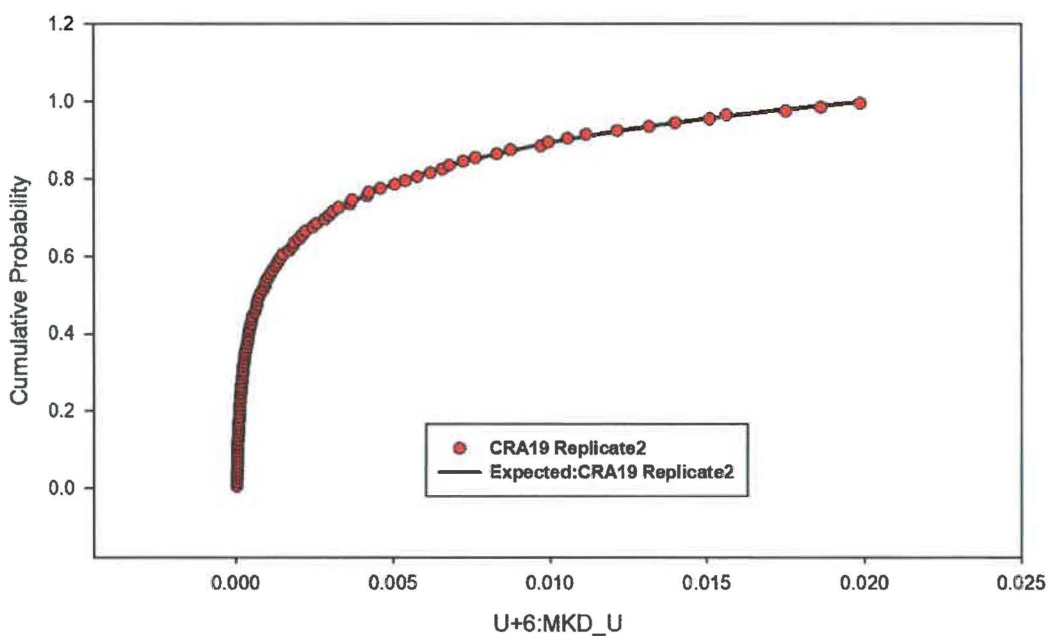

Figure 133 – Observed and Expected CDFs for U+6:MKD_U (Loguniform Distribution) Replicate 2.

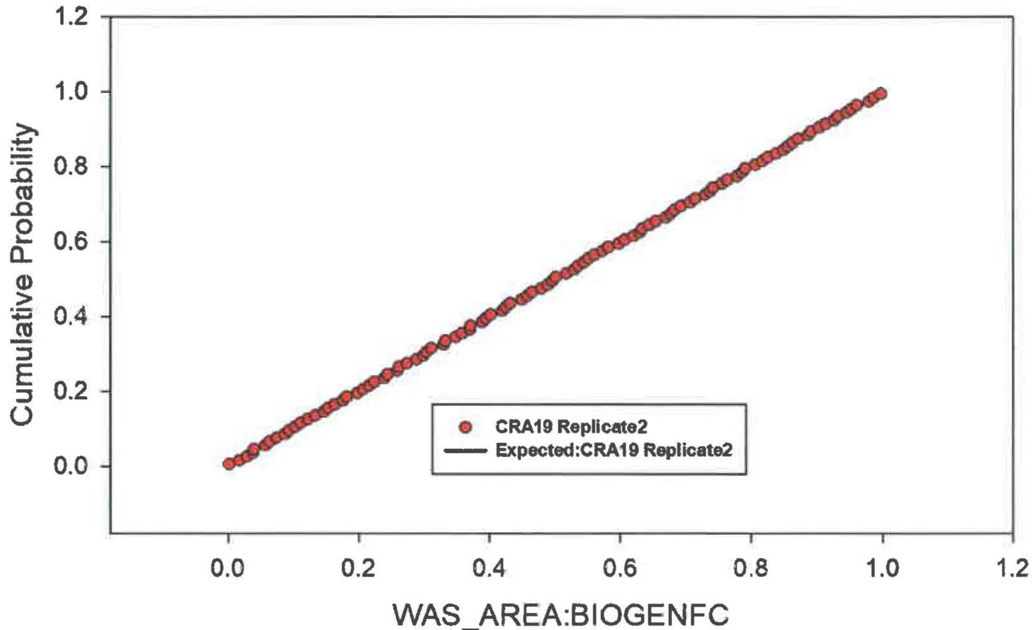

Figure 134 – Observed and Expected CDFs for WAS_AREA:BIOGENFC (Uniform Distribution) Replicate 2.

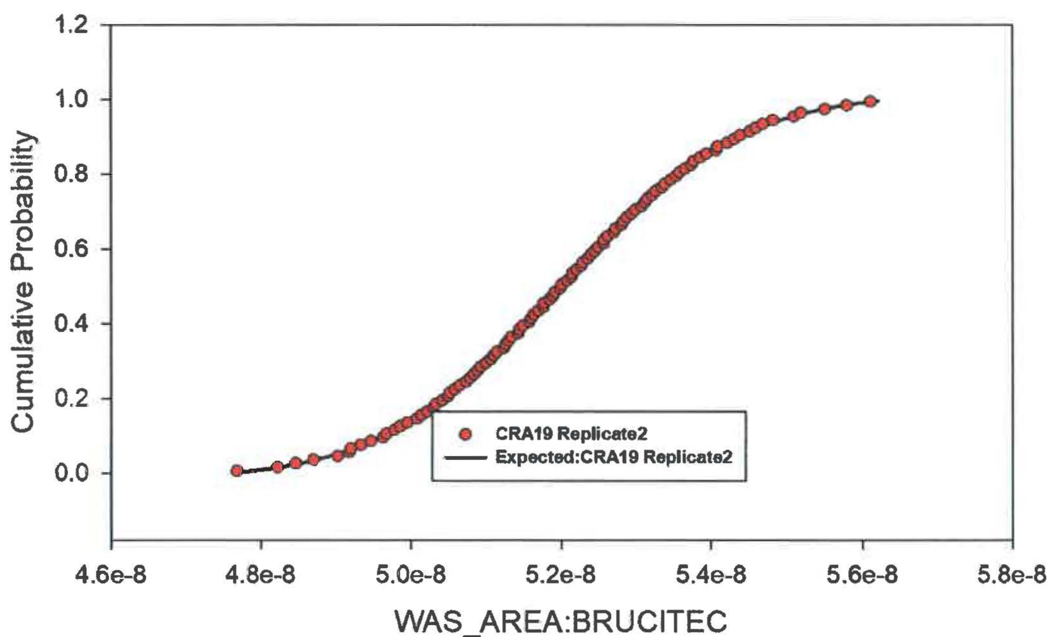

Figure 135 – Observed and Expected CDFs for WAS_AREA:BRUCITEC (Normal Distribution) Replicate 2.

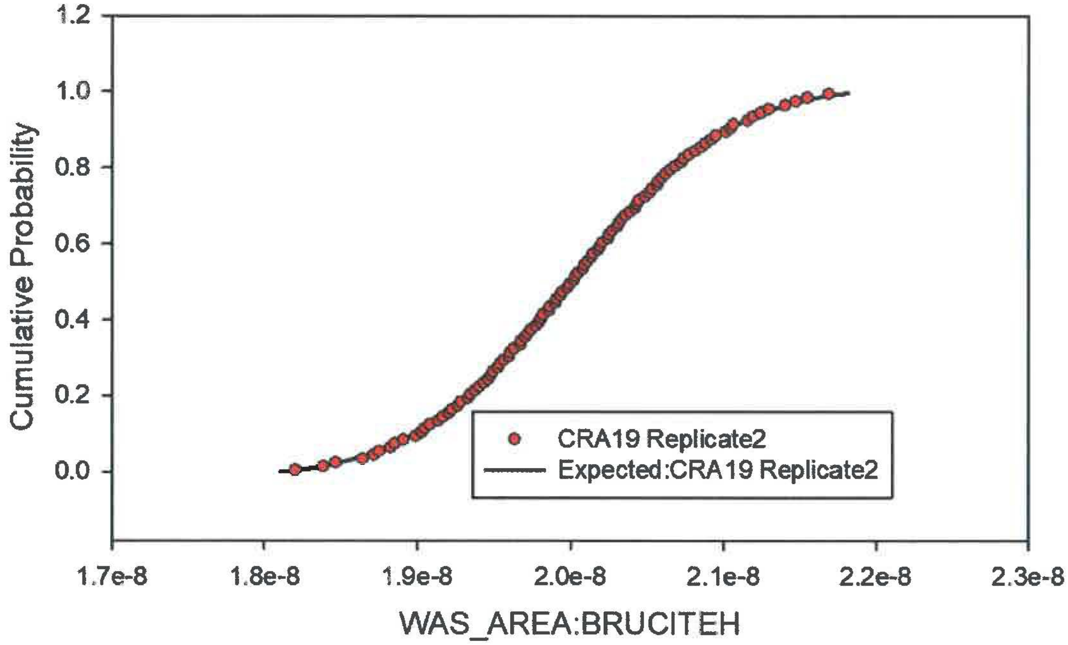

Figure 136 – Observed and Expected CDFs for WAS_AREA:BRUCITEH (Normal Distribution) Replicate 2.

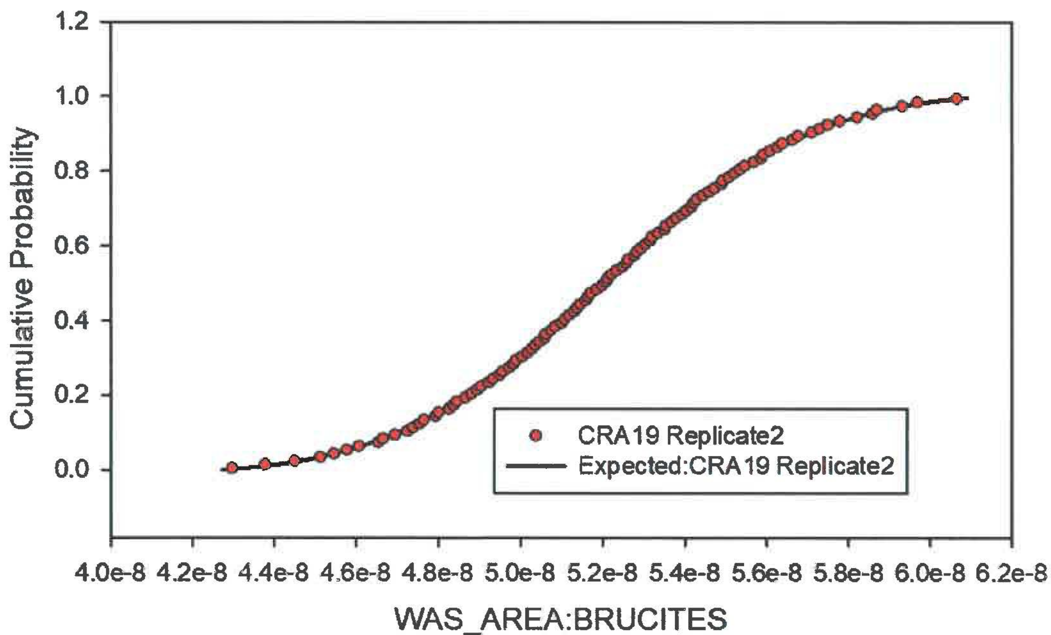

Figure 137 – Observed and Expected CDFs for WAS_AREA:BRUCITES (Normal Distribution) Replicate 2.

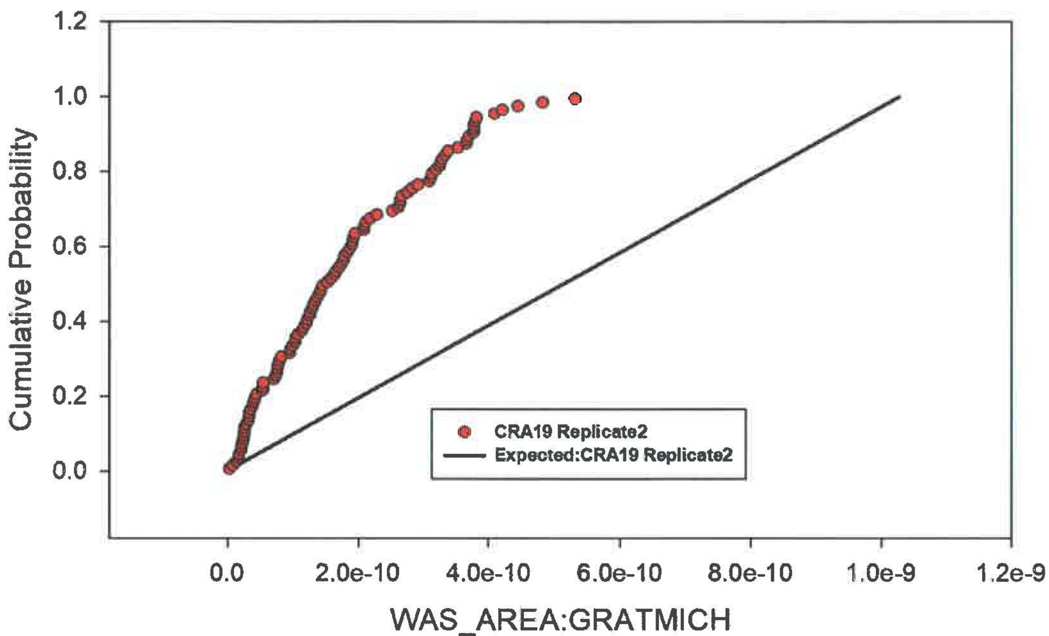

Figure 138 – Observed and Expected CDFs for WAS_AREA:GRATMICH (Uniform Distribution) Replicate 2.

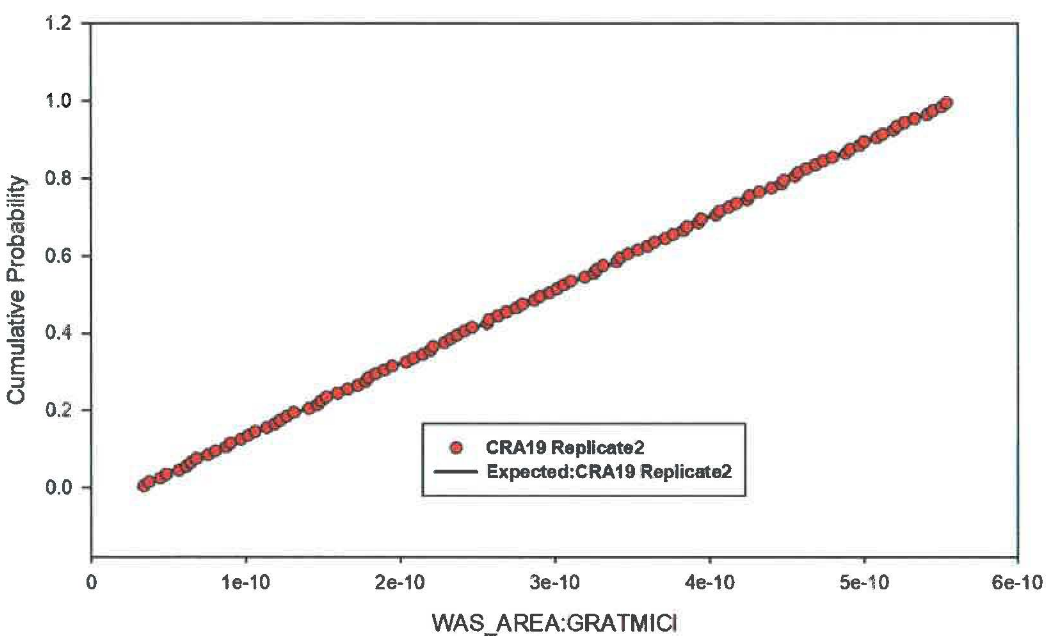

Figure 139 – Observed and Expected CDFs for WAS_AREA:GRATMICI (Uniform Distribution) Replicate 2.

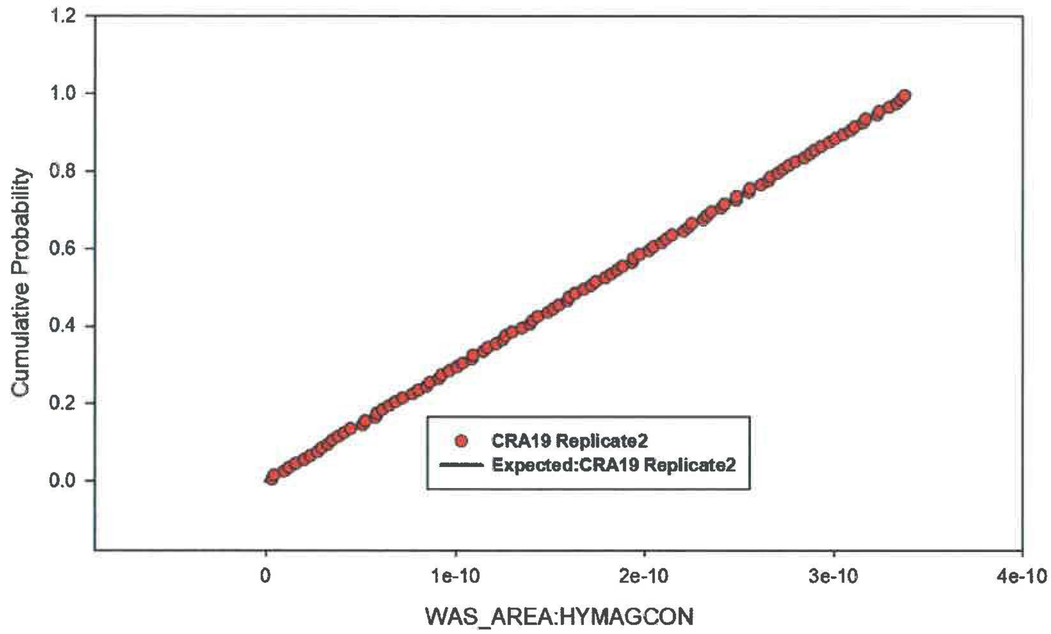

Figure 140 – Observed and Expected CDFs for WAS_AREA:HYMAGCON (Uniform Distribution) Replicate 2.

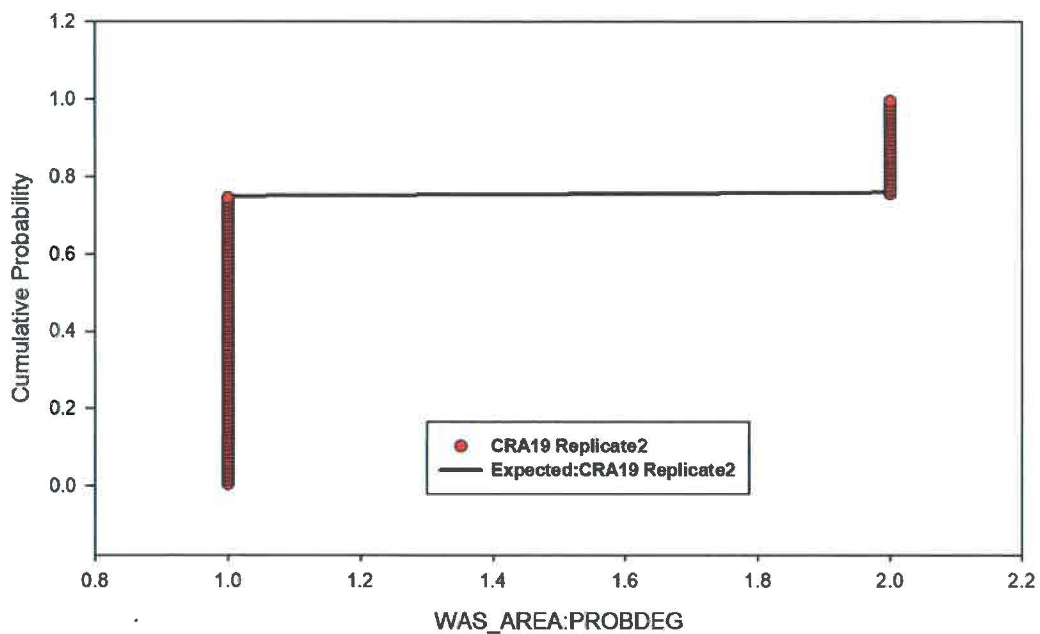

Figure 141 – Observed and Expected CDFs for WAS_AREA:PROBDEG (Delta Distribution) Replicate 2.

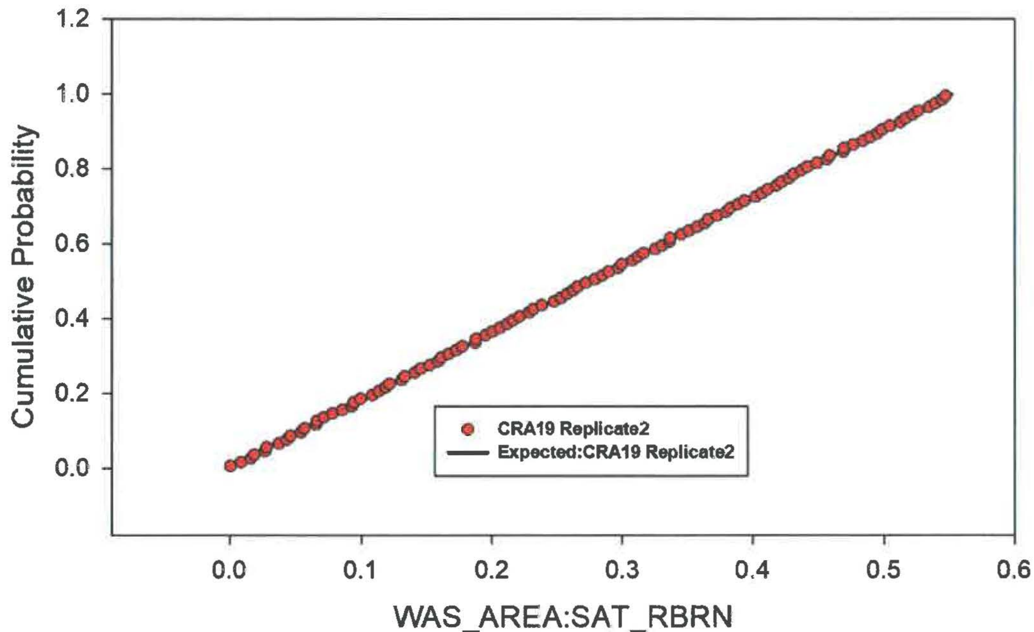

Figure 142 – Observed and Expected CDFs for WAS_AREA:SAT_RBRN (Uniform Distribution) Replicate 2.

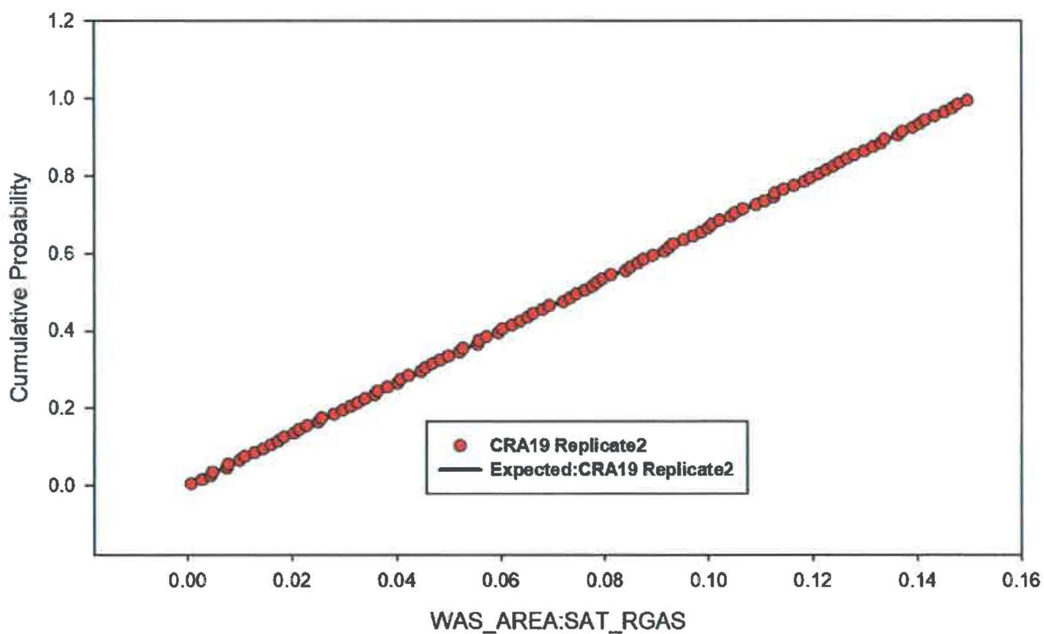

Figure 143 – Observed and Expected CDFs for WAS_AREA:SAT_RGAS (Uniform Distribution) Replicate 2.

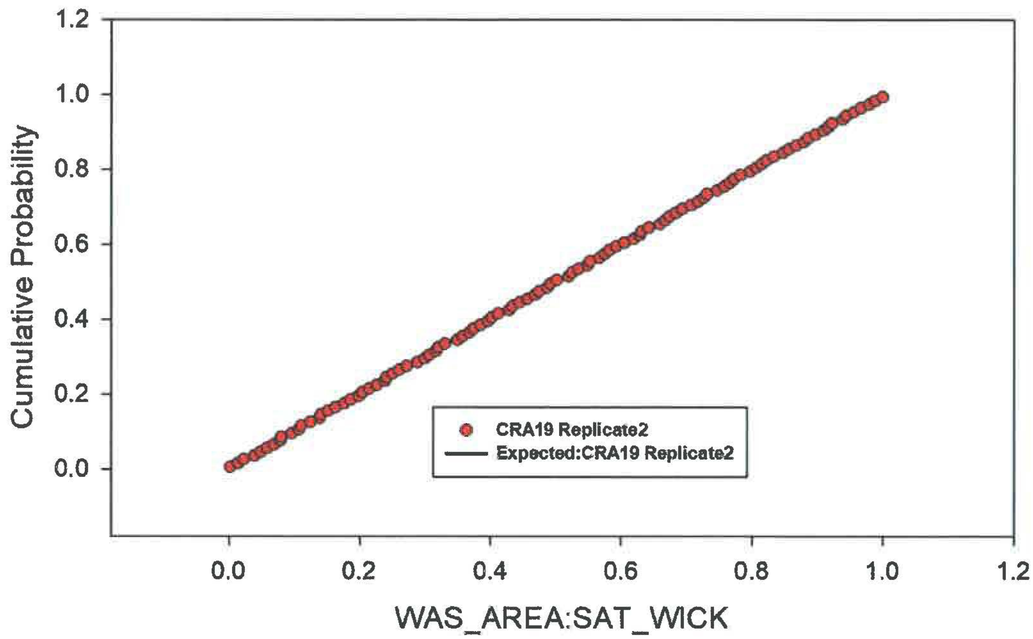

Figure 144 – Observed and Expected CDFs for WAS_AREA:SAT_WICK (Uniform Distribution) Replicate 2.

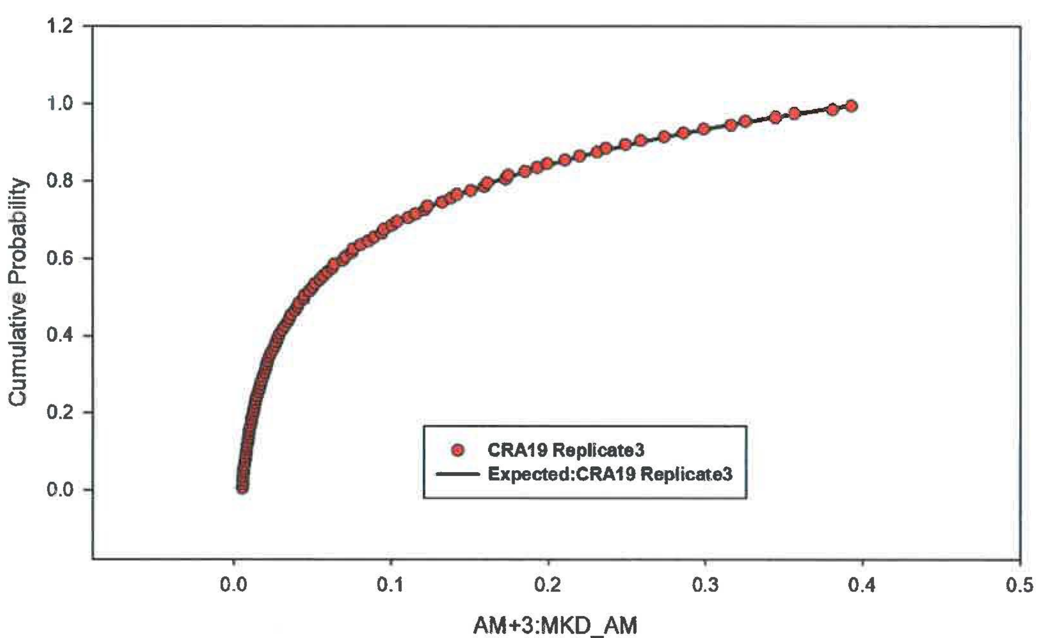

Figure 145 – Observed and Expected CDFs for AM+3:MKD_AM (Loguniform Distribution) Replicate 3.

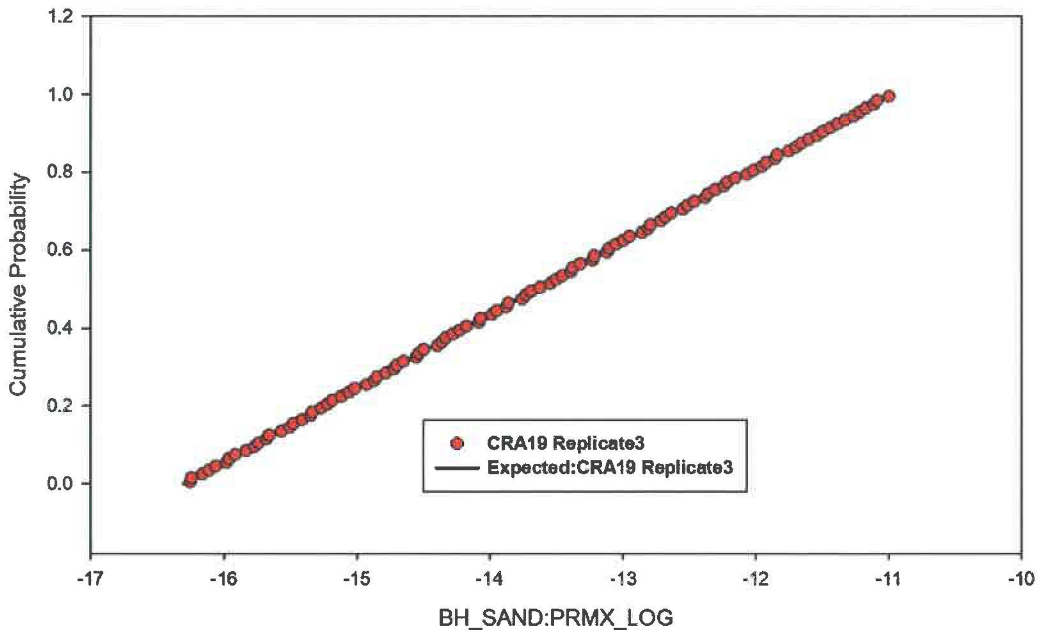

Figure 146 – Observed and Expected CDFs for BH_SAND:PRMX_LOG (Uniform Distribution) Replicate 3.

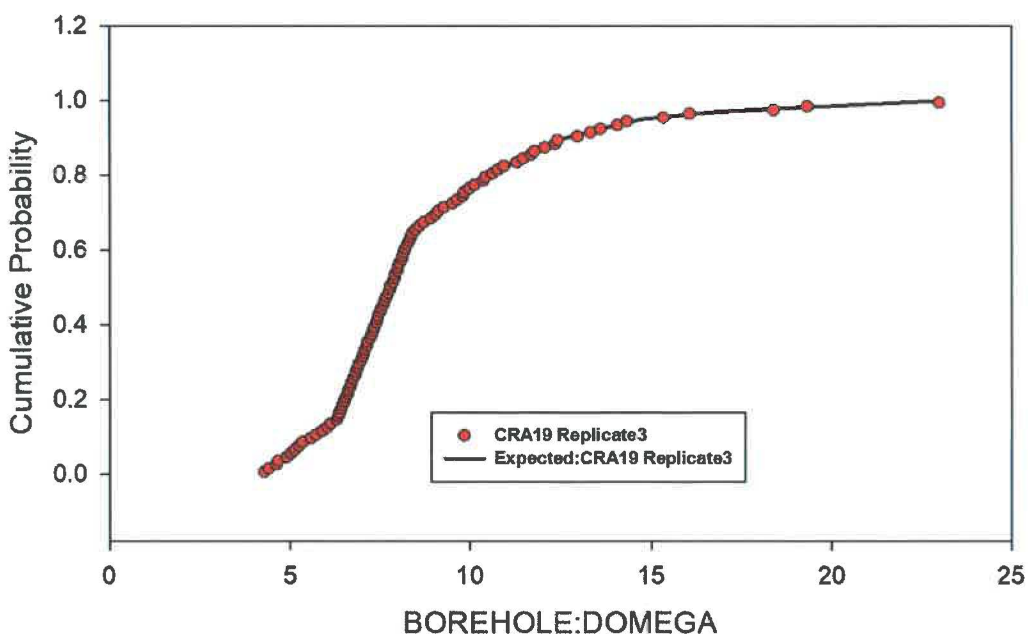

Figure 147 – Observed and Expected CDFs for BOREHOLE:DOMEGA (Cumulative Distribution) Replicate 3.

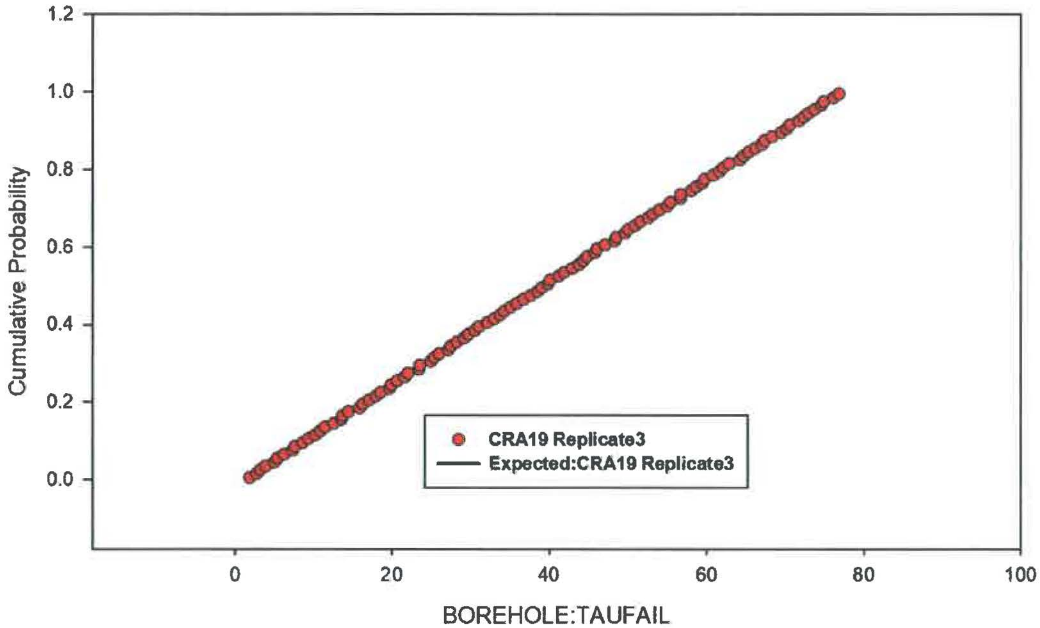

Figure 148 – Observed and Expected CDFs for BOREHOLE:TAUFAIL (Uniform Distribution) Replicate 3.

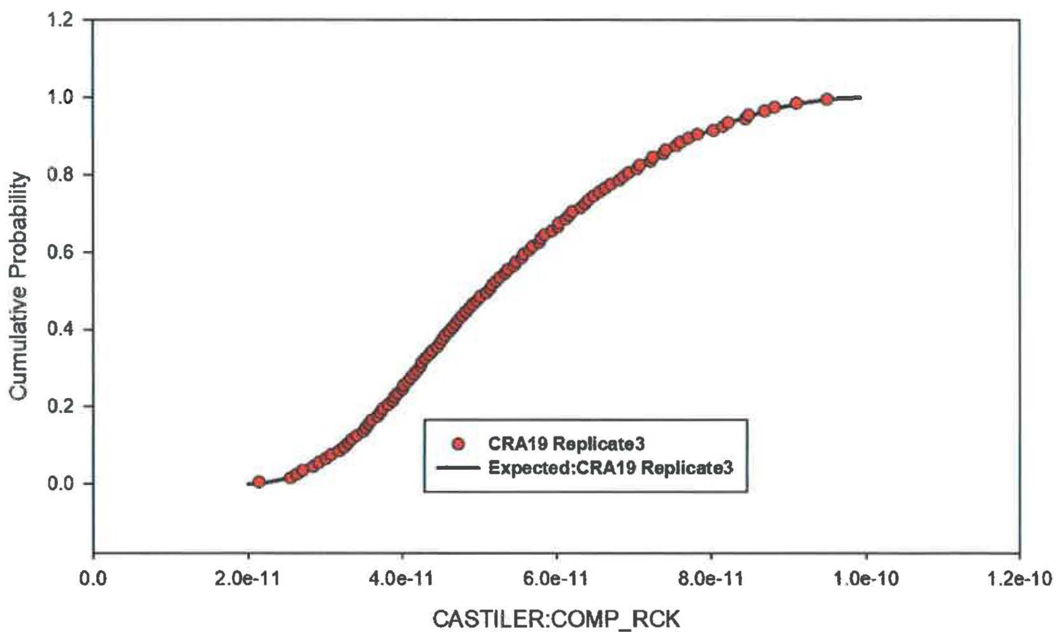

Figure 149 – Observed and Expected CDFs for CASTILER:COMP_RCK (Triangular Distribution) Replicate 3.

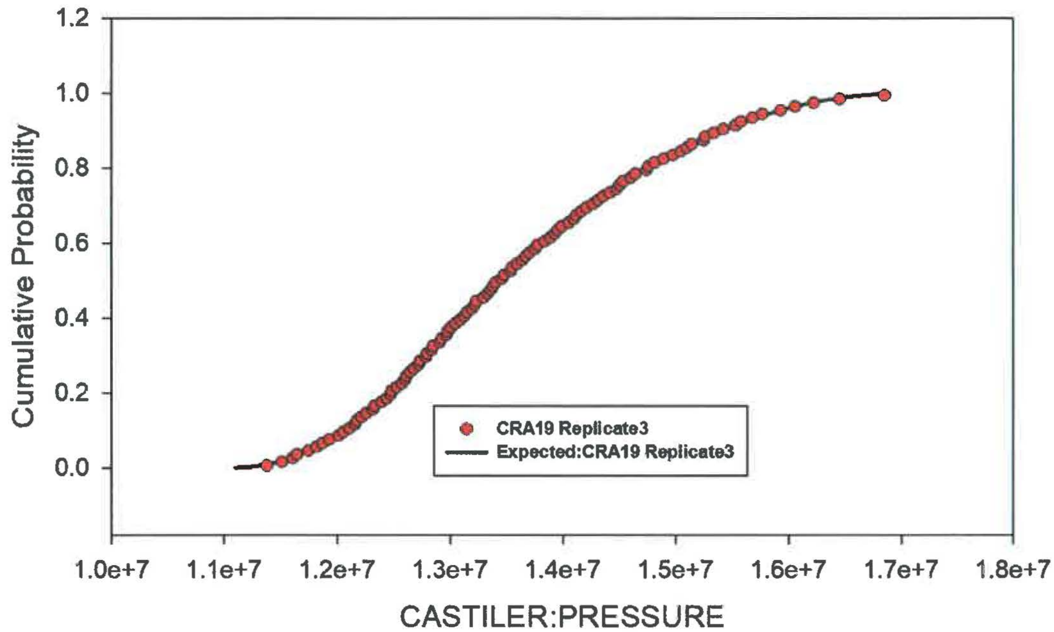

Figure 150 – Observed and Expected CDFs for CASTILER:PRESSURE (Triangular Distribution) Replicate 3.

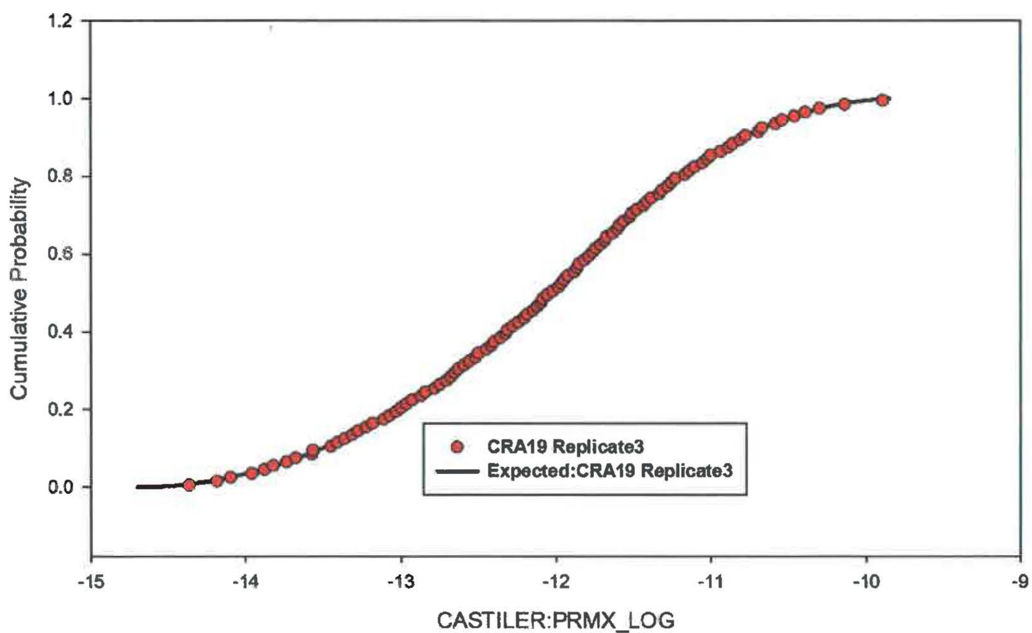

Figure 151 – Observed and Expected CDFs for CASTILER:PRMX_LOG (Triangular Distribution) Replicate 3.

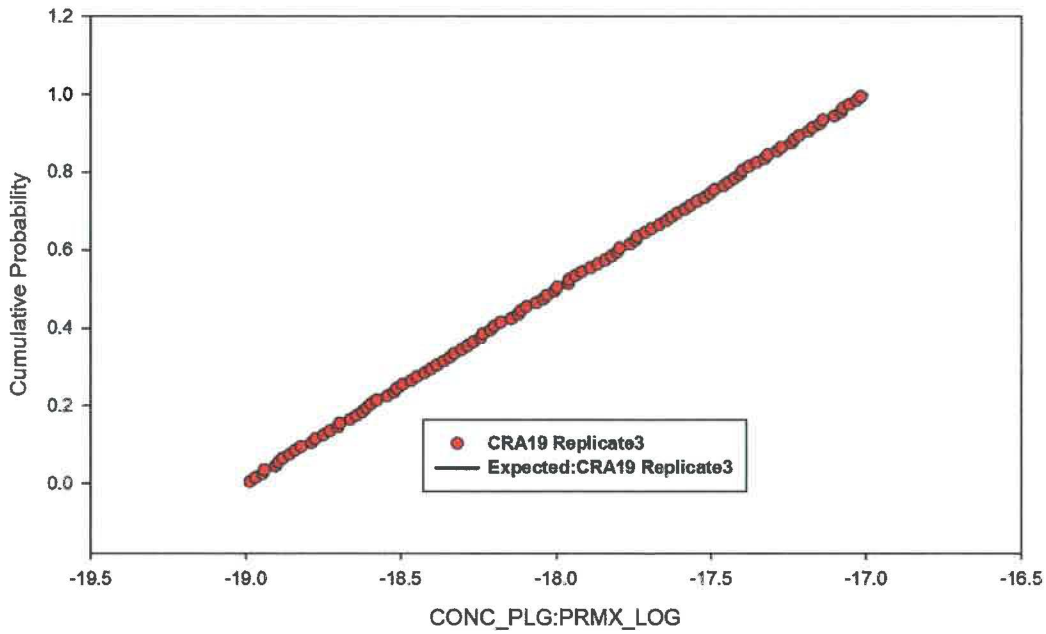

Figure 152 – Observed and Expected CDFs for CONC_PLG:PRMX_LOG (Uniform Distribution) Replicate 3.

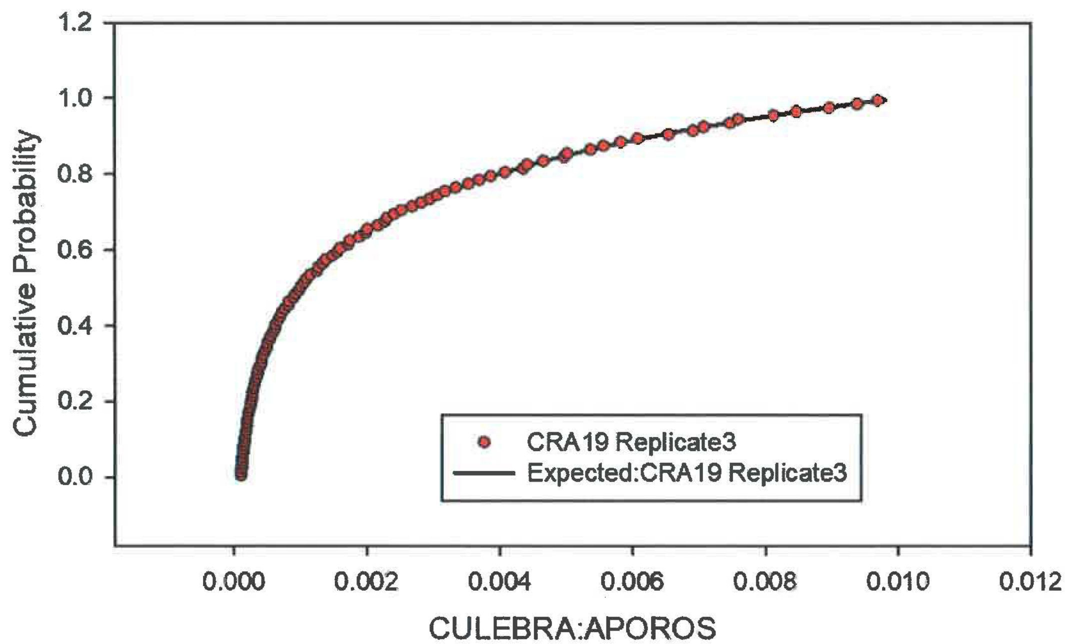

Figure 153 – Observed and Expected CDFs for CULEBRA:APOROS (Loguniform Distribution) Replicate 3.

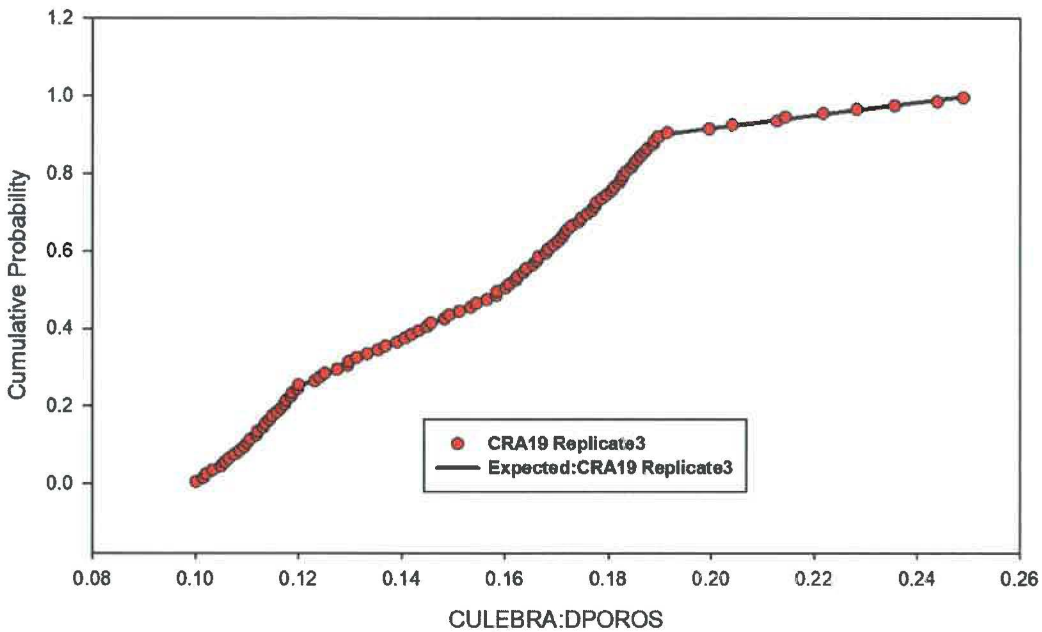

Figure 154 – Observed and Expected CDFs for CULEBRA:DPOROS (Cumulative Distribution) Replicate 3.

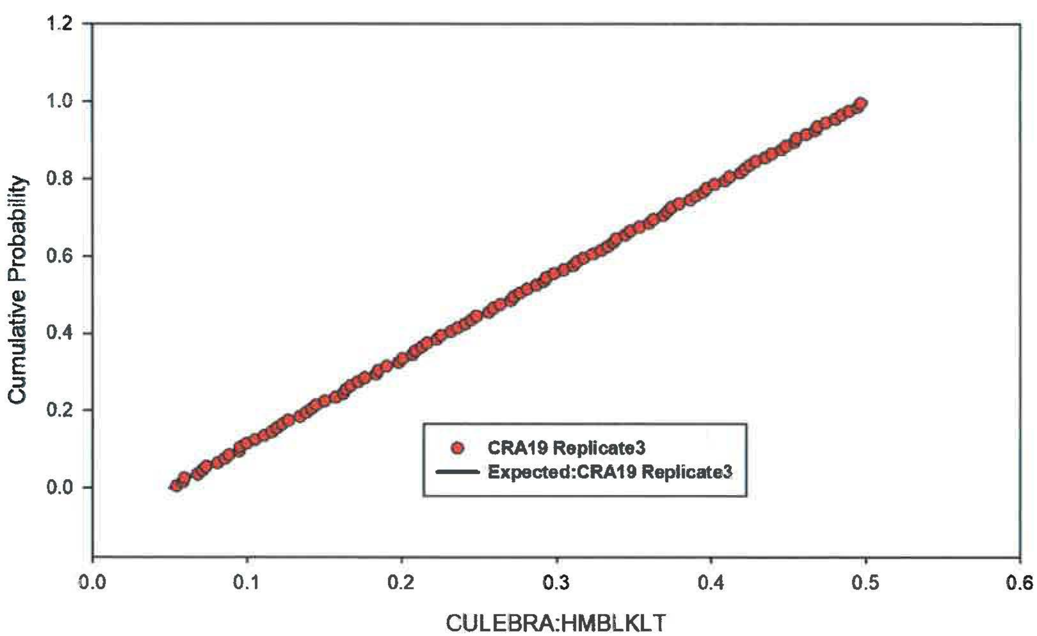

Figure 155 – Observed and Expected CDFs for CULEBRA:HMBLKLT (Uniform Distribution) Replicate 3.

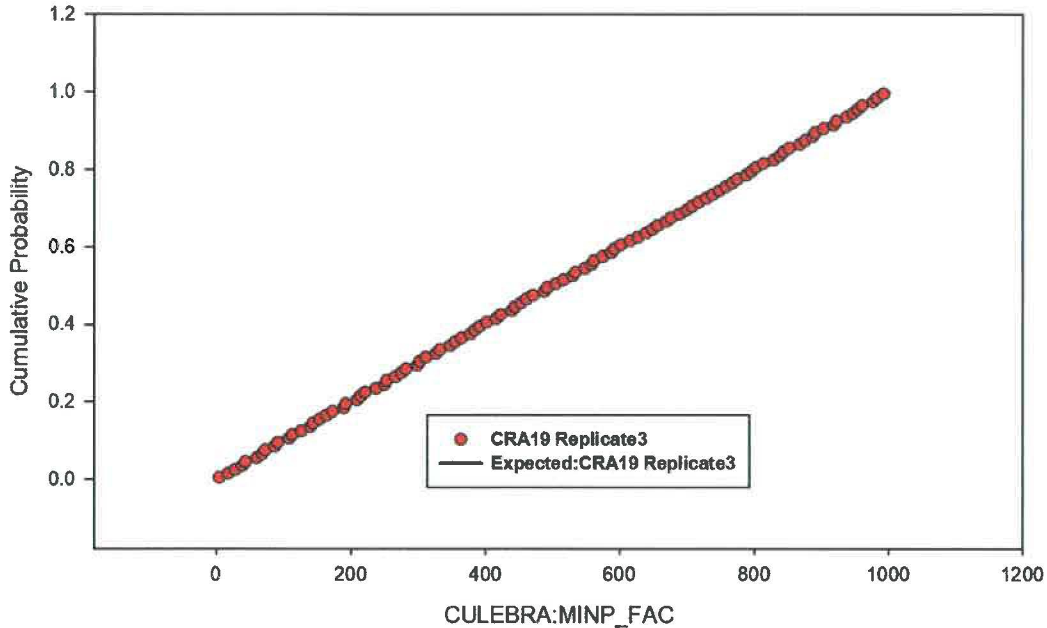

Figure 156 – Observed and Expected CDFs for CULEBRA:MINP_FAC (Uniform Distribution) Replicate 3.

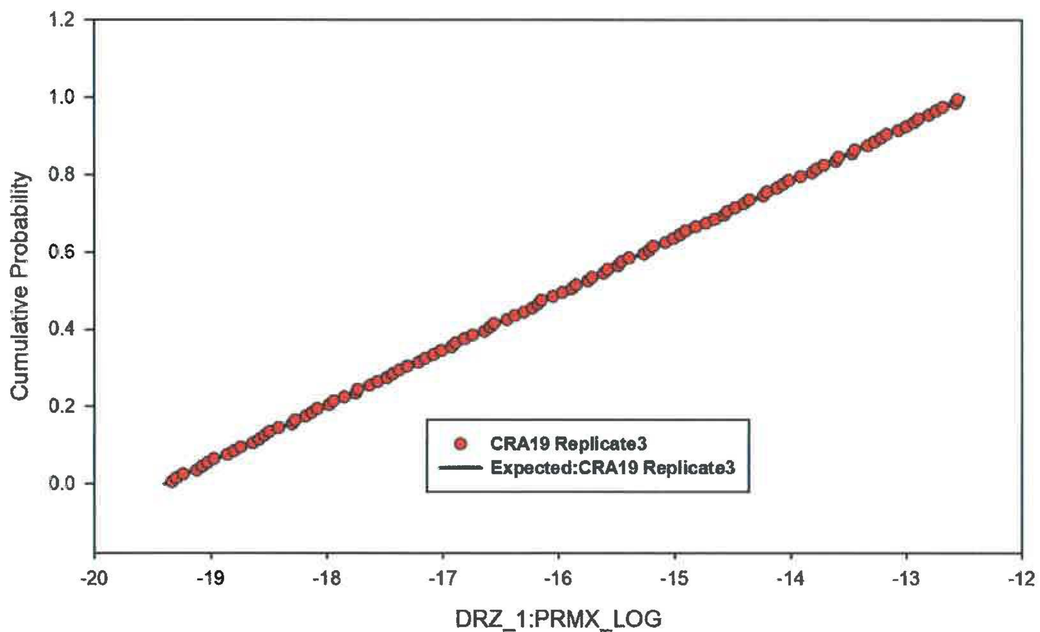

Figure 157 – Observed and Expected CDFs for DRZ_1:PRMX_LOG (Uniform Distribution) Replicate 3.

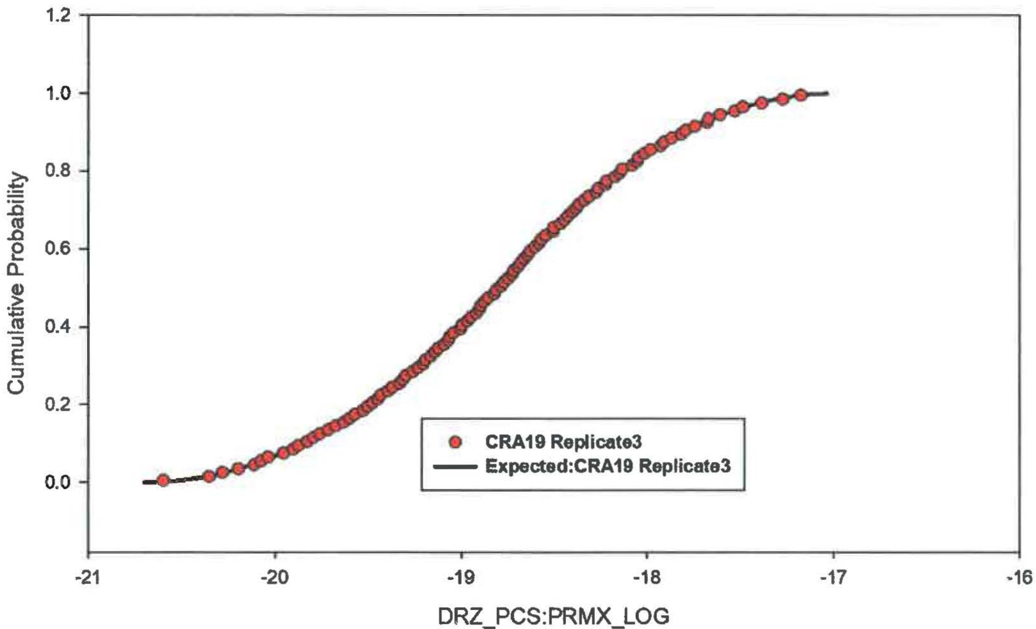

Figure 158 – Observed and Expected CDFs for DRZ_PCS:PRMX_LOG (Triangular Distribution) Replicate 3.

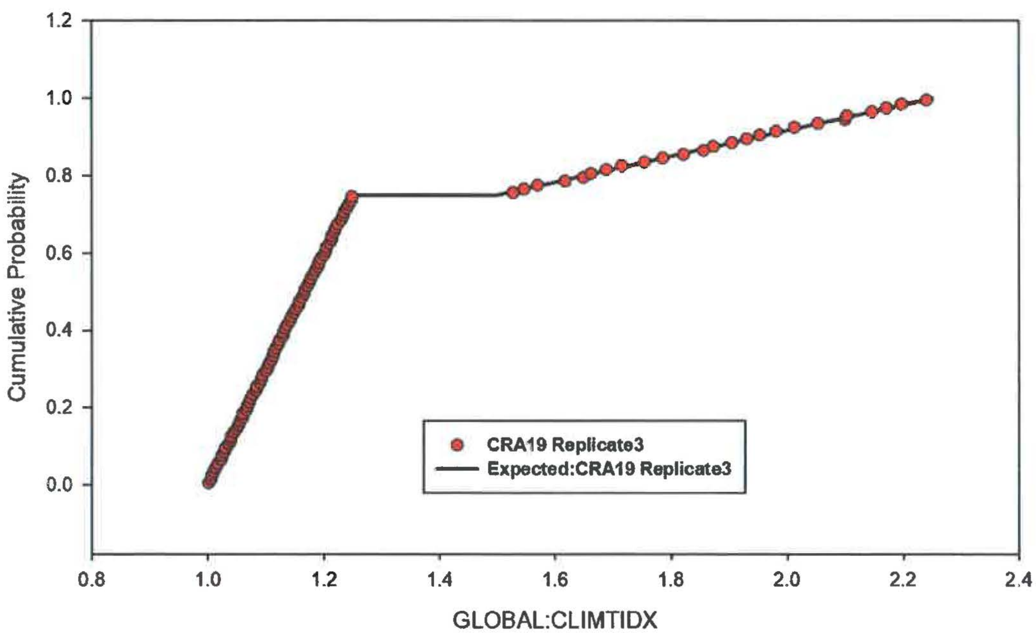

Figure 159 – Observed and Expected CDFs for GLOBAL:CLIMTIDX (Cumulative Distribution) Replicate 3.

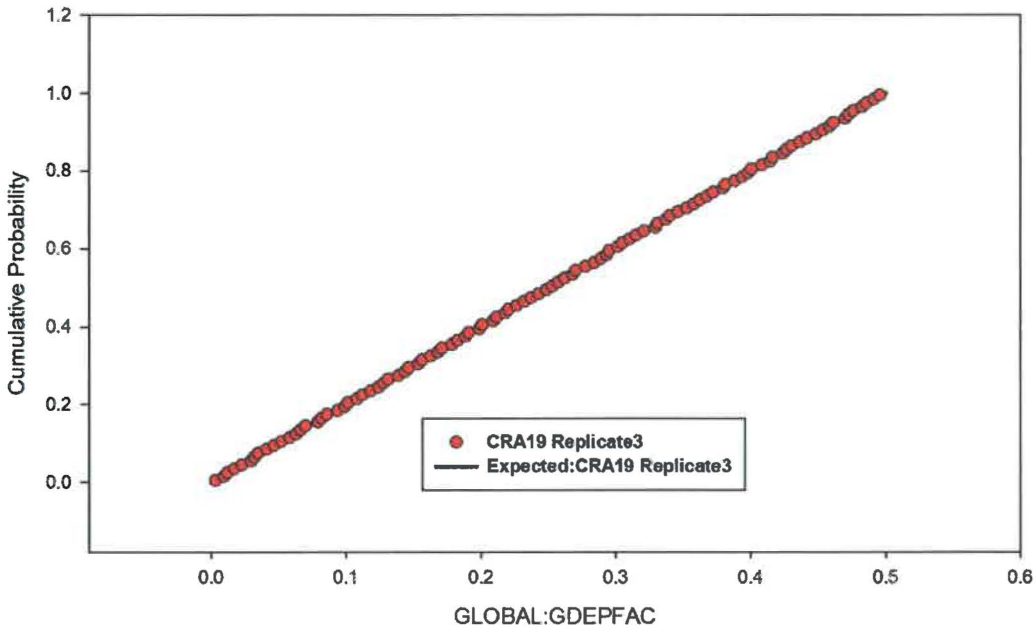

Figure 160 – Observed and Expected CDFs for GLOBAL:GDEPFAC (Uniform Distribution) Replicate 3.

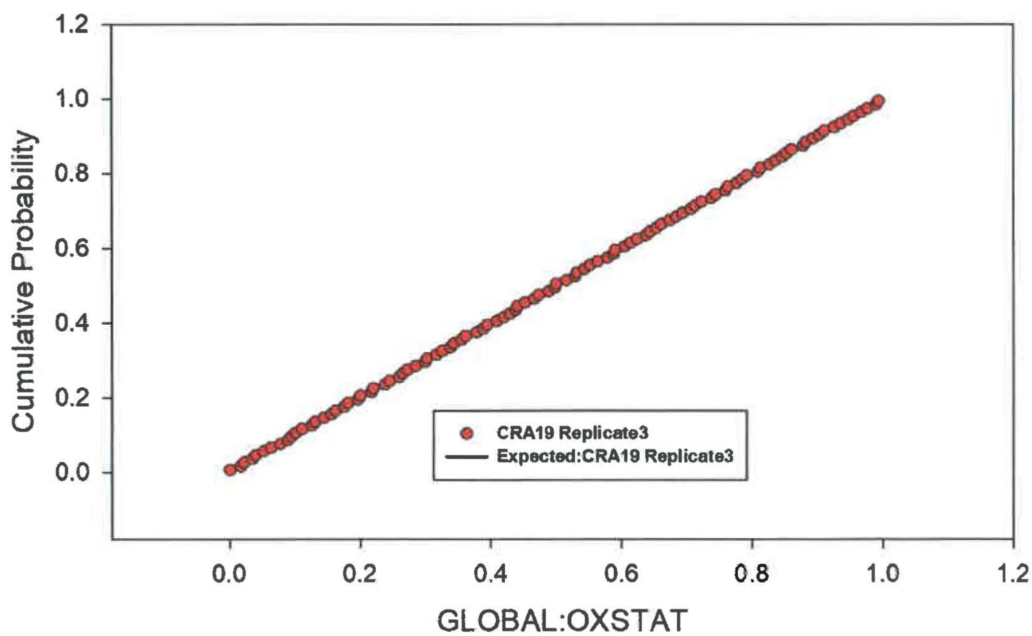

Figure 161 – Observed and Expected CDFs for GLOBAL:OXSTAT (Uniform Distribution) Replicate 3.

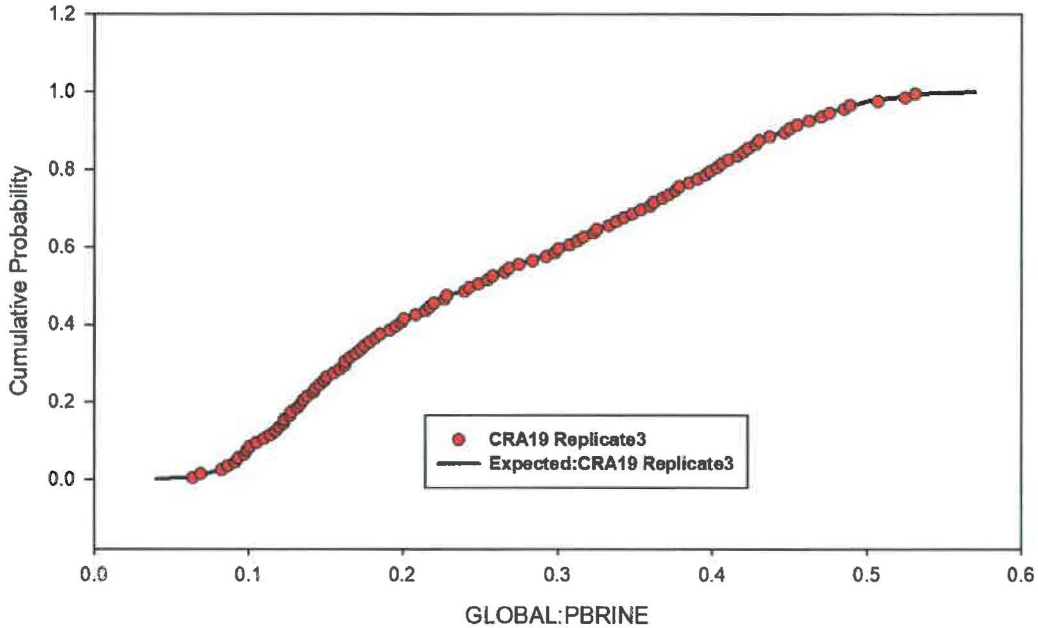

Figure 162 – Observed and Expected CDFs for GLOBAL:PBRINE (Cumulative Distribution) Replicate 3.

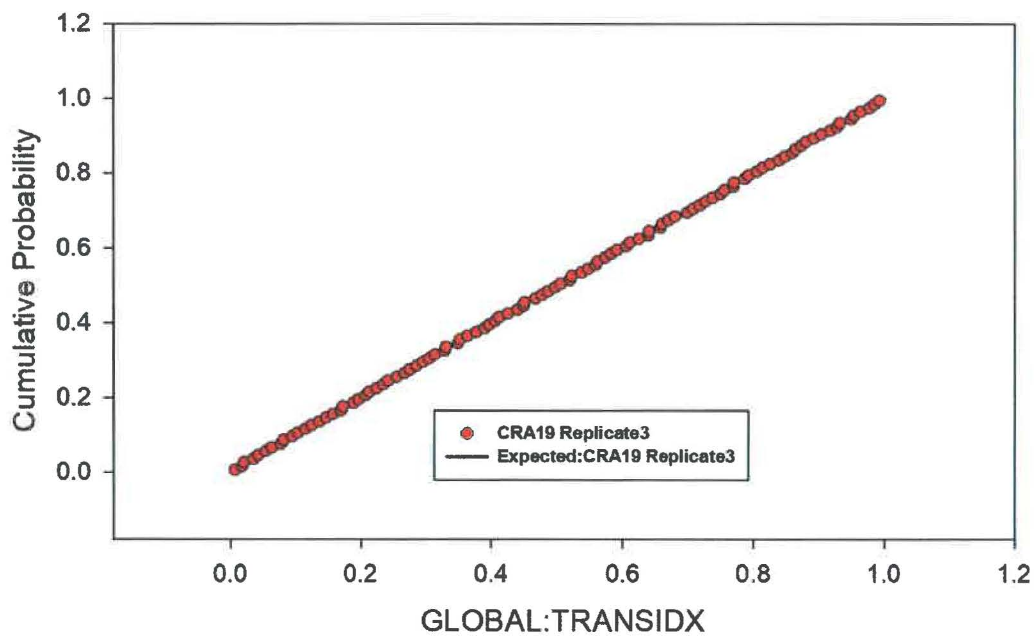

Figure 163 – Observed and Expected CDFs for GLOBAL:TRANSIDX (Uniform Distribution) Replicate 3.

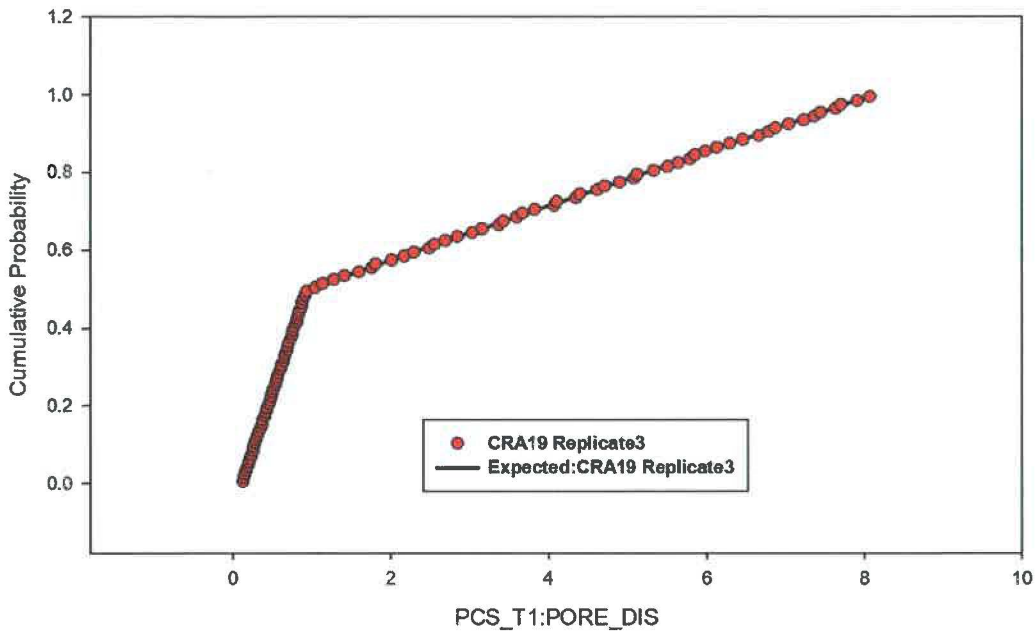

Figure 164 – Observed and Expected CDFs for PCS_T1:PORE_DIS (Cumulative Distribution) Replicate 3.

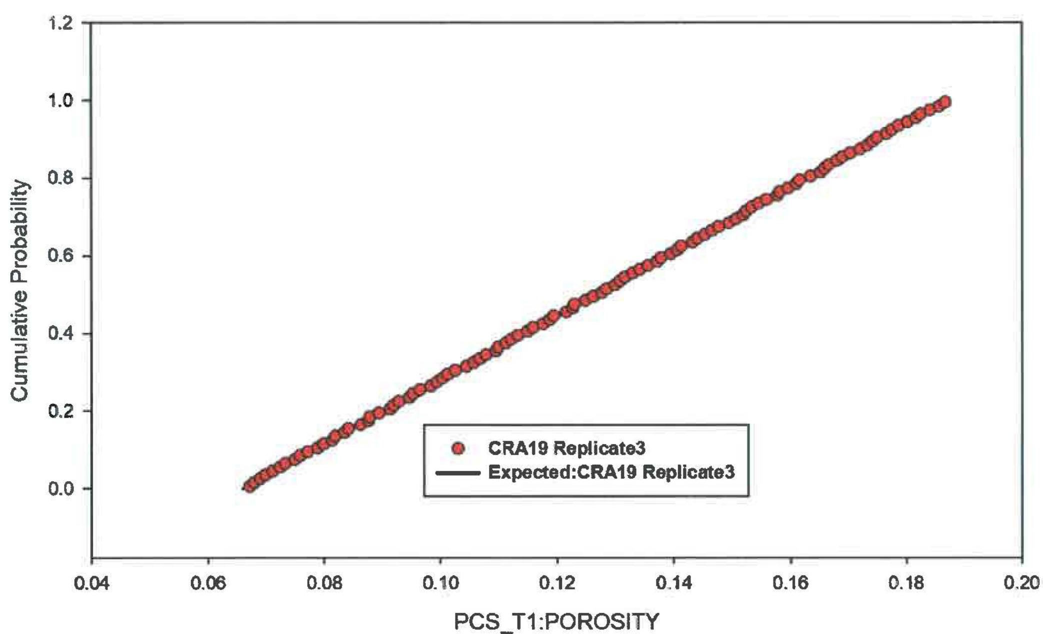

Figure 165 – Observed and Expected CDFs for PCS_T1:POROSITY (Uniform Distribution) Replicate 3.

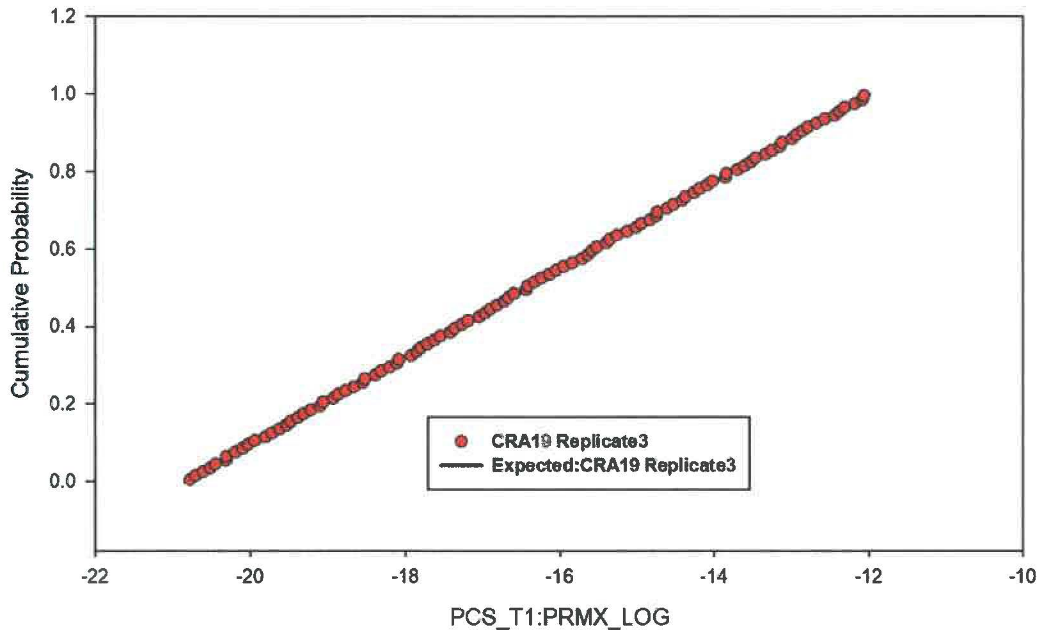

Figure 166 – Observed and Expected CDFs for PCS_T1:PRMX_LOG (Uniform Distribution) Replicate 3.

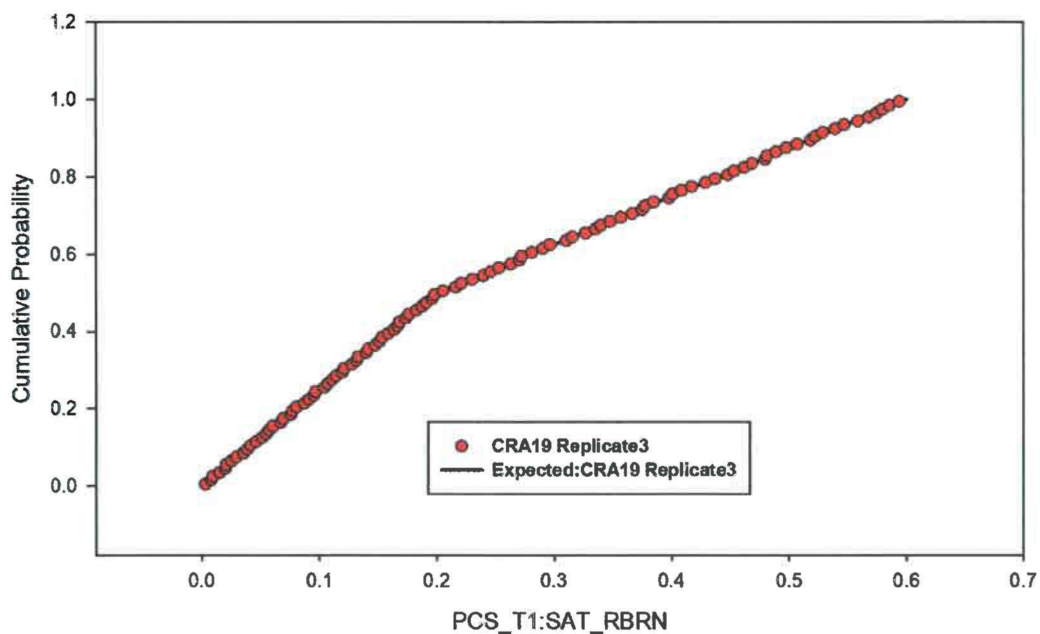

Figure 167 – Observed and Expected CDFs for PCS_T1:SAT_RBRN (Cumulative Distribution) Replicate 3.

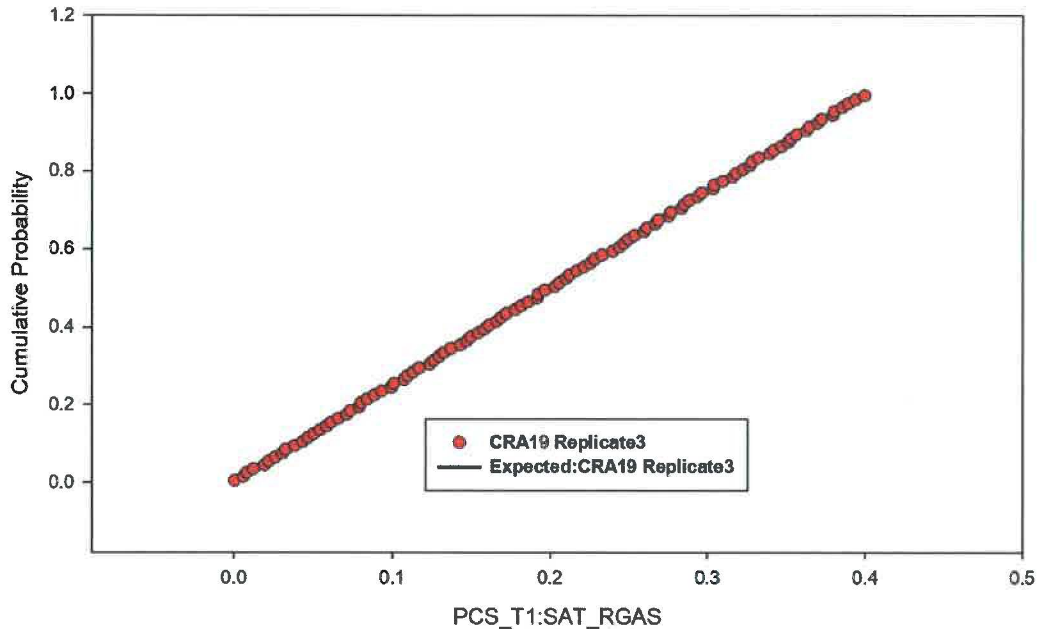

Figure 168 – Observed and Expected CDFs for PCS_T1:SAT_RGAS (Uniform Distribution) Replicate 3.

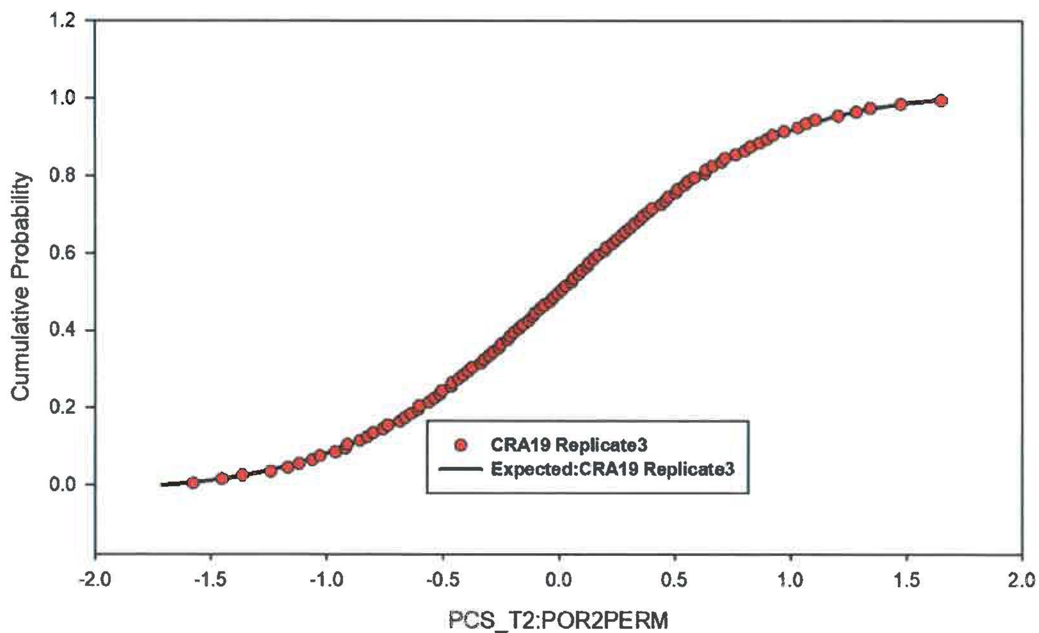

Figure 169 – Observed and Expected CDFs for PCS_T2:POR2PERM (Normal Distribution) Replicate 3.

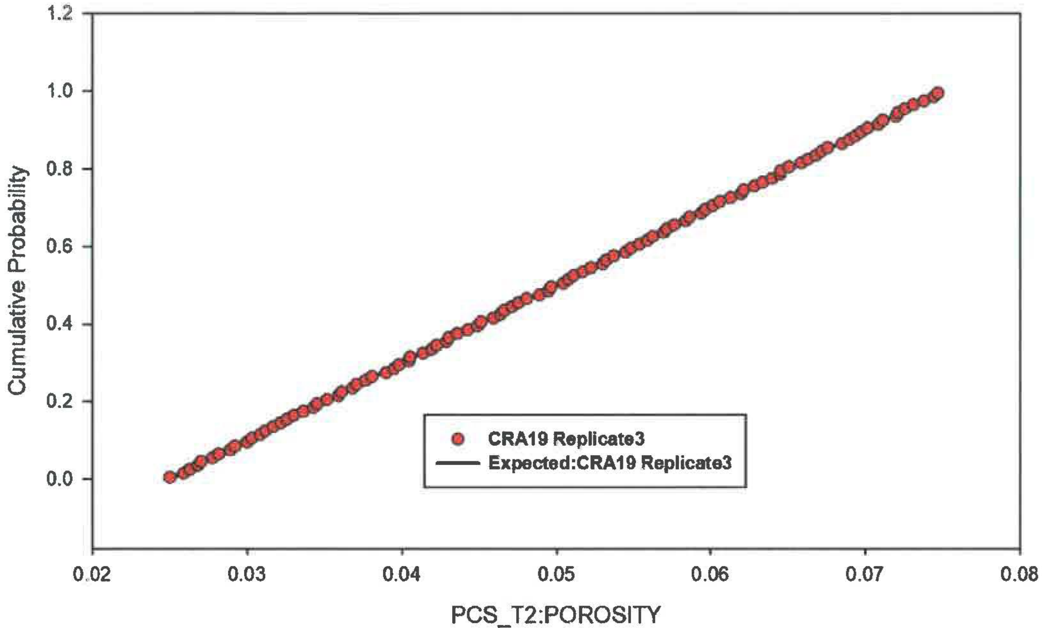

Figure 170 – Observed and Expected CDFs for PCS_T2:POROSITY (Uniform Distribution) Replicate 3.

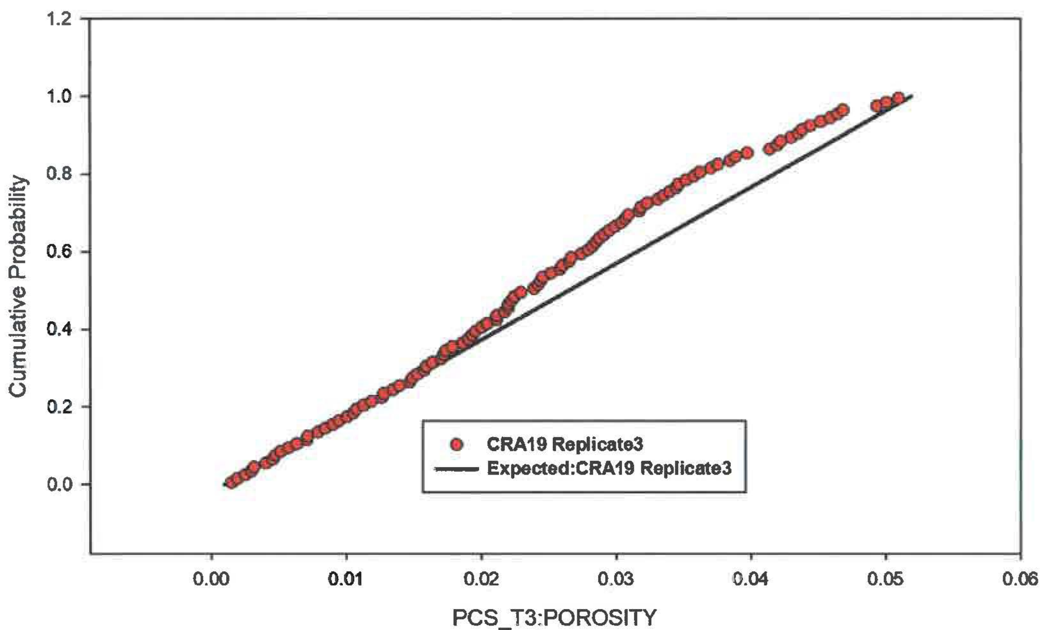

Figure 171 – Observed and Expected CDFs for PCS_T3:POROSITY (Uniform Distribution) Replicate 3.

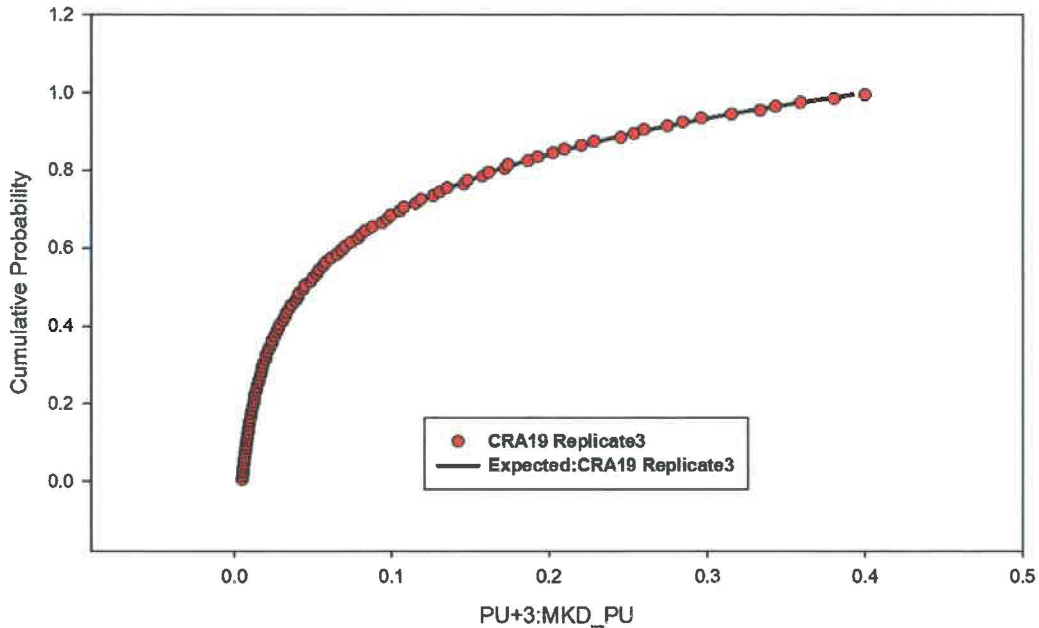

Figure 172 – Observed and Expected CDFs for PU+3:MKD_PU (Loguniform Distribution) Replicate 3.

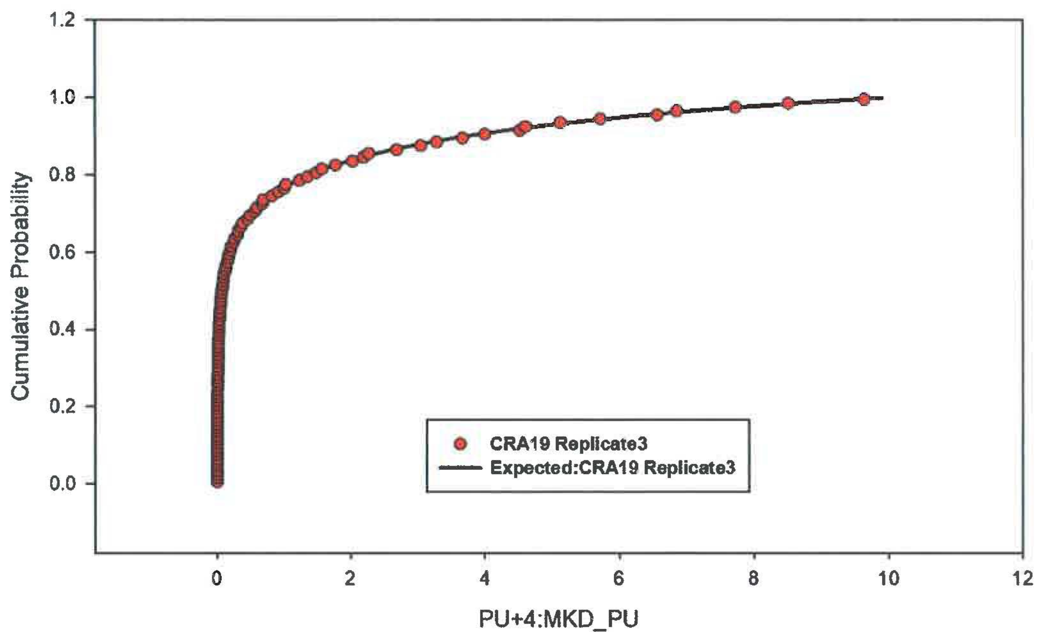

Figure 173 – Observed and Expected CDFs for PU+4:MKD_PU (Loguniform Distribution) Replicate 3.

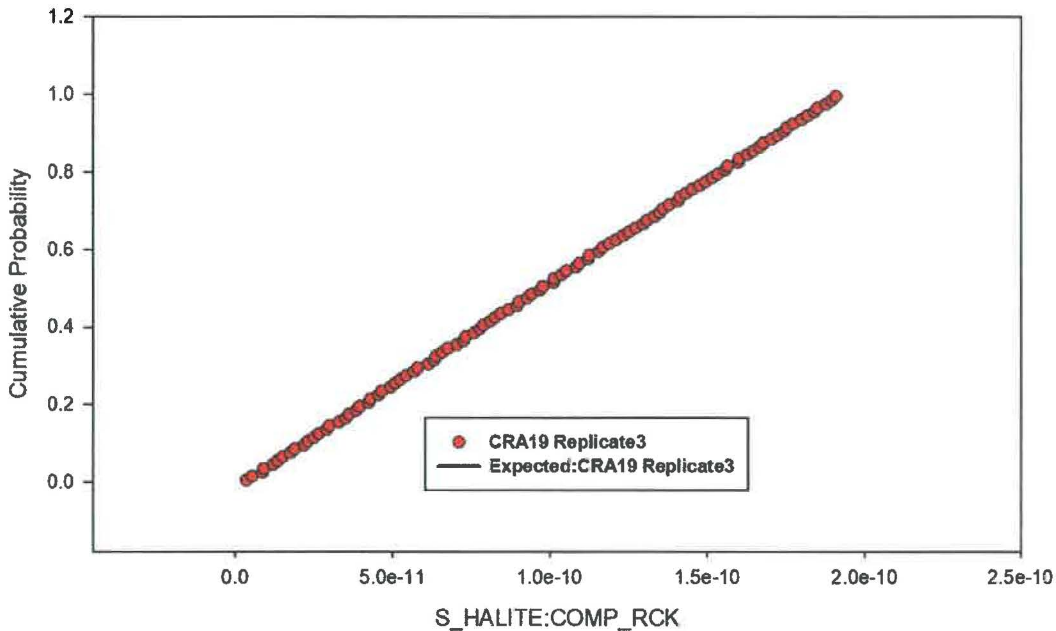

Figure 174 – Observed and Expected CDFs for S_HALITE:COMP_RCK (Uniform Distribution) Replicate 3.

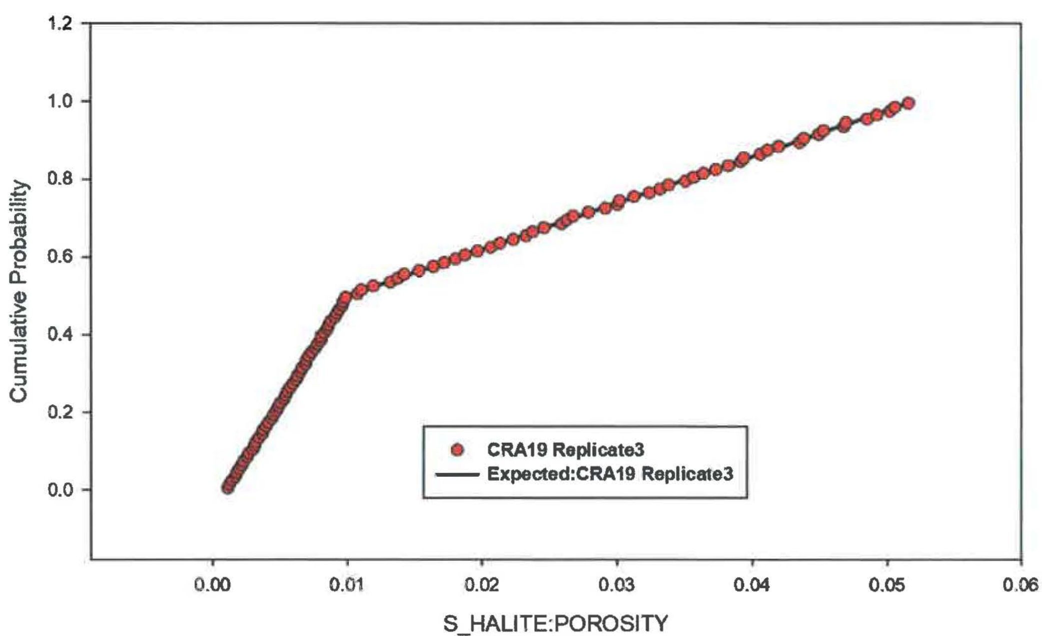

Figure 175 – Observed and Expected CDFs for S_HALITE:POROSITY (Cumulative Distribution) Replicate 3.

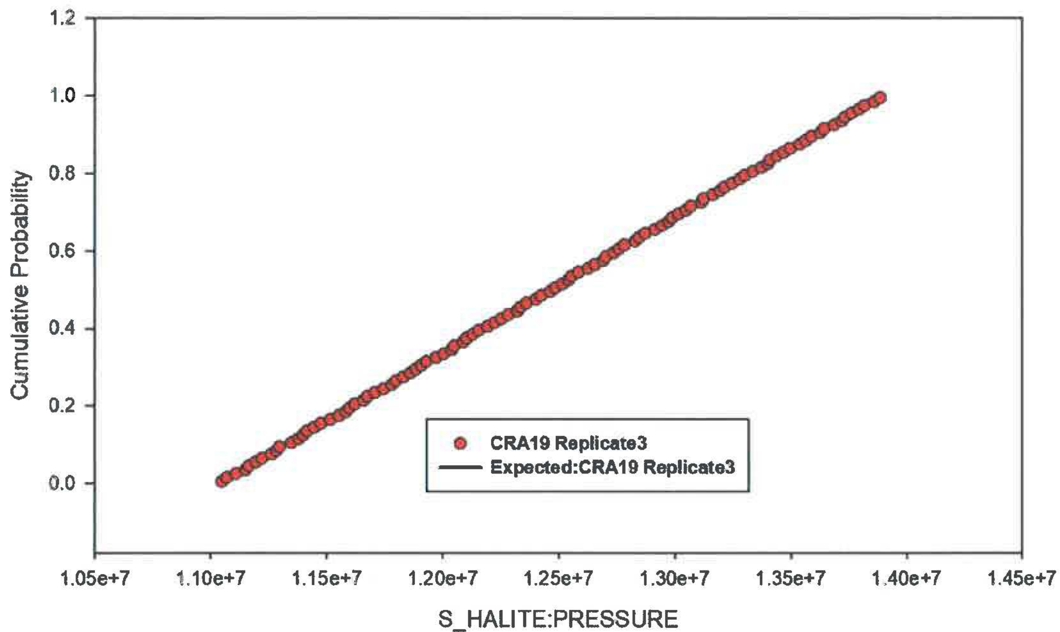

Figure 176 – Observed and Expected CDFs for S_HALITE:PRESSURE (Uniform Distribution) Replicate 3.

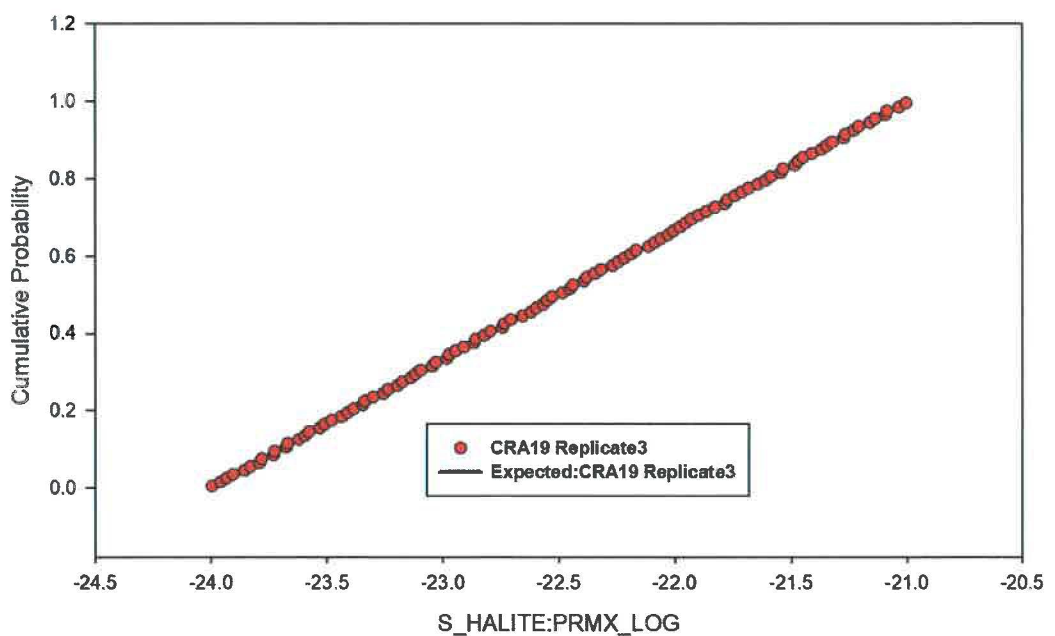

Figure 177 – Observed and Expected CDFs for S_HALITE:PRMX_LOG (Uniform Distribution) Replicate 3.

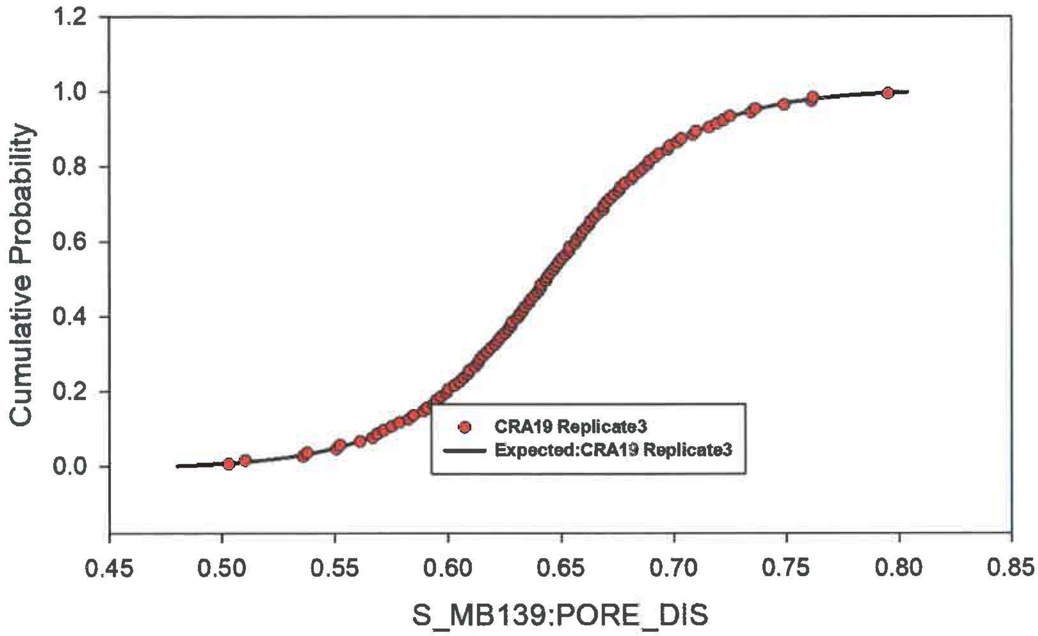

Figure 178 – Observed and Expected CDFs for S_MB139:PORE_DIS (Student Distribution) Replicate 3.

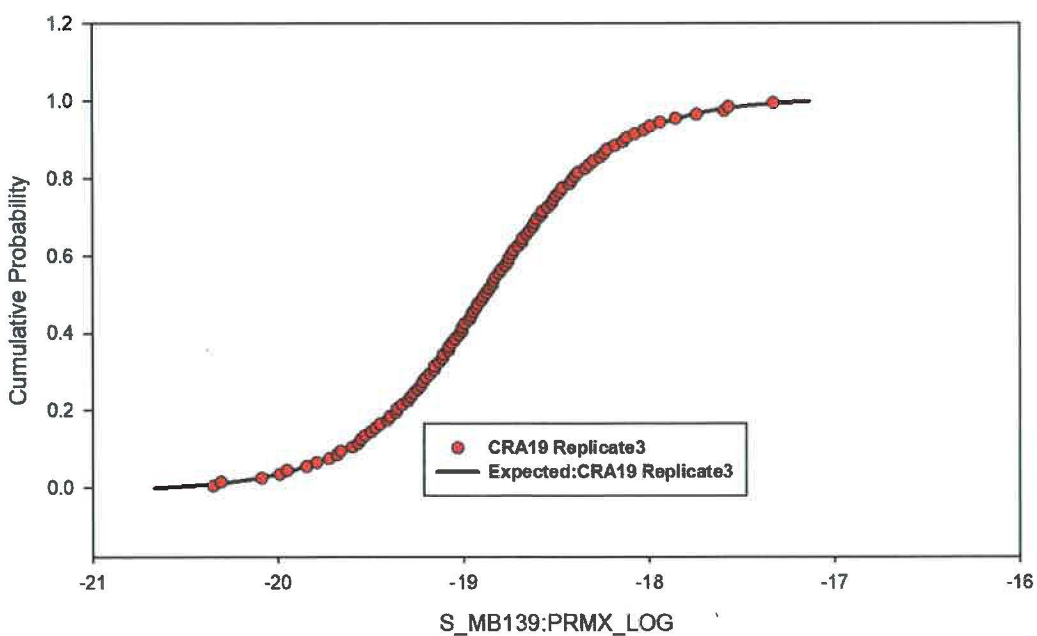

Figure 179 – Observed and Expected CDFs for S_MB139:PRMX_LOG (Student Distribution) Replicate 3.

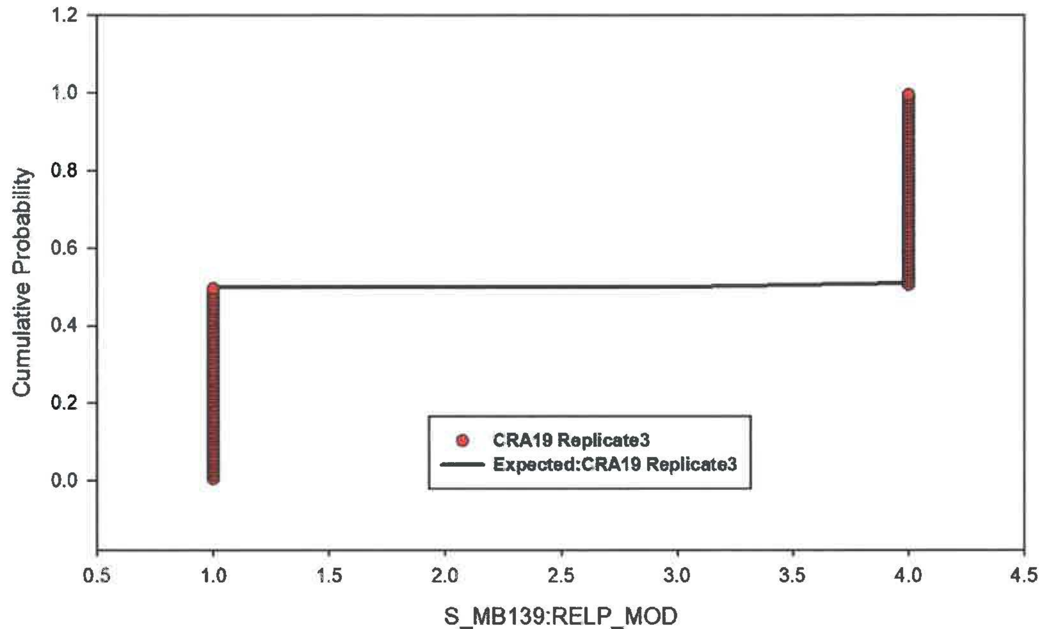

Figure 180 – Observed and Expected CDFs for S_MB139:RELP_MOD (Delta Distribution) Replicate 3.

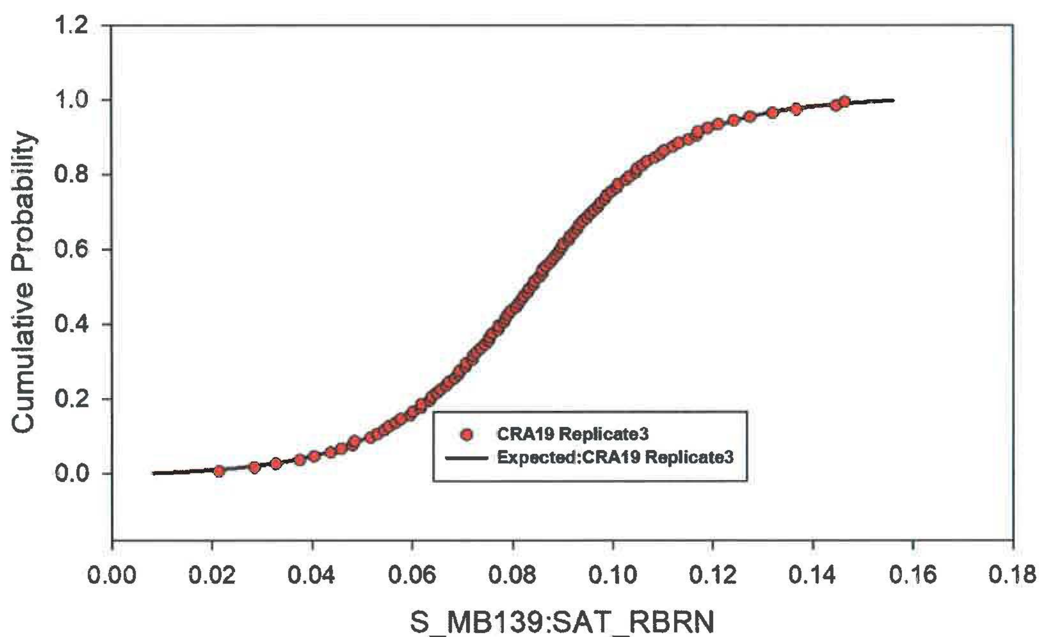

Figure 181 – Observed and Expected CDFs for S_MB139:SAT_RBRN (Student Distribution) Replicate 3.

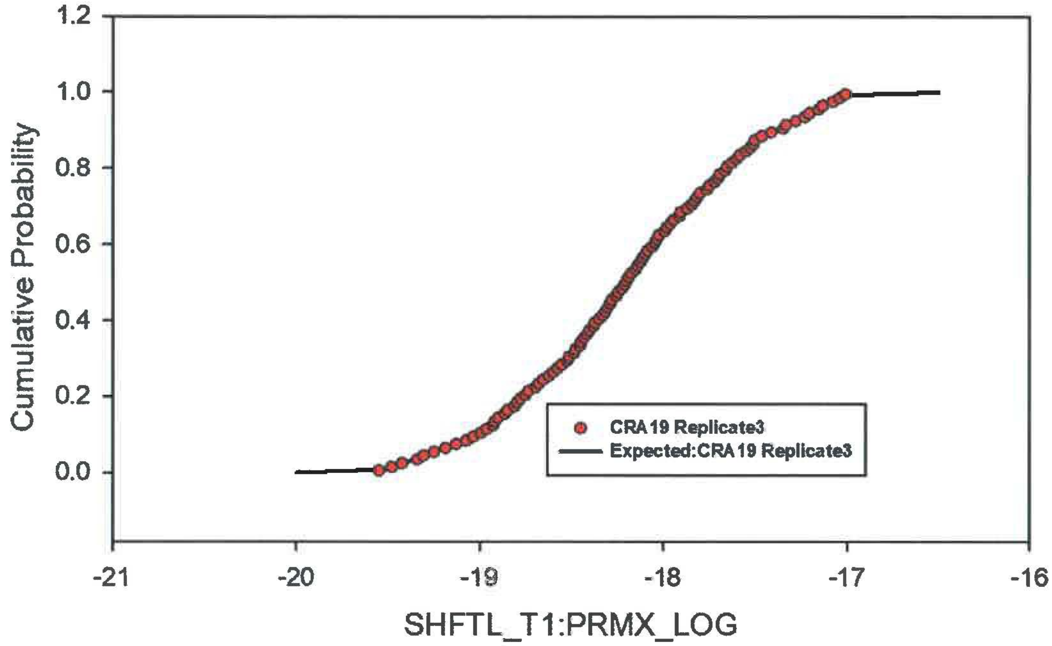

Figure 182 – Observed and Expected CDFs for SHFTL_T1:PRMX_LOG (Cumulative Distribution) Replicate 3.

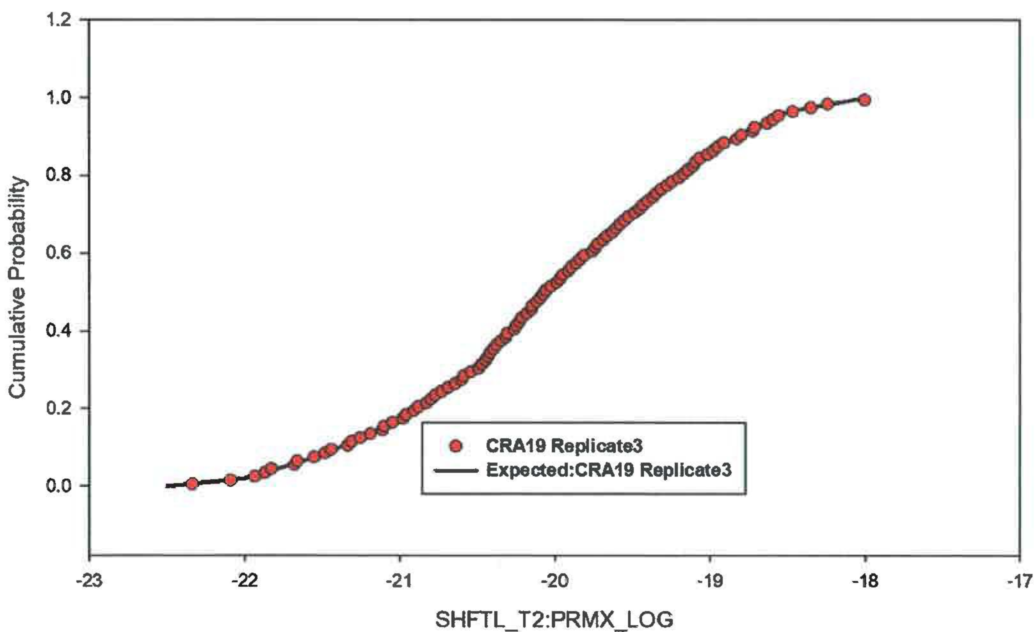

Figure 183 – Observed and Expected CDFs for SHFTL_T2:PRMX_LOG (Cumulative Distribution) Replicate 3.

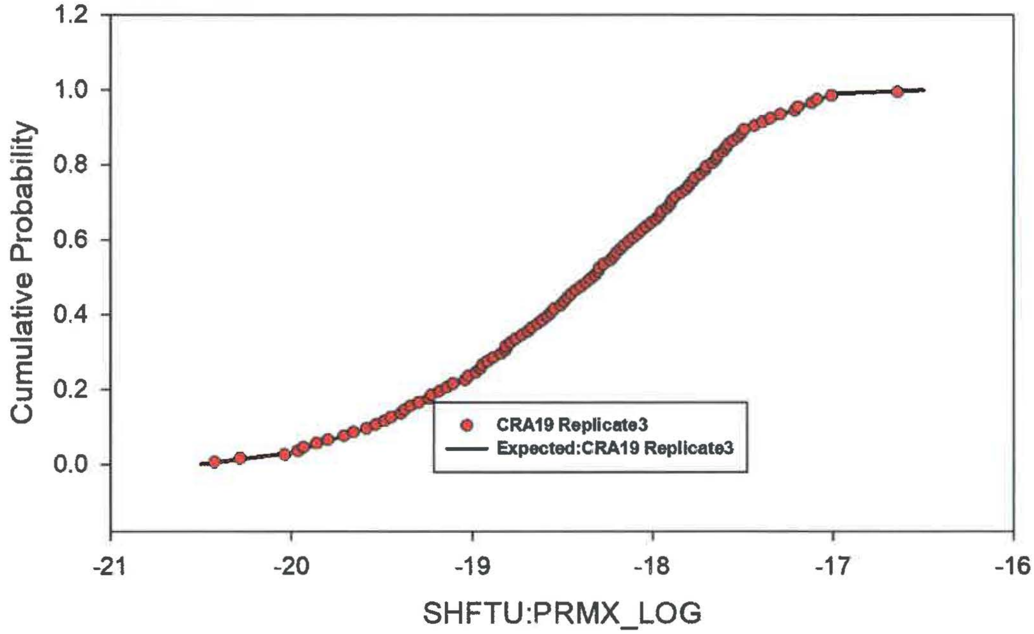

Figure 184 – Observed and Expected CDFs for SHFTU:PRMX_LOG (Cumulative Distribution) Replicate 3.

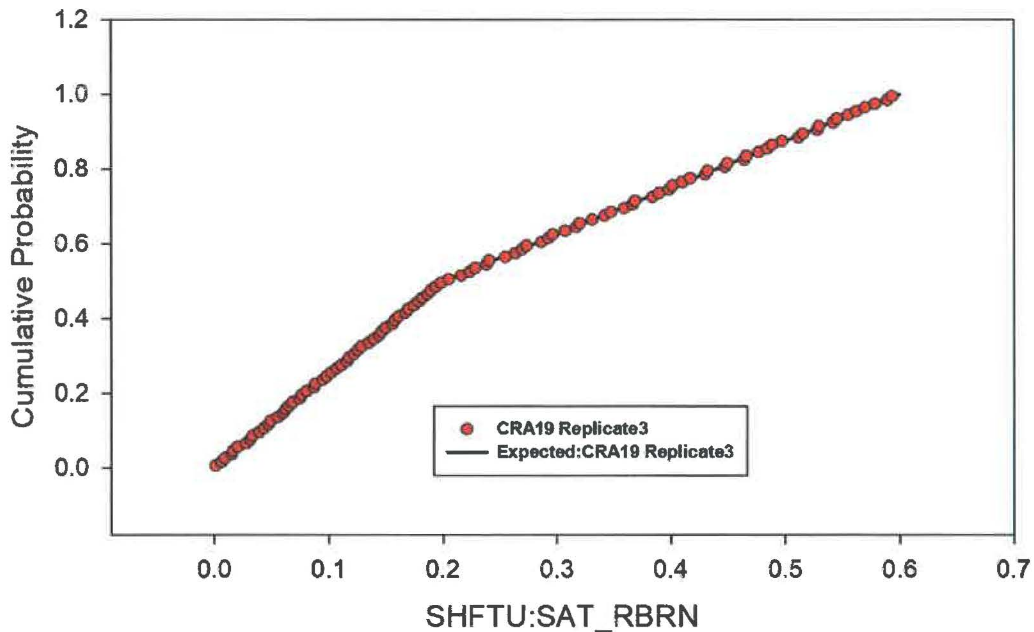

Figure 185 – Observed and Expected CDFs for SHFTU:SAT_RBRN (Cumulative Distribution) Replicate 3.

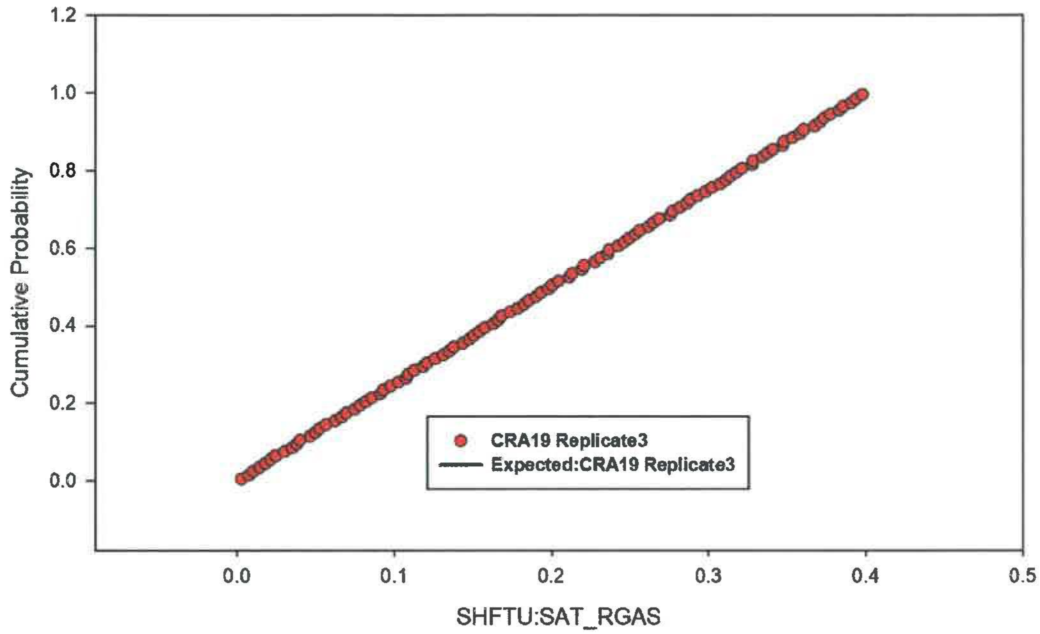

Figure 186 – Observed and Expected CDFs for SHFTU:SAT_RGAS (Uniform Distribution) Replicate 3.

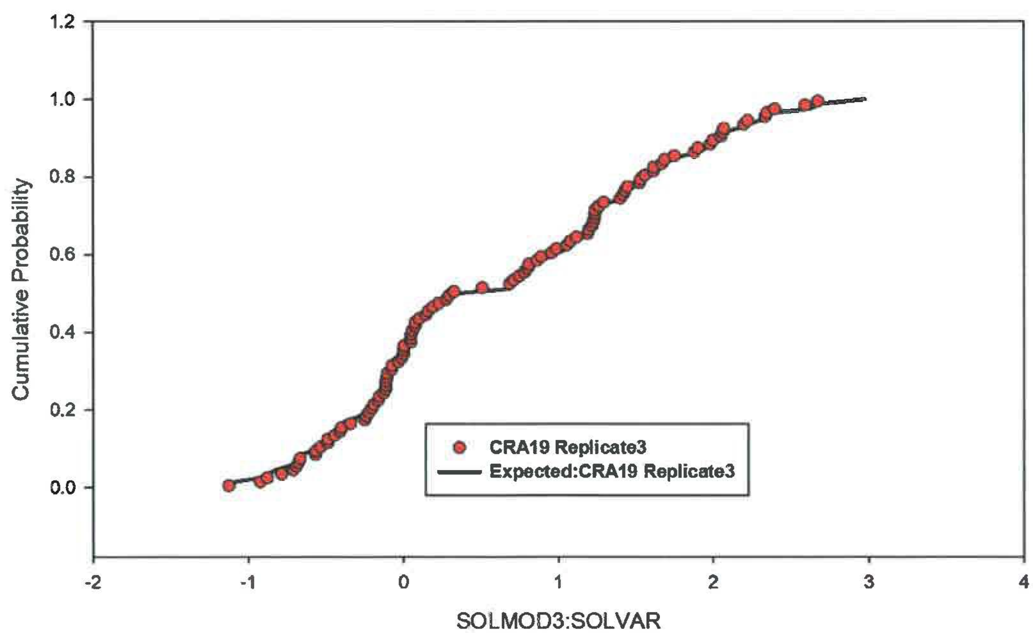

Figure 187 – Observed and Expected CDFs for SOLMOD3:SOLVAR (Cumulative Distribution) Replicate 3.

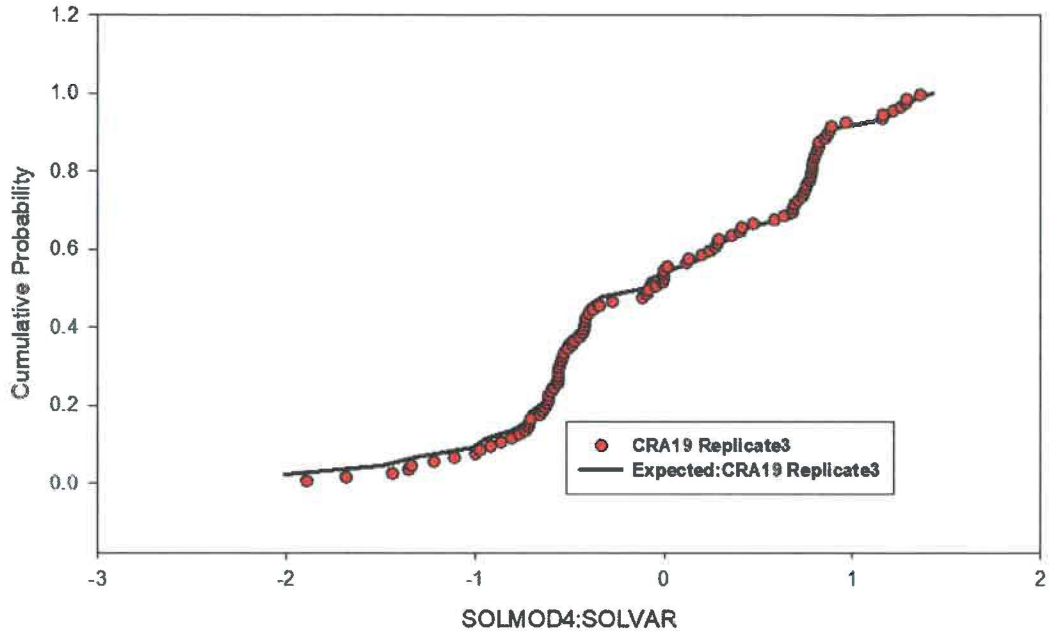

Figure 188 – Observed and Expected CDFs for SOLMOD4:SOLVAR (Cumulative Distribution) Replicate 3.

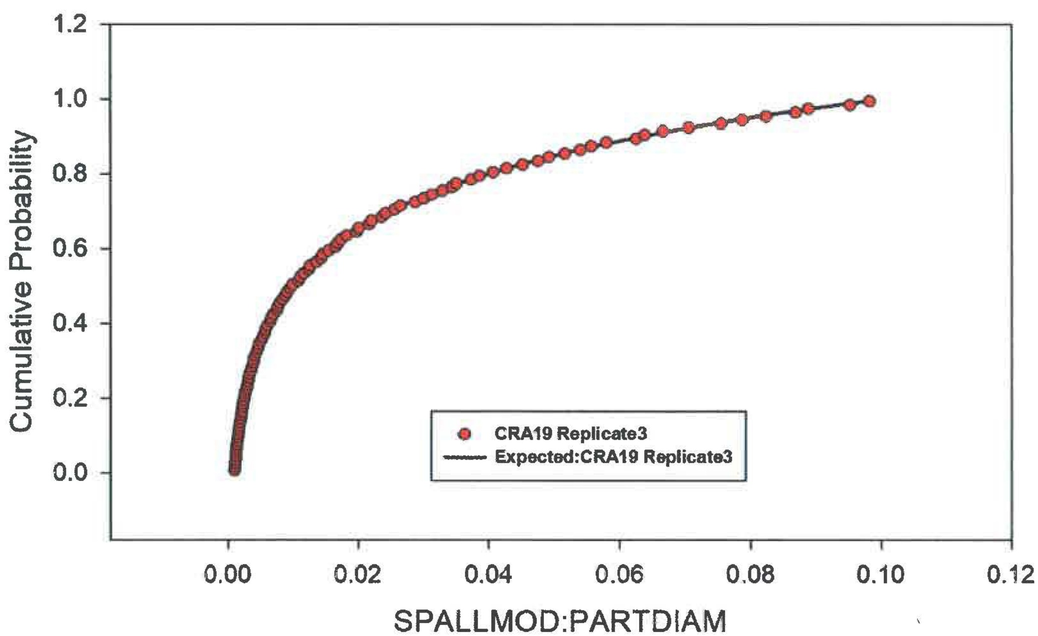

Figure 189 – Observed and Expected CDFs for SPALLMOD:PARTDIAM (Loguniform Distribution) Replicate 3.

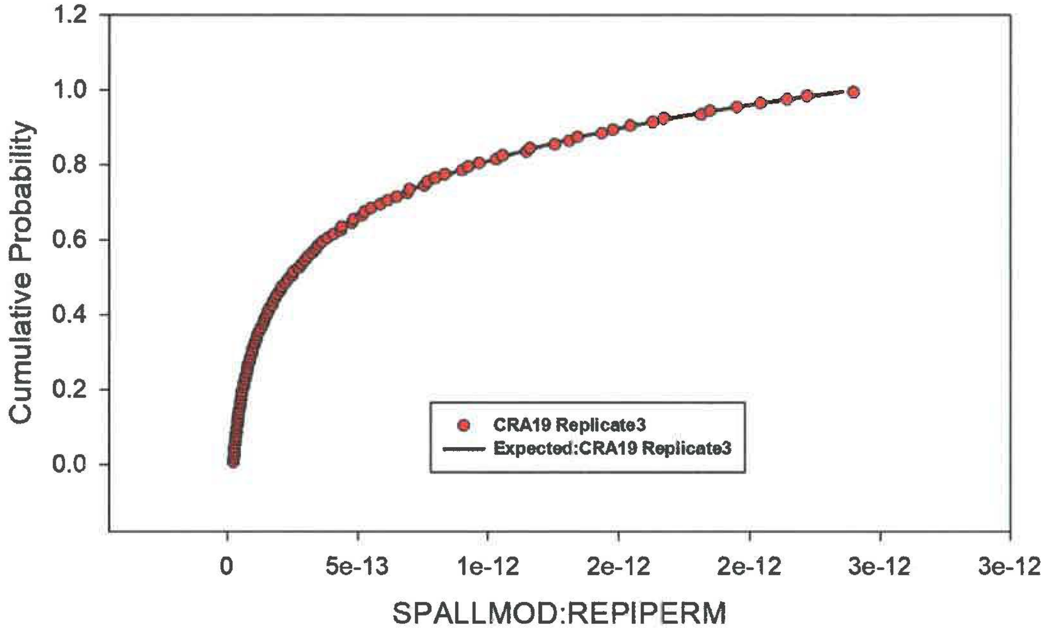

Figure 190 – Observed and Expected CDFs for SPALLMOD:REPIPERM (Loguniform Distribution) Replicate 3.

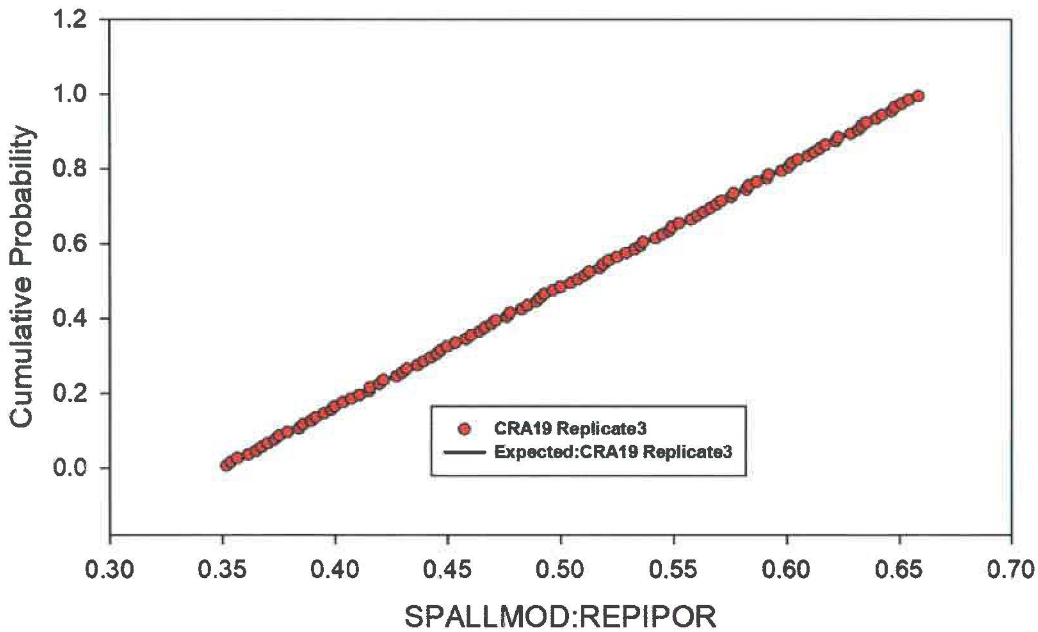

Figure 191 – Observed and Expected CDFs for SPALLMOD:REPIPOR (Uniform Distribution) Replicate 3.

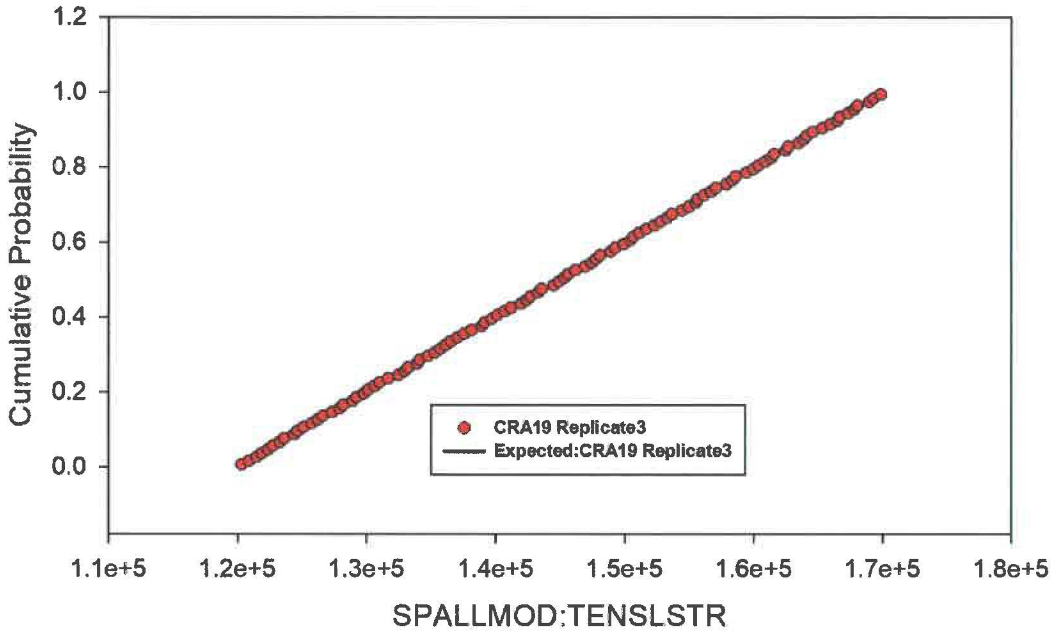

Figure 192 – Observed and Expected CDFs for SPALLMOD:TENSLSTR (Uniform Distribution) Replicate 3.

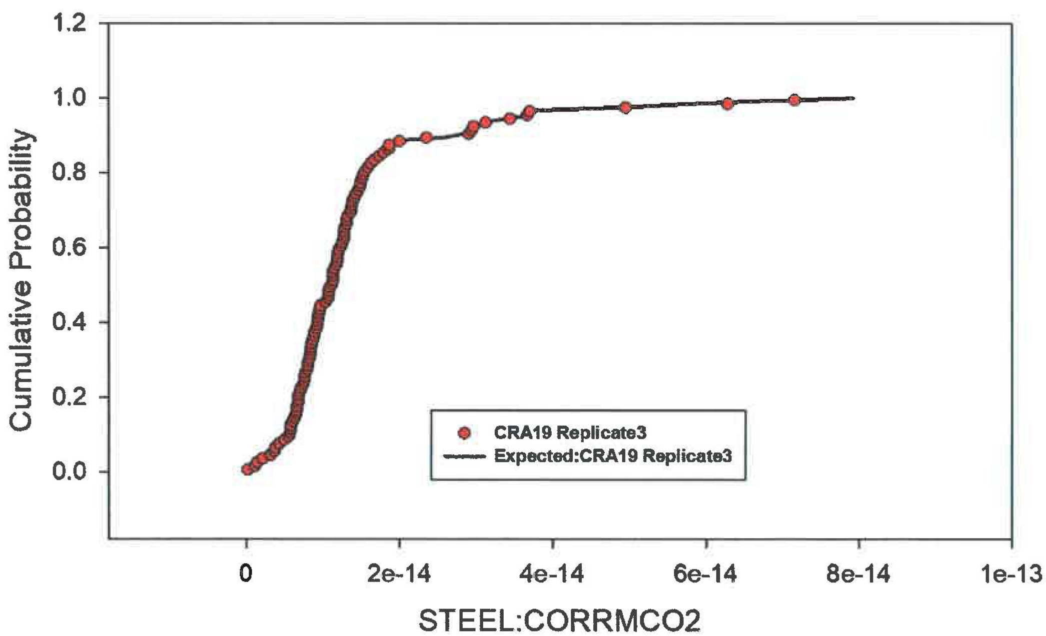

Figure 193 – Observed and Expected CDFs for STEEL:CORRMCO2 (Cumulative Distribution) Replicate 3.

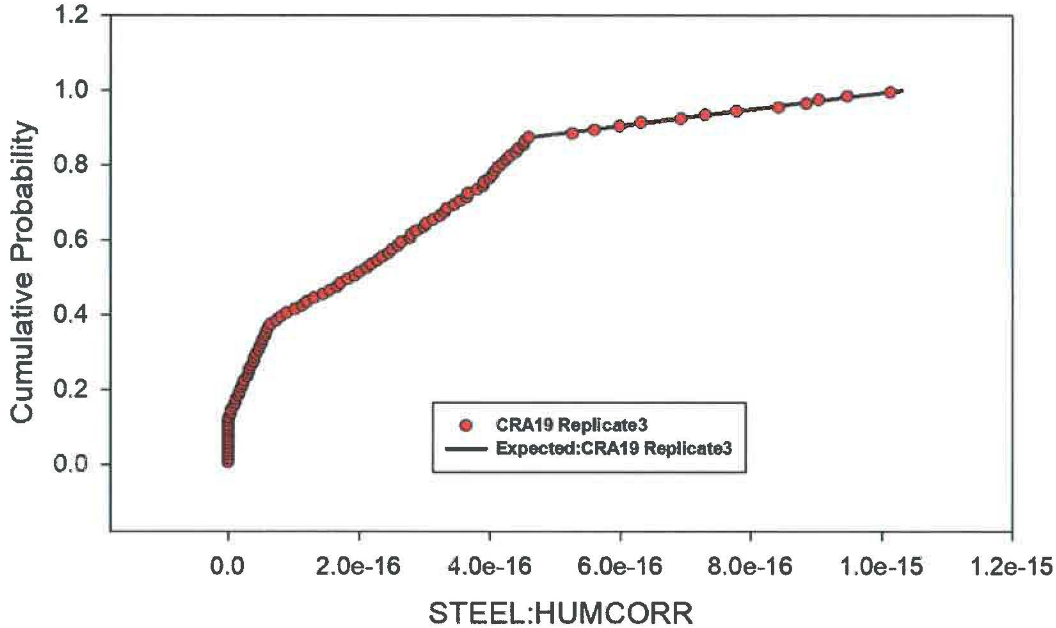

Figure 194 – Observed and Expected CDFs for STEEL:HUMCORR (Cumulative Distribution) Replicate 3.

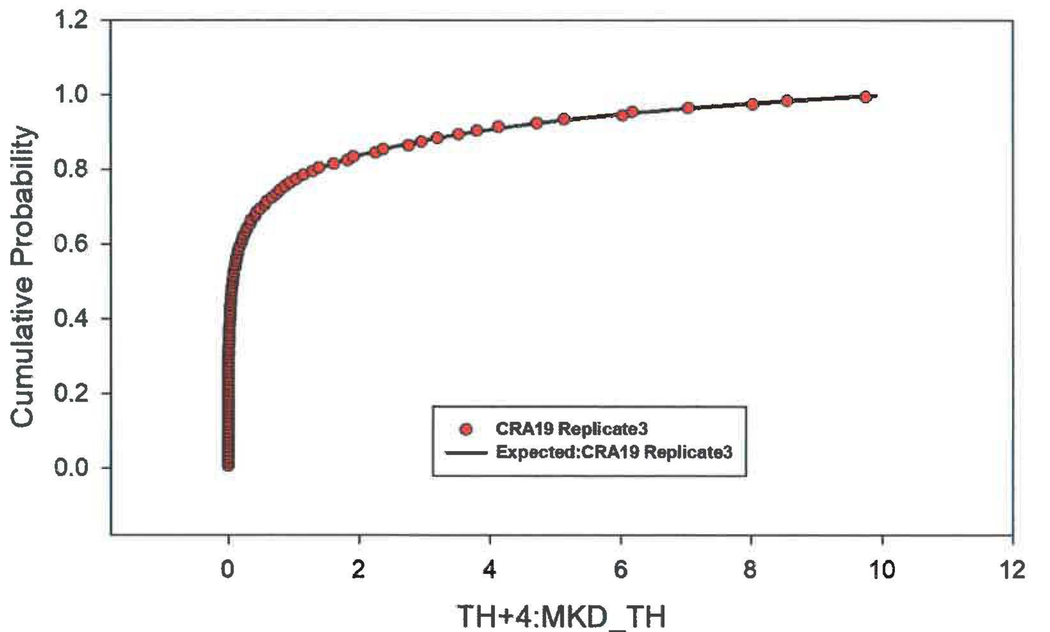

Figure 195 – Observed and Expected CDFs for TH+4:MKD_TH (Loguniform Distribution) Replicate 3.

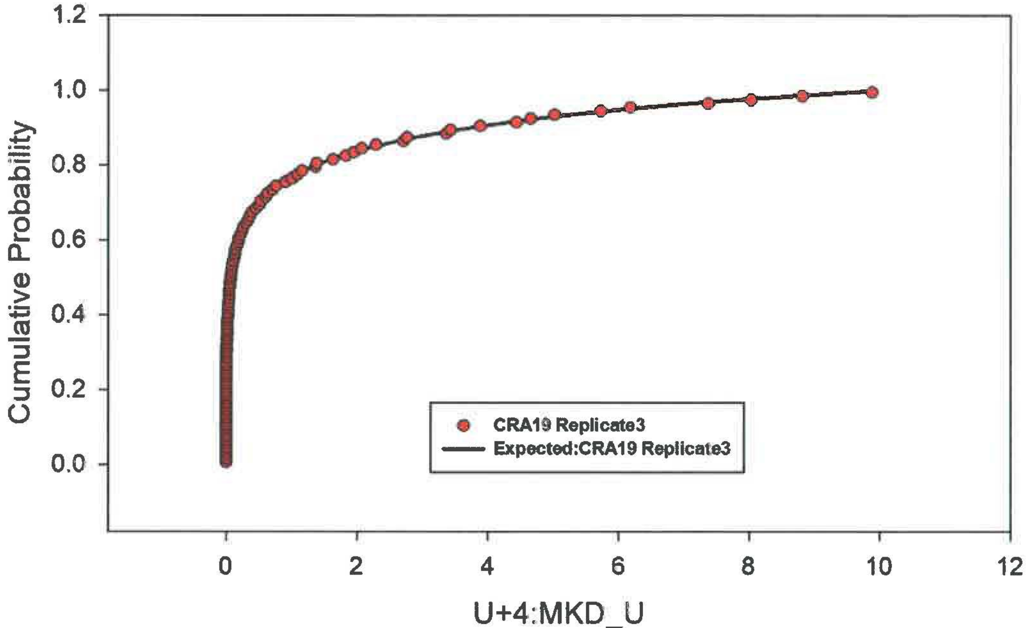

Figure 196 – Observed and Expected CDFs for U+4:MKD_U (Loguniform Distribution) Replicate 3.

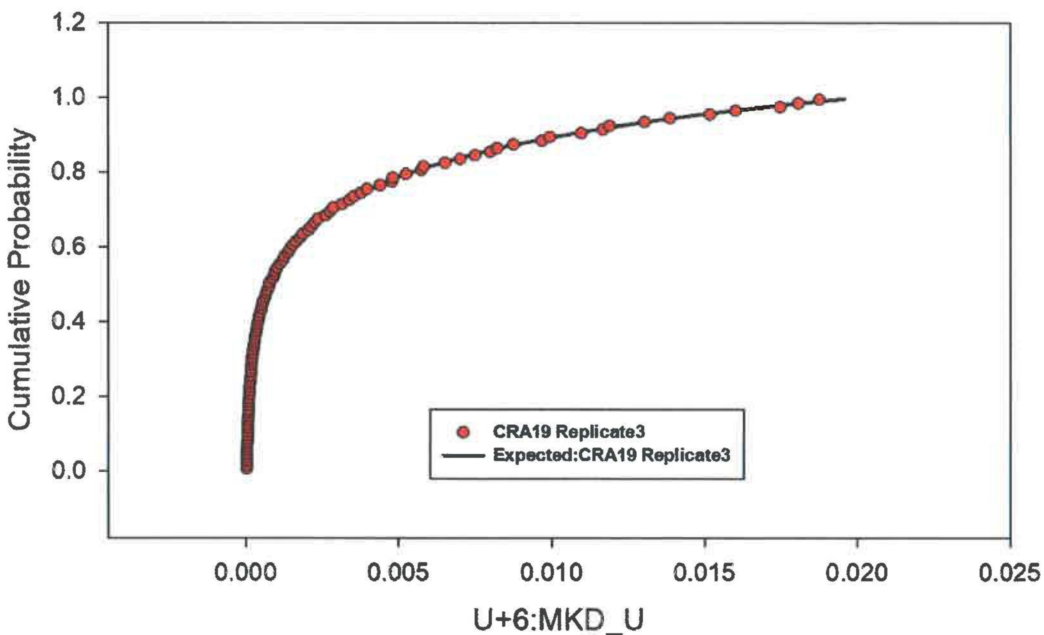

Figure 197 – Observed and Expected CDFs for U+6:MKD_U (Loguniform Distribution) Replicate 3.

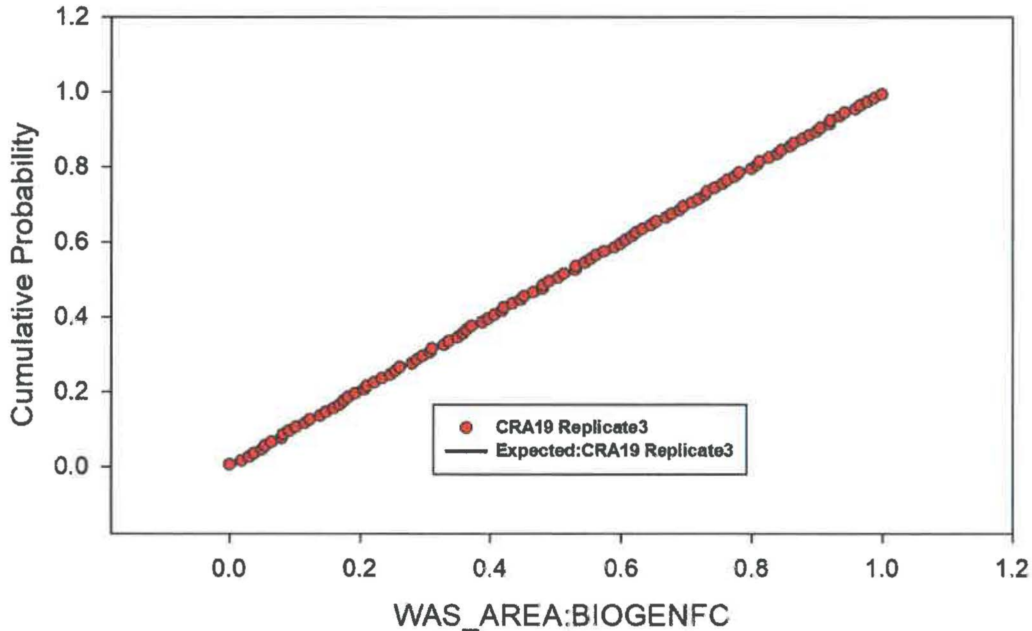

Figure 198 – Observed and Expected CDFs for WAS_AREA:BIOGENFC (Uniform Distribution) Replicate 3.

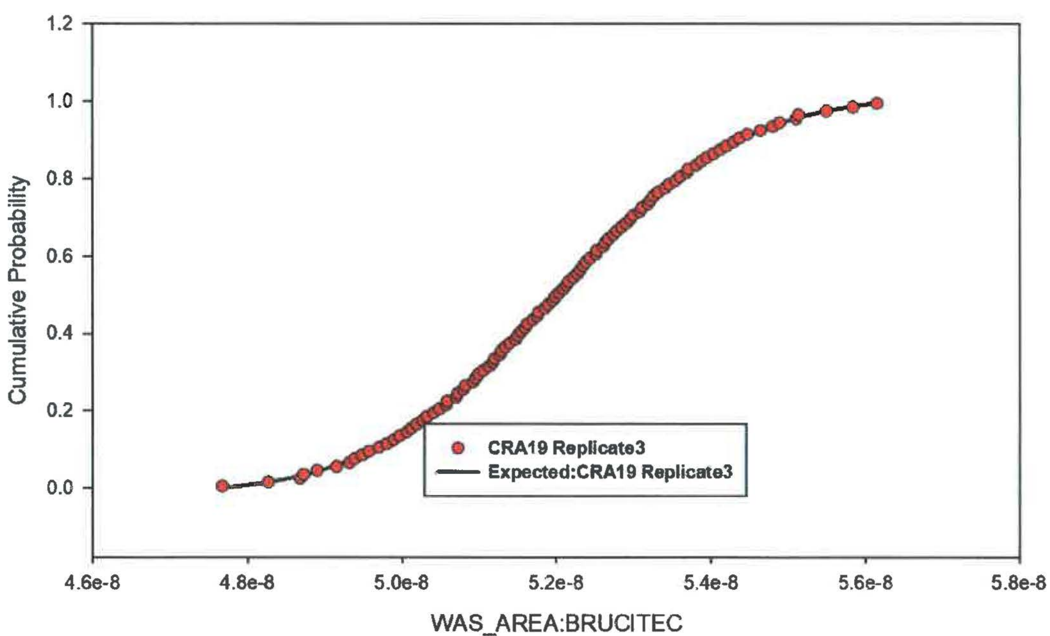

Figure 199 – Observed and Expected CDFs for WAS_AREA:BRUCITEC (Normal Distribution) Replicate 3.

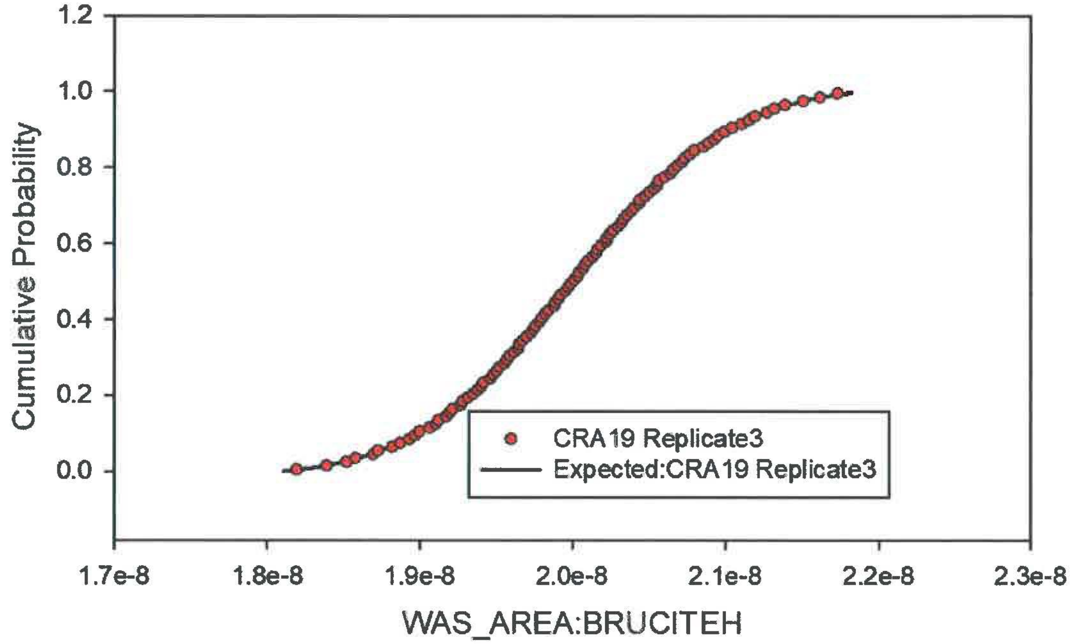

Figure 200 – Observed and Expected CDFs for WAS_AREA:BRUCITEH (Normal Distribution) Replicate 3.

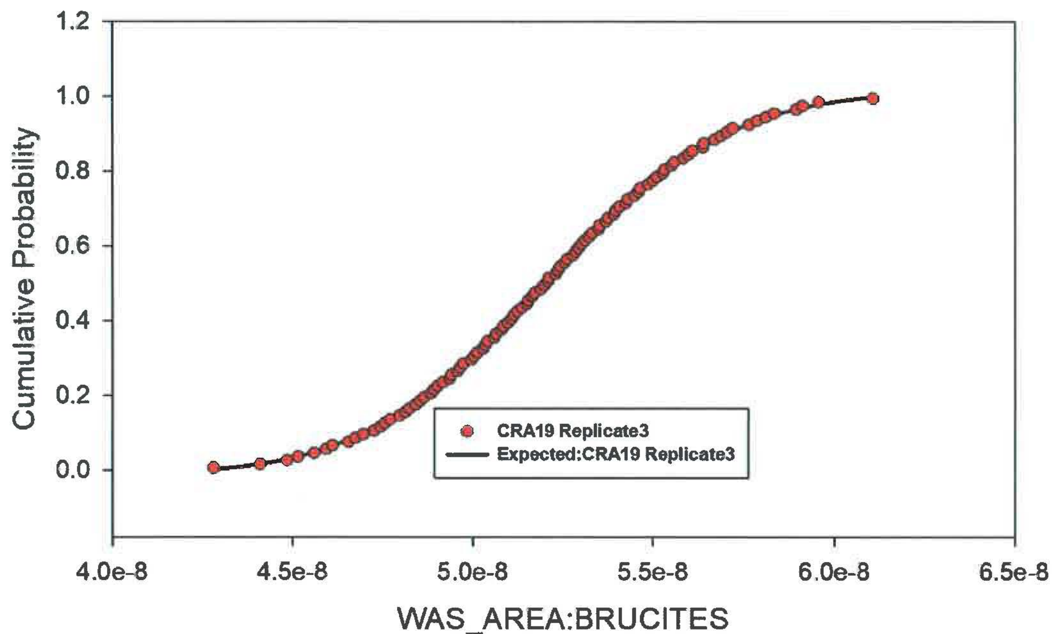

Figure 201 – Observed and Expected CDFs for WAS_AREA:BRUCITES (Normal Distribution) Replicate 3.

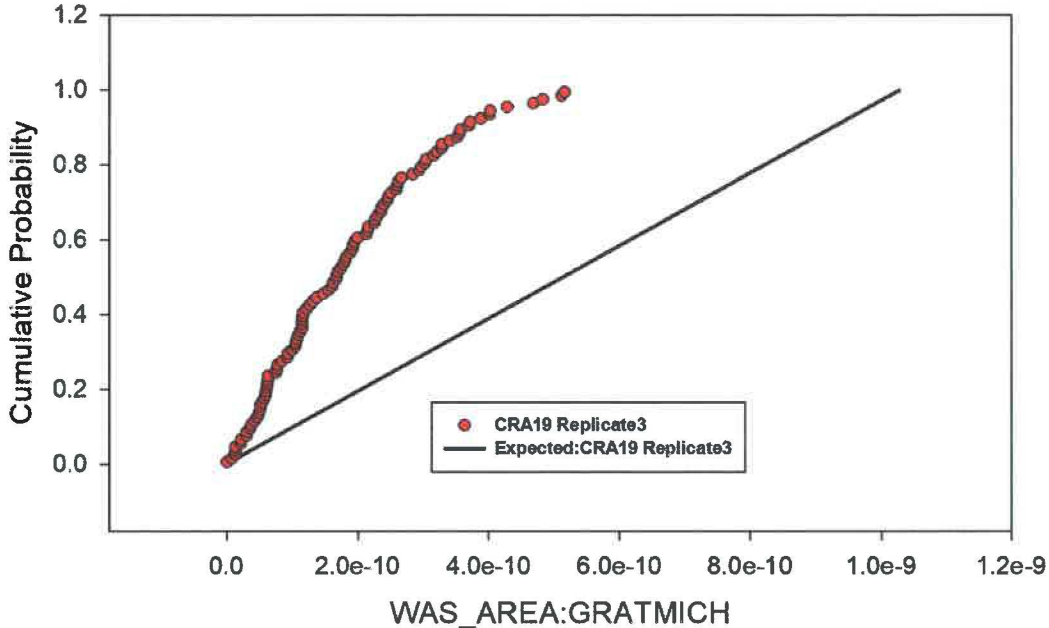

Figure 202 – Observed and Expected CDFs for WAS_AREA:GRATMICH (Uniform Distribution) Replicate 3.

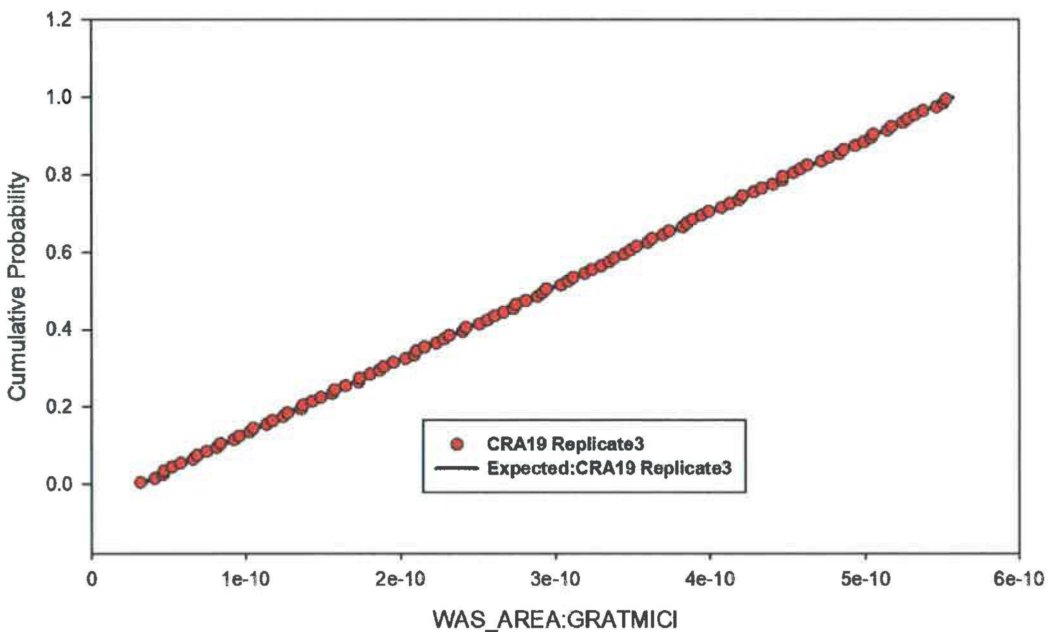

Figure 203 – Observed and Expected CDFs for WAS_AREA:GRATMICI (Uniform Distribution) Replicate 3.

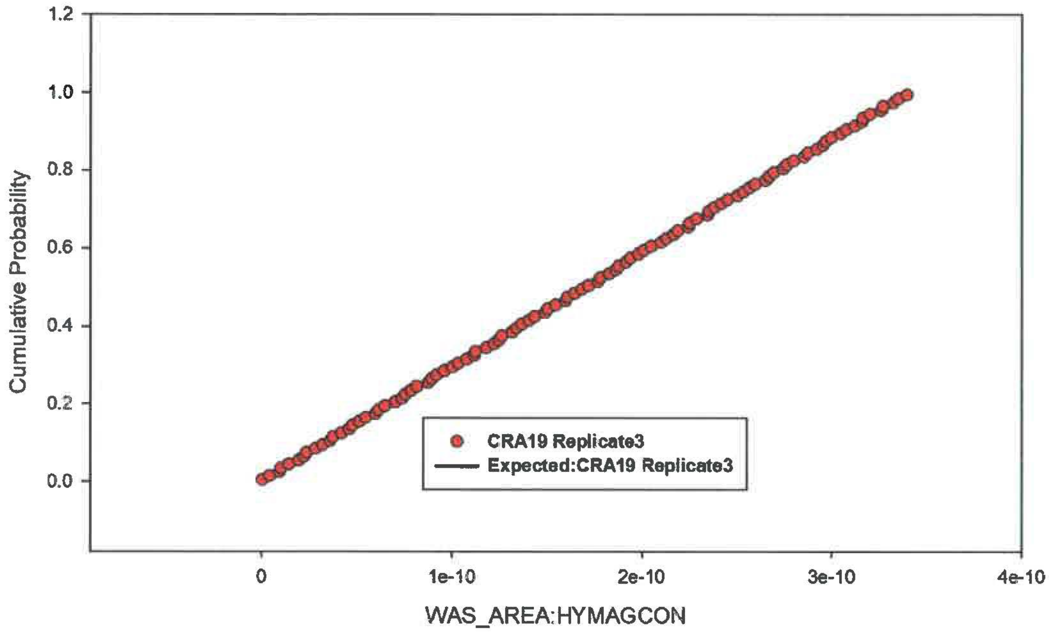

Figure 204 – Observed and Expected CDFs for WAS_AREA:HYMAGCON (Uniform Distribution) Replicate 3.

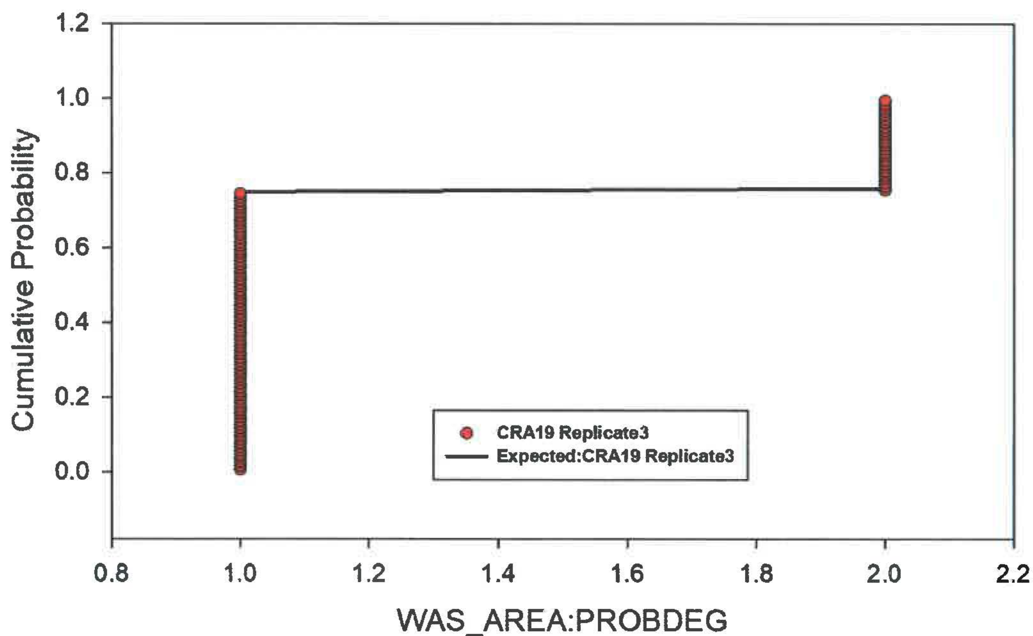

Figure 205 – Observed and Expected CDFs for WAS_AREA:PROBDEG (Delta Distribution) Replicate 3.

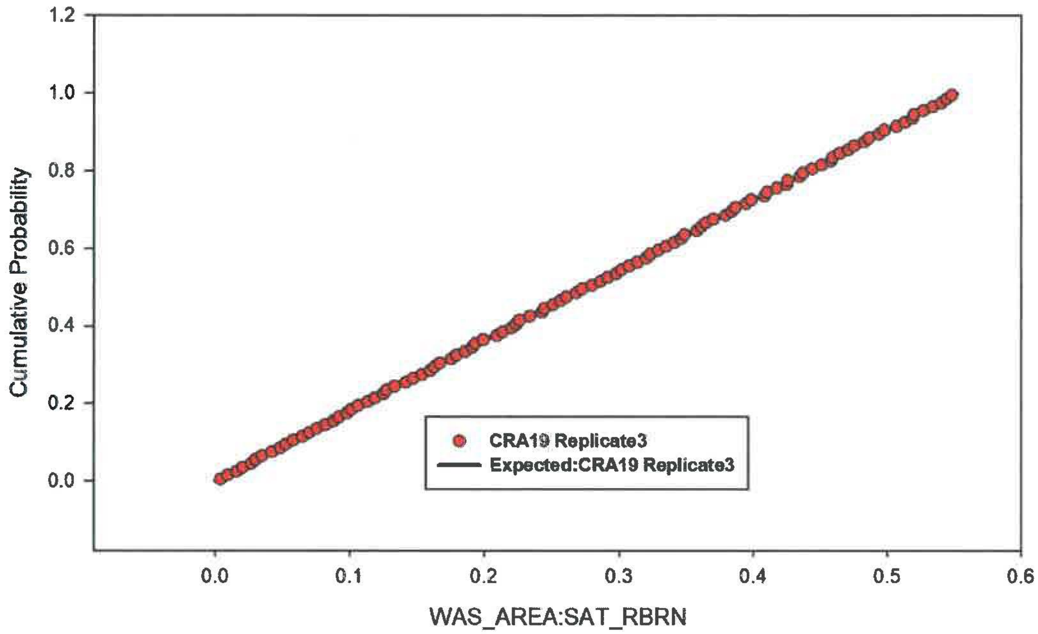

Figure 206 – Observed and Expected CDFs for WAS_AREA:SAT_RBRN (Uniform Distribution) Replicate 3.

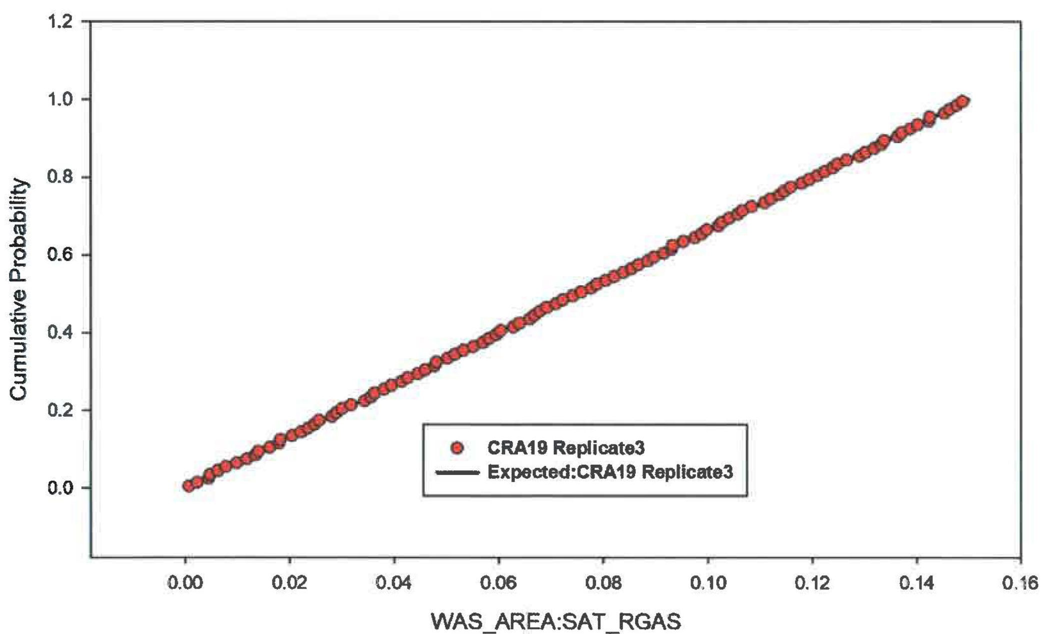

Figure 207 – Observed and Expected CDFs for WAS_AREA:SAT_RGAS (Uniform Distribution) Replicate 3.

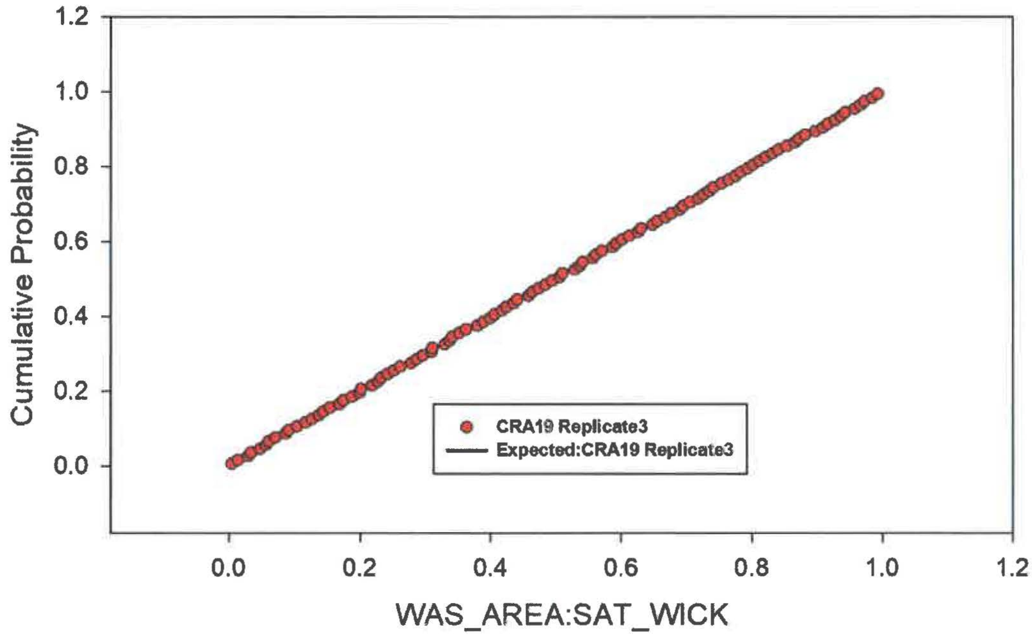

Figure 208 – Observed and Expected CDFs for WAS_AREA:SAT_WICK (Uniform Distribution) Replicate 3.

This page intentionally left blank.

5.0 SUMMARY

LHS was used to generate one hundred vectors of sampled parameter values for each of three replicates for the CRA19 analysis. A unique random number seed was assigned to each of the three replicates. These seed values were identical to those used in the CRA14 analysis. Correlations were assigned to two pairs of variables (S_HALITE:PRMX_LOG and S_HALITE:COMP_RCK, as well as CASTILER:PRMX_LOG and CASTILER:COMP_RCK) and applied during the LHS sampling process.

The LHS results were additionally influenced by an enforcement of a conditional relationship between three pairs of parameters: WAS_AREA:GRATMICH and WAS_AREA:GRATMICI, PCS_T3: POROSITY and PCS_T2: POROSITY, and PCS_T2: POROSITY and PCS_T1:POROSITY. Sixty-four parameters were sampled for the CRA19 analysis, including two new parameters (also, one parameter from the CRA14 analysis was not sampled). Updated distributions were sampled for six additional parameters. All 300 sets of sampled parameters were written to the WIPP PA Results Database (PA_Results) for use by other WIPP PA codes.

The resulting sampled data had the expected correlation structure and the values fell within the expected ranges. The distributions of sampled values matched the expected cumulative distribution functions (CDFs).

This page intentionally left blank.

6.0 REFERENCES

Camphouse, R.C. 2013. Analysis Plan for the 2014 WIPP Compliance Recertification Application Performance Assessment. Sandia National Laboratories, Carlsbad, NM. ERMS 559198.

Clayton, D. J. 2008. Analysis Plan for the Performance Assessment for the 2009 Compliance Recertification Application. Sandia National Laboratories, Carlsbad, N.M. ERMS 547515.

Clayton, D.J., S. Dunagan, J.W. Garner, A.E. Ismail, T.B. Kirchner, G.R. Kirkes, M.B. Nemer. 2008. Summary Report of the 2009 Compliance Recertification Application Performance Assessment. Sandia National Laboratories, Carlsbad, NM. ERMS 548862.

Clayton, D.J., R.C. Camphouse, J.W. Garner, A.E. Ismail, T.B. Kirchner, K.L. Kuhlman, M.B. Nemer. 2010. Summary Report of the CRA-2009 Performance Assessment Baseline Calculation. Sandia National Laboratories, Carlsbad, NM. ERMS 553039.

Clayton, D. 2013. Justification of Chemistry Parameters for Use in BRAGFLO for AP-164, Rev. 1. Sandia National Laboratories, Carlsbad, NM. ERMS 559466.

Cotsworth, E. 2005. EPA Letter on Conducting the Performance Assessment Baseline Change (PABC) Verification Test. U.S. EPA, Office of Radiation and Indoor Air, Washington, D.C. ERMS 538858.

Cotsworth, E. 2009. EPA Letter on CRA-2009 First Set of Completeness Comments. U.S. EPA, Office of Radiation and Indoor Air, Washington, D.C. ERMS 551444.

Day, B. 2019. Reassessment of Need and Parameter Justification for Modeling Gas Generation due to Radiolysis of Brine and Cellulose/Plastic/Rubber in WIPP for CRA-2019. Sandia National Laboratories, Carlsbad, NM. ERMS 570873.

Domski, P.S. 2019a. Th(IV), Np(V), and Am(III) Baseline Solubilities and Th(IV) and Am(III) Solubility Uncertainties for the CRA-2019 PA. Sandia National Laboratories, Carlsbad, NM. ERMS 571169.

Domski, P.S. 2019b. Uncertainty Analysis of Actinide Solubilities for CRA 2019. Sandia National Laboratories, Carlsbad, NM. ERMS 571179.

Kim, S. and L. Feng. 2019. Input Parameter Report for the 2019 Compliance Recertification Application Performance Assessment (CRA-2019 PA). Sandia National Laboratories, Carlsbad, NM. ERMS 571377.

Kirchner, T. 2009. Generation of the LHS Samples for the AP-137 Revision 0 (CRA09) PA Calculations. Sandia National Laboratories, Carlsbad, NM. ERMS 547971.

Kirchner, T. 2012. AP-162 Revision 0: Analysis Plan for the Migration of the Performance Assessment Codes to the Sun Solaris Blade Server Running with Intel Processors. Sandia National Laboratories, Carlsbad, NM. ERMS 557765.

Kirchner, T. 2013. Generation of the LHS Samples for the CRA-2014 (AP-164) PA Calculations. Sandia National Laboratories, Carlsbad, NM. ERMS 559950.

Kirchner, T., A. Gilkey, and J. Long. 2014. Summary Report on the Migration of the WIPP PA Codes from VMS to Solaris, AP-162 Revision 1. Sandia National Laboratories, Carlsbad, NM. ERMS 561757.

Kirchner, T., A. Gilkey, and J. Long. 2015. Addendum to the Summary Report on the Migration of the WIPP PA Codes from VMS to Solaris, AP-162. Sandia National Laboratories, Carlsbad, NM. ERMS 564675.

Leigh, C.D., J.F. Kanney, L.H. Brush, J.W. Garner, G.R. Kirkes, T. Lowry, M.B. Nemer, J.S. Stein, E.D. Vugrin, S. Wagner, and T.B. Kirchner. 2005. 2004 Compliance Recertification Application Performance Assessment Baseline Calculation, Revision 0. Sandia National Laboratories, Carlsbad, NM. ERMS 541521.

Long, J. 2013. Execution of Performance Assessment Codes for the CRA-2014 Performance Assessment. Sandia National Laboratories, Carlsbad, NM. ERMS 560016.

Long, J. 2019. Computational Code Execution and File Management for the 2019 Compliance Recertification Application Performance Assessment (CRA-2019 PA). Sandia National Laboratories, Carlsbad, NM. ERMS 571375.

MacKinnon, R.J., and G. Freeze. 1997a. Summary of EPA-Mandated Performance Assessment Verification Test (Replicate 1) and Comparison With the Compliance Certification Application Calculations, Revision 1. Sandia National Laboratories, Carlsbad, NM. ERMS 422595.

MacKinnon, R.J., and G. Freeze. 1997b. Summary of Uncertainty and Sensitivity Analysis Results for the EPA-Mandated Performance Assessment Verification Test, Rev. 1. Sandia National Laboratories, Carlsbad, NM. ERMS 420669.

MacKinnon, R.J., and G. Freeze. 1997c. Supplemental Summary of EPA-Mandated Performance Assessment Verification Test (All Replicates) and Comparison With the Compliance Certification Application Calculations, Revision 1. Sandia National Laboratories, Carlsbad, NM. ERMS 414880.

Mariner, P.E. 2019. A Summary of Humic Colloid Parameter Values to be Implemented in the CRA-2019 Deferred Performance Assessment. Sandia National Laboratories, Carlsbad, NM. ERMS 571250.

Nemer, M. B. and J. S. Stein. 2005. Analysis Package for BRAGFLO: 2004 Compliance Recertification Application Performance Assessment Baseline Calculation. Analysis Report, June 28, 2005. Carlsbad, NM: Sandia National Laboratories. ERMS 540527.

U.S. Congress. 1992. WIPP Land Withdrawal Act, Public Law 102-579, 106 Stat. 4777, 1992; as amended by Public Law 104-201, 110 Stat. 2422, 1996.

U.S. Department of Energy (DOE) 1996. Title 40 CFR Part 191 Compliance Certification Application for the Waste Isolation Pilot. U.S. Department of Energy Waste Isolation Pilot Plant, Carlsbad Area Office, Carlsbad, NM. DOE/CAO-1996-2184.

U.S. Department of Energy (DOE) 2004. Title 40 CFR Part 191 Compliance Recertification Application for the Waste Isolation Pilot Plant, , 10 vols., U.S. Department of Energy Waste Isolation Pilot Plant, Carlsbad Area Office, Carlsbad, NM. DOE/WIPP 2004-3231.

U.S. Environmental Protection Agency (EPA). 1998. 40 CFR 194, Criteria for the Certification and Recertification of the Waste Isolation Pilot Plant's Compliance with the Disposal Regulations: Certification Decision: Final Rule, Federal Register. Vol. 63, 27354-27406.

U.S. Environmental Protection Agency (EPA). 2006. 40 CFR 194, Criteria for the Certification and Recertification of the Waste Isolation Pilot Plant's Compliance with the Disposal Regulations: Certification Decision: Final Rule, Federal Register. Vol. 71, 18010-18021.

U.S. Environmental Protection Agency (EPA). 2010. 40 CFR Part 194 Criteria for the Certification and Recertification of the Waste Isolation Pilot Plant's Compliance With the Disposal Regulations: Recertification Decision, Federal Register No. 222, Vol. 75, pp. 70584-70595, November 18, 2010.

U.S. Environmental Protection Agency (EPA). 2017a. Criteria for the Certification and Recertification of the Waste Isolation Pilot Plant's Compliance with the Disposal Regulations; Recertification Decision. July 19, 2017. Office of Radiation and Indoor Air, Docket EPA-HQ-OAR-2014-0609-0079.

U.S. Environmental Protection Agency (EPA). 2017b. Probability of Encountering Castile Brine Beneath the WIPP Waste Panels Using the TDEM Block Method. June, 2017. Office of Radiation and Indoor Air, Docket EPA-HQ-OAR-2014-0609-0047.

U.S. Environmental Protection Agency (EPA). 2017c. Technical Support Document for Section 194.23, EPA Review of Proposed Modification to the Waste Shear Strength Parameter TAUFAIL. July, 2017. Office of Radiation and Indoor Air, Docket EPA-HQ-OAR-2014-0609-0052.

U.S. Environmental Protection Agency (EPA). 2017d. Technical Support Document for Section 194.24, Evaluation of the Compliance Recertification Actinide Source Term, Gas Generation, Backfill Efficacy, Water Balance and Culebra Dolomite Distribution Coefficient Values. June, 2017. Office of Radiation and Indoor Air, Docket EPA-HQ-OAR-2014-0609-0054.

WIPP PA. 2005. Design Document for LHS (Version 2.42). Sandia National Laboratories. Carlsbad, NM: ERMS 538371.

WIPP PA. 2015a. Addendum to User's Manual for PRELHS (Version 2.42). Sandia National Laboratories. Carlsbad, NM: ERMS 563987.

WIPP PA. 2015b. Addendum to Verification and Validation Plan/Validation Document for PRELHS (Version 2.43). Sandia National Laboratories. Carlsbad, NM: ERMS 564828.

WIPP PA. 2015c. Installation and Checkout for POSTLHS Version 4.09 Regression Testing for the Solaris Blade. Sandia National Laboratories. Carlsbad, NM: ERMS 563973.

WIPP PA. 2015d. Addendum to Verification and Validation Plan/Validation Document for POSTLHS Version 4.10. Sandia National Laboratories. Carlsbad, NM: ERMS 564906.

WIPP PA. 2016a. Software Installation and Checkout Attachment, PRELHS Version 2.44, Regression Test Report. Sandia National Laboratories. Carlsbad, NM: ERMS 566919.

WIPP PA. 2016b. Implementation Document for POSTLHS Version 4.11. Sandia National Laboratories. Carlsbad, NM: ERMS 566302.

Zeitler, T.R. 2018a. Bounding Calculation of the Cumulative Distribution for STEEL:HUMCORR. Sandia National Laboratories. Carlsbad, NM. ERMS 569807.

Zeitler, T.R. 2018b. Cumulative Distribution for STEEL:CORRMCO2 for the CRA-2019 PA. Sandia National Laboratories. Carlsbad, NM. ERMS 570869.

Zeitler, T.R. 2019a. Analysis Plan for the 2019 WIPP Compliance Recertification Application Performance Assessment. Sandia National Laboratories, Carlsbad, NM. ERMS 571150.

Zeitler, T.R. 2019b. A Summary of EPA/DOE Defined Parameters to be Implemented in the CRA-2019 PA. Sandia National Laboratories. Carlsbad, NM. ERMS 570879.

Appendix A. Comparison of Sampled Data to Expected Ranges

Table 5 below compares the mean and range observed in the unconditioned sampled data to the mean and range specified in the WIPP PA Parameter Database (ParamDB). The table also shows the relative percent difference (RPD) in the means, as well as the percent of the range covered by the sampled values. The equation used to calculate RPD is:

$$RPD = abs\left(\frac{\overline{X}_1 - \overline{X}_2}{\left(\overline{X}_1 + \overline{X}_2\right)/2}\right) \quad (2)$$

where $\overline{X}_1$ is the observed mean and $\overline{X}_2$ is the expected mean.

In general, the sampled ranges matched the expected ranges within a few percent. Notable exceptions (i.e, when the observed range is less than 90 % of the expected range) occur in some cases for triangular, cumulative, Student, and, in one case, uniform distributions. The relatively skewed nature of some triangular and and cumulative distributions is responsible for the lower range coverages for those types of distributions. As observed by Kirchner (2013), the observed range of the sampled data for Student distributions is much smaller than the range specified in the parameter database because the minimum and maximum values in the database are the extremes of the data whereas the sampled values represent the uncertainty on the mean. The uncertainty on the mean is based on the standard error of the data and that range will always be smaller than the range of the data. Finally, the case for which a uniform distribution is observed to show a low range coverage is that for the WAS_AREA:GRATMICH parameter, for which the low coverage is due to the condititional relationship assigned to this parameter (Section 4.4.1), which artificially alters the observed range.

The calculated RPD in the means is relatively low, typically less than 1 %. Notable exceptions (i.e., when RPD exceeds 4 %) are described below. The PCS_T2:POR2PERM parameter shows an RPD of 200 % because the expected mean is 0 and the RPD formula becomes:

$$RPD = abs\left(\frac{\overline{X}_1 - \overline{X}_2}{\left(\overline{X}_1 + \overline{X}_2\right)/2}\right) = \frac{2\overline{X}_1}{\overline{X}_1} = 2 \quad (3)$$

The S_MB139:RELP_MOD parameter has a large RPD because there are only two possible values, 1 and 4, so the observed mean lies between these two values whereas the mean from the database was assigned to 4 because previously the mean also represented the default value. The WAS_AREA:GRATMICH parameter shows a large RPD because its distribution was controlled after sampling to ensure the sampled value in each vector did not exceed the sampled value for WAS_AREA:GRATMICI, hence the observed mean is reduced compared to the expected mean. The PCS_T3:POROSITY parameter also shows elevated RPDs because it is controlled by PCS_T2:POROSITY (Section 4.4.3). The PCS_T2:POROSITY parameter was controlled by PCS_T1:POROSITY but the overlap was small and the control only modified one of 300 sampled values.

For the CRA-2019 PA, the SOLMOD4:SOLVAR parameter has a larger RPD (average ~100 % across replicates) than it did for the CRA-2014 PA (average ~3 %). While the skewed shape of the CRA-2019 PA distribution is somewhat different from that of the CRA-2014 PA distribution, the primary reason for the large change in RPD is due to the small value of the expected mean itself. For the CRA-2014 PA, the expected mean was 0.660 and sampled means were 0.685, 0.653, and 0.643 across the replicates for absolute differences of 0.025, 0.007, and 0.017 (Kirchner 2013). For the CRA-2019 PA, the expected mean was -0.00486 and sampled means were -0.0158, -0.0142, and -0.0171 across the replicates for absolute differences of 0.01094, 0.00934, and 0.01224. So, while the absolute differences (i.e., numerator in Equation 2) were similar between the two distributions, the RPDs were noticeably different due to the smaller denominator in the case of the CRA-2019 PA. This is a similar case to the PCS_T2:POR2PERM parameter discussed above, in which the expected mean was identically zero, forcing an RPD of 200 %. Additionally, the average absolute differences in means compared to the respective ranges of values were 0.35 % and 0.32 %, respectively for the CRA-2014 PA and CRA-2019 PA, so there is not a fundamental difference in the sampling of the SOLMOD4:SOLVAR parameter between the two analyses.

Table 5 – Comparison of Sampled Values with Prescribed Distributions

Material	Property	Rep	Observed			Parameter Database			RPD of Means	% Range Covered	Dist
			Min	Max	Mean	Min	Max	Mean			
AM+3	MKD_AM	1	5.02E-03	3.97E-01	9.00E-02	5.00E-03	4.00E-01	9.00E-02	0.05%	99.1%	Logunif.
AM+3	MKD_AM	2	5.17E-03	3.89E-01	9.03E-02	5.00E-03	4.00E-01	9.00E-02	0.31%	97.1%	Logunif.
AM+3	MKD_AM	3	5.21E-03	3.93E-01	9.00E-02	5.00E-03	4.00E-01	9.00E-02	0.03%	98.1%	Logunif.
BH_SAND	PRMX_LOG	1	-1.63E+01	-1.10E+01	-1.36E+01	-1.63E+01	-1.10E+01	-1.37E+01	0.01%	99.8%	Uniform
BH_SAND	PRMX_LOG	2	-1.63E+01	-1.10E+01	-1.36E+01	-1.63E+01	-1.10E+01	-1.37E+01	0.01%	99.6%	Uniform
BH_SAND	PRMX_LOG	3	-1.63E+01	-1.10E+01	-1.36E+01	-1.63E+01	-1.10E+01	-1.37E+01	0.02%	99.1%	Uniform
BOREHOLE	DOMEGA	1	4.34E+00	2.16E+01	8.63E+00	4.20E+00	2.30E+01	8.63E+00	0.06%	92.1%	Cum.
BOREHOLE	DOMEGA	2	4.27E+00	2.27E+01	8.62E+00	4.20E+00	2.30E+01	8.63E+00	0.14%	97.9%	Cum.
BOREHOLE	DOMEGA	3	4.27E+00	2.30E+01	8.64E+00	4.20E+00	2.30E+01	8.63E+00	0.12%	99.6%	Cum.
BOREHOLE	TAUFAIL	1	1.61E+00	7.70E+01	3.93E+01	1.60E+00	7.70E+01	3.93E+01	0.01%	99.9%	Uniform
BOREHOLE	TAUFAIL	2	1.81E+00	7.63E+01	3.93E+01	1.60E+00	7.70E+01	3.93E+01	0.06%	98.8%	Uniform
BOREHOLE	TAUFAIL	3	1.84E+00	7.67E+01	3.93E+01	1.60E+00	7.70E+01	3.93E+01	0.02%	99.3%	Uniform
CASTILER	COMP_RCK	1	2.07E-11	9.36E-11	5.33E-11	2.00E-11	1.00E-10	5.30E-11	0.54%	91.1%	Triang.
CASTILER	COMP_RCK	2	2.28E-11	9.48E-11	5.33E-11	2.00E-11	1.00E-10	5.30E-11	0.66%	90.0%	Triang.
CASTILER	COMP_RCK	3	2.14E-11	9.49E-11	5.33E-11	2.00E-11	1.00E-10	5.30E-11	0.51%	91.9%	Triang.
CASTILER	PRESSURE	1	1.12E+07	1.65E+07	1.36E+07	1.11E+07	1.70E+07	1.36E+07	0.03%	89.8%	Triang.
CASTILER	PRESSURE	2	1.14E+07	1.67E+07	1.36E+07	1.11E+07	1.70E+07	1.36E+07	0.04%	90.4%	Triang.

Material	Property	Rep	Observed			Parameter Database			RPD of Means	% Range Covered	Dist
			Min	Max	Mean	Min	Max	Mean			
CASTILER	PRESSURE	3	1.14E+07	1.68E+07	1.36E+07	1.11E+07	1.70E+07	1.36E+07	0.02%	92.7%	Triang.
CASTILER	PRMX_LOG	1	-1.45E+01	-9.94E+00	-1.21E+01	-1.47E+01	-9.80E+00	-1.21E+01	0.01%	92.4%	Triang.
CASTILER	PRMX_LOG	2	-1.45E+01	-1.01E+01	-1.21E+01	-1.47E+01	-9.80E+00	-1.21E+01	0.01%	91.3%	Triang.
CASTILER	PRMX_LOG	3	-1.44E+01	-9.90E+00	-1.21E+01	-1.47E+01	-9.80E+00	-1.21E+01	0.03%	91.2%	Triang.
CONC_PLG	PRMX_LOG	1	-1.90E+01	-1.70E+01	-1.80E+01	-1.90E+01	-1.70E+01	-1.80E+01	0.00%	98.9%	Uniform
CONC_PLG	PRMX_LOG	2	-1.90E+01	-1.70E+01	-1.80E+01	-1.90E+01	-1.70E+01	-1.80E+01	0.00%	99.5%	Uniform
CONC_PLG	PRMX_LOG	3	-1.90E+01	-1.70E+01	-1.80E+01	-1.90E+01	-1.70E+01	-1.80E+01	0.00%	98.5%	Uniform
CULEBRA	APOROS	1	1.01E-04	9.82E-03	2.14E-03	1.00E-04	1.00E-02	2.10E-03	1.79%	98.1%	Logunif.
CULEBRA	APOROS	2	1.02E-04	9.58E-03	2.15E-03	1.00E-04	1.00E-02	2.10E-03	2.46%	95.7%	Logunif.
CULEBRA	APOROS	3	1.01E-04	9.70E-03	2.14E-03	1.00E-04	1.00E-02	2.10E-03	2.11%	96.9%	Logunif.
CULEBRA	DPOROS	1	1.00E-01	2.46E-01	1.55E-01	1.00E-01	2.50E-01	1.60E-01	3.21%	97.1%	Cum.
CULEBRA	DPOROS	2	1.00E-01	2.48E-01	1.55E-01	1.00E-01	2.50E-01	1.60E-01	3.18%	98.3%	Cum.
CULEBRA	DPOROS	3	1.00E-01	2.49E-01	1.55E-01	1.00E-01	2.50E-01	1.60E-01	3.18%	99.3%	Cum.
CULEBRA	HMBLKLT	1	5.26E-02	4.99E-01	2.75E-01	5.00E-02	5.00E-01	2.75E-01	0.09%	99.2%	Uniform
CULEBRA	HMBLKLT	2	5.39E-02	4.96E-01	2.75E-01	5.00E-02	5.00E-01	2.75E-01	0.01%	98.3%	Uniform
CULEBRA	HMBLKLT	3	5.41E-02	4.96E-01	2.75E-01	5.00E-02	5.00E-01	2.75E-01	0.06%	98.3%	Uniform
CULEBRA	MINP_FAC	1	1.02E+00	9.95E+02	5.01E+02	1.00E+00	1.00E+03	5.01E+02	0.04%	99.5%	Uniform
CULEBRA	MINP_FAC	2	5.56E+00	9.96E+02	5.01E+02	1.00E+00	1.00E+03	5.01E+02	0.00%	99.2%	Uniform
CULEBRA	MINP_FAC	3	4.34E+00	9.92E+02	5.00E+02	1.00E+00	1.00E+03	5.01E+02	0.03%	98.9%	Uniform
DRZ_1	PRMX_LOG	1	-1.94E+01	-1.25E+01	-1.59E+01	-1.94E+01	-1.25E+01	-1.60E+01	0.32%	99.8%	Uniform

Material	Property	Rep	Observed Min	Observed Max	Observed Mean	Parameter Database Min	Parameter Database Max	Parameter Database Mean	RPD of Means	% Range Covered	Dist
DRZ_1	PRMX_LOG	2	-1.94E+01	-1.26E+01	-1.60E+01	-1.94E+01	-1.25E+01	-1.60E+01	0.31%	98.8%	Uniform
DRZ_1	PRMX_LOG	3	-1.93E+01	-1.26E+01	-1.59E+01	-1.94E+01	-1.25E+01	-1.60E+01	0.33%	98.3%	Uniform
DRZ_PCS	PRMX_LOG	1	-2.05E+01	-1.72E+01	-1.88E+01	-2.07E+01	-1.70E+01	-1.88E+01	0.01%	88.9%	Triang.
DRZ_PCS	PRMX_LOG	2	-2.06E+01	-1.72E+01	-1.88E+01	-2.07E+01	-1.70E+01	-1.88E+01	0.01%	91.8%	Triang.
DRZ_PCS	PRMX_LOG	3	-2.06E+01	-1.72E+01	-1.88E+01	-2.07E+01	-1.70E+01	-1.88E+01	0.00%	92.5%	Triang.
GLOBAL	CLIMTIDX	1	1.00E+00	2.24E+00	1.31E+00	1.00E+00	2.25E+00	1.31E+00	0.16%	98.7%	Cum.
GLOBAL	CLIMTIDX	2	1.00E+00	2.25E+00	1.31E+00	1.00E+00	2.25E+00	1.31E+00	0.21%	99.7%	Cum.
GLOBAL	CLIMTIDX	3	1.00E+00	2.24E+00	1.31E+00	1.00E+00	2.25E+00	1.31E+00	0.16%	99.1%	Cum.
GLOBAL	GDEPFAC	1	4.21E-03	4.99E-01	2.50E-01	0.00E+00	5.00E-01	2.50E-01	0.04%	98.9%	Uniform
GLOBAL	GDEPFAC	2	2.94E-03	4.96E-01	2.50E-01	0.00E+00	5.00E-01	2.50E-01	0.05%	98.6%	Uniform
GLOBAL	GDEPFAC	3	3.21E-03	4.96E-01	2.50E-01	0.00E+00	5.00E-01	2.50E-01	0.04%	98.5%	Uniform
GLOBAL	OXSTAT	1	4.38E-03	9.95E-01	5.00E-01	0.00E+00	1.00E+00	5.00E-01	0.02%	99.1%	Uniform
GLOBAL	OXSTAT	2	7.89E-03	9.92E-01	5.01E-01	0.00E+00	1.00E+00	5.00E-01	0.14%	98.4%	Uniform
GLOBAL	OXSTAT	3	8.10E-04	9.94E-01	5.00E-01	0.00E+00	1.00E+00	5.00E-01	0.03%	99.3%	Uniform
GLOBAL	PBRINE	1	6.61E-02	5.51E-01	2.65E-01	4.00E-02	5.70E-01	2.63E-01	0.44%	91.4%	Cum.
GLOBAL	PBRINE	2	6.25E-02	5.40E-01	2.65E-01	4.00E-02	5.70E-01	2.63E-01	0.45%	90.1%	Cum.
GLOBAL	PBRINE	3	6.37E-02	5.31E-01	2.65E-01	4.00E-02	5.70E-01	2.63E-01	0.46%	88.1%	Cum.
GLOBAL	TRANSIDX	1	7.95E-03	9.98E-01	5.00E-01	0.00E+00	1.00E+00	5.00E-01	0.05%	99.0%	Uniform
GLOBAL	TRANSIDX	2	6.83E-03	9.92E-01	5.00E-01	0.00E+00	1.00E+00	5.00E-01	0.07%	98.5%	Uniform
GLOBAL	TRANSIDX	3	6.61E-03	9.92E-01	5.00E-01	0.00E+00	1.00E+00	5.00E-01	0.05%	98.6%	Uniform

Material	Property	Rep	Observed			Parameter Database			RPD of Means	% Range Covered	Dist
			Min	Max	Mean	Min	Max	Mean			
PCS_T1	PORE_DIS	1	1.20E-01	8.06E+00	2.52E+00	1.10E-01	8.10E+00	2.52E+00	0.01%	99.3%	Cum.
PCS_T1	PORE_DIS	2	1.10E-01	8.02E+00	2.52E+00	1.10E-01	8.10E+00	2.52E+00	0.12%	99.0%	Cum.
PCS_T1	PORE_DIS	3	1.26E-01	8.06E+00	2.52E+00	1.10E-01	8.10E+00	2.52E+00	0.12%	99.4%	Cum.
PCS_T1	POROSITY	1	6.62E-02	1.87E-01	1.26E-01	6.60E-02	1.87E-01	1.27E-01	0.05%	99.5%	Uniform
PCS_T1	POROSITY	2	6.65E-02	1.87E-01	1.27E-01	6.60E-02	1.87E-01	1.27E-01	0.01%	99.2%	Uniform
PCS_T1	POROSITY	3	6.71E-02	1.87E-01	1.26E-01	6.60E-02	1.87E-01	1.27E-01	0.03%	98.9%	Uniform
PCS_T1	PRMX_LOG	1	-2.08E+01	-1.21E+01	-1.64E+01	-2.08E+01	-1.20E+01	-1.64E+01	0.01%	98.4%	Uniform
PCS_T1	PRMX_LOG	2	-2.08E+01	-1.21E+01	-1.64E+01	-2.08E+01	-1.20E+01	-1.64E+01	0.02%	99.2%	Uniform
PCS_T1	PRMX_LOG	3	-2.08E+01	-1.21E+01	-1.64E+01	-2.08E+01	-1.20E+01	-1.64E+01	0.01%	98.4%	Uniform
PCS_T1	SAT_RBRN	1	1.96E-03	5.95E-01	2.50E-01	0.00E+00	6.00E-01	2.50E-01	0.03%	98.9%	Cum.
PCS_T1	SAT_RBRN	2	6.93E-04	5.95E-01	2.50E-01	0.00E+00	6.00E-01	2.50E-01	0.09%	99.0%	Cum.
PCS_T1	SAT_RBRN	3	2.91E-03	5.94E-01	2.50E-01	0.00E+00	6.00E-01	2.50E-01	0.05%	98.5%	Cum.
PCS_T1	SAT_RGAS	1	9.61E-04	3.98E-01	2.00E-01	0.00E+00	4.00E-01	2.00E-01	0.05%	99.2%	Uniform
PCS_T1	SAT_RGAS	2	2.78E-03	3.99E-01	2.00E-01	0.00E+00	4.00E-01	2.00E-01	0.09%	99.0%	Uniform
PCS_T1	SAT_RGAS	3	5.95E-04	3.99E-01	2.00E-01	0.00E+00	4.00E-01	2.00E-01	0.09%	99.7%	Uniform
PCS_T2	POR2PERM	1	-1.63E+00	1.68E+00	5.66E-04	-1.72E+00	1.72E+00	0.00E+00	200%	96.1%	Normal
PCS_T2	POR2PERM	2	-1.58E+00	1.70E+00	1.13E-03	-1.72E+00	1.72E+00	0.00E+00	200%	95.5%	Normal
PCS_T2	POR2PERM	3	-1.58E+00	1.65E+00	1.19E-03	-1.72E+00	1.72E+00	0.00E+00	200%	93.8%	Normal
PCS_T2	POROSITY	1	2.51E-02	7.47E-02	5.00E-02	2.50E-02	7.50E-02	5.00E-02	0.00%	99.2%	Uniform
PCS_T2	POROSITY	2	2.55E-02	7.47E-02	4.99E-02	2.50E-02	7.50E-02	5.00E-02	0.13%	98.4%	Uniform

Material	Property	Rep	Observed			Parameter Database			RPD of Means	% Range Covered	Dist
			Min	Max	Mean	Min	Max	Mean			
PCS_T2	POROSITY	3	2.50E-02	7.47E-02	5.00E-02	2.50E-02	7.50E-02	5.00E-02	0.01%	99.3%	Uniform
PCS_T3	POROSITY	1	1.44E-03	5.05E-02	2.47E-02	1.00E-03	5.19E-02	2.65E-02	7.12%	96.5%	Uniform
PCS_T3	POROSITY	2	1.46E-03	5.12E-02	2.44E-02	1.00E-03	5.19E-02	2.65E-02	8.23%	97.8%	Uniform
PCS_T3	POROSITY	3	1.49E-03	5.10E-02	2.40E-02	1.00E-03	5.19E-02	2.65E-02	9.80%	97.2%	Uniform
PU+3	MKD_PU	1	5.02E-03	3.96E-01	9.03E-02	5.00E-03	4.00E-01	9.00E-02	0.30%	99.0%	Logunif.
PU+3	MKD_PU	2	5.06E-03	3.95E-01	9.02E-02	5.00E-03	4.00E-01	9.00E-02	0.18%	98.7%	Logunif.
PU+3	MKD_PU	3	5.04E-03	4.00E-01	9.01E-02	5.00E-03	4.00E-01	9.00E-02	0.16%	99.9%	Logunif.
PU+4	MKD_PU	1	5.19E-04	9.69E+00	1.01E+00	5.00E-04	1.00E+01	1.00E+00	0.51%	96.9%	Logunif.
PU+4	MKD_PU	2	5.21E-04	9.55E+00	1.01E+00	5.00E-04	1.00E+01	1.00E+00	1.40%	95.5%	Logunif.
PU+4	MKD_PU	3	5.38E-04	9.64E+00	1.01E+00	5.00E-04	1.00E+01	1.00E+00	1.27%	96.4%	Logunif.
S_HALITE	COMP_RCK	1	3.77E-12	1.92E-10	9.75E-11	2.94E-12	1.92E-10	9.75E-11	0.04%	99.4%	Uniform
S_HALITE	COMP_RCK	2	3.20E-12	1.90E-10	9.75E-11	2.94E-12	1.92E-10	9.75E-11	0.02%	98.9%	Uniform
S_HALITE	COMP_RCK	3	3.46E-12	1.91E-10	9.74E-11	2.94E-12	1.92E-10	9.75E-11	0.06%	99.0%	Uniform
S_HALITE	POROSITY	1	1.13E-03	5.11E-02	1.82E-02	1.00E-03	5.19E-02	1.82E-02	0.17%	98.3%	Cum.
S_HALITE	POROSITY	2	1.05E-03	5.12E-02	1.82E-02	1.00E-03	5.19E-02	1.82E-02	0.13%	98.4%	Cum.
S_HALITE	POROSITY	3	1.11E-03	5.16E-02	1.82E-02	1.00E-03	5.19E-02	1.82E-02	0.24%	99.1%	Cum.
S_HALITE	PRESSURE	1	1.11E+07	1.39E+07	1.25E+07	1.10E+07	1.39E+07	1.25E+07	0.04%	99.4%	Uniform
S_HALITE	PRESSURE	2	1.11E+07	1.39E+07	1.25E+07	1.10E+07	1.39E+07	1.25E+07	0.04%	99.4%	Uniform
S_HALITE	PRESSURE	3	1.10E+07	1.39E+07	1.25E+07	1.10E+07	1.39E+07	1.25E+07	0.03%	99.5%	Uniform
S_HALITE	PRMX_LOG	1	-2.40E+01	-2.10E+01	-2.25E+01	-2.40E+01	-2.10E+01	-2.25E+01	0.00%	98.8%	Uniform

Material	Property	Rep	Observed			Parameter Database			RPD of Means	% Range Covered	Dist
			Min	Max	Mean	Min	Max	Mean			
S_HALITE	PRMX_LOG	2	-2.40E+01	-2.10E+01	-2.25E+01	-2.40E+01	-2.10E+01	-2.25E+01	0.00%	99.5%	Uniform
S_HALITE	PRMX_LOG	3	-2.40E+01	-2.10E+01	-2.25E+01	-2.40E+01	-2.10E+01	-2.25E+01	0.01%	99.7%	Uniform
S_MB139	PORE_DIS	1	4.99E-01	8.02E-01	6.44E-01	4.91E-01	8.42E-01	6.44E-01	0.04%	86.1%	Student
S_MB139	PORE_DIS	2	5.00E-01	7.99E-01	6.44E-01	4.91E-01	8.42E-01	6.44E-01	0.01%	85.1%	Student
S_MB139	PORE_DIS	3	5.03E-01	7.95E-01	6.44E-01	4.91E-01	8.42E-01	6.44E-01	0.00%	83.2%	Student
S_MB139	PRMX_LOG	1	-2.04E+01	-1.71E+01	-1.89E+01	-2.10E+01	-1.71E+01	-1.89E+01	0.05%	84.8%	Student
S_MB139	PRMX_LOG	2	-2.07E+01	-1.72E+01	-1.89E+01	-2.10E+01	-1.71E+01	-1.89E+01	0.04%	88.0%	Student
S_MB139	PRMX_LOG	3	-2.03E+01	-1.73E+01	-1.89E+01	-2.10E+01	-1.71E+01	-1.89E+01	0.03%	77.4%	Student
S_MB139	RELP_MOD	1	1.00E+00	4.00E+00	2.50E+00	1.00E+00	4.00E+00	4.00E+00	46.15%	100.0%	Delta
S_MB139	RELP_MOD	2	1.00E+00	4.00E+00	2.50E+00	1.00E+00	4.00E+00	4.00E+00	46.15%	100.0%	Delta
S_MB139	RELP_MOD	3	1.00E+00	4.00E+00	2.50E+00	1.00E+00	4.00E+00	4.00E+00	46.15%	100.0%	Delta
S_MB139	SAT_RBRN	1	1.50E-02	1.57E-01	8.36E-02	7.78E-03	1.74E-01	8.36E-02	0.01%	85.5%	Student
S_MB139	SAT_RBRN	2	2.13E-02	1.57E-01	8.38E-02	7.78E-03	1.74E-01	8.36E-02	0.20%	81.5%	Student
S_MB139	SAT_RBRN	3	2.14E-02	1.46E-01	8.38E-02	7.78E-03	1.74E-01	8.36E-02	0.17%	75.3%	Student
SHFTL_T1	PRMX_LOG	1	-2.00E+01	-1.69E+01	-1.82E+01	-2.00E+01	-1.65E+01	-1.80E+01	1.18%	88.6%	Cum.
SHFTL_T1	PRMX_LOG	2	-1.99E+01	-1.70E+01	-1.82E+01	-2.00E+01	-1.65E+01	-1.80E+01	1.18%	83.4%	Cum.
SHFTL_T1	PRMX_LOG	3	-1.96E+01	-1.70E+01	-1.82E+01	-2.00E+01	-1.65E+01	-1.80E+01	1.16%	72.6%	Cum.
SHFTL_T2	PRMX_LOG	1	-2.24E+01	-1.80E+01	-2.01E+01	-2.25E+01	-1.80E+01	-1.98E+01	1.32%	96.3%	Cum.
SHFTL_T2	PRMX_LOG	2	-2.23E+01	-1.81E+01	-2.01E+01	-2.25E+01	-1.80E+01	-1.98E+01	1.32%	92.1%	Cum.
SHFTL_T2	PRMX_LOG	3	-2.23E+01	-1.80E+01	-2.01E+01	-2.25E+01	-1.80E+01	-1.98E+01	1.33%	96.2%	Cum.

Material	Property	Rep	Observed			Parameter Database			RPD of Means	% Range Covered	Dist
			Min	Max	Mean	Min	Max	Mean			
SHFTU	PRMX_LOG	1	-2.05E+01	-1.69E+01	-1.84E+01	-2.05E+01	-1.65E+01	-1.82E+01	1.21%	88.6%	Cum.
SHFTU	PRMX_LOG	2	-2.04E+01	-1.68E+01	-1.84E+01	-2.05E+01	-1.65E+01	-1.82E+01	1.20%	90.6%	Cum.
SHFTU	PRMX_LOG	3	-2.04E+01	-1.66E+01	-1.84E+01	-2.05E+01	-1.65E+01	-1.82E+01	1.21%	94.6%	Cum.
SHFTU	SAT_RBRN	1	1.79E-03	6.00E-01	2.50E-01	0.00E+00	6.00E-01	2.50E-01	0.04%	99.7%	Cum.
SHFTU	SAT_RBRN	2	2.76E-03	5.97E-01	2.50E-01	0.00E+00	6.00E-01	2.50E-01	0.03%	99.1%	Cum.
SHFTU	SAT_RBRN	3	9.67E-04	5.93E-01	2.50E-01	0.00E+00	6.00E-01	2.50E-01	0.03%	98.7%	Cum.
SHFTU	SAT_RGAS	1	9.09E-04	3.98E-01	2.00E-01	0.00E+00	4.00E-01	2.00E-01	0.06%	99.3%	Uniform
SHFTU	SAT_RGAS	2	2.05E-03	3.98E-01	2.00E-01	0.00E+00	4.00E-01	2.00E-01	0.00%	98.9%	Uniform
SHFTU	SAT_RGAS	3	2.70E-03	3.98E-01	2.00E-01	0.00E+00	4.00E-01	2.00E-01	0.01%	98.7%	Uniform
SOLMOD3	SOLVAR	1	-1.08E+00	2.88E+00	6.45E-01	-1.14E+00	2.97E+00	6.40E-01	0.81%	96.4%	Cum.
SOLMOD3	SOLVAR	2	-9.97E-01	2.95E+00	6.49E-01	-1.14E+00	2.97E+00	6.40E-01	1.31%	95.8%	Cum.
SOLMOD3	SOLVAR	3	-1.13E+00	2.67E+00	6.16E-01	-1.14E+00	2.97E+00	6.40E-01	3.92%	92.4%	Cum.
SOLMOD4	SOLVAR	1	-1.83E+00	1.35E+00	-1.58E-02	-2.01E+00	1.43E+00	-4.86E-03	106.0%	92.6%	Cum.
SOLMOD4	SOLVAR	2	-1.87E+00	1.37E+00	-1.42E-02	-2.01E+00	1.43E+00	-4.86E-03	97.85%	94.1%	Cum.
SOLMOD4	SOLVAR	3	-1.89E+00	1.36E+00	-1.71E-02	-2.01E+00	1.43E+00	-4.86E-03	111.3%	94.6%	Cum.
SPALLMOD	PARTDIAM	1	1.01E-03	9.65E-02	2.15E-02	1.00E-03	1.00E-01	2.15E-02	0.10%	96.5%	Logunif.
SPALLMOD	PARTDIAM	2	1.00E-03	9.76E-02	2.16E-02	1.00E-03	1.00E-01	2.15E-02	0.28%	97.6%	Logunif.
SPALLMOD	PARTDIAM	3	1.04E-03	9.82E-02	2.16E-02	1.00E-03	1.00E-01	2.15E-02	0.32%	98.2%	Logunif.
SPALLMOD	REPIPERM	1	2.42E-14	2.32E-12	5.15E-13	2.40E-14	2.40E-12	5.16E-13	0.26%	96.4%	Logunif.
SPALLMOD	REPIPERM	2	2.49E-14	2.37E-12	5.15E-13	2.40E-14	2.40E-12	5.16E-13	0.21%	98.6%	Logunif.

Material	Property	Rep	Observed Min	Observed Max	Observed Mean	Parameter Database Min	Parameter Database Max	Parameter Database Mean	RPD of Means	% Range Covered	Dist
SPALLMOD	REPIPERM	3	2.45E-14	2.40E-12	5.16E-13	2.40E-14	2.40E-12	5.16E-13	0.01%	99.8%	Logunif.
SPALLMOD	REPIPOR	1	3.51E-01	6.58E-01	5.05E-01	3.50E-01	6.60E-01	5.05E-01	0.04%	99.0%	Uniform
SPALLMOD	REPIPOR	2	3.51E-01	6.58E-01	5.05E-01	3.50E-01	6.60E-01	5.05E-01	0.00%	99.1%	Uniform
SPALLMOD	REPIPOR	3	3.52E-01	6.58E-01	5.05E-01	3.50E-01	6.60E-01	5.05E-01	0.02%	99.0%	Uniform
SPALLMOD	TENSLSTR	1	1.20E+05	1.70E+05	1.45E+05	1.20E+05	1.70E+05	1.45E+05	0.01%	98.8%	Uniform
SPALLMOD	TENSLSTR	2	1.20E+05	1.70E+05	1.45E+05	1.20E+05	1.70E+05	1.45E+05	0.02%	99.4%	Uniform
SPALLMOD	TENSLSTR	3	1.20E+05	1.70E+05	1.45E+05	1.20E+05	1.70E+05	1.45E+05	0.01%	99.0%	Uniform
STEEL	CORRMCO2	1	5.37E-16	7.42E-14	1.34E-14	0.00E+00	7.92E-14	1.33E-14	0.75%	93.0%	Cum.
STEEL	CORRMCO2	2	5.89E-16	6.60E-14	1.33E-14	0.00E+00	7.92E-14	1.33E-14	0.01%	82.5%	Cum.
STEEL	CORRMCO2	3	1.39E-16	7.16E-14	1.34E-14	0.00E+00	7.92E-14	1.33E-14	0.42%	90.2%	Cum.
STEEL	HUMCORR	1	3.23E-20	1.02E-15	2.42E-16	0.00E+00	1.03E-15	2.43E-16	0.04%	98.9%	Cum.
STEEL	HUMCORR	2	7.79E-21	9.88E-16	2.42E-16	0.00E+00	1.03E-15	2.43E-16	0.11%	95.9%	Cum.
STEEL	HUMCORR	3	1.56E-20	1.01E-15	2.43E-16	0.00E+00	1.03E-15	2.43E-16	0.01%	98.3%	Cum.
TH+4	MKD_TH	1	5.20E-04	9.69E+00	1.01E+00	5.00E-04	1.00E+01	1.00E+00	1.07%	96.9%	Logunif.
TH+4	MKD_TH	2	5.25E-04	9.76E+00	1.02E+00	5.00E-04	1.00E+01	1.00E+00	1.52%	97.6%	Logunif.
TH+4	MKD_TH	3	5.24E-04	9.75E+00	1.01E+00	5.00E-04	1.00E+01	1.00E+00	0.97%	97.5%	Logunif.
U+4	MKD_U	1	5.45E-04	9.42E+00	1.00E+00	5.00E-04	1.00E+01	1.00E+00	0.34%	94.2%	Logunif.
U+4	MKD_U	2	5.20E-04	9.74E+00	1.01E+00	5.00E-04	1.00E+01	1.00E+00	0.81%	97.4%	Logunif.
U+4	MKD_U	3	5.07E-04	9.88E+00	1.01E+00	5.00E-04	1.00E+01	1.00E+00	1.38%	98.8%	Logunif.
U+6	MKD_U	1	3.14E-05	1.97E-02	3.07E-03	3.00E-05	2.00E-02	3.10E-03	0.93%	98.3%	Logunif.

Material	Property	Rep	Observed			Parameter Database			RPD of Means	% Range Covered	Dist
			Min	Max	Mean	Min	Max	Mean			
U+6	MKD_U	2	3.11E-05	1.99E-02	3.08E-03	3.00E-05	2.00E-02	3.10E-03	0.67%	99.3%	Logunif.
U+6	MKD_U	3	3.06E-05	1.88E-02	3.07E-03	3.00E-05	2.00E-02	3.10E-03	0.81%	93.8%	Logunif.
WAS_AREA	BIOGENFC	1	2.82E-03	9.97E-01	5.01E-01	0.00E+00	1.00E+00	5.00E-01	0.11%	99.4%	Uniform
WAS_AREA	BIOGENFC	2	1.80E-03	9.97E-01	5.00E-01	0.00E+00	1.00E+00	5.00E-01	0.07%	99.5%	Uniform
WAS_AREA	BIOGENFC	3	2.65E-04	9.99E-01	5.00E-01	0.00E+00	1.00E+00	5.00E-01	0.07%	99.9%	Uniform
WAS_AREA	BRUCITEC	1	4.80E-08	5.63E-08	5.20E-08	4.76E-08	5.64E-08	5.20E-08	0.01%	94.5%	Normal
WAS_AREA	BRUCITEC	2	4.77E-08	5.61E-08	5.20E-08	4.76E-08	5.64E-08	5.20E-08	0.01%	95.7%	Normal
WAS_AREA	BRUCITEC	3	4.77E-08	5.61E-08	5.20E-08	4.76E-08	5.64E-08	5.20E-08	0.00%	96.4%	Normal
WAS_AREA	BRUCITEH	1	1.82E-08	2.18E-08	2.00E-08	1.81E-08	2.19E-08	2.00E-08	0.00%	95.9%	Normal
WAS_AREA	BRUCITEH	2	1.82E-08	2.17E-08	2.00E-08	1.81E-08	2.19E-08	2.00E-08	0.01%	91.7%	Normal
WAS_AREA	BRUCITEH	3	1.82E-08	2.17E-08	2.00E-08	1.81E-08	2.19E-08	2.00E-08	0.00%	93.1%	Normal
WAS_AREA	BRUCITES	1	4.34E-08	6.06E-08	5.20E-08	4.27E-08	6.13E-08	5.20E-08	0.01%	92.4%	Normal
WAS_AREA	BRUCITES	2	4.30E-08	6.06E-08	5.20E-08	4.27E-08	6.13E-08	5.20E-08	0.02%	95.1%	Normal
WAS_AREA	BRUCITES	3	4.28E-08	6.11E-08	5.20E-08	4.27E-08	6.13E-08	5.20E-08	0.00%	98.2%	Normal
WAS_AREA	GRATMICH	1	5.57E-12	5.54E-10	1.80E-10	0.00E+00	1.03E-09	5.14E-10	96.34%	53.4%	Uniform
WAS_AREA	GRATMICH	2	2.65E-12	5.31E-10	1.78E-10	0.00E+00	1.03E-09	5.14E-10	97.00%	51.4%	Uniform
WAS_AREA	GRATMICH	3	6.73E-13	5.16E-10	1.84E-10	0.00E+00	1.03E-09	5.14E-10	94.70%	50.2%	Uniform
WAS_AREA	GRATMICI	1	3.26E-11	5.55E-10	2.94E-10	3.08E-11	5.57E-10	2.94E-10	0.05%	99.4%	Uniform
WAS_AREA	GRATMICI	2	3.40E-11	5.53E-10	2.94E-10	3.08E-11	5.57E-10	2.94E-10	0.09%	98.7%	Uniform
WAS_AREA	GRATMICI	3	3.15E-11	5.52E-10	2.94E-10	3.08E-11	5.57E-10	2.94E-10	0.04%	99.0%	Uniform

Material	Property	Rep	Observed			Parameter Database			RPD of Means	% Range Covered	Dist
			Min	Max	Mean	Min	Max	Mean			
WAS_AREA	HYMAGCON	1	3.49E-13	3.40E-10	1.70E-10	0.00E+00	3.40E-10	1.70E-10	0.06%	99.9%	Uniform
WAS_AREA	HYMAGCON	2	3.10E-12	3.37E-10	1.70E-10	0.00E+00	3.40E-10	1.70E-10	0.06%	98.2%	Uniform
WAS_AREA	HYMAGCON	3	5.60E-13	3.39E-10	1.70E-10	0.00E+00	3.40E-10	1.70E-10	0.06%	99.7%	Uniform
WAS_AREA	PROBDEG	1	1.00E+00	2.00E+00	1.25E+00	1.00E+00	2.00E+00	1.25E+00	0.00%	100.0%	Delta
WAS_AREA	PROBDEG	2	1.00E+00	2.00E+00	1.25E+00	1.00E+00	2.00E+00	1.25E+00	0.00%	100.0%	Delta
WAS_AREA	PROBDEG	3	1.00E+00	2.00E+00	1.25E+00	1.00E+00	2.00E+00	1.25E+00	0.00%	100.0%	Delta
WAS_AREA	SAT_RBRN	1	2.71E-03	5.51E-01	2.76E-01	0.00E+00	5.52E-01	2.76E-01	0.07%	99.3%	Uniform
WAS_AREA	SAT_RBRN	2	6.63E-04	5.47E-01	2.76E-01	0.00E+00	5.52E-01	2.76E-01	0.05%	99.0%	Uniform
WAS_AREA	SAT_RBRN	3	3.97E-03	5.48E-01	2.76E-01	0.00E+00	5.52E-01	2.76E-01	0.11%	98.6%	Uniform
WAS_AREA	SAT_RGAS	1	7.72E-04	1.49E-01	7.50E-02	0.00E+00	1.50E-01	7.50E-02	0.01%	98.5%	Uniform
WAS_AREA	SAT_RGAS	2	6.34E-04	1.50E-01	7.50E-02	0.00E+00	1.50E-01	7.50E-02	0.04%	99.3%	Uniform
WAS_AREA	SAT_RGAS	3	7.07E-04	1.49E-01	7.51E-02	0.00E+00	1.50E-01	7.50E-02	0.10%	98.7%	Uniform
WAS_AREA	SAT_WICK	1	3.06E-03	9.92E-01	5.00E-01	0.00E+00	1.00E+00	5.00E-01	0.05%	98.9%	Uniform
WAS_AREA	SAT_WICK	2	2.32E-03	9.99E-01	5.00E-01	0.00E+00	1.00E+00	5.00E-01	0.09%	99.7%	Uniform
WAS_AREA	SAT_WICK	3	4.40E-03	9.93E-01	5.00E-01	0.00E+00	1.00E+00	5.00E-01	0.02%	98.8%	Uniform